Studies on Preparation, Characterization and Pharmacokinetics of Etoposide Loaded Nanoparticles

THESIS

Submitted in partial fulfilment
of the requirements for the degree of

DOCTOR OF PHILOSOPHY

by

MOVVA SNEHALATHA

Under the supervision of

Prof. Ranendra N. Saha

BIRLA INSTITUTE OF TECHNOLOGY AND SCIENCE

PILANI (RAJASTHAN) INDIA

2006

BIRLA INSTITUTE OF TECHNOLOGY AND SCIENCE
PILANI (RAJASTHAN)

CERTIFICATE

This is to certify that the thesis entitled "**Studies on Preparation, Characterization and Pharmacokinetics of Etoposide Loaded Nanoparticles**" and submitted by **MOVVA SNEHALATHA,** ID No 2001PHXF024 for award of Ph. D. Degree of the Institute and embodies original work done by her under my supervision.

Date:

(Dr. RANENDRA N. SAHA)

Professor of Pharmacy
Dean, Faculty Division III & Educational Development Division
B.I.T.S., Pilani

Dedicated

To

My Family

Acknowledgements

It gives me immense pleasure in expressing my gratitude to my guide, Prof.R.N.Saha, Dean, Faculty Division III and Educational Development Division, BITS, Pilani, for his supervision and support for completion of this work. I sincerely acknowledge the guidance and help rendered by him at all times, especially for seeing me through the tough patches of my stay in Pilani.

I convey my sincere thanks to Prof. S. Venkateswaran, Ex. Vice chancellor, BITS, Pilani, Prof. L.K. Maheshwari, Vice chancellor, BITS, Pilani, Prof. K.E. Raman, Deputy Director (Administration), BITS, Pilani, for permitting me and providing necessary facilities to carryout my doctoral research.

My heartfelt gratitude to Prof. Ravi Prakash, Dean, Research and Consultancy Division, BITS, Pilani, for monitoring my progress. I would like to thank Dr. R. Mahesh, Group Leader, Pharmacy Group, BITS, Pilani, for his constructive criticism. I am also grateful to him for permitting me to avail the various laboratory facilities for my work.

I am obliged to Dr. Tripathi, Director, Institute of Nuclear Medicine and Allied Sciences (INMAS, New Delhi), for giving me access to facilities at INMAS. I am highly obliged to Dr. Rakesh Kumar Sharma, Joint Director, INMAS, for providing me training, necessary input to carryout part of my work at INMAS. I offer my thanks to Mr. Anil Kumar Babbar for helping me for biodistribution studies at INMAS. Without his help and valuable suggestions biodistribution study of radiolabeled nanoparticles would not have been complete.

I am deeply grateful to the Council of Scientific and Industrial Research (CSIR, New Delhi), for awarding me with Senior Research Fellowship and also for generously granting travel grant to present my research paper at conference abroad. I express my sincere thanks to Dabur Research Foundation, Sahibabad for the generous gift sample of Etoposide. I am indebted to Indian Institute of Chemical Technology (IICT, Hyderabad), All India Institute of Medical Sciences (AIIMS, New Delhi), Central Electronics Engineering Research Institute (CEERI, Pilani), and Panacea Biotech, Lalru for extending their help in analyzing my samples. I am grateful to Dr. K.C. Jindal, President, and Mr. Munish Talwar, General Manager, Formulations Panacea Biotech for providing access to use particle size analyzer.

I thank INMAS staff, Dr. Adhikari, Mr. Lakshman, Mrs. Krishna Chuttani, Dr.Prem, Mrs. Nidhi Bharadhwaj, Dr. Sheetal, Shri. Dev Singh and Mrs. Kanchan for their support. My sincere thanks to Dr. Souri Banerjee, BITS, Pilani, Dr. P.K. Gupta and Mr. Ashok Sharma, CEERI, Pilani for helping me in Atomic Force Microscopy Studies.

All faculty members of Pharmacy Group (Dr. A.N. Nagappa, Dr. S.M. Ray, Dr. D. Sriram, Dr. P. Yogeeswari, Dr. Sajeev Chandran, Mr. Murali Raman, Mr. Prashant Kole, Mr. Shrikant Charde, Mrs. Archna Roy, Mr. Punna Rao, and Dr. Hemant R. Jadhav), BITS, Pilani, deserve special mention for their co-operation in discharging my academic responsibilities and research activity.

I would like to thank Dr. S.D. Pohekar and Mr. Deshmukh, and other office staff of Research and Consultancy Division, BITS, Pilani, Raghuvirji, Mahipal, and Soniji for various help during my doctoral research. I take this opportunity to thank all the non-teaching staff of Pharmacy Group, Hari Ramji, Gokulji, Mathu Ramji, Sita Ramji, Soniji, Sharmaji, Yasinji and Navin for their help.

At this moment, I feel nostalgic and go down the memory lane to recall all the wonderful moments that I spent with my friends Praveen, Shrikant, Punna, Girish, Venu, and Laila for filling my surroundings with life and laughter. My special thanks to Laila for providing valuable suggestions during thesis preparation. I also take this opportunity to thank Dr. Vijay, Joy, Dr. Ravi, Dr. Thirumurugan, Dr. Venkatesh, Dr. Pandi, Dr. Rahul, Dr. Tanushree, Dr. Raju, Mr. Ramachandran, Mrs. Meenakshi, Mrs. Shalini, Mr. Raghavendran, Mr. Rajkumar, Mr. Kundu, Mr. Prakash, Mrs. Vanita and all others. I express my hearty thanks to my beloved friends and well wishers Mr. Shivaprakash, Dr. Kumaran, Buchi, Uday, Akshant, Thirupati, Ashok, K.V.G. Chandrasekhar, Purna and Haritha for making my stay in Pilani a memorable experience of my life. There are so many fond memories attached with them. I would like to specially mention Duppy who gave me innumerable sweet memories to treasure for life. My friends Chayapathy, Sankar, Madhuri, Pavan, Rambabu, Manikandan and Milan deserve a special mention. I deeply cherish their concern for me.

I feel exultant and proud to have Venugopal as my soul mate. His understanding and love saw me accomplish this task. I truly cherish his warm and friendly help and his concern for my work at all times. I thank my in laws and brother in law for their affection and encouragement.

Needless to say, I owe it all to my parents who have been with me always. It is wholly and solely their dream that I am happy to realize today. Their faith in me and their spirit of love has kept the candle of perseverance glowing incessantly. Without their blessings I would have not achieved this goal.

M. Snehalatha

Summary

Present research aims at design and development of nanoparticulate delivery system, for better delivery of etoposide for extended period of time for better therapeutic efficacy. Main objective of the present work was to prepare and characterize etoposide loaded nanoparticles using different biodegradable and/or bioacceptable polymers alone and in combination and their characterization and in vivo study of their pharmacokinetic and distribution in animal model.

As a part of this study, suitable analytical methods were developed for the estimation of etoposide in formulations and different study samples. According to the need, UV spectrophotometric, spectrofluorimetric and HPLC method with UV detection were developed and validated. These methods were sensitive, accurate, precise and found to be suitable for analysis of etoposide in formulations and study samples. Under preformulation studies, pH - solubility, pH - stability, partition coefficient and drug-excipient interaction studies at different storage conditions were carried out for etoposide. These studies indicated the poor aqueous solubility and degradation of etoposide at extreme acidic and alkaline conditions.

Nanoparticle formulations encapsulating etoposide were prepared using nanoprecipitation method or solvent evaporation method depending on the polymer used. Biodegradable and biocompatible polymers, poly lactic glycolic acid co polymers (PLGA 50/50, PLGA 75/25 and PLGA 85/15), poly-e-caprolactone and Eudragit® L 100 were selected for preparation. Formulations were optimized by changing various process parameters during preparation. Concentration of stabilizers (Pluronic F 68 and Poly vinyl alcohol), amount of polymer and etoposide, volume of aqueous phase and organic phase used for preparation of nanoparticles were optimized. Morphology of the prepared nanoparticles was studied by transmission electron microscopic and atomic force microscopic techniques. Size distribution, polydispersity index and zeta potential for the prepared nanoparticles were measured by photon correlation spectroscopy using zetasizer. The methods used for preparation of nanoparticles were simple, reproducible and produced nanoparticles with narrow size distribution and good entrapment efficiency. Use of different biodegradable polymers individually and in combination produced etoposide loaded nanoparticles with low polydispersity index and high drug entrapment efficiency. Change in the concentration of stabilizer, polymer and amount of etoposide found to influence size, polydispersity index and entrapment efficiency of the prepared nanoparticles.

In vitro release of etoposide from the prepared nanoparticles was studied by dialysis bag diffusion technique. Release from nanoparticles prepared with PLGA co polymers

extended with increase in lactide content in the polymer. In vitro release of etoposide was extended upto 48 h from formulations prepared with PLGA 85/15, PCL individually and their combination (1:1). For selected formulations, stability was checked at different temperatures by measuring their size, polydispersity index, zeta potential and entrapment efficiency after storage. Freeze dried formulations were found to be stable without change in their size, entrapment efficiency and redispersibility for 1 year.

Biodistribution and pharmacokinetic studies were performed in mice after administering radiolabeled free etoposide and nanoparticle formulations through intravenous and oral routes. Radiolabeling of etoposide and nanoparticle formulations was done with technetium (Tc^{99m}). Labeling method was optimized by changing different process parameters like amount of stannous chloride and pH. Quality control tests done by thin layer chromatography showed high labeling efficiency with very less percentage of free pertechnetate and radio colloids. Different organs/tissues were extracted from mice at different time points and were estimated for radioactivity present in organs/tissues using gamma counter. The uptake and distribution of free etoposide and nanoparticles was found to be different for various organs/tissues. Distribution of nanoparticles found to be more to liver, blood, lungs, bone and less to heart, kidney compared to distribution of free etoposide. Thus modified distribution can lead to organ specific distribution with better therapeutic efficacy and low side effects or toxicity.

Tumor uptake of radio labeled etoposide and formulations was determined and biodistribution studies were also performed in Dalton's lymphomacyte solid tumor bearing mice after intravenous administration. Gamma scintigraphic imaging was done for the tumor bearing mice at 4 and 24 h post administration. This study indicated higher tumor affinity and targeting properties of etoposide loaded nanoparticles than free etoposide.

Pharmacokinetic studies were done by measuring radioactivity in blood samples collected at different time points, using gamma counter, after i.v. and oral administration of radio labeled preparations in mice and rabbits. Pharmacokinetic parameters calculated after fitting into non-compartmental model showed increased AUC, MRT and lower clearance for nanoparticles compared to free etoposide. Scintigraphic imaging was done at 4 and 24 h after intravenous administration of radio labeled preparations in healthy rabbits and tumor induced mice. Scintigraphic images confirmed the localization of nanoparticles at the site of tumor. Images indicated modified distribution of nanoparticles in rabbit also. Improved bioavailability and selective biodistribution were observed in nanoparticle delivery systems.

Table of Contents

List of Abbreviations and Symbols

% A/g	Percentage activity
% RSD	Percentage relative standard deviation
% RTD	Percentage remaining to be degraded
λ_{em}	Emission wavelength
λ_{exc}	Excitation wavelength
(IL)-2	Interleukin
λ_{max}	Wavelength maximum
µg	Microgram
µg/ml	Microgram per milli litre
^{99m}Mo	Molybdenum
^{99m}Tc	Technetium - 99m
$^{99m}TcO_4^-$	Pertechnetate
ACN	Acetonitrile
AFM	Atomic force microscopy
AIDS	Auto immunodeficiency syndrome
approx.	Approximately
AUC	Area under the curve
Cl	Clearance
C_{max}	Maximum concentration reached
Conc.	Concentration
CSF	Cerebro spinal fluid
DL	Detection limit
DLS tumor	Daltons lymphoma solid tumor
DMA	Dimethyl acetamide
DMF	Dimethyl formamide
DMSO	Dimethyl sulfoxide
DNA	Deoxyribo nucleic acid
DSC	Differential scanning calorimetry
EE	Entrapment efficiency
EO	Ethylene oxide
EPR	Enhanced permeability retention
EuL-100	Eudragit® L 100
F 68	Pluronic F 68
GIT	Gastro intestinal tract
HCl	Hydrochloric acid

HEC	Hydroxyethylcellulose
HPC	Hydroxypropylcellulose
HPLC	High performance liquid chromatography
HPMC	Hydroxypropyl methylcellulose
i.m.	Intramuscular
i.p.	Intraperitoneal
i.v.	Intravenous
ICH	International conference on harmonization
IR	Infra red spectroscopy
ITLC	Instant thin layer chromatography
KH_2PO_4	Potassium dihydrogen phosphate
LD	Laser diffraction
LLE	Liquid-liquid extraction
Log $P_{o/w}$	Logarithm of partition coefficient
M	Molarity
MC	Methylcellulose
mg/ml	Milligram Per milli liter
MPS	Mono phagocytic system
MRT	Mean residence time
Na_2HCO_3	Sodium hydrogen carbonate
$NaBH_4$	Sodium borohydride
NaCl	Sodium chloride
NaOH	Sodium hydroxide
nm	Nano meters
PAW	Pyridine: Acetic Acid: Water
PCL	Poly e caprolactone
$P_{Cl/w}$	Partition coefficient in Chloroform/Water systems
PCS	Photon correlation spectroscopy
PECA	Poly (ethylcyanoacrylate)
PEG	Poly (ethylene glycol)
PGA	Poly glycolic acid
P-gp	P-glycoprotein
PHCA	Poly (hexylcyanoacrylate)
PI	Polydispersity index
PIHCA	Poly (isohexylcyanoacrylate)
pK_a	Ionization constant

PLA	Poly (lactic acid)
PLGA	Poly (lactic and glycolic acid)
PMCA	Poly (methylcyanoacrylate)
PNP	Polymeric nanoparticles
$P_{o/w}$	Partition coefficient in Octanol/Water systems
POE	Polyoxyethylene
POP	Polyoxypropylene
PVA	Poly vinyl alcohol
QL	Quantitation limit
RBC	Red blood corpuscles
RES	Reticuloendothelial system
RP	Reverse phase
RSD	Relative standard deviation
SLN	Solid lipid nanoparticles
$SnCl_2$. 2 H_2O	Stannous chloride dihydrate
SPE	Solid phase extraction
$t_{1/2}$	Half life
TDW	Triple distilled water
TEM	Transmission electron microscope
Tg	Glass transition temperature
TLC	Thin layer chromatography
Tm	Melting temperature
T_{max}	Time to reach maximum concentration
TPP	Tri polyphosphate
USP	United states pharmacopoeia
UV	Ultra violet

List of Tables

List of Figures

Chapter 1

Introduction, Literature Review and Objective

1.1. Cancer and Chemotherapy

An ideal treatment of disease is the delivery of efficacious medication at the appropriate concentration to the site of action in a controlled and continuous manner.

Cancer is one of the most dangerous diseases tough to beat. Cancer can be defined as the emergence of cellular clusters resulting from continuous production of abnormal cells that invade and destroy normal tissues. Two characteristic features of any type of cancer are, unregulated cell growth and tissue invasion/metastasis. Unregulated cell growth without invasion is a feature of benign neoplasms or new growths. Cancers of epithelial tissues are called carcinomas; cancers of non-epithelial tissues are called sarcomas. Leukemia and Lymphomas are those arising from blood cells forming tissue and involving lymph nodes with an overproduction of lymphocytes. Tumors often arise first in renewing tissues and tumor cells are able to divide endlessly, without differentiating into a mature state and regardless of the function of the tissue they are in. Tumor cells are believed to be genetically unstable and subject to a high degree of random mutations during clonal expansion. This gives rise to lethal or disadvantageous mutations, as well as greater autonomy and growth advantages to those cells that will go on to become tumor producers. They may arise in different parts of the body, and they vary in retention of normal differentiation pattern, grade, and extent of expansion into surrounding normal tissue, and metastases (Brigger et al, 2002).

Use of proper drugs in the management of cancer has made a significant impact on the outcome of most types of malignancies. One of the main challenges in cancer therapy is how to improve the cancer treatment by optimal and careful application of anticancer drugs without affecting normal cells. Drug development and delivery process in cancer therapy is complex and associated with special challenges and considerations compared to other diseases. The proper delivery of anticancer drugs and drug carriers to the tumor at concentrations required for effective tumor therapy and low systemic toxicity still remained a challenge. In the most common cancer types, currently available drugs have limited efficacy combined with significant toxicity. The ideal anticancer chemotherapy is one that is specific for cancer cells yet capable of diverse application to multiple tumor types while effectively, but safely, shrinking primary tumors, as well as preventing or eliminating metastatic nodules.

1.1.1. Cancer Treatment

The goal of cancer treatment is first to eradicate cancer. If this primary goal cannot be accomplished, the goal of cancer treatment shifts to palliative care, the amelioration of

symptoms, and preservation of quality of life while striving to extend life. The treatment of most human cancers with conventional cytoreductive agents has been unsuccessful due to growth kinetics of solid tumors and the genetic instability that predisposes to the development of intrinsic and acquired drug resistance. When cure of cancer is possible, cancer treatments may be undertaken despite the certainty of severe and perhaps life threatening toxicities. Every cancer treatment has the potential to cause harm, and treatment may be given that produces toxicity with no benefit. Radical surgical procedures, radiation therapy, high doses of cytokines such as interleukin (IL)-2 are all used in certain settings where most of the patients will experience toxicity and side effects from the intervention and only a fraction of the patients will experience benefit.

One of the challenges of cancer treatment is to use the various treatment modalities alone and together in a fashion that maximizes the chances of patient benefit. Cancer treatments are divided into four main types: surgery, radiation therapy, chemotherapy and biologic therapy. Surgery and radiation therapy are considered local treatments, though their effects can influence the behavior of tumor at remote sites. Chemotherapy and biologic therapy are usually systemic treatments. Chemotherapeutic agents may be used for the treatment of active, clinically apparent cancer.

Oral delivery of anticancer drugs suffers many drawbacks. Unfortunately, most anticancer drugs are not bioavailable due to their poor solubility, stability and permeability and thus orally administered anticancer drugs have little chance to reach the tumor site (DeMario and Ratain, 1999; Bottomley, 2002). These problems make formulation development of anticancer drugs a major challenge. In addition, oral drug delivery of many anticancer drugs presents such problems as the lack of good bioavailability, slow drug absorption, variability in achievable plasma/tissue concentrations owing to inter and intra individual differences in drug absorption and disposition. The reason has been under intensive investigation and it has been found that the orally administered anticancer drugs would be eliminated by the first metabolic process with cytochrome P450 and by the efflux pump of P-glycoprotein (P-gp) (Sparreboom et al, 1997; Malingre et al, 2001). Medical solutions, which are currently being developed, propose to apply P450/P-gp suppressors such as cyclosporine A to make oral chemotherapy feasible. However, these suppressors would fail the immune system of the patients and thus may lead to complex medication to the patients. Also, most of the suppressors may have side effects and/or difficulties in formulation of their own (Van Zuylen et al, 2000; Khin and Si-Shen, 2005).

Though, oral delivery of anticancer drugs is a challenge, but has advantages over the current regime of chemotherapy by injection or infusion. Oral chemotherapy can provide a

long term, continuous exposure of the cancer cells to the anticancer drugs of a relatively lower and safer concentration and thus gives little chance for the tumor blood vessels to grow, and resulting in much better efficacy and fewer side effects than the current intermittent chemotherapy could do. Oral chemotherapy is convenient and thus preferred by patients, which can greatly improve the quality of life of the patients. Oral chemotherapy can eventually promote a new concept of chemotherapy: “chemotherapy at home”. This is especially important for the patients with advanced or metastatic cancer (Ajani and Takiuchi, 1999; Feng and Chien, 2003).

Intravenous (i.v.) administration of anticancer agents is much more problematic. Specificity for intravenously injectable drugs is often low, necessitating large amounts of a drug be injected into a patient, creating a high concentration of the drug in the blood stream that could potentially lead to toxic side effects. Further, poor water solubility aggravates the problem. After i.v. injection, the drugs or drug carriers enter the tumor vasculature and reach the cancer cells via distribution through the vascular compartment, transport across the micro vessel wall and diffusion through the interstitium with in the tumor tissue. In addition during the transport they may bind nonspecifically to proteins or other tissue components, bind specifically to targets or metabolized. Disadvantages of systemic delivery of anticancer drugs are the cost in comparison with that of the oral route of delivery. Compared to oral means of drug delivery, systemic delivery is invasive, and often requires the use of a secured catheter in a major blood vessel (Ewesuedo and Ratain, 2004).

Various other approaches were taken to improve the tumor delivery of anticancer agents, such as intravesical injection and intraperitoneal administration, localized drug delivery through intratumoral administration. Intratumoral administration of an anticancer drug mitomycin C has been shown to reduce its side effects by concentrating the drug at the tumor site by modifying the pharmacokinetic and biological properties (Ewesuedo and Ratain, 2004).

1.1.2. Problems Associated with Drug Delivery to Tumors

Tumor vasculature forms a major barrier in drug delivery to tumors because of its highly disorganized and unpredictable structure and function (Brigger et al, 2002). Tumor blood vessels present several abnormalities in comparison with normal physiological vessels, often including a relatively high proportion of proliferating endothelial cells, an increased tortuosity, a deficiency in pericytes and an aberrant basement membrane formation (Seymour, 1992; Baban and Seymour, 1998). Transport pathways across tumor vessels have been shown to occur via open gaps (inter-endothelial junctions and trans-

endothelial channels), vesicular vacuolar organelles and fenestrae. It remains, however, controversial as to which pathways are predominantly responsible for tumor hyper permeability and macromolecular trans-vascular transport (Hobbs et al, 1998). Regardless of the transport mechanism, the pore cutoff size of several tumor models has been reported ranging between 380 and 780 nm (Yuan et al, 1995; Hobbs et al, 1998).

For efficient delivery of drugs in tumor therapy, they must be able to traverse through the circulatory system and reach the tumor mass in sufficient concentration, get transported across the micro vessels, and diffuse into the interstitial space (Jain, 2001a). Unfortunately, the irregular blood supply, high interstitial pressure, low pH and hypoxia, and lack of lymphatic system contribute to inefficient drug uptake and distribution in the tumor mass after systemic administration. The problem of optimum delivery to tumors is further compounded by many potent anticancer drugs, with poor permeability and poor solubility characteristics.

The transport of an anticancer drugs in the interstitium will be governed by physiological (i.e. pressure) and physicochemical (i.e. composition, structure, charge) properties of the interstitium and by the physicochemical properties of the drug molecule (size, configuration, charge, hydrophobicity) itself (Jain, 1987). Thus, to deliver therapeutic agents to tumor cells in vivo, one must overcome the following problems: (i) drug resistance at the tumor level due to physiological barriers (non cellular based mechanisms), (ii) drug resistance at the cellular level (cellular mechanisms), and (iii) distribution, biotransformation and clearance of anticancer drugs in the body (Links and Brown, 1999).

Apart from the above, there are also formulation issues, such as in vivo formulation stability, degree of drug entrapment and ability to make the agent bioavailable at the site of action, that determine the degree of success of a delivery specific approach for treating cancer. In order to carry a cytotoxic agent specifically to solid tumors while avoiding healthy tissues, the drug must be stably encapsulated in the carrier when in the general circulation.

In chemotherapy, clinical drug resistance may be defined either as a lack of tumor size reduction or as the occurrence of clinical relapse after an initial positive response to antitumor treatment (Links and Brown, 1999). Non-cellular drug resistance mechanisms could be due to poorly vascularized tumor regions, which can effectively reduce drug access to the tumor and thus protect cancerous cells from cytotoxicity. The acidic environment in tumors can also confer a resistance mechanism against basic drugs. These compounds would be ionized, preventing their diffusion across cellular membrane. The resistance of tumors to therapeutic intervention may be due to cellular mechanisms, which are

categorized in term of alterations in the biochemistry of malignant cells. They comprise altered activity of specific enzyme systems (for example topoisomerase activity), altered apoptosis regulation, or transport based mechanisms, like P-glycoprotein efflux system, responsible for the multi drug resistance (MDR), or the multi-drug resistance associated protein (MRP) (Krishna and Mayer, 2000). As cancer fighting drugs are toxic to both tumor and normal cells, the efficacy of chemotherapy is often limited by important side effects. Traditional chemotherapy treats tumors by systemic treatment via parenteral or oral application, by intratumoral injection or by interstitial placement of drugs. Oral delivery via tablets or capsules is largely inefficient due to exposure of the pharmaceutical agent to the metabolic processes of the body. Therefore, a more than necessary dose is often required and the maximum effectiveness of the drug is limited.

1.1.3. Need for Better Drug Delivery Approaches

Above problems associated with cancer therapy necessitated to develop better drug delivery systems for anticancer drugs. One of the lingering challenges in cancer therapeutics is how to influence the outcome of cancer treatment by optimal and careful delivery of anticancer drugs. The majority of drugs used in cancer treatment is administered systemically, orally or loco regionally. Of these, only loco regional delivery presumes restriction of an administered tumor. But the loco regional delivery of drugs could present unique and/or similar adverse events in comparison to systemically administered neoplastics.

Systemic delivery of cytotoxic anticancer drugs has and will continue to play a crucial role in cancer therapeutics. However, one of the major problems with this form of drug delivery is the exposure of normal tissues/organs to the administered drug. Most anticancer drugs are not usually administered orally because lack of availability and/or suitable oral formulations. In addition, oral drug delivery presents following problems: lack of bioequivalence of oral formulations, poor drug absorption, variability in achievable plasma/tissue concentrations owing to inter and intra individual variation in drug absorption and disposition, and drug-drug interactions because most cancer patients are also using other medications. Disadvantages of systemic delivery of anticancer drugs are the cost in comparison with that of the oral route of delivery. This could be significant in situations where effective oral anticancer drugs are available.

With all the associated problems in the present cancer therapy, there is always need for a better drug delivery system which delivers the drug particularly at the site of tumor or to the specific tumor cell where it will slowly release the drug. It is well known that

anticancer drugs not only kill cancerous cells but also they are toxic and can kill normal cells in the body with many other side effects. Delivery system, which identifies and delivers drugs to cancer cells, only can reduce the exposure of normal cells to the anticancer drugs, thus reducing side effects associated with the treatment.

Present approaches in seeking to achieve this end include

1. Tumor targeting and promotion of drug accumulation in solid tumor masses or nodules.
2. Tumor specific or selectively acting agents based upon a unique feature of cancer cells.
3. Tumor selective drugs using a cancer specific activation mechanism or metabolic requirements.

1.1.4. New and Novel Drug Delivery Systems for the Treatment of Cancer

New drug delivery systems can be used for specific delivery of drugs to reduce side effects, to improve the bioavailability or to target specific sites. Most of these specially designed dosage forms in cancer treatment are based on polymeric materials to control the release of the active agent via dissolution, matrix erosion and degradation, diffusion or cleavage of prodrugs. Tremendous opportunities exist for utilizing advanced drug delivery systems for cancer treatments. Controlled release formulations of pharmacologically active substances using biodegradable polymers as carriers provide interesting options for stable and convenient drug formulations. When colloidal particles are formulated from a biodegradable polymer and a drug, a modified drug delivery/drug targeting or an improved pharmacokinetic profile of the compound is feasible. Also, improvements in selectivity, protection of the drug against fast metabolism, and more effective diffusion through biological barriers may become attainable (Kreuter, 1994).

The design of novel drug delivery systems has primary objective to control the delivery of a pharmacological agent to its site of action at a therapeutically optimal rate and dosage regimen. The improvement of therapeutic index can be obtained by site specific or targeted delivery, combined with controlled release, which promote the efficacy of the drug and would also reduce its toxic side effects. Colloidal drug delivery systems, including liposomes, microemulsions, nanocapsules and nanospheres are the most promising to achieve this goal. All these formulations have different advantages and disadvantages, despite their very similar characteristics of size, shape and mode of administration. However, nanoparticles are very stable systems and their solid polymeric structure can be engineered for targeting and/or controlled release purposes (Soppimath et al, 2001).

Colloidal drug carrier systems hold the promise of overcoming physiological barriers to provide a successful therapy. Based on the size of the colloidal particles and the route of administration, drugs can be passively targeted to certain areas of the body. This selective delivery of chemotherapeutic agents has two advantages. It allows for the maximum fraction of the delivered drug molecules to reach and react with the cancer cells without having any harmful effect on normal cells, and it increases the distribution of the drug to the cancer cells (Yuan, 1998). The end result of such delivery is an increase in effectiveness of the chemotherapeutic agent and, due to lower systemic concentrations, decreased incidence of side effects.

One strategy for such could be to associate antitumor drugs with colloidal polymeric nanoparticles, with the aim to overcome non-cellular and cellular based mechanisms of resistance and to increase selectivity of drugs towards cancer cells while reducing their toxicity towards normal tissues. Nanoparticles of biodegradable polymers may also provide an alternative solution for oral delivery of anticancer drugs across the gastrointestinal barrier due to their extremely small size and their appropriate surface coating to escape from the recognition by P 450/P-gp (Brigger et al, 2002).

Nanoparticles represent very promising drug delivery systems, which can be considered for a very wide range of applications. Optimization of earlier techniques combined with the development of new procedures using biodegradable polymeric materials has enabled the development of nanoparticulate systems with increased acceptance and potential. The entrapment of hydrophilic compounds still faces some limitations; the many possible variations in structure and type of nanoparticles allow the entrapment of a great number of molecules. The technology of nanoparticles being now quite well mastered and the main objective is the improvement of their bioavailability and targeting properties following their administration (Soppimath et al, 2001).

1.2. Nanoparticles

In the recent years, significant effort has been devoted to develop nanotechnology for drug delivery since it offers a better means of delivering small as well as high molecular weight drugs, proteins, peptides or genes to cells and tissue. Nanotechnology has opened up new vistas of research in the development of novel drug delivery systems. They have been studied extensively as particulate carriers in several pharmaceutical and medical fields.

Nanoparticles are generally defined as particles between 1 nm to 1000 nm in size, and can be either spherical or vesicular. These are colloidal particles in which biologically active molecules can be trapped, dissolved, and/or encapsulated. Depending on the method of preparation of nanoparticles, nanospheres or nanocapsules can be produced (Figure 1). Nanocapsules are vesicular systems in which the drug is confined to a cavity surrounded by a unique polymer membrane, while nanospheres are matrix system in which the drug is physically and uniformly dispersed. The size and surface characteristics of nanoparticles, such as charge, hydrophilic-hydrophobic balance, and presence of site-specific components influence their body distribution and targeting attitude.

Figure 1: Schematic representation of nanosphere and nanocapsule.

Nanoparticles can be prepared by several techniques, depending on the nature of the polymeric material and the characteristics of the drug to be loaded. Various biocompatible and biodegradable polymers have been used in drug delivery research as they can effectively deliver the drug and thus increase the therapeutic benefit, while minimizing the side effects (Ravi kumar and Kumar, 2001).

1.2.1. Materials Used in the Preparation of Polymeric Nanoparticles

a) Polymers

The challenge in the design of nanoparticulate drug delivery lies in the fact that polymeric materials are required to possess a unique combination of apparently conflicting, but indispensable properties. Such polymers should be non-toxic, encapsulate drugs, proteins and antigens without changing their bioactivities, confer impermeability sufficient

to protect them from acidic and enzymatic degradation and still maintain the ability to release the substrate at the target site at a certain rate. In addition the ability of polymers to form stable nanoparticles with desirable sizes and surface characteristics should be considered prerequisite for their selection. Nanoparticles can be prepared with non-biodegradable and non-biocompatible polymers, but it is always preferable to use biocompatible or biodegradable polymers to avoid toxic and life threatening tissue and immunological reactions after administered into the body. In general, for the preparation of nanoparticles, both hydrophilic and hydrophobic polymers are used. A list of polymers along with their preparation techniques is given in Table 1.

Table 1: Summary of nanoparticle preparation techniques and employed polymeric materials (Allemann et al, 1993 and Quintanar-Guerrero et al, 1998).

Technique	Material
Emulsion Polymerization	Poly (alkyl methacrylate), Poly (alkyl cyanoacrylate), Poly (styrene), Poly (vinyl pyridine), Poly (acroleine), Poly (gluteraldehyde)
Interfacial Polymerization	Poly (alkyl cyanoacrylate), Poly (lysine) derivatives
Emulsion Evaporation	Poly (lactic acid), Poly (lactide-co-glycolide), Poly (e-caprolactione), Poly (ß-hydroxybutyrate), Ethyl Cellulose
Solvent Displacement	Poly (alkyl methacrylate), Poly (lactic acid) Poly (lactide-co-glycolide), Poly (e-caprolactione),
Salting Out	Cellulose acetate phthalate, Poly (alkyl methacrylate), Ethyl Cellulose, Poly (lactic acid), Poly (lactide-co-glycolide)
Emulsification Diffusion	Poly (lactic acid), Poly (e-caprolactione)
Desolvation, Denaturation	Albumin, Casein. Gelatin, Alginate, Chitosan, Ethyl cellulose

i) Natural Hydrophilic Polymers

Among the natural macromolecules available for the manufacture of nanoparticles, albumin, gelatin, chitosan, alginates or agarose have been extensively studied and characterized (Truong-Le, 1997). These macromolecules have attracted wide interest due to their intrinsic biodegradability and biocompatibility. The polymers of natural origin suffer some disadvantages including a) batch to batch quality variation (b) conditional biodegradability and (c) antigenicity. Alginate based delivery systems are reported as homo-compatible and acceptable system for parenteral administration of bioactive materials. In contrast dextran, albumin and gelatin which are though accepted materials for parenteral

administration manifest immunogenicity due to use of cross linking agents, which are employed during their preparations. Chitosan is a homo-non-compatible material and hence it should be restricted to extra corporeal uses only (Mitra et al, 2001; Mao et al, 2001).

ii) Synthetic Hydrophobic Polymers

Most of the polymers used for nanoparticle preparations are typically hydrophobic in nature. They are either pre-polymerized or synthesized before or during the process of nanoparticle preparation. Polymers from the ester class poly (lactic acid) (PLA) and poly (lactic co glycolic acid) (PLGA) co polymers are representative of first group along with poly (caprolactone) (PCL) and are already been approved for human use. Poly (alkyl cyanoacrylates) (PACA) group of polymers have received the greatest attention as polymeric nanoparticulate systems but a number of controversies are there regarding the toxicity of the corresponding alkyl cyanoacrylates monomer.

A number of different polymers have been investigated for formulating biodegradable nanoparticles, PLA and its copolymers with glycolic acid, PLGA have been extensively used for controlled drug delivery systems. The lactide/glycolide polymers chains are cleaved by hydrolysis into natural metabolites (lactic and glycolic acids), which are eliminated from the body by the citric acid cycle. PLGA provides a wide range of degradation rates, from months to years, depending on its composition and molecular weight (Shive and Anderson, 1997; Gorner et al, 1999; Uhrich et al, 1999; Jain, 2000; Panyam and Labhasetwar, 2003).

PCL is another biodegradable, biocompatible and water insoluble polymer suitable for controlled drug delivery due to slow degradation and high permeability of many drugs and at the same time being free from toxicity. It has the ability to form compatible blends with other polymers. Due to higher permeability of PCL, it is blended with other polymers to improve stress, crack resistance and control over release rate of drugs. Within the last decades, PCL polymers have been the major area of interest to develop controlled delivery systems especially for peptides and proteins. Other advantages of PCL include its hydrophobicity, in vitro stability and low cost. Moreover, this polymer has been under clinical evaluation for sustained delivery of levonorgestrel (Pitt, 1990).

b) Stabilizers

A stabilizer is required to avoid coalescence and formation of agglomerates during and after the preparation of nanoparticles. The large interfacial tension of small droplets drives the system to coalescence. Adsorption of stabilizers at the interface prevents this

coalescence by lowering the interfacial tension and the energy of the system. The type and concentration of stabilizer used may influence the particle size and particle properties such as zeta potential and mucoadhesion (Scholes et al, 1999; Feng and Huang, 2001). Both particle size and zeta potential are important physicochemical properties because they determine the physical stability and biopharmaceutical properties of nanoparticles, influencing drug release rate, biodistribution, mucoadhesion, and cellular uptake (Vandervoort and Ludwig, 2002). The type and concentration of the stabilizer selected may affect the particle size.

Poloxamers and poly vinyl alcohol (PVA) are the most popular stabilizers used for the production of polymeric nanoparticles. Polyoxyethylene based copolymers like poloxamer, and poloxamine are of considerable interest because of their extremely low toxicity and low immunogenic response. The use of poloxamer during particle formation provides a hydrophilic layer of polyoxyethylene chains extending from the surface and anchored in the hydrophobic PLA shell by the polyoxypropylene blocks (Kabanov et al, 2002).

Sometimes other polymers were also used as stabilizers since they provide a surface coating of the metastable micro phase, thus lowering its tendency to phase-aggregation. The polymers evaluated as stabilizers are cellulose derivatives such as methylcellulose (MC), hydroxyethylcellulose (HEC), hydroxypropylcellulose (HPC) and hydroxypropyl methylcellulose (HPMC), as well as gelatin type A and B and carbomer. Some of these have been reported as adjuvants in the preparation of PLGA particles, such as poloxamer (Couvreur et al, 1997; Scholes et al, 1999; De Rosa et al, 2000; O'Hara and Hickney, 2000), gelatin (Arshady, 1991; Tobio et al, 1998), HPMC (Sansdrap and Moes, 1993; Gabor et al, 1999), MC (Arshady, 1991) and carbopol (Wang et al, 1991). Moreover, HPMC, poloxamer and carbomer are interesting compounds because of their mucoadhesive properties. Tween 80 and triton X100 are also used to stabilize nanoparticle preparations alone or in combination. Deciding the phase in which stabilizer should be added is very important as it effects the drug loading. The use of stabilizers in the preparation of nanoparticles would affect particle size and zeta potential value (Feng and Huang, 2001).

c) Solvents

Solvent selection in the preparation of nanoparticulate formulation is critical. Criteria for solvent selection depend on the preparation technique of nanoparticles, miscibility of solvent with water, polymer characters and drug solubility, etc. All these parameters have an impact on particle size and encapsulation efficiency. In general, the

organic solvent should have low miscibility with water to yield a more stable emulsion that eventually leads to high quality nanoparticles. Another aspect to be considered during selection of a solvent is its toxicity as traces of solvent may remain in the nanoparticles (Birnbaum et al, 2000). So usually after the formation of nanoparticles, it should be ensured that organic solvent is completely removed/washed out.

Based on the preparation technique employed, water miscible solvent like acetone, or water immiscible solvents like dichloromethane can be used. Acetone and dichloromethane are the most commonly used solvents for the preparation of nanoparticles by PLGA, PCL polymers. Combination of solvents can be used to improve the solubility of the polymers. The emulsion/evaporation method uses a water-immiscible organic solvent, such as methylene chloride or chloroform; while the emulsion/diffusion and solvent displacement techniques uses a partially water miscible solvent, such as benzyl alcohol, acetone, or dimethylsulfoxide (DMSO). Jeon et al, (2000) studied the effect of solvent on the particle size and drug encapsulation efficiency and their effect on release kinetics of PLGA nanoparticles loaded with norfloxacin, using dimethyl acetamide (DMA), dimethyl formamide (DMF), DMSO, and acetone as initial solvents. The size of PLGA nanoparticles prepared from DMA, DMF, and DMSO as solvent were about 200-400 nm, smaller than those obtained by the use of acetone.

1.2.2. Polymeric nanoparticles (PNP)

These are solid colloidal particles consisting of non-biodegradable synthetic polymers or biodegradable macromolecular materials of synthetic, semi synthetic or natural origin. The choice of appropriate polymer, particle size and manufacturing process will primarily depend on the bioacceptability of the polymer, followed by physicochemical properties of the drug and the therapeutic objective. Drug or any biologically active compound can be dissolved, entrapped or encapsulated into the nanoparticle or simply adsorbed onto its surface. Drug release from these carriers is dependent on both the type of the carrier and the loading mechanism involved. Polymeric nanoparticles have the potential to completely transform drug delivery technology (Gref et al, 1994).

PNP are significant improvement over traditional oral and intravenous system of administration in terms of efficiency and effectiveness. Also, PNP can have engineered specificity, allowing them to deliver a higher concentration of pharmaceutical agent to a desired location. The most important advantage of using PNP in drug delivery is that they generally increase the stability of pharmaceutical agents and they can be easily fabricated in large quantities by a number of available methods. The use of PNP allows the design of

individual delivery systems for highly specific applications. Among the adaptations that can be made are surface modifications of the polymer, use of different fabrication methods, selection of a variety of pre-existing polymers or copolymers, and formulation of novel polymeric materials (Uhrich et al, 1999).

Polymeric nanoparticles are able to deliver drugs to specific sites of action for a prolonged period of time and represent an alternative drug delivery system to liposomes. They usually exhibit a long shelf life and good stability on storage. Polymeric nanoparticles are superior to liposomes in targeting them to specific organs or tissues by adsorbing and coating their surface with different substances (Damge et al, 1988). This feature makes PNP ideal candidates for cancer therapy, delivery of vaccines, and delivery of targeted antibiotics. Polymeric nanoparticles are the future of drug delivery technology and represent the best way to increase specificity in pharmaceutical therapy, a key to defeat cancer and other incurable diseases (Birrenbach et al, 1976; Kreuter, 1994; Soppimath et al, 2001).

1.2.3 Solid Lipid Nanoparticles (SLN)

SLN are sub micron colloidal carriers (50-1000 nm) which are composed of physiological lipid, dispersed in water or in an aqueous surfactant solution. SLN combine advantages of polymeric nanoparticles, fat emulsions and liposomes but simultaneously avoid some of their disadvantages. They are biodegradable, biocompatible and non-toxic. Nanoparticle drug delivery, utilizing biodegradable and absorbable lipids, provides a more efficient, less risky solution to many drug delivery challenges (Mehnert and Mader, 2001). Proposed advantages of SLN include possibility of controlled drug release and drug targeting, increased drug stability, high drug payload, incorporation of both lipophilic and hydrophilic drugs, no biotoxicity of the carrier, avoidance of organic solvents, ease of scale up and sterilization. Disadvantages include low drug-loading capacities, the presence of alternative colloidal structures (micelles, liposomes, mixed micelles, drug nanocrystals), the complexity of the physical state of the lipid (transformation between different modifications, possibility of supercooled melts) which cause stability problems during storage or administration (gelation, particle size increase, drug expulsion) (Mehnert and Mader, 2001).

1.2.4. Methods for the Preparation of Nanoparticles

Various methods are used for the preparation of nanoparticles. The selection of appropriate method for the preparation of nanoparticles depends on the physicochemical characters of the polymer and the drug to be loaded. Preparation techniques determine the

structural characters, in vitro release profile and biodistribution of these polymeric delivery systems. Two types of systems with different inner structures are possible.

1. Matrix type system consisting of an entanglement of polymer units in which drug is dispersed - nanospheres.
2. Reservoir type system comprised of an oily core surrounded by polymeric membrane - nanocapsules.

The main characteristic of colloidal dispersions is their extremely large interface area between the dispersed phase and the continuous phase. Production of nanoparticles relies essentially upon their kinetic stabilization, and effective recovery of the final formulation. Several methods have been developed by researchers to obtain particles in the nanosize range.

a) Emulsion and Solvent Evaporation Method

This is one of the most frequently used methods for preparation of nanoparticles. The preformed polymer and drug are first dissolved in a water-immiscible organic solvent, which is then emulsified in an aqueous solution, containing stabilizer. The emulsification is brought about by subsequent exposure to a high-energy source such as an ultrasonic device, homogenizer, or colloid mill. The organic phase is evaporated under reduced pressure or vacuum, resulting in the formation of fine aqueous dispersion of nanoparticles. The nanoparticles are collected by ultracentrifugation and washed with distilled water to remove stabilizer residues or any free drug and lyophilized for storage (Guarrero et al, 1998; Song et al, 1997).

Modification of this method, known as high-pressure emulsification and solvent evaporation, has been reported by Jaiswal et al, (2004). This method involves preparation of a coarse emulsion, which is then subjected to homogenization under high-pressure followed by overnight stirring to remove organic solvent. This method has the advantages of obtaining small, mono-dispersed nanoparticles with high encapsulation efficiency and reproducibility.

The emulsion evaporation method can be used for preparation of particles with sizes varying from a few nanometers to micrometers by controlling the stirring rates and conditions showing high efficiency in incorporation of lipophilic drugs (Mu and Feng, 2003a; Feng et al, 2004). Variables in this method may include volume ratio of organic phase and aqueous phase, concentration of polymer and drug in organic phase and aqueous phase, presence of oil soluble surfactant in organic phase, stabilizer/surfactant in organic/aqueous phase, saturation solubility of drug in aqueous phase, and stirring speed

(Whateley, 1993). Polymers normally used in this method are polysaccharides, PLA, PLGA, poly (glycolic acid) (PGA), and other synthetic polymers such as poly (ethylene glycol) (PEG) copolymers.

b) Double-Emulsion and Evaporation Method

The emulsion and evaporation method suffers from the limitation of poor entrapment of hydrophilic drugs because of their diffusion and partitioning from the dispersed oil phase into the aqueous continuous phase. Therefore, to encapsulate hydrophilic drugs and proteins, the double-emulsion technique is employed, which involves the addition of aqueous drug solution to organic polymer solution under vigorous stirring to form a w/o emulsion. This w/o emulsion is added into second aqueous phase containing stabilizer with stirring to form the w/o/w emulsion. The emulsion is then subjected to solvent removal by evaporation under reduced pressure, and nanoparticles can be isolated by centrifugation at high speed. The formed nanoparticles must be thoroughly washed before lyophilization (Vandervoort and Ludwig, 2002).

Several variables that affect the characteristics of nanoparticles formed by this method include the amount of hydrophilic drug to be incorporated, the concentration of stabilizer used, the polymer concentration, and the volume of external aqueous phase. The double emulsion technique used by Lamprecht et al, (1999) was found to give high encapsulation efficiency of the protein studies. Using propranolol HCl as a model drug, it has been shown that the double-emulsion/evaporation method can be applied for preparation of nanoparticles loaded with both low molecular weight and hydrophilic drugs (Ubrich et al, 2004).

c) Salting-Out Method

This involves the addition of polymer and drug solution in a slightly water-miscible solvent such as acetone to an aqueous solution containing the salting-out agent and a colloidal stabilizer under vigorous mechanical stirring. When this o/w emulsion is diluted with a sufficient volume of water, it induces the formation of nanoparticles by enhancing the diffusion of acetone into the aqueous phase. The remaining solvent and salting-out agent are eliminated by cross-flow filtration. Several manufacturing parameters can be varied including stirring rate, internal/ external phase ratio, concentration of polymer in the organic phase, type of electrolyte, concentration, and type of stabilizer in the aqueous phase (Allemann et al, 1992).

d) Emulsion-Diffusion Method

This is another widely used method involving polymer solution in partially water miscible solvent (such as ethyl acetate, benzyl alcohol, propylene carbonate) pre-saturated with water, added to an aqueous solution containing stabilizer under vigorous stirring. The subsequent addition of water to the system destabilizes the equilibrium between the two phases and causes the solvent to diffuse into the external phase, resulting in reduction of the interfacial tension and in nanoparticle formation, which gradually becomes poorer in solvent. This method is a modification of the salting out procedure; it provides the advantage of avoiding the use of salts and thus eliminates the need for intensive purification steps. While this method also suffers from low entrapment efficiency of hydrophilic drugs in nanoparticles, incorporation of medium chain glyceride into aqueous solution has been found to improve the encapsulation efficiency of water-soluble drugs into nanospheres offering the advantages of simplicity, narrow particle size distribution, and ready dispersibility of the resultant particles (Takeuchi et al, 2001).

e) Solvent Displacement/Nanoprecipitation Method

With appropriate modifications, this method is suitable for producing both nanocapsules and nanospheres. Nanoprecipitation method is usually employed to incorporate lipophilic drugs into the carriers based on the interfacial deposition of a polymer following displacement of a semi polar or a non polar solvent from a lipophilic solution (Molpeceres et al, 1996). Polymer, drug, and/or lipophilic surfactant are dissolved in a semipolar water miscible solvent, such as acetone or ethanol. The solution is then poured or injected into an aqueous solution containing stabilizer under magnetic stirring. Nanoparticles are formed instantaneously by rapid solvent diffusion. The solvent is then removed from the suspension under reduced pressure. The rate of addition of the organic phase into the aqueous phase affects the particle size. It was observed that a decrease in both particle size and drug entrapment occurs as the rate of mixing of the two phases increases. This method gave relatively narrow particle size distribution for different formulations evaluated.

Nanoprecipitation method is well suited for most of the poorly water soluble drugs. Nanospheres size, drug release kinetics and yield were shown to be effectively controlled by readily adjustable preparation parameters. Adjusting polymer concentration in the organic phase was found to be useful in production of smaller sized nanospheres, though restricted to a limited range of the polymer to drug ratio. Therefore it is desirable to identify and characterize additional tools for nanospheres size control (Chorny et al, 2002).

The drug loading efficiency was found to be lower for the hydrophilic drugs than lipophilic drugs in this method, because of their poor interaction with the polymer leading to diffusion of the drug, from the polymer in the organic phase, to the external aqueous environment, although exceptions were found, as seen in case of proteins and peptides. Improved bioavailability of proteins and peptides was demonstrated using PLGA nanoparticles by the nanoprecipitation method (Barichello et al, 1999). Govender et al, (1999) showed improved incorporation of the water soluble drug, procaine hydrochloride into PLGA nanoparticles by increasing pH of the aqueous phase and replacing procaine hydrochloride by procaine dihydrate base. The method of solvent displacement allows the production of a large variety of carriers such as nanospheres, nanocapsules, liposomes, and nanoemulsions (Bala et al, 2004).

Important parameters, which affect the final formulation, are the concentration of the polymers in the organic phase, the ratio between the phases, and their nature. However, few reports were presented concerning the influence of molecular weight of the polymer, nature of the oil phase (interfacial tension and viscosity), type and concentration of surfactants on the size, polydispersity, surface charge, heterogeneity, and structure of nanocapsule formed by solvent displacement process (Mosqueira et al, 2000).

f) Polymerization Methods

Nanoparticles can also be prepared by in situ polymerization of monomers. PACA, being biodegradable, has been used as tissue adhesives in surgery since these are well tolerated in vivo (Pani et al, 1968). This has prompted intense research activity to study polymerization reactions.

Couvreur et al, (1979a) reported the production of nanoparticles (~ 200 nm diameter) by polymerizing mechanically the dispersed methyl or ethyl cyanoacrylate in aqueous acidic medium in the presence of polysorbate-20 as a surfactant without irradiation or an initiator. The cyano acrylic monomer is added to an aqueous solution of a surface active agent (polymerization medium) under vigorous mechanical stirring to polymerize alkyl cyanoacrylate at ambient temperature. Drug is dissolved in the polymerization medium either before the addition of the monomer or at the end of the polymerization reaction. The nanoparticle suspension is then purified by ultracentrifugation or by re-suspending the particles in an isotonic surfactant free medium.

To produce stable nanoparticles by this method, polymerization must be carried out in an acidic medium (pH 1.0-3.5). After dispersing the monomer in an aqueous acidic medium containing surfactant and stabilizer, polymerization is continued for 3 to 4 hrs by

increasing the pH of the medium to obtain the desired products. During polymerization, various stabilizers like dextran-70, 40 and 10, poloxamer-188, 184, 237, etc are added. In addition, some surfactants like polysorbate-20, 40 or 80 are also used. Particle size and molecular mass of these nanoparticles depend upon the type and concentration of the stabilizer and/or surfactant used (Couvreur et al, 1979a). The size and molecular mass of nanoparticles depend upon the pH of the polymerization medium, but nanoparticle production is not possible above a pH of 3.0, probably due to the aggregation and stepwise molecular mass increase at lower pH. Other factors that influence the formation of nanoparticles include the concentration of monomer and the speed of stirring (Behan et al, 1999).

Ethyl-2-ethoxycarbonylmethylenoxycarbonyl acrylate, a new derivative of poly (methylidene malonate) is prepared and used for nanoparticle formation. Nanoparticles from these monomers were prepared by the same methods as those adopted for the preparation of PACA nanoparticles by anionic polymerization. The pH of the polymerization medium critically influenced the physicochemical properties of nanoparticles, but the minimum sized nanoparticles were produced in the pH range of 5.5-6.0 when compared to pH 2.0 and pH 7.6 for the poly (butyl cyanoacrylate) (PBCA) and poly (methylidene malonate), respectively (Lescure et al, 1994).

g) Hydrophilic Polymers in the Preparation of Nanoparticles

Other than the commonly used synthetic hydrophobic polymers, active research is now focused on the preparation of nanoparticles using hydrophilic polymers like chitosan, sodium alginate, gelatin, etc. Several hydrophobic-hydrophilic carriers having limited protein-loading capacity have been prepared by using organic solvents (Gref et al, 1994).

Calvo et al, (1997) have reported a method to prepare hydrophilic chitosan nanoparticles. The preparation method involves ionic gelation, with a mixture of two aqueous phases, of which one contains chitosan and a diblock copolymer of ethylene oxide (EO), and the other contains a polyanion sodium tri polyphosphate (TPP). In this method, the positively charged amino group of chitosan interacts with the negatively charged TPP. The size (200-1000 nm) and zeta potential (120 mV and 160 mV) of the nanoparticles produced were modulated by varying the composition of chitosan with the PEO-PPO diblock polymer. These nanoparticles have shown good association with proteins, such as bovine serum albumin, tetanus toxoid and diphtheria toxoid (Calvo et al, 1997), insulin (Fernandez-urrusuno et al, 1999) as well as oligonucleotide (Calvo et al, 1998).

The complex coacervation technique was also used to prepare the DNA-gelatin nanoparticles (Truong-Le 1998). The chitosan nanoparticles are proved to be better carriers than the gelatin-based nanoparticles for loading the immunological and antineoplastic proteins (Tian and Groves 1999). The chitosan nanoparticles were also produced by the emulsion coacervation method (Tokumitsu et al, 1999). In this method, chitosan and the drug to be loaded were dissolved in water and water-in-oil emulsion prepared in liquid paraffin using an emulsifying agent. To this stable emulsion, another emulsion of sodium hydroxide (NaOH) in liquid paraffin was added. When in contact with NaOH, chitosan nanoparticles were produced by the coacervation of the polymer.

Magnetic nanoparticles were prepared by incorporating iron oxide in albumin and/or dextran at neutral pH. These nanoparticles altered the pattern of uptake (Berry et al, 2004). Nanoparticles were prepared by gelation of alginate solutions with calcium ions. After strengthening the resulting microgels with poly (L-lysine), nanoparticles of well defined sizes that presented an unusual high surface hydrophilicity were obtained. Alginate-based nanoparticles were also developed and used for the delivery of oligonucleotides (Vautheir et al, 1998).

1.2.5. Characterization of Nanoparticles

As any other dosage form intended to be used in medicine, nanoparticulate formulations are also required to be characterized and evaluated. Nanoparticles are usually characterized in terms of their size, morphology, drug content, and in vitro drug release. The determination of these properties is of great relevance for quality control as well as evaluating the influence of process parameters on the resulting formulation and their ultimate efficacy. In addition, to these pharmaceutical considerations, a major challenge is to establish a correlation between the physicochemical properties of the systems and their ability to make the drug available in blood and sites of action. A wide range of techniques is available for a comprehensive physicochemical examination of nanoparticle characters. There are many sensitive techniques for characterizing nanoparticles, depending upon the parameter being looked at; laser light scattering or photon correlation spectroscopy (PCS) for particle size and size distribution; scanning electron microscopy (SEM), transmission electron microscopy (TEM), and atomic force microscopy (AFM) for morphological properties; X-ray photoelectron spectroscopy (XPS), fourier transform infrared spectroscopy (FTIR), nuclear magnetic resonance spectroscopy (NMR) for surface analysis; and thermo gravimetric analysis (TGA), X ray diffraction, differential scanning calorimetry (DSC) to study crystalline behavior; size exclusion chromatography (SEC), hydrophobic

interaction chromatography (HIC) for polymer characterization (Figure 2). Parameters such as density, molecular weight, and crystallinity affect release and degradation properties, whereas surface charge, hydrophilicity, and hydrophobicity signi?cantly in?uence interaction with the biological environment.

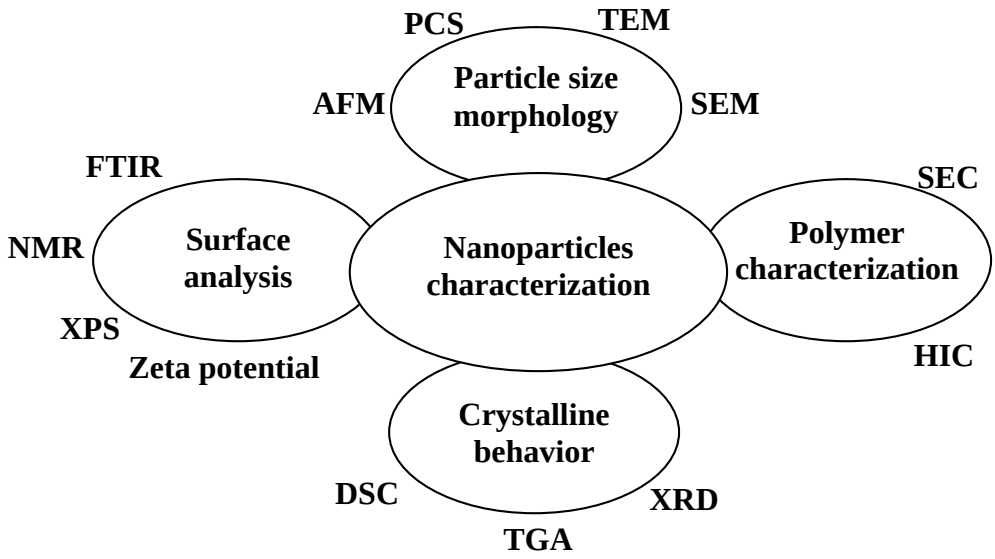

Figure 2: Various techniques available to characterize nanoparticles (Bala et al, 2004).

a) Morphology and Size Distribution

Particle size distribution and morphology are the most important parameters of characterization of nanoparticles. Morphology and size are measured by electron microscopy, AFM, freeze fracture microscopy etc., Two main techniques are used to determine the particle size distribution of nanoparticles include PCS and laser diffraction (LD). The Coulter Counter method is also used some times to measure particle size. PCS is a good tool to characterize nanoparticles, but it is not able to detect larger particles. They can be visualized by means of LD measurements. This method is based on the dependence of the diffraction angle on the particle radius. Smaller particles cause more intense scattering at high angles compared to the larger ones. A clear advantage of LD is the coverage of a broad size range from the nanometer to the lower millimeter range.

The mean size and width of distribution (polydispersity index) is typically determined by PCS (Muller and Muller 1984). The measuring range of PCS is limited to approximately 3 nm-3 mm. The LD data are volume data; typical characterization parameters are the diameters 50, 90, 95, and 99% (i.e. a diameter of 99% means that 99% of the volume of the particles is below the given size in micrometers) (Muller et al, 2001).

Electron microscopy helps in morphological characterization of nanoparticles. It covers SEM, TEM. It provides, in contrast to PCS and LD, direct information on the

particle shape. SEM is becoming the analytical method of choice among researchers in micro and nanoparticle development. The possibility to revisit the results and interpret the data using the real images of the particles provides scientists with a much better and faster understanding of the product under investigation. Three primary benefits of using SEM are the capabilities for image analysis, a wide analysis range from millimeter to nanometer scale, the ability to provide shape information (Lemarchand et al, 2003). TEM, with or without staining, is used for particles size determination. TEM was found useful in studying distribution of PLGA nanoparticles in cells and tissues using 6-coumarin as a fluorescent marker, osmium tetroxide as an electron microscopy marker and bovine serum albumin as a model protein (Panyam et al, 2003).

AFM is an advanced method for characterization of nanoparticles. AFM is attracting increasing attention as it offers the capability of 3D visualization. This technique utilizes the force acting between a surface and a probing tip resulting in a spatial resolution of up to 0.01 nm for imaging. Striking advantages of AFM are the real time investigation, simplicity of sample preparation and that the sample does not need to be conductive (Mehnert and Mader, 2001). Therefore, it has the potential for the direct analysis of the originally hydrated, solvent containing samples. It provides both quantitative and qualitative information on many physical properties, including size, surface area and volume of distribution (Dubes et al, 2003).

b) Surface Charge

The nature and intensity of the surface charge of nanoparticles is very important as it determines their interaction with the biological environment as well as their electrostatic interaction with bioactive compounds. The surface charge of nanoparticles in particular can be determined by measuring the particle velocity in an electric field. Laser light scattering technique i.e. laser Doppler anemometry has become available as fast and high resolution technique for the determination of nanoparticle velocities (Panagi et al, 2003). The measurement of the zeta potential allows for predictions about the storage stability of colloidal dispersion. High zeta potential values, either positive or negative, should be achieved in order to ensure stability and avoid aggregation of the particles. The extent of surface hydrophobicity can then be predicted from the values of zeta potential. These values can be altered by varying stabilizer concentration or by surface modification (Soppimath et al, 2001).

c) Crystallinity

The physical state of both drug and polymer are important because this will have an influence in the in vitro and in vivo release characteristics of the drug. The crystalline behavior of the polymeric nanoparticles is studied using X-ray diffraction (XRD) and thermo analytical methods such as DSC and differential thermal analysis (DTA) (Oh et al, 1999). DSC thermograms depict the phase transition temperatures of pure material and drug loaded nanoparticles, revealing the physical strength of the polymer. It also depicts the effect of various solvents and stabilizers on these transition temperatures. Different drug/polymer combinations may coexist in the polymeric carriers, such as amorphous drug in either an amorphous or a crystalline polymer and crystalline drug in either an amorphous or a crystalline polymer. DSC and XRD techniques are often combined to get useful information on the structural characteristics of both drugs and polymers. The XRD pattern of PLGA nanoparticles containing ciprofloxacin HCL revealed that the ciprofloxacin, which was initially crystalline powder, was present in an amorphous state in nanoparticles (Dillen et al, 2004).

d) Drug Loading

A successful nanoparticulate system may be the one, which has a high loading capacity to reduce the quantity of the carrier required for administration. Drug loading into the nanoparticles is achieved by two methods: one, by incorporating the drug at the time of nanoparticle production or secondly, by adsorbing the drug after the formation of nanoparticles by incubating them in the drug solution. It is thus evident that a large amount of drug can be entrapped by the first method when compared to the secondn (Alenso et al, 1991, Ueda et al, 1998). Adsorption isotherms for the nanoparticulate drug delivery system give vital information on the best possible formulation, the drug binding capacity onto the surface of nanoparticles and the amount of drug adsorbed. For instance, Couvreur et al, (1979b) reported the adsorption of two antineoplastic drugs, dactinomycin and methotrexate onto biodegradable poly (methylcyanoacrylate) and poly (ethylcyanoacrylate). It was observed that methotrexate was bound to the nanoparticles to a lesser extent than dactinomycin. Generally, in the case of PACA, it is observed that longer the alkyl chain length higher the affinity for the drugs. The capacity of adsorption is thus related to the hydrophobicity of the polymer and the specific area of the nanoparticles (Couvreur et al, 1979a). In case of entrapment method, an increase in concentration of the monomer increases the association of drug, but a reverse trend is observed with the drug concentration

in the dispersed solution (Radwan, 1995). These findings suggest that there is a need to optimize the amount of monomer to be used for the drug entrapment.

The type of surface active materials and stabilizers has an effect on drug loading. Chukwu et al, (1999) studied the adsorption of different psychopharmacological agents onto nanoparticles of poly (isobutylcyanoacrylate), (PIBCA), in the pH range between 2.0 and 7.4. Adsorption of drugs onto nanoparticles followed the Langmuir mechanism. In addition to adsorption and incorporation, a new method of drug loading for the water soluble drugs with high entrapment efficiency was proposed in which drug was chemically conjugated into nanoparticles (Yoo et al, 1999). In this study, doxorubicin is conjugated with PLGA. PEG conjugates (PEGylation) of drugs are also used now a days.

e) In vitro Drug Release

Drug release from nanoparticles and subsequent biodegradation are important for developing the successful formulations. The release rate of drug from nanoparticles depend upon: (i) desorption of the surface-bound /adsorbed drug; (ii) diffusion through the nanoparticle matrix; (iii) diffusion through the nanocapsules polymer wall; iv) nanoparticle matrix erosion; and (v) combined erosion and diffusion process. Thus, diffusion and biodegradation govern the process of drug release. Methods to study the in vitro release are: (i) side-by-side diffusion cells with artificial or biological membranes; (ii) dialysis bag diffusion technique; (iii) reverse dialysis sac technique; (iv) ultra-centrifugation; (v) ultra-filtration; or (vi) centrifugal ultra-filtration technique.

Despite the continuous efforts in this direction, there are still some technical difficulties to study in vitro drug release from nanoparticles (Washington, 1990; Magenheim and Benita 1991). These are attributed to the separation of nanoparticles from the release media. In order to separate nanoparticles and avoid the tedious and time-consuming separation techniques, dialysis has been used; here, the suspension of nanoparticles is added to the dialysis bags/ tubes of different molecular mass cut-off. These bags are then incubated in the dissolution medium (Fresta et al, 1995). Another technique involves the use of a diffusion cell consisting of donor and acceptor compartments; this technique was used to separate through the artificial / biological membranes. In this method, kinetic study was not performed under the perfect sink conditions, because the nanoparticles were not directly diluted in the release media, but were separated from the release media through the membrane. Thus, the amount of drug in the release media did not reflect the real amount released (Cavallaro et al, 1994). In order to avoid the enclosure of nanoparticles in the dialysis bag, Leavy and Benita, (1990) used a reverse dialysis technique for the O/W

emulsion. In this method, nanoparticles were added directly into the dissolution medium. Calvo et al, (1996) adopted the same technique for the evaluation of nanoparticles including nanocapsules and nanoemulsions. However, the method is not very sensitive for studying the rapid release formulations; but can only be used for the release of formulations having the release time longer than 1 h.

Release profiles of the drugs from nanoparticles depend upon the nature of the delivery system. In the case of matrix device, drug is uniformly distributed / dissolved in the matrix and the release occurs by diffusion or erosion of the matrix. If the diffusion of the drug is faster than matrix degradation, then the mechanism of drug release occurs mainly by diffusion, otherwise it depends upon degradation. Normally rapid initial release is attributed to the fraction of the drug adsorbed or weakly bound to the large surface area of the nanoparticles. Following the dilution of the dissolution media under perfect sink conditions the drug partition showed an increase due to the immediate release phase. Later, an exponential delayed release rate is observed probably due to the drug diffusion from the matrix (Niwa et al, 1993).

Release in the matrix type of nanoparticles follows the first-order kinetics. In the case of nanocapsules (reservoir-type drug delivery systems) the release occurs by diffusion of the drug from the core across the polymeric barrier layer. Hence, theoretically, the drug release expected to follow the zero-order kinetics. Calvo et al, (1996) obtained almost the similar release profiles for indomethacin from both nanoparticles and nanocapsules. This indicated that the polymer coating does not show any barrier properties for the drug release. The drug release from the nanocapsule takes place mainly by the partitioning of the drug; however, the main factor controlling the release is the volume of the aqueous medium.

Lu et al, (1999) reported that the release of bovine serum albumin from PLA nanocapsule depends upon the molecular mass of the polymer, which indicates that the release may not occur by partitioning of the drug, but may be due to diffusion across the polymer coating. The method of drug incorporation into nanoparticles has also shown an effect on drug release. Fresta et al, (1995) reported a higher initial burst effect up to 60-70% for the nanoparticles loaded with drug by adsorption. In case of incorporation method, the burst effect is less and the remaining drug release is quite slow. This study demonstrated that the incorporation technique has shown better sustained release characteristics. When the drug is chemically conjugated with PLGA nanoparticles, the release took place over 25 days, whereas with those nanoparticles containing un-conjugated free drug, a rapid release in about 5 days occurred. Here, the controlled release properties have been attributed to chemical degradation of the conjugated PLGA, which permitted water solubilization and

subsequent release of the drug-conjugated PLGA oligomers into the medium (Yoo et al, 1999). In case of drug release from hydrogel nanoparticles, release occurs mainly due to swelling, which can be controlled by either adding the hydrophilic functional groups or by changing cross-linking of the matrix.

1.2.6. Nanoparticles for Delivery of Anticancer Drugs

One of the most promising applications of nanoparticles is their use as carriers for anticancer drugs. Interestingly, nanoparticles exhibited a significant tendency to accumulate in a number of tumors after intravenous administration. This particular behavior has been related to the frequently observed high endocytic activity of cancer cells. In addition, some tumors have been shown to exhibit an increased vascular permeability, which may favor the accessibility of nanoparticles to extra vascular tumor cells.

The binding of a variety of anticancer drugs (e.g., doxorubicin, 5-fluorouracil, dactinomycin, and methotrexate), immonomodulators (muramyl dipeptide-L-analyl-cholesterol) or antisense oligonucleotides mainly to polyalkylcyanoacrylaete (PACA) or albumin nanoparticles enhanced their efficacy against experimental tumors in comparison to free drugs. Doxorubicin, chemically conjugated to the terminal end group of PLGA by an ester linkage to form nanoparticles, exhibited sustained release over 1 month. Also it was found that the released fraction of doxorubicin had similar cytotoxic activity, comparable to that of free doxorubicin (Yoo et al, 2000). Paclitaxel, one of the best naturally occurring antineoplastic drugs, has posed challenges in clinical administration resulting from its poor solubility and low permeability associated with mucosal P-glycoprotein (PGP) efflux. Mu and Feng, (2001) formulated a novel PLGA nanoparticle formulation of taxol containing vitamin E d-α-tocopheryl polyethylene glycol 1000 succinate (vitamin E TPGS) as emulsifier. Later they showed that the incorporation of TPGS has improved drug encapsulation, size distribution, morphological and physicochemical properties, and in vitro drug release (Mu and Feng 2003a).

In a number of cases a reduction of the general toxicity of anticancer drugs was also demonstrated. This is usually attributed to the modification of the drug pharmacokinetic parameters specifically the distribution profile of the drug-carrier it self. When associated with nanoparticles, drugs concentrate mainly in liver and spleen and are precluded to exert their acute toxicity in other organs (Leroux et al, 1996).

One of the promising applications of anticancer drug loaded nanoparticles may be their use in the treatment of hepatic metastases. The kuppfer cells mainly take up intravenously injected nanoparticles. These cells later act as reservoir for the drug, allowing

its massive and prolonged diffusion into the neighboring neoplastic cells. Besides the use of this passive targeting, the incorporation of magnetic particles into albumin nanoparticles and subsequent electromagnetic guidance has been shown to improve the antimetastatic potential of the anticancer drug carrier by facilitating the access to extravascular tumors (Kreuter, 1994).

New and attractive possibilities have recently become available with the development of polyethylene oxide (PEO) surface modified nanoparticles. In the recent study involving PLA nanoparticles loaded with a photoactive sensitizer ($ZnPcF_{16}$), coating the nanoparticles with PEO 20,000 by adsorption was shown to significantly increase their blood circulation time and in turn their tumor accumulation in mice. Efficient photodynamic therapy could be performed, as demonstrated by significant tumor regression following light treatment (Allemann et al, 1996).

1.2.7. Improving Oral Bioavailability

Nanoparticles have been employed as oral drug carriers with several objectives like improvement of the bioavailability of drugs with poor absorption characteristics, delivery of vaccine antigens to the gut associated lymphatic tissue (GALT), controlled or sustained release of drug, reduction of the gastrointestinal (GI) mucosa irritation caused by drugs, assurance of the stability of drugs in the gastro intestinal tract (GIT).

Some workers have supported the idea that nanoparticles may improve the bioavailability of peptide or protein drugs administered orally. The rationale for this approach is that nanoparticles can protect these labile drugs from extensive enzyme degradation in the GIT and enhance their absorption by optimizing their interaction with the absorption site in the gut wall or by directly transporting them through the intestinal mucosa to the systemic circulation. Precursors in this field, Maincent et al, (1986) reported that the relative per oral bioavailability of vincamine in rabbits was considerably increased when this drug was associated with PACA nanoparticles. The bioavailability of vincamine was about 25% when administered in aqueous solution to rabbits. After oral administration of vincamine adsorbed on poly (hexylcyanoacrylate) (PHCA) nanoparticles, the bioavailability reached 40%, due to a prolonged period of contact of the drug delivery system with the mucosa.

The pharmacokinetics of several drugs, after oral administration, has been improved by means of nanoparticles. Most of these studies have been achieved with conventional formulations, which mean that the carriers were generally not specifically designed for improving the bioadhesion performances of the particles. Later, Michel et al, (1991) found

that insulin encapsulated in PACA nanocapsules reduced glycaemia by 50-60%, whereas free insulin did not affect glycaemia when administered orally to diabetic rats. This effect was attributed to the protection of insulin from proteolytic degradation. It was also suggested that this effect could result from the retarded passage of intact nanocapsules through rat mucosa.

In fact, the most probable mechanism by which nanoparticles increase the oral bioavailability of drugs is by protecting them against degradation and by releasing them in GIT in a way that favors their absorption. In a study the per oral efficiency of PACA nanoparticles loaded with vincamine was attributed to the bioadhesive behavior of particles, allowing the slow release of the drug close to its absorption window and its subsequent diffusion into the vascular compartment (Pimienta et al, 1990).

Matrix tablets with various biphasic release patterns can be prepared by altering the molecular weight or copolymer ratio of PLGA. Altering the tablet weight and size changed the release pattern, but the drug release rate was found to be dependent mainly on the surface area of matrix tablets. Thus, PLGA nanoparticles provide long acting matrix tablets by direct compression with the drug and the drug release rate could be controlled simply by choosing the polymer species, mixing ratio, and surface area of the matrix tablets (Murakami et al, 2000).

Majority of studies, however, deal with the stability aspects of the nanoparticle associated drugs against challenges from luminal proteases in the GIT. Polyalkylcyanoacrylates nanoparticles and nanocapsules were developed as peptide carriers for insulin and growth hormone releasing factor. PACA nanoparticles were also proposed as possible drug delivery system for cyclosporine A, a cyclic oligopeptide having a specific immunosuppressive activity. Attempts were made for delivery of proteins and peptides especially using biodegradable nanoparticles (PLA/PLG nanoparticles).

1.2.8. Delivery of Vaccines

As previously mentioned, although it is restricted, particulate uptake does take place in the intestinal mucosa. This uptake was shown to occur mainly in the lymphoid regions of the intestine called the Peyer's patches, through the action of specialized epithelial cells, called M cells. These cells play a determining role in the sampling and transport of luminal antigens into the lymphoid tissues for immunologic surveillance and initiation of appropriate immunologic response. It has been postulated that the use of nanoparticles would be profitable for the oral delivery of antigens because of their ability to control the

release of proteins and to protect them from enzymatic degradation in the GIT (Florence, 1997).

1.2.9. Other Applications of Nanoparticles

Nanoparticles can be utilized to better delivery of several other drugs also including antiinfectious agents. Most antiinfectious agents display limited efficacies against intracellular infections. Because most of the cells that are frequently infected include phagocytic cells, it was suggested that nanoparticles should be of great interest to improve antiinfectious chemotherapy. This approach has been extensively investigated with PACA nanoparticles loaded with ampicillin as a model of acidic antibiotic (Pinto-Alphandary et al, 1994). The efficacy of this formulation against *Listeria monocytogenes* and *Salmonella typhimurium* infections has been demonstrated in numerous studies, both in cell cultures and in mouse models. The effective up take of ampicillin loaded nanoparticles as demonstrated in murine macrophages by confocal and transmission electron microscopy studies. In addition, the authors reported that the nanoparticles were localized in the same vacuoles as the infecting bacteria.

Nanoparticles also hold promise as drug carriers for the treatment of parasitic infections such as visceral leishmaniasis. Most of the drugs (primaquine, dehydroemetine) used to treat this infection exert, apart from the desired activity, very toxic and adverse side effects. The binding of these drugs to various types of nanoparticles was shown to significantly increase their therapeutic index as a result of passive targeting to the mono phagocytic system (MPS) (Kreuter 1994).

In the field of viral infections, a very important challenge is the targeting of human immunodeficiency virus (HIV) infected macrophages. It is now well established that macrophages of MPS play an important role in the immunopathogenesis of HIV infection by acting as a reservoir for the virus and its dissemination throughout the body. Therefore nanoparticles represent an interesting system for the specific transport of antiviral agents displaying poor selectivity and/or short plasma half life. PACA nanoparticles loaded with the protease inhibitor saquinavir were shown to be effective in HIV infected human macrophage cultures (Bender et al, 1996). In another study azidothymidine bound to PACA nanoparticles was successfully targeted into macrophage rich organ in rats (Lobenberg and Kreuter, 1996). These initial positive results have suggested that the new perspectives in the treatment of HIV related diseases might be open. Substances whose development has been halted because of their unfavorable pharmacokinetic properties could be made efficient and available, using nanoparticle technology.

Besides the previously described main applications, nanoparticles can be administered by the intramuscular and subcutaneous routes in addition to intravenous and per oral routes. These routes have been so far rarely employed with nanoparticles; they may present some advantages in the attempt to prolong the plasma level of drugs, to protect from enzymatic degradation or to reduce their irritant effect when applied intramuscularly. Depending on the rate of release, which is desired for the drug, PACA or polylactide (PLA, PLGA) nanoparticles appear to be particularly suitable for those routes, due to their particular and controllable degradation properties.

Another possible route of administration for nanoparticles is their topical application to the eye. The use of nanoparticles by ocular route has been investigated for the treatment of chronic diseases such as glaucoma, following the observation that various types of nanoparticles tend to adhere to the ocular epithelial surface. The polymers seem to have the best potential for these applications are PLGA, PCL and PACA. They have been used in the form of either nanospheres or nanocapsules. Because of their low viscosity in suspension, these systems can be administered as easily as eye drops with the advantage of having reservoir like behavior that is able to deliver the drug progressively (Bourlais et al, 1998).

1.2.10. In vivo Fate of Nanoparticles

Nanoparticles have easy accessibility in the body and can be transported to different body sites through systemic circulation of blood. Targeting the drug through selective polymeric nanoparticles as carrier can enhance therapeutic efficacy of drugs. But like other colloidal carriers used for drug targeting, they are sometimes taken up by reticuloendothelial system (RES) such as kuppfer cells of liver and macrophages of spleen. Numerous recent investigations have been aimed at reducing RES uptake and increasing the concentrations of particulate carriers at the desired sites in the body (Moghimi and Hunter, 2001; Otsuka et al, 2003).

One of the most suitable methods of studying the biodistribution and pharmacokinetics is to label these nanoparticles with radio isotopes like technetium-99m (^{99m}Tc) and to measure their radioactivity in various tissues or to perform gamma imaging of the whole body after their administration (Babbar et al, 1991; Bhatnagar et al, 1997; Arulsudar et al, 2003). The biodistribution of radio labeled doxorubicin incorporated into PBCA nanocapsules has been reported by Harivardhan et al, (2004). Colloidal carriers incorporating gamma emitters have been prepared and injected by different routes of administration such as i.v or pulmonary route. As most of these colloids are found in the MPS after i.v administration, the potential of gamma scintigraphy techniques have been

outlined using nanoparticles labeled with Indium-111, ^{99m}Tc, Rhenium (^{188}Re) and In-Oxine (Krenning et al, 1993; Knapp et al, 1997; Virgolini et al, 2002; Forrer et al, 2004; Harivardhan et al, 2004). In these studies, the particle distribution in body was followed as a function of time.

Due to the hyper-permeability of the tumor vasculature and the lack of lymphatic drainage, blood-borne polymeric conjugate and nanoparticles are preferentially distributed in the tumor due to the enhanced permeability and retention (EPR) effect. The concentrations of polymer-drug conjugates in tumor tissues can reach levels 10-100 times higher than would be seen after administration of the free drug (Senger et al, 1983). The enhanced vascular permeability of the tumor, developed through secretion of vascular permeability factors such as bradykinin, vascular endothelial growth factor (VEGF), and nitric oxide, allows for preferential uptake and increased residence time for polymeric drugs and colloidal systems in the vicinity of the tumor mass (Maeda et al, 1998). Using PEG modified liposomes, Jain (2001a,b) has shown that the effective vascular pore size of most peripheral human tumors ranged from 200 to 600 nm in diameter, with a mean of about 400 nm. Systemically administered nanoparticles are rapidly cleared from the circulation by a process of opsonization, which is initiated by complement activation and preferential uptake of the nanoparticles by the organs of RES (Leong et al, 1998; Roy et al, 1999; Mao et al, 2001; Moghimi and Hunter, 2001; Kaul and Amiji, 2002; Li et al, 2003; Cui and Mumper, 2003). Harivardhan et al, (2004) showed in their study that greater concentrations of doxorubicin loaded PBCA nanoparticles in Dalton's lymphoma tumor bearing mice were present for enhanced period of time when compared to free doxorubicin.

For delivery to solid tumor, surface modification of nanoparticles with water soluble polymers, such as PEG affords long circulation time and passive targeting potential to the tumor mass (Otsuka et al, 2003). Surface-bound PEG chains prevent protein binding, complement activation, and preferential uptake by the RES through steric repulsion mechanism (Otsuka et al, 2003; Moghimi and Hunter, 2001).

Transport studies have shown that the intestine both in vivo and in vitro is selective in its uptake and is able to transport closely related substances at widely different rates. Absorption of polymeric nanoparticles from GIT has been extensively studied for the last two decades (Florence 1997). The factors controlling intestinal absorption of particles are now better known: size, nature of polymer, zeta potential, vehicle, coating with lectins or other adhesion factors, presence of nutrients have been determined as critical factors influencing particle uptake. Despite the amount of information, however, no clearly defined parameters can be determined to design the best carrier for oral administration of

nanospheres. Radio isotopes: Radio labeled particles have been used extensively to determine fate and the route of uptake of orally administered particles. It has been found that the size of the nanoparticles plays a key role in their adhesion to and interaction with the biological cells. The possible mechanisms for the particles to pass through the gastro intestinal (and other physiological) barriers could be (Lefevre et al, 1978; Florence, 1997)

1. Paracellular passage - particles kneading between intestinal epithelial cells due to their extremely small size (< 50 nm)
2. Endocytotic uptake - particles absorbed by intestinal enterocytes through endocytosis (particles size < 500 nm)
3. Lymphatic uptake - particles adsorbed by M cells of peyer's patches (particle size < 5 microns).

Coating the particles by appropriate bioadhesive materials such as polyvinyl alcohol (PVA), PEG, etc can greatly improve their adhesion to and absorption into intestinal cells as well as the ability to escape from the multi drug resistance pump proteins (Mu and Feng 2003b). Nanoparticles hold promise for the targeted delivery of drugs to inflamed areas of the body after administration by number of possible routes. Nanoparticles have been investigated for lymphatic targeting also. These have potential to deliver drugs to the lymph node through tissue spaces by local administration.

1.2.11. Nanoparticles for Tumor Tissue Targeting and Delivery

The association of drug loaded polymeric nanoparticles can modify the drug biodistribution profile. Once in the bloodstream, they are mainly delivered to the MPS organs such as liver, spleen, lungs and bone marrow (Grislain et al, 1983). This was demonstrated in mice treated with doxorubicin incorporated into poly (isohexylcyanoacrylate) (PIHCA) nanospheres, where higher concentrations of doxorubicin were found in the liver, spleen and lungs, as compared to the treatment with free doxorubicin (Verdun et al, 1990). At the same time, the concentration of doxorubicin in the heart and kidneys of mice were comparatively lower. When actinomycin D was adsorbed on poly (methylcyanoacrylate) (PMCA) nanospheres, it concentrated mainly in the lungs of the rats (Brasseur et al, 1980). However, when this compound was incorporated into the more slowly biodegradable poly (ethylcyanoacrylate) (PECA) nanospheres, the drug accumulated mainly in the small intestine of rats. When vinblastine was incorporated into the same PECA nanospheres, the drug concentrated highly in the spleen of rats. Thus, both the polymeric composition (type, hydrophobicity, biodegradation profile) of the nanoparticles and the associated drug (molecular weight, charge, localization in the nanospheres:

adsorbed or incorporated) has a great influence on the drug distribution pattern in the RES (Couvreur et al, 1980).

Such affinity of nanoparticles to MPS macrophages for endocytosis/phagocytosis provides an opportunity to efficiently deliver therapeutic agents to these cells, using polymeric conventional nanoparticles. This modified biodistribution can be benefitial for the chemotherapeutic treatment of MPS localized tumors like hepatocarcinoma or hepatic metastasis arising from digestive tract or gynaecological cancers, bronchopulmonary tumors, myeloma and leukemia. The increased antitumor efficacy with drugs associated with conventional nanoparticles was demonstrated on a hepatic matastases model in mice (M 5076 reticulum cell sarcoma). Doxorubicin-PIHCA nanoparticles had an improved antimetastatic efficacy, since their use resulted in a greater reduction of the number of metastases than free doxorubicin was used. Additionally, it appeared to increase the life span of the matastasis bearing mice (Brigger et al, 2002).

Since the usefulness of conventional nanoparticles is limited by their massive capture by the macrophages of the MPS after intravenous administration, other nanoparticulate devices must be considered to target tumors, which are not localized in the MPS area. A major breakthrough in the nanoparticles field consisted in using hydrophilic polymers (PEG, poloxamines, poloxamers, polysaccharides) to efficiently coat conventional nanoparticle surface (Jeon et al, 1991, Storm et al, 1995). These coating provide dynamic cloud of hydrophilic and neutral chains at the particle surface, which repel plasma proteins. Hydrophilic polymers can be introduced at the surface in two ways, either by adsorption of surfactants or by use of block or branched co polymers (Jeon et al, 1991). These Stealth nanoparticles were characterized by a prolonged half life in the blood compartment. This allows them to selectively extravasate in pathological sites, like tumors or inflamed regions with a leaky vasculature. As a result, such long-circulating nanoparticles are supposed to be able to directly target most tumors located outside the MPS regions. The size of the colloidal carriers as well as their surface characteristics are the key for the biological fate of nanoparticles, since these parameters can prevent their uptake by MPS macrophages (Gref et al, 1994; Stolnik et al, 1995).

1.2.12. Advantages of Nanoparticles

In general nanoparticles can be used to provide targeted delivery of drugs to cells and tissues, to sustain drug effect in target tissue, to improve oral bioavailability, to solubilize drugs for intra vascular delivery and to improve the stability of therapeutic agents against enzymatic degradation. Considerable progress has been made in the preparation of

well characterized nanoparticle formulations loaded with a variety of anticancer agents. The use of biodegradable materials avoids the problems related to the removal of the delivery device after drug depletion. Moreover, biodegradable matrices can provide a further control of release rates, by joining the typical diffusive mechanism with polymer degradation (Bala et al, 2004).

These are currently the most well studied drug delivery systems used in the treatment of cancer. They are being employed in the treatment of a wide variety of human malignancies. They have many other potential advantages over the corresponding free drugs like improved efficacy, reduced toxicity, favorable pharmacokinetic properties, enhanced half life, improved patient compliance, and better therapeutic efficacy (Grislain et al, 1983). In addition, encapsulation of a normally labile therapeutic agent, such as DNA, antisense oligonuclides or the lactone ring of campothecins, can protect the agent from premature degradation by enzymes in the plasma or from simple hydrolysis. Nanoparticle formulation results in substantial increase in antitumor efficacy when compared to free drug or standard chemotherapy regimens (Damge et al, 1990; Gulyaev et al, 1999). Nanoparticles, as a drug vehicle, able to target tumor tissues or cells, to a certain extent, while protecting the drug from degradation during its transport. They are being employed in the treatment of a wide variety of malignancies. Nanoparticles represent very promising carrier systems for targeting of anticancer agents to tumors. They exhibit a significant tendency to accumulate in a number of tumors after administration.

1.3. Objective of the Research

Though etoposide is a first line anticancer drug and was used in the treatment of various malignancies, but presently available formulations, like intravenous injections and soft gelatin capsules, have some drawbacks. Non-selective distribution of etoposide causes side effects. Oral formulations found to have poor bioavailability with high intra and inter patient variability in the rate and extent of etoposide absorption, due to poor solubility and dissolution.

Thus present research aims at design and development of nanoparticulate delivery system, for better delivery of etoposide in a controlled pattern for a prolonged period of time with modified and selective biodistribution profile.

Objectives of the present work were to

- Prepare etoposide loaded nanoparticles using different biodegradable and/or biocompatible polymers, alone and in combination
- Characterize the prepared nanoparticles for
    - Morphology and size distribution
    - Zeta potential and Polydispersity Index
    - Drug content and Entrapment efficiency
- Optimize various formulation parameters
- Study the in vitro release character of etoposide from the prepared nanoparticles
- Study the stability of prepared nanoparticles for optimized formulations
- Perform biodistribution and pharmacokinetic studies in mice for the Tc^{99m} labeled etoposide and nanoparticle formulations after intravenous and oral administration
- Carryout tumor uptake studies for radio labeled etoposide and formulations along with biodistribution studies. Gamma scintigraphic imaging was proposed to be used for the study
- Carryout pharmacokinetic studies on rabbits after administering radiolabeled etoposide and nanoparticle formulations through i.v and oral routes

The proposed work requires analysis and estimation of drug at different levels of sensitivity at various stages. As formulation design and characterization essentially needs a suitable and sensitive analytical method (s), it was also planned to develop and validate analytical methods for various study. Thus for preformulation, formulation characterization following methods were planned to be developed.

- UV Spectrophotometer method
- Spectrofluorimetric method
- HPLC method

References

Ajani, J.A., Takiuchi, H., 1999. Recent developments in oral chemotherapy options for gastric carcinoma. Drugs. 58, 85-90.

Alenso, M.J., Losa, C., Calvo, P., Vila-Jato, J.L., 1991. Approaches to improve the association of amikacin sulphate to poly (cyanoacrylate) nanoparticles. Int. J. Pharm. 68, 69-76.

Allemann, E., Gurny, R., Doelker, E., 1992. Preparation of aqueous polymeric nanodispersions by a reversible salting-out process: influence of process parameters on particle size. Int. J. Pharm. 87, 247-253.

Allemann, E., Gurny, R., Doelker, E., 1993. Drug loaded nanoparticles preparation methods and drug targeting issues. Eur. J. Pharm. Biopharm. 39, 173-191.

Allemann, E., Rousseau, J., Brasseur, N., Kudrevich, S.V., Lewis, K., van Lier, J.E., 1996. Photodynamic therapy of tumours with hexadecafluoro zinc phthalocynine formulated in PEG-coated poly (lactic acid) nanoparticles. Int. J. Cancer. 11, 821-824.

Arshady, R., 1991. Preparation of biodegradable microspheres and microcapsules: 2. Polylactides and related polyesters. J. Control. Release. 17, 1-22.

Arulsudar, N., Subramanian, N., Mishra, P., Sharma, R.K., Murthy, R.S.R., 2003. Preparation, characterization and biodistribution of ^{99m}Tc-labeled liposome encapsulated cyclosporine. J. Drug Targeting. 11, 187-196.

Baban, D., Seymour, L.W., 1998. Control of tumor vascular permeability. Adv. Drug Del. Rev. 34, 109-119.

Babbar, A., Kashyap, R., Chauhan, U.P., 1991. A convenient method for the preparation of 99mTc-labelled pentavalent DMSA and its evaluation as a tumour imaging agent. J. Nucl. Biol. Med. 35, 100-104.

Bala, I., Hariharan, S., Kumar, M.N., 2004. PLGA nanoparticles in drug delivery: the state of the art. Crit. Rev. Ther. Drug Carrier. Syst. 21, 387-422.

Barichello, J.M., Morishita, M., Takayama, K., Nagai, T., 1999. Absorption of insulin from Pluronic F-127 gels following subcutaneous administration in rats. Int. J. Pharm. 184, 189-198.

Behan, N., Birkinshaw, C., Clarke, N., 1999. A study of the factors affecting the formation of poly (*n*-butylcyanoacrylate) pro-nanoparticles. Proced. Intern. Symp. Control. Rel. Bioact. Mater. 26, 1134-1135.

Bender ,A.R., von Briesen, H., Kreuter, J., Duncan, I.B., Rubsamen-Waigmann, H., 1996. Efficiency of nanoparticles as a carrier system for antiviral agents in human

immunodeficiency virus-infected human monocytes/macrophages in vitro. Antimicrob. Agents. Chemother. 40, 1467-1471.

Berry, C.C., Wells, S., Charles, S., Aitchison, G., Curtis, A.S., 2004. Cell response to dextran-derivatised iron oxide nanoparticles post internalisation. Biomaterials, 25, 5405-5413.

Bhatnagar, A., Singh, A.K., Babbar, A., Soni, N.L., Singh, T., 1997. Renal imaging with 99Tc(m)-dextran. Nucl. Med. Commun. 18, 562-566.

Birnbaum, D.T., Kosmala, J.D., Henthorn, D.B., Brannon-Peppas, L., 2000. Controlled release of beta-estradiol from PLAGA microparticles: the effect of organic phase solvent on encapsulation and release. J. Control. Release. 65, 375-387.

Birrenbach, G., Speiser, P.P., 1976. Polymerized micelles and their use as adjuvants in immunology. J. Pharm. Sci. 65, 1763-1766.

Bottomley, A., 2002. The cancer patient and quality of life. The Oncologist.7, 120-125.

Bourlais, C.L., Acar, L., Zia, H., Sado, P.A., Needham, T., Leverge, R., 1998. Ophthalmic drug delivery systems--recent advances. Prog. Retin. Eye. Res. 17, 33-58.

Brasseur, F., Couvreur, P., Kante, B., Deckers-Passau, L., Roland, M., Deckers, C., Speiser, P., 1980. Actinomycin D adsorbed on polymethylcyanoacrylate nanoparticles: increased efficiency against an experimental tumor. Eur. J. Cancer. 10, 1441-1445.

Brigger, I., Dubernet, C., Couvreur, P., 2002. Nanoparticles in cancer therapy and diagnosis. Adv. Drug Del. Rev. 54, 631-651.

Calvo, P., Vila-Jato, J.L., Alonso, M.J., 1996. Comparative in vitro evaluation of several colloidal systems, nanoparticles, nanocapsules and nanoemulsions as ocular drug carriers, J. Pharm. Sci. 85, 530-536.

Calvo, P., Remunan-Lopez, C., Vila-Jato, J.L., Alonso, M.J., 1997. Novel hydrophilic chitosan and chitosan / polyethylene oxide nanoparticles as protein carriers, J. Appl. Polym. Sci. 63, 125-132.

Calvo P., Boughaba, A.S., Appel, M., Fattal, E., Alonso, M.J., Couvreur, P., 1998. Oligonucleotide-chitosan nanoparticles as new gene therapy vector, Proc. 2nd World Meeting APGI/APV Paris. 1111-1112.

Cavallaro, G., Fresta, M., Giammona, G., Puglisi, G., Villari, A., 1994. Entrapment of β-lactams antibiotics in poly ethylcyanoacrylate nanoparticles: studies on the possible in vivo application of this colloidal delivery system. Int. J. Pharm. 111, 31-41.

Chorny, M., Fishbein, I., Danenberg, H., Golomb, G., 2002. Lipophilic drug loaded nanospheres by nanoprecipitation: effect of formulation variables on size, drug recovery and release kinetics. J. Control. Release. 83, 389-400.

Chukwu, K., Ishroder, U., Sommerfeld, P., Sabel, B.A., 1999. Loading some psychopharmacologic agents onto poly (butylcyanoacrylate) nanoparticles - a means of targeting to the brain and improving therapeutic efficiency. Proced. Intern. Symp. Control. Rel. Bioact. Mater. 26, 1148-1149.

Couvreur, P., Kante, B., Roland, M., Goit, P., Bauduin, P., Speiser, P., 1979a. Polycyanoacrylate nanocapsules as potential lysosomotropic carriers: preparation, morphology and sorptive properties. J. Pharm. Pharmacol. 31, 331-332.

Couvreur, P., Kante, B., Roland, M., Speiser, P., 1979b. Adsorption of antineoplastic drugs to polyalkylcyanoacrylate nanoparticles and their release in calf serum. J. Pharm. Sci. 68, 1521-1523.

Couvreur, P., Blanco-Prieto, M.J., Puisieux, F., Roques, B., Fattal, E., 1997. Multiple emulsion technology for the design of microspheres containing peptides and oligopeptides. Adv. Drug Del. Rev. Rev. 28, 85-96.

Couvreur, P., Kante, B., Lenaerts, V., Scailteur, V., Roland, M., Speiser, P., 1980. Tissue distribution of antitumor drugs associated with polyalkylcyanoacrylate nanoparticles, J. Pharm. Sci. 69, 199-202.

Cui, Z., Mumper, R.J., 2003. Microparticles and nanoparticles as delivery systems for DNA vaccines. Crit. Rev. Ther. Drug. Carrier. Syst. 20, 103-137.

Damge, C., Michel, C., Aprahamian, M., Couvreur, P., 1988. New approach for oral administration of insulin with poly-alkycyanoacrylate nanocapsules as drug carrier. Diabetes. 37, 246-251.

Damge, C., Michel, C., Aprahamian, M., Couvreur, P., Devissaguet, J.P., 1990. Nanocapsules as carriers for oral peptide delivery. J. Control. Release. 13, 233-239.

De Rosa, G., Iomelli, R., La Rotonda, M.I., Miro, A., Quaglia, F., 2000. Influence of the co-encapsulation of different non-ionic surfactants on the properties of PLGA insulin-loaded microspheres. J. Control. Release. 69, 283-295.

DeMario, M.D., Ratain, M.J., 1999. Oral chemotherapy: rationale and future directions. J. Clin. Oncol.16, 2557-2567.

Dillen, K., Vandervoort, J., Mooter, G.Vd., Verheyden, L., Ludwig, A., 2004. Factorial design, physicochemical characterisation and activity of ciprofloxacin-PLGA nanoparticles. Int. J. Pharm. 275, 171-187.

Dubes, A., Parrot-Lopez, H., Abdelwahed, W., Degobert, G., Fessi, H., Shahgaldian, P., Coleman, A.W., 2003. Scanning electron microscopy and atomic force microscopy imaging of solid lipid nanoparticles derived from amphiphilic cyclodextrins. Eur. J. Pharm. Biopharm. 55, 279-282.

Ewesuedo, R.B., Ratain, M.J., 2004. Systemically administered drugs. In: Brown, B.M., (Ed.), Cancer drug discovery and development: Drug delivery systems in cancer therapy. Humana Press, New Jersey, pp. 3-14.

Feng, S., Huang, G., 2001. Effects of emulsifiers on the controlled release of paclitaxel (Taxol®) from nanospheres of biodegradable polymers. J. Control Release. 71, 53–69.

Feng, S.S., Chien, S., 2003. Chemotherapeutic engineering: application and further development of chemical engineering principles for chemotherapy of cancer and other diseases. Chem. Eng. Sci. 58, 4087-4114.

Feng, S.S., Mu, L., Win, K.Y., Huang, G., 2004. Nanoparticles of biodegradable polymers for clinical administration of paclitaxel. Curr. Med. Chem. 11, 413-424.

Fernandez-urrusuno, R., Calvo, P., Remunan-Lopez, C., Vila-Jato, J.L., Alonso, M.J., 1999. Enhancement of nasal absorption of polyinsulin using chitosan nanoparticles, Pharm. Res. 16, 1576-1591.

Florence, A.T., 1997. The oral absorption of micro- and nanoparticulates: neither exceptional nor unusual. Pharm. Res. 14, 259-266.

Forrer, F., Uusijarvi, H., Waldherr, C., Cremonesi, M., Bernhardt, P., Mueller-Brand, J., Maecke, H.R., 2004. A comparison of ^{111}In-DOTATOC and ^{111}In-DOTATATE: biodistribution and dosimetry in the same patients with metastatic neuroendocrine tumors. Eur. J. Nucl. Med. 31, 1257–1262.

Fresta, M., Puglisi, G., Giammona, G., Cavallaro, G., Micali, N., Furneri, P.M., 1995. Pefloxacin mesilate and ofloxacin loaded polyethylcyanoacrylate nanoparticles; characterization of the colloidal drug carrier formulation. J. Pharm. Sci. 84, 895-901.

Gabor, F., Ertl, B., Wirth, M., Mallinger, R., 1999. Ketoprofen- poly (D,L-lactic-co-glycolic acid) microspheres: influence of manufacturing parameters and type of polymer on the release characteristics. J. Microencaps. 16, 1-12.

Gorner, T., Gref, R., Michenot, D., Sommer, F., Tran, M.N., Dellacherie, E., 1999. Lidocaine-loaded biodegradable nanospheres. I. Optimization Of the drug incorporation into the polymer matrix. J. Control. Release. 22, 259-268.

Govender, T., Stolnik, S., Garnett, M.C., Illum, L., Davis, S.S., 1999. PLGA nanoparticles prepared by nanoprecipitation: Drug loading and release studies of a water soluble drug. J. Control. Release. 57, 171-185.

Gref, R., Minamitake, Y., Peracchia, M.T., Trubetskoy, V., Torchilin, V.P., Langer, R., 1994. Biodegradable long circulating polymeric nanospheres. Science. 18, 1600-1603.

Grislain, L., Couvreur, P., Lenaerts, V., Roland, M., Deprez-Decampeneere, D., Speiser, P., 1983. Pharmacokinetics and distribution of a biodegradable drug-carrier, Int. J. Pharm. 15, 335-345.

Guarrero, Q., Allemann, E., Fessi, H., Doelker, E., 1998. Preparation techniques and mechanisms of formation of biodegradable nanoparticles from preformed polymers. Drug Dev. Ind. Pharm. 24, 1113-1128.

Gulyaev, A.E., Gelperina, S.E., Skidan, I.N., Antropov, A.S., Kivman, G.Y., Kreuter, J., 1999. Significant transport of doxorubicin into the brain with polysorbate 80-coated nanoparticles. Pharm. Res. 16, 1564-1569.

Harivardhan R.L., Sharma, R.K., Murthy, R.S.R., 2004. Enhanced tumor uptake of doxorubicin loaded poly (butyl cyanoacrylate) nanoparticles in mice bearing Dalton's Lymphoma Tumor. J. Drug Targeting. 12, 443-451.

Hobbs, S.K., Monsky, W.L., Yuan, F., Roberts, W.G., Griffith, L., Torchilin, V.P., Jain, R.K., 1998. Regulation of transport pathways in tumor vessels: role of tumor type and microenvironment. Proc. Natl. Acad. Sci. USA. 95, 4607-4612.

Jain, R.K., 1987. Transport of molecules in the tumor interstitium: Review, Cancer. Res. 47, 3039-3051.

Jain, R.A., 2000. The manufacturing techniques of various drug loaded biodegradable poly (lactide-co-glycolide) (PLGA) devices. Biomaterials. 21, 2475-2490.

Jain, R.K., 2001a. Delivery of molecular medicine to solid tumors: lessons from in vivo imaging of gene expression and function. J. Control. Release. 74, 7-25.

Jain, R.K, 2001b. Delivery of molecular and cellular medicine to solid tumors. Adv. Drug Del. Rev. 46, 149-168.

Jaiswal, J., Gupta, S.K., Kreuter, J., 2004. Preparation of biodegradable cyclosporine nanoparticles by high-pressure emulsification-solvent evaporation process. J. Control. Release. 96. 169-178.

Jeon, S.I., Lee, J.H., Andrade, J.D., de Gennes, P.G., 1991. Protein surface interactions in the presence of polyethylene oxide. I. Simplified theory. J. Colloid Interface. Sci. 142, 149-158.

Jeon, H.J., Jeong, Y., Jang, M.K., Park, Y.H., Nah, J.W., 2000. Effect of solvent on the preparation of surfactant-free poly (lactide co glycolide) nanoparticles and norfloxacin release characteristics. Int. J. Pharm. 207, 99-108.

Kabanov, A., Batrakova, E.V., Alakhov, V.Y., 2002. Pluronic block copolymers for overcoming drug resistance in cancer. Adv. Drug Del. Rev. 54, 759-779.

Kaul, G., Amiji, M., 2002. Long-circulating poly (ethylene glycol)-modified gelatin nanoparticles for intracellular delivery. Pharm. Res. 19, 1061-1067.

Khin, Y.W., Si-Shen, F., 2005. Effects of particle size and surface coating on cellular uptake of polymeric nanoparticles for oral delivery of anticancer drugs. Biomaterials. 26, 2713-2722.

Knapp, F.F., Beets, A.L., Guhlke, S., Zamora, P.O., Bender, H., Palmedo,H., Biersack, H.J., 1997. Availability of rhenium-188 from the aluminabased tungsten-188/rhenium-188 generator for preparation of rhenium-188-labeled radiopharmaceuticals for cancer treatment. Anticancer Res. 17, 1783.

Krenning, E.P., Kwekkeboom, D.J., Bakker, W.H., Breeman, W.A., Kooij, P.P., Oei, H.Y., van, H.M., Postema, P.T., de, J.M., Reubi, J.C., 1993. Somatostatin receptor scintigraphy with [111In-DTPA-D-Phe1]- and [123I-Tyr3]-octreotide: the Rotterdam experience with more than 1000 patients. Eur. J. Nucl. Med. 20, 716-731.

Kreuter, J., 1994. Nanoparticles. In: Kreuter, J., (Ed.), Colloidal drug delivery systems. Marcel Dekker, New York, pp. 219-315.

Krishna, R., Mayer, L.D., 2000. Multidrug resistance (MDR) in cancer mechanisms, reversal using modulators of MDR and the role of MDR modulators in influencing the pharmacokinetics of anticancer drugs. Eur. J. Cancer. Sci. 11, 265-283.

Lamprecht, A., Ubrich, N., Perez, M.H., Lehr, C.M., Hoffman, M., Maincent, P., 1999. Biodegradable monodispersed nanoparticles prepared by pressure homogenization-emulsification. Int. J. Pharm. 184, 97-105.

Leavy, M.Y., Benita, S., 1990. Drug release from submicron O/W emulsion: A new in vitro kinetic evaluation model. Int. J. Pharm. 66, 29-37.

Lefevre, M.E., Vanderhoff, J.W., Laussue, J.A., Joel, D.D., 1978. Accumulation of 2-mm latex particles in mouse Peyer's patches during chronic latex feeding. Experimentia. 34, 120-122.

Lemarchand, C., Couvreur, P., Besnard, M., Costantini, D., Gref, R., 2003. Novel polyester-polysaccharide nanoparticles. Pharm. Res. 20, 1284-1292.

Leong, K.W., Mao, H.Q., Truong-Le, V.L., Roy, K., Walsh, S.M., August, J.T., 1998. DNA-polycation nanospheres as non-viral gene delivery vehicles. J. Control. Release. 53, 183-193.

Leroux, J.C., Doelker, E., Gurny, R., 1996. In Benita, S., (Eds.), Microencapsulation methods and industrial applications, Dekker, New York, pp. 535-575.

Lescure, F., Seguin, C., Breton, P., Bourrinet, P., Roy, D., Couvreur, P., 1994. Preparation and characterization of novel poly (methylidene malonoate)-made nanoparticles. Pharm. Res. 11, 1270-1277.

Li, Y., Ogris, M., Wagner, E., Pelisek, J., Ruffer, M., 2003. Nanoparticles bearing polyethyleneglycol-coupled transferrin as gene carriers: preparation and in vitro evaluation. Int. J. Pharm. 18, 93-101.

Links, M., Brown, R., 1999. Clinical relevance of the molecular mechanisms of resistance to anticancer drugs. Expert Rev. Mol. Med. 1, 1-21.

Lobenberg, R., Kreuter, J., 1996. Macrophage targeting of azidothymidine: a promising strategy for AIDS therapy. AIDS. Res. Hum. Retroviruses. 10, 1709-1715.

Lu, Z., Bei, J., Wang, S., 1999. A method of the preparation of polymeric nanocapsules without stabilizer. J. Control. Release. 61, 107-112.

Maeda, T., Matsumura, S., Hiranuma, H., Jikko, A., Furukawa, S., Ishida, T., Fuchihata, H., 1998. Expression of vascular endothelial growth factor in human oral squamous cell carcinoma: its association with tumour progression and gene status. J. Clin. Pathol. 51, 771-775.

Magenheim, B., Benita, S., 1991. Nanoparticle characterization: a comprehensive physicochemical approach. S.T.P. Pharm. Sci. 1, 221-224.

Maincent, P., Le Verge, R., Sado, P., Couvreur, P., De-vissaguet, J.P., 1986. Deposition kinetics and oral bioavailability of vincamine-loaded polyalkyl cyanoacrylate nanoparticles. J. Pharm. Sci. 75, 955-958.

Malingre, M.M., Beijnen, J.H., Schellens, J.H.M., 2001. Oral delivery of taxanes. Invest New Drug. 19, 155-162.

Mao, H.Q., Roy, K., Troung-Le, V.L., Janes, K.A., Lin, K.Y., Wang, Y., August, J.T., Leong, K.W., 2001. Chitosan-DNA nanoparticles as gene carriers: synthesis, characterization and transfection efficiency. J. Control. Release. 23, 399-421.

Mehnert, W., Mader, K., 2001. Solid lipid nanoparticles: Production, characterization and applications. Adv. Drug Del. Rev. 47, 165-196.

Michel, C., Aprahamian, M., Defontaine, L., Couvreur, P., Damge, C., 1991. The effect of site of administration in the gastrointestinal tract on the absorption of insulin from nanocapsules in diabetic rats. J. Pharm. Pharmacol. 43, 1-5.

Mitra, S., Gaur, U., Ghosh, P.C., Maitra, A.N., 2001. Tumour targeted delivery of encapsulated dextran-doxorubicin conjugate using chitosan nanoparticles as carrier. J. Control. Release. 74, 317-323.

Moghimi, S.M., Hunter, A.C., 2001. Capture of stealth nanoparticles by the body's defences. Crit. Rev. Ther. Drug. Carrier. Syst. 18, 527-50.

Molpeceres, J., Guzman, M., Aberturas, M.R., Chacon, M., Berges, L., 1996. Application of central composite designs to the preparation of polycaprolactone nanoparticles by solvent displacement. J Pharm Sci. 85, 206-213.

Mosqueira, V.C.F., Legrand, P., Barrat, G., 2000. Poly (D,L-Lactide) nanocapsules prepared by a solvent displacement process: Influence of the composition on physiochemical and structural properties. J. Pharm. Sci. 89, 614-626.

Mu, L., Feng, S.S., 2001. Vitamin E TPGS used as emulsifier in the solvent evaporation/extraction technique for fabrication of polymeric nanospheres for controlled release of paclitaxel (Taxol®). J. Control. Release. 80, 129-144.

Mu, L., Feng, S.S., 2003a. A novel controlled release formulation for the anticancer drug paclitaxel (Taxol®): PLGA nanoparticles containing vitamin E TPGS. J. Control. Release. 86, 33-48.

Mu, L., Feng, S.S., 2003b. PLGA/TPGS nanoparticles for controlled release of paclitaxel: effects of the emulsifier and the drug loading ratio. Pharm. Res. 20, 1864-1872.

Muller, B.W., Muller, R.H., 1984. Particle size analysis of latex suspensions and microemulsions by photon correlation spectroscopy. J. Pharm. Sci. 73, 915-918.

Muller, R.H., Jacobs, C., Kayser, O., 2001. Nanosuspensions as particulate drug formulations in therapy rationale for development and what we can expect for the future. Adv. Drug Del. Rev. 47, 3-19.

Murakami, H., Kobayashi, M., Takeuchi, H., Kawashima, Y., 2000. Utilization of poly(dl-lactide-*co*-glycolide) nanoparticles for preparation of mini-depot tablets by direct compression. J. Control. Release. 67, 29-36.

Niwa, T., Takeuchi, H., Hino, T., Kunou, N., Kawashima, Y., 1993. Preparations of biodegradable nanospheres of water-soluble and insoluble drugs with D,L-lactide / glycolide copolymer by a novel spontaneous emulsification solvent diffusion method and the drug release behavior. J. Control. Release. 25, 89-98.

O'Hara, P., Hickney, A.J., 2000. Respirable PLGA microspheres containing rifampicin for the treatment of tuberculosis: Manufacture and characterization. Pharm. Res. 17, 955-961.

Oh, I., Lee, K., Kwon, H.Y., Lee, Y.B., Shin, S.C., Chom C.S., Kim, C.K., 1999. Release of adriamycin from poly (gamma-benzyl.glutamate)/poly (ethylene oxide) nanoparticles. Int. J. Pharm. 181, 107-115.

Otsuka, H., Nagasaki, Y., Kataoka, K., 2003. PEGylated nanoparticles for biological and pharmaceutical applications. Adv. Drug Del. Rev. 24, 403-419.

Panagi, Z., Beletsi, A., Evangelatos, G., Livaniou, E., Ithakissios, D.S., Avgoustakis, K., 2003. Effect of dose on the biodistribution and pharmacokinetics of PLGA and PLGA-mPEG nanoparticles. Int. J. Pharm. 221, 143-152.

Pani, K.C., Gladieux, G., Brandes, G., Kulkarni, R.K., Leonarda, F., 1968. The degradation of *n*-butyl alpha-cyanoacrylate tissue adhesive II. Surgery. 63, 481-489.

Panyam, J., Labhasetwar, V., 2003. Dynamics of endocytosis and exocytosis of poly(D,L-lactide-co-glycolide) nanoparticles in vascular smooth muscle cells. Pharm. Res. 20, 212-220.

Panyam, J., Sahoo, S.K., Prabha, S., Bargar, T., Labhasetwar, V., 2003. Fluorescence and electron microscopy probes for cellular and tissue uptake of poly (,-lactide-*co*-glycolide) nanoparticles. Int. J. Pharm. 262, 1-11.

Pimienta, C., Lenaerts, V., Cadieux, C., Raymond, P., Juhasz, J., Simard, M.A., Jolicoeur, C., 1990. Mucoadhesion of hydroxypropylmethacrylate nanoparticles to rat intestinal ileal segments in vitro. Pharm. Res. 7, 49-53.

Pinto-Alphandary, H., Balland, O., Laurent, M., Andremont, A., Puisieux, F., Couvreur, P., 1994. Intracellular visualization of ampicillin-loaded nanoparticles in peritoneal macrophages infected in vitro with Salmonella typhimurium. Pharm. Res. 11, 38-46.

Pitt, C.G., 1990. Poly (e-caprolactone) and its copolymers. In: Chasin, M., Langer, R. (Eds.), Biodegradable Polymers as Drug Delivery Systems. Marcel Dekker, New York, pp. 71-120.

Quintanar-Guerrero, D., Allemann, E., Fessi, H., Doelker, E., 1998. Preparation techniques and mechanisms of formation of biodegradable nanoparticles from preformed polymers. Drug. Dev. Ind. Pharm. 24, 1113-1128

Radwan, M.A., 1995. In vitro evaluation of polyisobutylcyanoacrylate nanoparticles as a controlled drug carrier for theophylline. Drug. Dev. Ind. Pharm. 21, 2371-2375.

Ravi kumar, M.N.V., Kumar, N., 2001. Polymeric controlled drug delivery systems: Perspective issues and opportunities, Drug. Dev. Ind. Pharm. 27, 1-30.

Roy, K., Mao, H.Q., Huang, S.K., Leong, K.W., 1999. Oral gene delivery with chitosan-DNA nanoparticles generates immunologic protection in a murine model of peanut allergy. Nat. Med., 5, 387-391.

Sansdrap, P., Moes, A.J., 1993. Influence of manufacturing parameters on the size characteristics and release profiles of nifedipine from poly (D,L-lactide-co-glycolide) microspheres. Int. J. Pharm. 98, 157-164.

Scholes, P.D., Coombes, A.G.A., Illum, L., Davis, S.S., Watts, J.F., Ustariz, C., Vert, M., Davis, M.C., 1999. Detection and determination of surface levels of poloxamer and PVA surfactant on biodegradable nanospheres using SSIMS and XPS. Int. J. Pharm. 59, 261-278.

Senger, D.R., Galli, S.J., Dvorak, A.M., Perruzzi, C.A., Harvey, V.S., Dvorak, H.F., 1983. Tumor cells secrete a vascular permeability factor that promotes accumulation of ascites fluid. Science. 25, 983-985.

Seymour, L.W., 1992. Passive tumor targeting of soluble macroreversion molecules and drug conjugates. Crit. Rev. Ther. Drug Carrier. Syst. 9, 135-187.

Shive, M.S., Anderson, J.M., 1997. Biodegradation and biocompatibility of PLA and PLGA microspheres. Adv. Drug Del. Rev. 13, 5-24.

Song, C.X., Labhasetwar, V., Murphy, H., Qu, X., Humphrey, W.R., Shebuski, R.J., Levy, R.J., 1997. Formulation and characterization of biodegradable nanoparticles for intravascular local drug delivery. J. Control. Release. 43, 197-212.

Soppimath, K.S., Aminabhavi, T.M., Kulkarni, A.R., Rudzinski, W.E., 2001. Biodegradable polymeric nanoparticles as drug delivery devices. J. Control. Release. 70, 1-20.

Sparreboom, A., van, A.J., Mayer, U., Schinkel, A.H., Smit, J.W., Meijer, D.K., Borst, P., Nooijen, W.J., Beijnen, J.H., van, T.O., 1997. Limited oral bioavailability and active epithelial excretion of paclitaxel (Taxol) caused by P-glycoprotein in the intestine. Proc. Natl. Acad. Sci. U. S. A, 94, 2031-2035.

Stolnik, S., Illum, L., Davis, S.S., 1995. Long circulating microparticulate drug carriers. Adv. Drug. Del. Rev. 16, 195-214.

Storm, G., Belliot, S.O., Daemen, T., Lasic, D.D., 1995. Surface modification of nanoparticles to oppose uptake by the mononuclear phagocyte system. Adv. Drug. Del. Rev. 17, 31-48.

Takeuchi, H., Yamamoto, H., Kawashima, Y., 2001. Mucoadhesive nanoparticulate systems for peptide drug delivery. Adv. Drug Del. Rev. 47, 39-54.

Tian, X.X., Groves, M.J., 1999. Formulation and biological activity of antineoplastic proteoglycans derived from *Mycobacterium vaccae* in chitosan nanoparticles. J. Pharm. Pharmacol. 51, 151-157.

Tobio, M., Gref, R., Sanchez, A., Langer, R., Alonso, M.J., 1998. Stealth PLA-PEG nanoparticles as protein carriers for nasal administration. Pharm. Res. 15, 270-275.

Tokumitsu, H., Ichikawa, H., Fuukumori, Y., 1999. Chitosan-gadopentetic acid complex nanoparticles for gadolinium neutron-capture therapy of cancer: preparation by novel

emulsion-droplet coalescence technique and characterization. Pharm. Res. 16, 1830-1835.

Truong-Le, V.L., Mao, H., Walsh, S., Leong, K.W., August, J.T., 1997. Delivery of DNA vaccine using gelatin-DNA nanoparticles. Proc. Intern. Symp. Control. Rel. Bioact. Mater. 24, 39-40.

Truong-Le, V.L., August, J.T., Leong, K.W., 1998. Controlled gene delivery by DNA-gelatin nanospheres. Hum. Gene Ther. 9, 1709-1717.

Ubrich, N., Bouillot, P., Pellerin, C., Hoffman, M., Maincent, P., 2004. Preparation and characterization of propranolol hydrochloride nanoparticles: A comparative study. J. Control. Release. 291-300.

Ueda, M., Iwara, A., Kreuter, J., 1998. Influence of the preparation methods on the drying release behavior of loperamide-loaded nanoparticles. J. Microencapsulation. 15, 361-372.

Uhrich, K.E., Cannizzaro, S.M., Langer, R.S., Shakesheff, K.M., 1999. Polymeric systems for controlled drug release. Chem. Rev. 10, 3181-3198.

Van Zuylen, L., Nooter, K., Sparreboom, A., Verweij, J., 2000. Development of multidrug-resistance convertors: sense or nonsense? Invest. New Drug. 18, 205-220.

Vandervoort, J., Ludwig, A., 2002. Biocompatible stabilizers in the preparation of PLGA nanoparticles: a factorial design study. Int. J. Pharm. 238, 77-92.

Vautheir, C., Aynie, I., Couvreur, P., Fattal, E., 1998. Pharmacokinetic and tissue disposition of oligonucleotide associated with alginate nanoparticles. Proc. Intern. Symp. Control. Rel. Bioact. Mater. 25, 228-229.

Verdun, C., Brasseur, F., Vranckx, H., Couvreur, P., Roland, M., 1990. Tissue distribution of doxorubicin associated with polyhexylcyanoacrylate nanoparticles. Cancer. Chemother. Pharmacol. 26, 13-18.

Virgolini, I., Traub, T., Novotny, C., Leiner, M., Fuger, B., 2002. Experience with indium-111 and yttrium-90-labeled somatostatin analogs. Curr. Pharm. Des. 8, 1781–1787.

Wang, H.T., Schmitt, E., Flanagan, D.R., Linhardt, R.J., 1991. Influence of formulation methods on the in vitro controlled release of protein from poly(ester) microspheres. J. Control. Release. 17, 23-32.

Washington, C., 1990. Drug release from microdisperse systems. A critical review. Int. J. Pharm. 58, 1-12.

Whateley, T.L., 1993. Biodegradable microspheres for controlled drug delivery. In: Karsa, D.R, Stephenson, R.A., (Ed.), Encapsulation of controlled release. Cambridge: The Royal Society of Chemistry, pp.52-57.

Yoo, H.S., Oh, J.E., Lee, K.H., Park, T.G., 1999. Biodegradable nanoparticles containing doxorubicin-PLGA conjugate for sustained release. Pharm. Res. 16, 1114-1118.

Yoo, H.S., Lee, K.H., Oh, J.E., Park, T.G., 2000. In vitro and in vivo antitumor activities of nanoparticles based on doxorubicin-PLGA conjugates. J. Control. Release. 68, 419-431.

Yuan, F., Dellian, M., Fukumura, D., Leuning, M., Berk, D.D., Yorchilin, V.P., Jain, R.K., 1995. Vascular permeability in a human tumor xenograft: molecular size dependence and cutoff size. Cancer. Res. 55, 3752-3756.

Yuan, F., 1998. Transvascular drug delivery in solid tumors. Semin. Radiat. Oncol. 8, 164-175.

Chapter 2

Drug Profile - Etoposide

2.1. Etoposide

Etoposide is a semi synthetic derivative of epipodophyllotoxin. Several podophyllin components possess considerable antitumor activity but are considered to be unacceptable for the human use because of their side effects. Their toxicity prevents administration of doses high enough to give sufficient to give therapeutic effect. Etoposide proved to be one of the most promising compounds with significant in vitro and in vivo antineoplastic action among podophyllin components and has been clearly demonstrated to have greater efficacy in humans when used with more prolonged schedules of administration (Issell et al, 1984). Chemical structure of etoposide is given in Figure 1.

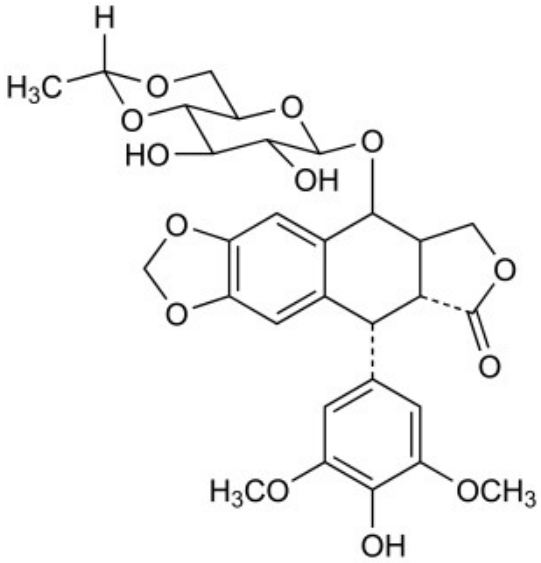

Figure 1: Structure of Etoposide.

2.2. Description

2.2.1. Nomenclature, Formula and Molecular Weight

The generic name is etoposide (33419-42-0). The chemical abstracts name is 4‘-o-demethyl-1-o-(4,6-o-ethylidene-ß-D-glucopyranosyl)epipodophyllotoxin (IUPAC). Molecular formula of etoposide is $C_{29}H_{32}O_{13}$; its molecular weight is 588.6 (Holthuis et al, 1989).

2.2.2. Appearance, Odour and Colour

Etoposide is a white, odorless and amorphous powder.

2.2.3. Melting Range

The reported melting ranges are: etoposide crystallized from methanol: 251-260ºC, etoposide as obtained from the manufacturer: 221-222 ºC (Keller-Juslen et al, 1971).

2.2.4. Optical Rotation

The optical rotation $[a]^{20}_{D}$ of etoposide crystallized from methanol in chloroform (C=0.6g/v) was -110.5 ºC (Keller-Juslen et al, 1971).

2.2.5. Differential Scanning Calorimetry

An exothermic peak appears between approx. 190 and 210 ºC, an endothermic peak between 255 and 264 ºC with a maximum at 258 ºC (Holthuis et al, 1989).

2.2.6. Solubility

It is very soluble in methanol and chloroform, slightly soluble in ethanol, and sparingly soluble in water and ether. It is made more miscible with water by means of organic solvents (Holthuis et al, 1989).

2.2.7. Dissociation Constant

The pKa of etoposide was determined spectrometrically. From the inflection in the plot of the absorbance as a function of pH, a pKa of 9.7 was found. At ionic strength of 0.1 M, the spectrometrically determined pKa was reported to be 9.8 (Beijnen et al, 1988).

2.3. Pharmacology

2.3.1. Mechanism of Action

Etoposide differs in its biological action from its parent podophyllotoxin, which is a spindle poison. Etoposide does not interact with the microtubule assembly but prevents cells from entering mitosis (Brewer et al, 1979; Loike et al, 1978). Etoposide arrests cells in the late S or G2 phase of the cell cycle and the cells accumulate in the G2 phase. Cells treated with etoposide show a rapid decrease of the mitotic index, with a simultaneous reduction of cell proliferation. Etoposide has been shown to induce double stranded break and single stranded breaks in DNA in intact cells and in nuclei, but not in purified DNA. The DNA degradation is dose dependent and temperature dependent and reversible after removal of the drug (Slevin, 1991).

Etoposide is thought to be activated in the cell nucleus by oxidation of the phenolic group to reactive intermediates. Interaction of these intermediates with DNA could also result in DNA damage. Studies indicate that type II topoisomerase is probably the intracellular target in the DNA strand breaking property of etoposide. Etoposide inhibits the cellular uptake of thymidine, uridine, adenosine and guanosine (Slevin, 1991).

2.3.2. Therapeutic Use and Clinical Activity

In clinical studies, etoposide proved to be active against a variety of tumors. In single agent therapy, etoposide is one of the most active compounds against small cell lung cancer and is primarily used in the treatment of testicular cancer, non Hodgkin lymphoma, neuroblastoma, acute myelomonocytic leukemia, acute non lymphomatic leukemia, bladder cancer, brain tumors, cervical cancer, ependyoma, germ cell tumor, gestational trophoblastic neoplasia, head and neck cancer, lung cancer, small cell lung cancer, non-small cell lymphoma, ovarian cancer, prostate cancer, and kaposi's sarcoma associated with AIDS. Other tumors sensitive to etoposide are Ewing's sarcoma, hepatoma, AIDS related leukemia, acute myeloid leukemia, acute lymphocytic neuroblastoma, rhabdomyosarcoma and Wilm's tumour (O'Dwyer et al, 1985). In chemotherapy sometimes etoposide is combined with other anti-neoplastic agents.

2.3.3. Therapeutic Dose

Intravenous dose of etoposide for testicular cancer in combination therapy is 50 to 100 mg/sq. m for 5 days, or 100 mg/m^2 on alternate days for three doses. For small cell carcinoma of the lung, the dose in combination therapy is 50-120 mg/m^2 per day i.v. for 3 days or 50 mg per day orally for 21 days. Cycles of therapy are usually repeated every 3 to 4 weeks. The drug should be administered slowly during a 30 to 60 min infusion to avoid hypotension and bronchospasm, which likely to result from the additives used to dissolve etoposide, a relatively insoluble compound. In combination with ifosfamide and carboplatin, it is frequently used for high dose chemotherapy in total doses of 1500 to 2000 mg/m^2 (O'Dwyer and Weiss, 1984; Holthuis et al, 1989).

The currently available commercial dosage forms are non aqueous i.v. parenteral solutions (strength of 100 mg etoposide per 5 ml) and oral gelatin capsules containing etoposide solution in mixed solvent system (strength of 50 and 100 mg). The i.v. administration of etoposide on chronic situation is inconvenient for patients. In addition, etoposide precipitates from the parenteral solution as diluted with other i.v. fluids for infusion delivery and too rapid infusion of etoposide causes hypotension of the patient. The capsule formulation has a reported bioavailability of 50%. Several investigational oral formulations have been evaluated, namely hydrophilic, soft gelatin capsules containing etoposide solution, lipophilic capsules of etoposide suspension and drinking ampoules. But all these formulations yielded poor oral bioavailabilities with high inter and intra patient variability in rate and extent of etoposide absorption (Shah et al, 1989).

2.3.4. Clinical Toxicities

The dose limiting toxicity of etoposide is leucopenia. Thrombocytopenia occurs less often and usually is not severe. Nausea, vomiting, stomatitis and diarrhea occur in approx 15 % of patients treated intravenously and about 55% of patients who receive the drug orally. Alopecia is common but reversible. Fever, phlebitis, dermatitis and allergic reactions including anaphylaxis and acute hypersensitivity reactions have been observed (Hudson et al, 1993). Hepatic toxicity is particularly evident after high dose treatment. For both etoposide and teneposide, toxicity is increased in patients with decreased serum albumin, an effect related to decrease protein binding of the drug. It was shown to have cytotoxic activity against testicular and small cell lung cancers, lymphoma, leukemia and Kaposi's sarcoma associated with AIDS (O'Dwyer et al, 1985). Bone marrow recovery is usually complete by day 20, and cumulative toxicity has not been reported. Mucositis is an adverse reaction, which is observed after high doses of etoposide (O'Dwyer and Weiss, 1984).

2.4. Pharmacokinetics

An open two-compartment model or an open three-compartment model describes the pharmacokinetics of etoposide after i.v or oral administration. No difference is observed in the pharmacokinetics after i.v administration of high and low doses indicating dose independent. Upon oral administration to human subjects of hydrolytic capsules or a diluted intravenous preparation, peak etoposide levels were seen at 35 - 240 min and 30 - 160 min, respectively (D'Incalci et al, 1982). Etoposide demonstrates incomplete and variable bioavailability after oral dosing, which may be due to its concentration and pH dependent stability in artificial gastric and intestinal fluids.

2.4.1. Absorption, Fate and Excretion

Oral administration of etoposide results absorption that averages about 50% of the drug with considerable variability being observed both within and between patients (Harvey et al, 1985) and with decreasing bioavailability occurring with increasing dose (Smyth et al, 1985). After intravenous injection, peak plasma concentrations of 30 µg/mL are achieved; there is a biphasic pattern of clearance with a terminal half life of about 6 to 8 hrs in patients with normal renal function. Approximately 40% of an administered dose is excreted intact in the urine. In patients with compromised renal function, dosage should be reduced in proportion to the reduction in creatinine (level) clearance. In patients with advanced liver disease, low serum albumin and elevated bilirubin (which displaces etoposide from

albumin) tend to increase the unbound fraction of drug, increasing the toxicity of any given dose. However, guidelines for dose reduction in this circumstance have not been defined. Drug concentration in the CSF averages 1 % to 10 % in plasma.

Upon oral administration to human subjects of hydrophilic capsules or diluted intravenous preparation, peak etoposide blood levels were seen at 35-160 min respectively. Drug absorption varies within wide limits, the mean values for the biological availability being 57% (± 35%) for the capsules and 91% (± 35%) for the diluted i.v. preparation. Other investigators found an oral absorption after administration of soft gelatin capsules varying from 24.9 to 73.7%. Etoposide has low aqueous solubility and surface electrical charges that might contribute to low and erratic bioavailability (Shah et al, 1989). Pharmacological studies indicated that oral administration of low dose etoposide for a prolonged period time might be more effective than higher dose administration with periodic intravenous infusion (Slevin et al, 1989; Hande, 1993). In clinical practice, prolonged oral etoposide has been reported to show antitumor response in traditionally etoposide-insensitive malignancies and in traditionally etoposide- sensitive malignancies, which have already failed to prior bolus etoposide (Waits et al, 1992; Rose et al, 1998). Oral etoposide has been tested in many solid and hematological tumors and found to have an activity small cell carcinoma of the lung, non-small cell carcinoma of the lung, ovarian, prostate, germ cell and breast tumors and lymphoma (Slevin, 1990). Beside its efficacy, it has also several advantages in clinical practice such as its ease administration, comparatively lower cost and more favorable toxicity profile (Comis et al, 1999).

The major metabolite of etoposide is glucuronide derivative of etoposide, the glucuronic acid being attached to the phenol group at C-4. After incubation of cellular suspensions with etoposide in vitro, two metabolites were found: the reactive o-quinone derivative of etoposide and its reduction product, the catechol of etoposide. In humans, urinary excretion of unchanged drug accounts for an appreciable amount of drug elimination: according to the literature 26.2 - 53.4% of unchanged drug is recovered from urine after intravenous administration (Holthuis et al, 1986).

References

Beijnen, J.H., Holthuis, J.J.M., Kerkdijk, H.G., van der Houwen, O.A.G.J., Paalman, A.C.A., Bult, A., Underberg, W.J.M., 1988. Degradation kinetics of etoposide in aqueous solution. Int. J. Pharm. 41, 169-183.

Brewer, C.F., Loike, J.D., Horwitz, S.B., Sternlicht, H., Gensler, W.J., 1979. Conformational analysis of podophyllotoxin and its congeners. Structure--activity relationship in microtubule assembly. J. Med. Chem., 22, 215-221.

Comis, R.L., Friedland, D.M., Good, B.C., 1999. The role of oral etoposide in non-small cell lung carcinoma. Drugs. 3, 21-30.

D'Incalci, M., Farina, P., Sessa, C., Mangioni, C., Conter, V., Masera, G., Rocchetti, M., Pisoni, M.B., Piazza, E., Beer, M., Cavalli, F., 1982. Pharmacokinetics of VP16-213 given by different administration methods. Cancer. Chemother. Pharmacol. 7, 141-145.

Hande, K.R., Krozely, M.G., Greco, F.A., Hainsworth, J.D., Johnson, D.H., 1993. Bioavailability of low-dose oral etoposide. J. Clin. Oncol. 11, 374-377.

Harvey, V.J., Slevin, M.L., Joel, S.P., Smythe, M.M., Johnston, A., Wrigley, P.F.M., 1985. Variable bioavailability following repeated oral doses of etoposide. Eur J. Clin. Oncol. 21, 1315–1319.

Holthuis, J.J.M., Bosch, K.V., Bult A., 1989. Etoposide. In: Florey, K., (Ed.), Analytical profiles of drug substances, Academic Press: San Diego, CA, pp. 121-151.

Holthuis, J.J.M., Postmus, P.E., Van Oort, W.J., Hulshoff, B., Verleun, H., Sleijfer, D.T., Mulder, N.H., 1986. Pharmacokinetics of high dose etoposide (VP 16-213). Eur. J. Cancer. Clin. Oncol. 22, 1149-1155.

Hudson, M.M., Weinstein, H.J., Donaldson, S.S., Greenwald, C., Kun, L., Terbell, N.J., Humphrey, W.A., Rupp, C., Marina, N.M., Wilimas, J., Link, M.P., 1993. Acute hypersensitivity reactions of etoposide in a VEPA regimen for Hodgkin's disease. J. Clin. Oncol. 11, 1080-1084.

Issell, B.F., Rudolph, A.R. and Louie, A.C., 1984. Etoposide (VP-16-213): An overview. In Issell, B.F., Muggia, F.M. and Carter, S.K. (Eds), Etoposide (VP-16), Academic Press, Orlando, FL, pp. 4-6.

Keller-Juslen, C., Kuhn, M., Stahelin, H., von Wartburg, A., 1971. Synthesis and antimitotic activity of glycosidic lignan derivatives related to podophyllotoxin. J. Med. Chem. 14, 936-940.

Loike, J.D., Brewer, C.F., Sternlicht, H., Gensler, W.J., Horwitz, S.B., 1978. Structure-activity study of the inhibition of microtubule assembly in vitro by podophyllotoxin and its congeners. Cancer Res., 38, 2688-2693.

O'Dwyer, P.J., Leyland-Jones, B., Alonso, M.T., Marsoni, S. Wittes, R.E., 1985. Drug therapy - etoposide (VP-16-213) - current status of an active anticancer drug. N. Engl. J, Med, 312, 692-700.

O'Dwyer, P.J., Weiss, R.B., 1984. Hypersensitivity reactions induced by etoposide. Cancer Res. 68, 959-961.

Rose, P.G., Blessing, J.A., Le, L.V., 1988. Prolonged oral etoposide in recurrent or advanced squamous cell carcinoma of the cervix: A Gynecologic Oncology Group Study. Gynecol. Oncol. 70, 263-266.

Shah, J., Chen, J.R., Chow, D., 1989. Preformulation study of etoposide: Identification of physicochemical characteristics responsible for the low and erratic oral bioavailability of etoposide. Pharm. Res. 6, 408-412.

Slevin, M.L., 1990. Low-dose oral etoposide: a new role for and old drug? J Clin Oncol. 8, 1607-1609.

Slevin, M.L., 1991. The clinical pharmacology of etoposide. Cancer, 67, 319-329.

Slevin, M.L., Joel, S.P., Whomsley, R., Devenport, K., Harvey, V.J., Osborne, R.J.O., Wrigley, P.F.M., 1989. The effect of dose on the bioavailability of oral etoposide: confirmation of a clinically relevant observation. Cancer. Chemother. Pharmacol. 24, 329–331.

Smyth, R.D., Pfeffer, M., Scalzo, A., Comis, R.L., 1985. Bioavailability and pharmacokinetics of etoposide (VP16). Semin. Oncol. 12, 48-51.

Waits, T.M., Jonson, D.H., Hainsworth, J.D., Hande, K.R., 1992. Prolonged administration of oral etoposide in non-small cell lung cancer: a phase II trial. J Clin. Oncol. 10, 292-296.

Chapter 3

Analytical Method Development

3.1. Introduction

Analytical method is an important and integral part of the formulation development of any drug candidate and characterization of the formulation. A simple and suitable method for accurate estimation of drug in the prepared formulation is necessary. Though, literature sometimes may provide analytical method(s) for drug estimation, however such methods are not always found suitable for the specific formulation development purpose. In such case it becomes essential to develop a need based sensitive, simple and cost effective method for the estimation of routine drug samples. Different sensitive methods like UV, visible, fluorescence and high performance liquid chromatography can be developed and applied according to the requirement of the project. Development of such an accurate, precise, sensitive as well as simple method for routine estimation is always tedious process and need special attention.

There were several methods reported in literature for the estimation of etoposide. Most of the reported methods are based on liquid chromatographic technique utilizing UV (Beijnen et al, 1988; Strife et al, 1980), fluorescence (Strife et al, 1981) and electrochemical (Werkhoven-Goewie et al, 1983; Mross et al, 1994; McLeod and Relling, 1992; Eisenberg and Eickhoff, 1993) detectors. Along with these, USP also has HPLC method utilizing gradient technique (USP, 2003). These reported methods are tedious, expensive, complicated, and not suitable for routine formulation analysis of present work as they have lengthy extraction procedures (Sinkule and Evans, 1984; Igwemezie et al, 1995) and column switching techniques (Van Opstal et al, 1989). They were quite time consuming for the analysis of etoposide to determine drug content, entrapment efficiency, etc, particularly for the analysis of large number of samples. Thus, there was a need for a simple and inexpensive methods for the determination of etoposide for analysis of drug present in formulations especially nanoparticles. Simple UV and spectrofluorimetric methods are found to be very suitable for the estimation of etoposide in samples of drug content, entrapment efficiency and in vitro release studies. Such methods are not only rapid to perform but are also simple and practical in many laboratories with relatively modest facilities.

Though, UV and spectrofluorimetric methods are simple, yet are not sensitive enough to be able to estimate etoposide at lower concentrations. There was a need for developing more sensitive method for the estimation of etoposide at very low level. As the proposed formulations are nanoparticles loaded with etoposide using different polymers, there is a possibility of drug releasing very slowly from them. If the analytical method is not sensitive enough, there is a possibility of erroneous results, which will lead to false

conclusions. To avoid this, high performance liquid chromatographic (HPLC) method was also developed in the present study. Method was developed to estimate etoposide present in marketed formulations as well as nanoparticle formulations. Bio analytical method was also developed in serum for the estimation of etoposide present in blood after in situ absorption study. Earlier reported methods were meant for estimation of etoposide in biological matrices like blood (Eisenberg and Eickhoff, 1993), plasma (Strife et al, 1981; Werkhoven-Goewie et al, 1983; Van Opstal et al, 1989), urine, CSF (Sinkule and Evans, 1984; Igwemezie et al, 1995) and leukemic cells (Liliemark et al, 1995) with complicated extraction procedures. Very few HPLC methods are reported for the estimation of etoposide in injectable formulations (Floor et al, 1985) and its stability and solubility studies (Shah et al, 1989). These methods were developed using phenyl and cyano columns, requiring internal standard for estimation of etoposide and retention times were high. There was a need for a better and simple method for the estimation of etoposide released during in vitro release studies of nanoparticles.

Thus according to the need of present work, a new UV spectrophotometric, spectrofluorimetric and HPLC methods were developed for estimation of etoposide in stability samples, drug content, entrapment efficiency, in vitro release studies. The developed methods are validated according to the guidelines provided (International Conference on Harmonization, ICH, 1996, United States Pharmacopoeia, USP, 2003).

3.2. Materials, Equipment/Instruments and Reagents

3.2.1. Materials

Pure Etoposide was obtained as gift sample from Dabur Research Foundation, Sahibabad, India. Acetonitrile and methanol were of HPLC grade and purchased from Spectrochem, Mumbai. Potassium dihydrogen phosphate, ortho phosphoric acid and ammonium acetate were purchased from Qualigens, India. For buffer preparations, in-house prepared triple distilled water (TDW) was used. Buffers and TDW were filtered through 0.22 µ filters (Millipore, USA).

Formulations of etoposide used for the study were soft gelatin capsules (Etosid, Cipla Ltd, India) containing 50 mg etoposide, U.S.P., in each capsule and injections (Etosid, Cipla Ltd, India and Fytosid, Dabur India Ltd, India) containing etoposide U.S.P. 100mg/5 ml and were procured from Indian market. Etosid capsules contain excipients like ferric oxide red and titanium dioxide. Etosid and Fytosid injections contain excipients like benzyl alcohol I.P., ethyl alcohol I.P. in a sterile non-aqueous vehicle.

3.2.2. Equipment/Instruments

A double-beam UV-Vis spectrophotometer (Perkin Elmer, Japan), model LAMBDA EZ210 connected to computer loaded with PESSW software (Version 1.2 and Revision E) was employed. It has an automatic wavelength accuracy of 0.1 nm and matched quartz cells of 10 mm path length.

A Spectrofluorimeter (Jasco, FP777, Japan) with a xenon lamp and inbuilt software was used for all fluorescence measurements using 1 cm quartz cells. Experimental parameters were: excitation band width - 5 nm, emission band width - 10 nm, photo-multiplier tube response - high, slit width - 0.5 nm, λ_{ex} = 240 nm and λ_{em} = 324 nm.

HPLC equipment (Jasco, Japan) with intelligent pumps of model PU-1580, UV-1575 model intelligent UV/Visible detector and AS-1559 model intelligent sampler was used. Chromatograms were analyzed using Borwin software provided with the system.

3.2.3. Reagents:

Phosphate buffer (pH 7.4): KH_2PO_4 (6.804 g) was dissolved in 500 ml of triple distilled water and 195.5 ml of NaOH (0.2 M) was added, then volume was made upto 1000 ml using TDW.

Ortho phosphoric acid (0.1 M): Ortho phosphoric acid, 6.88 ml was transferred to a 50 ml volumetric flask and volume was made up to the mark with TDW.

Ammonium acetate buffer 50 mM, (pH 6.0): Ammonium acetate, 1.947 g was weighed accurately, dissolved in TDW and volume was made up to 500 ml with TDW. Solution pH was adjusted with freshly prepared 0.1 M ortho phosphoric acid. Ammonium acetate buffer solution was filtered through 0.22 µ filters (Millipore, USA).

3.3. Analytical Method 1: UV Spectrophotometric Method

3.3.1. Experimental

a) Selection of Media

Different media were investigated to develop a suitable UV-spectrophotometric method for the analysis of etoposide in formulations. For selection of media the criteria employed was sensitivity of the method, ease of sample preparation, solubility of the drug, cost of solvents and the applicability of method to various purposes. The finalized medium was Acetonitrile (ACN): TDW (50:50 v/v). The developed method was validated as per guidelines provided by ICH (ICH, 1996) and USP (USP, 2003). Suitable statistical tests were performed on validation data (Bolton, 1997).

b) Preparation of Calibration Curve

Stock solution of 100 µg/ml of etoposide was prepared in acetonitrile by dissolving 5 mg of etoposide in 50 ml of medium. For preparation of different concentrations, aliquots of stock solutions were transferred into a series of 10 ml volumetric flasks and volumes were made up with selected media. Five different concentrations were prepared in the range of 5-40 µg/ml of etoposide for calibration curve. Etoposide was estimated at 240 nm in the medium. To establish linearity of the proposed method, six separate series of solutions of the drug (5-40 µg/ml) were prepared from the stock solutions and analyzed. Least square regression analysis was done for the obtained data. The calibration data for this method is presented in Table 1. Average absorbance of each concentration was substituted in the regression equation to calculate predicted concentration for that particular concentration.

c) Analytical Method Validation

Specificity and selectivity of the method was assessed by preparing a drug concentration (10 µg/ml) from pure drug stock and commercial sample stock in selected medium and analyzed. Solutions of different excipients used in formulations were prepared, with and without drug and analyzed for any change in spectra of etoposide.

As a part of determining accuracy of the proposed methods, different levels of drug concentrations (Lower Quality Control sample (LQC) - 7 µg/ml, Medium Quality Control sample (MQC)- 15 µg/ml and Higher Quality Control sample (HQC)- 35 µg/ml) were prepared from independent stock solution and analyzed. Accuracy was assessed as the mean percentage recovery and percentage relative error. To give additional support to accuracy of the developed assay method, standard addition method was done. In this study, different concentrations of pure drug (10, 20 and 30 µg/ml) were added to a known pre-analyzed formulation sample (Drug concentration - 10.09 µg/ml) and the total concentration was determined using the proposed method. The percent recovery of the added pure drug was calculated as, % Recovery = [(Cv-Cu)/Ca] × 100, where Cv is the total drug concentration measured after standard addition; Cu, drug concentration in the formulation; Ca, amount of pure drug (per ml) added to formulation.

Repeatability was determined by using different levels of drug concentrations (same concentration levels taken in accuracy study), prepared from independent stock solution and analyzed. Inter-day and intra-day variation was studied to determine intermediate precision of the method. Different levels of drug concentrations (as mentioned in accuracy) were prepared at two different times in a day by different analysts and studied for intra-day variation. Same protocol was followed for three different days to study inter-day variation.

The relative standard deviation (in %) of the predicted concentrations from the regression equation was taken as precision.

The detection limit (DL) and quantitation limit (QL) of etoposide by the spectrophotometric method were determined using calibration standards. DL and QL were calculated as 3.3s/S and 10s/S respectively, where S is the slope of the calibration curve and s is the standard deviation of y-intercept of regression equation (ICH guide lines, 1996). Robustness of the developed method was determined by changing composition of acetonitrile by ± 1%. Stability of the etoposide in the selected medium was observed by spectral changes at room temperature for 24 hrs.

d) Estimation of Etoposide in Commercial Formulations

Contents of 10 capsules of etoposide were emptied and mixed properly. Quantity equivalent to 2 mg of etoposide was taken and dissolved in 10 ml of ACN. Final dilutions were made with selected medium (ACN: TDW: 50:50 v/v) in order to obtain concentrations within the linearity range and the samples were analyzed using proposed method.

Contents of 5 injection vials were emptied and mixed. From this, volume equivalent to 2 mg etoposide was taken and dissolved in acetonitrile and same steps were repeated to obtain concentrations in the linearity range.

3.3.2. Results and Discussion

a) Selection of Media

For media optimization various aqueous media like only TDW, acetate buffer (pH 3.6), phosphate buffers (pH 5.8 to 8.0) were investigated. The final decision of using a combination of acetonitrile and TDW (50:50 v/v) as medium was based on criteria like; sensitivity, ease of preparation and applicability of the method to routine analysis. The spectra of etoposide in the present medium are shown in Figure 1. The λ_{max} of etoposide in particular medium was found to be 284 nm. But absorbance at this wavelength was less there by decreasing the sensitivity and linearity range of the method. Therefore 240 nm was used as etoposide has shown higher absorbance at this wavelength without interference from any. No extraction step was involved in the proposed method, there by decreasing the time and error in quantification.

b) Calibration Curve

Different drug concentrations and their absorbance are shown in the Table 1. At all concentration levels the standard deviation was low and the relative standard deviation

(RSD) did not exceed 2.4 %. The predicted concentrations were matching with the nominal concentration (Table 1). Linearity range was found to be 5-40 µg/ml. The linear regression equation obtained was: Absorbance = 0.022 × Concentration (in µg/ml) + 0.009; with a regression coefficient of 0.9993. The values of slope and intercept were found to be within the 95% confidence limits. Lower values of standard error of slope (6.3×10^{-5}), standard error of intercept (1.6×10^{-3}), standard error of estimate (0.353) and MSSR (0.12) indicates high precision of the proposed method.

c) Analytical Method Validation

Estimation of etoposide in formulations and comparison with pure drug has shown that common excipients used in formulations like benzyl alcohol, ethyl alcohol etc, did not interfere with the estimation of etoposide at the wavelength used (240 nm) in this method. Presence of excipients did not change the absorbance confirming specificity and selectivity of the method.

Accuracy expressed as % relative error ranged from -0.02 to 0.28 % in the selected medium (Table 2). The high mean % recovery values (> 99.82%) and their low standard deviation values (SD < 1.25) represented accuracy. The validity and reliability of the proposed method was established by recovery studies using standard addition method. The mean percentage analytical recoveries (± SD) for 10, 20 and 30 µg/ml concentrations were found to be 100.94 (± 1.58), 99.38 (± 1.69) and 100.93 (± 0.81) respectively. This result revealed that any small change in the drug concentration in the solution could be accurately determined by these proposed methods.

Precision was determined by studying repeatability and intermediate precision. Repeatability (% RSD) ranged from 0.14 to 1.24 % at all three levels of concentrations (Table 2). In intermediate precision study, RSD values were not more than 1.3 % in all the cases indicating no appreciable inter-day and intra-day variation (Table 3). RSD values were within the acceptable range indicating that these methods have excellent repeatability and intermediate precision.

DL and QL were found to be 1.17 µg/ml and 3.53 µg/ml respectively. Variation of composition of ACN by ± 1 % did not affect absorbance. In the selected medium no changes of absorbance was observed for 24 h when stored at room temperature (Figure 2).

d) Estimation of Etoposide in Commercial Formulations

Etoposide content for different formulations ranged from 98.33 to 100.10 % of the claimed amount with standard deviation not more than 2.3 % (Table 4). This indicated that the interference of excipients matrix is insignificant in estimation of etoposide by proposed

method. The estimated drug content with low values of standard deviation established the precision of the proposed method.

3.4. Analytical Method 2: Spectrofluorimetric Method

3.4.1. Experimental

a) Selection of Media

Different media, prepared using methanol and different buffers individually and in combinations, were investigated to develop a suitable spectrofluorimetric method for the analysis of etoposide. For selection of medium the criteria employed was sensitivity of the method and the applicability of method to various purposes. A combination of methanol and phosphate buffer pH 7.4 in ratio of 70:30 % v/v was selected for the spectrofluorimetric estimation of etoposide. Etoposide solutions were scanned for excitation and emission wavelengths. Excitation and emission wavelengths fixed for this method are 240 nm and 324 nm respectively.

b) Preparation of Calibration Curve

Primary stock solution of 200 µg/ml etoposide was prepared in methanol. Secondary stock of 20 µg/ml was prepared by diluting primary stock with selected medium. The concentration range of 200-1000 ng/ml was prepared by suitable dilution of secondary stock of appropriate volume by the medium. The Fluorescence intensity was measured at λ_{em}=324 nm, irradiating at λ_{ex}=240 nm. Nine replicates of all the solutions were prepared and analyzed. The calibration curve was then prepared by plotting the fluorescence intensity versus concentration of the drug. Linearity of the method was established by preparing six separate series of five concentrations (200, 400, 600, 800 and 1000 ng/ml) and analyzed. Least square regression analysis was done for the obtained data. Average absorbance of each concentration was substituted in the regression equation and predicted concentration was calculated for that particular concentration.

c) Analytical Method Validation

Spectrofluorimetric method developed for etoposide was validated for the same parameters as mentioned under UV spectrophotometric method (Section 3.3.1.c). Specificity and selectivity of the method was assessed by preparing a drug concentration (500 ng/ml) from pure drug stock and commercial sample stock in selected medium and analyzed. Solutions of excipients used in formulations were prepared, with and without drug and analyzed for any change in emission and excitation scans of etoposide.

To determine accuracy of the proposed method, different concentrations of drug (LQC - 300 ng/ml, MQC - 500 ng/ml and HQC - 900 ng/ml) were prepared and analyzed. Standard addition method was done to check recovery by adding different concentrations of pure drug solutions (100, 200, 400 and 600 ng/ml) to a known pre-analyzed formulation sample (400.10 ng/ml) and the total concentration was analyzed. The recovery of the added pure drug was calculated same as mentioned in earlier method (section 3.3.1.c).

Repeatability was also calculated similarly (section .3.1.c) by analyzing different drug concentrations taken same as given in accuracy. Inter-day and intra-day variation was carried out to determine intermediate precision of the method.

The DL and QL of etoposide for the proposed method were determined as mentioned in earlier method 1 (section 3.3.1.c). Robustness of the developed spectrofluorimetric method was determined by changing pH of the phosphate buffer by ± 0.1 and composition of methanol by ± 1%. Stability of the etoposide in the selected medium was observed by spectral changes at room temperature for 24 hrs.

d) Estimation of Etoposide in Commercial Formulations

Contents of 10 capsules of etoposide were emptied and mixed properly. Quantity equivalent to 2 mg of etoposide was taken and dissolved in 7 ml of methanol. Phosphate buffer pH 7.4 was added to make up the volume to 10 ml. Final dilutions were done with same medium in order to obtain concentrations within the linearity range

Contents of 5 injection vials were emptied and mixed. From this, volume equivalent to 2 mg etoposide was taken and dissolved in methanol and diluted similarly.

3.4.2. Results and Discussion

a) Selection of Media

The spectral characters of etoposide estimated using Fluorimetry were found to be independent of pH of the solution. Addition of methanol in various proportions with phosphate buffer (pH 7.4) has improved the sensitivity of the analysis. The final decision of using mixture of methanol and phosphate buffer (pH 7.4) in 70:30 v/v was made based on optimization of sensitivity of the method and cost of solvents. Emission spectra of different concentrations of etoposide in selected medium are shown in Figure 3.

b) Preparation of Calibration Curve

Different drug concentrations and their relative fluorescence intensities are shown in the Table 5. At all concentration levels the standard deviation was low and the relative

standard deviation did not exceed 1.8 %. The linearity range was found to be 200-1000 ng/ml. The linear regression equation obtained was: Fluorescence Intensity = 6.704 × Concentration (in ng/ml). + 115.4, with a regression coefficient of 0.9994. These mean values were found to be within the 95% confidence limits. Lower values of standard error of slope (0.04), standard error of intercept (27.12), standard error of estimate (1.78) and MSSR (7.56) indicates high precision of the proposed method.

c) Analytical Method Validation

Comparison with pure drug with the etoposide estimated from formulations has shown that common excipients used in formulations like benzyl alcohol, ethyl alcohol etc, did not interfere with the estimation of etoposide at the wavelengths used in this method. Presence of excipients did not change the fluorescence intensity confirming specificity and selectivity of λ_{em} and λ_{ex} for the drug.

The results of accuracy for the proposed method are summarized in the Table 6. Percentage relative error ranged from -1.03 to 1.24, indicating high accuracy of the method. The mean percentage analytical recoveries (± SD) for 100, 200, 400 and 600 ng/ml concentrations were found to be 100.69 (± 1.32), 99.45 (± 1.52), 99.83 (± 0.48) and 100.48 (± 1.10) respectively. High recoveries by standard addition method and low RSD show that the method can estimate etoposide accurately. Overall precision (RSD) ranged from 1.06 to 1.27 % (Table 6).

Relative standard deviations (RSDs) in intra-day variation study were found lower than 2.22 % and the RSDs in inter-day variation were lower than 0.40 % for all concentration levels (Table 7). The observed RSD values were within the limits, indicating intermediate precision of the developed method (Table 7).

DL and QL were found to be 23.92 ng/ml and 72.47 ng/ml respectively. Variation of pH of the medium by ± 0.1 and strength of methanol by ± 1 % did not have any significant effect on the relative intensity. The etoposide solution in selected medium exhibited no emission spectral changes on keeping at room temperature for a study period of 24 hrs.

d) Estimation of Etoposide in Commercial Formulations

The developed method was used for estimation of etoposide in pharmaceutical formulations and the results were shown in Table 8. For different formulations % recovery ranged from 99.40 to 100.21 with standard deviation not more than 1.76. The estimated drug content with low values of standard deviation established the precision of the proposed method. In all the formulations, etoposide was estimated accurately and precisely by this

method. Assay values of formulations were close to the label claim (as mentioned in Table 8) indicating that there is no interference of excipients matrix in estimation of etoposide by the proposed method.

3.5. Analytical Method 3: HPLC Method

3.5.1. Experimental

a) Selection of Mobile Phase

For mobile phase optimization various buffers of different pH like phosphate buffers, acetate buffers (pH 3.5 to 6.0) (20 mM to 50 mM), and different combinations of organic phase (acetonitrile and methanol) along with buffers were investigated. Main purpose is to develop a simple, precise, sensitive and selective HPLC method for quantitation of etoposide in bulk and dosage forms. Medium selected for this was a combination of ammonium acetate buffer 50 mM (pH 6.0) with methanol in 50:50 v/v ratio.

b) Chromatographic conditions

Etoposide was eluted using a reverse phase LiChrocart RP-18 (250 x 4.6 mm, 5 µm) column. Injection volume 50 µl of was used. Flow rate was adjusted to 1 ml/min of mobile phase and the wavelength was set to 240 nm.

c) Preparation of Calibration Curve

Primary stock of etoposide was prepared dissolving 2 mg of etoposide in 10 ml of methanol. Secondary stock of 20 µg/ml was prepared by diluting primary stock with mobile phase. Stock solution was diluted suitably with mobile phase to get calibration standards in a concentration range of 50 to 1000 ng/ml. Calibration curve was plotted between mean peak areas of etoposide against concentration of drug. Linearity of the proposed method was established as mentioned in methods 1 and 2. Concentrations of etoposide taken are 50, 200, 400, 600, 800 and 1000 ng/ml. Least square regression analysis was done for the obtained data and calibration equation was developed. ANOVA test (one-way) was performed based on the area of the peak observed for each pure drug concentration during the replicate measurement of the standard solutions. Average area of each concentration was substituted in the regression equation to calculate predicted concentration.

d) Analytical Method Validation

Validation parameters were determined according to standard procedures given in the ICH guidelines (1996) and USP (2003). Specificity and selectivity of the method was assessed by preparing a drug sample (500 ng/ml) both from pure drug stock and commercial sample stock in selected mobile phase. This was analyzed by HPLC using chromatographic conditions mentioned above.

Accuracy and precision were calculated according to earlier procedures. Different levels of drug concentrations taken for determining accuracy of this method are, LQC - 100 ng/ml, MQC - 500 ng/ml and HQC - 800 ng/ml. These were prepared independently from stock solution and analyzed. Standard addition method was done to give additional support to accuracy. Different concentrations of pure drug solutions (100, 300 and 600 ng/ml) were added to a known pre-analyzed formulation sample (400.07 ng/ml) and the total concentration analyzed. The recovery of the added pure drug was calculated.

As a part of precision, repeatability was calculated by taking different levels of drug concentrations (as mentioned in accuracy) prepared from fresh stock solution and were analyzed. Inter-day and intra-day variation studies were carried out to determine intermediate precision of the method. As mentioned in earlier methods same protocol was followed to study inter and intra day variability.

Signal-to-noise ratio of 3 was taken as DL and signal-to-noise ratio of 10 was taken as QL (ICH guidelines, 1996). The QL samples were prepared in three replicates using same procedure followed for calibration standards and analyzed. Robustness of the method was determined by changing composition of mobile phase by ± 1%, by changing the pH of ammonium acetate buffer by ± 0.1 units and by establishing the bench-top and stock solution stability of etoposide at room temperature.

e) Estimation of Etoposide in Commercial Formulations

For analysis of etoposide in capsules (10 capsules were taken for study), quantity equivalent to 2 mg of etoposide was taken and dissolved in 10 ml of methanol. Subsequent dilutions were made with mobile phase in order to obtain concentrations within the linearity range. For injections (5 vials), volume equivalent to 2 mg etoposide was taken and dissolved in methanol and diluted similarly.

3.5.2. Results and Discussion

a) Selection of Mobile Phase

Changing the buffer composition, their pH and addition of organic solvent in various proportions changed the retention time of the drug and symmetry of the peak. The final

decision of using 50 mM ammonium acetate buffer (pH 6.0) with methanol in 50:50 %v/v as a mobile phase was based on asymmetric factor, retention time of the drug, and sensitivity of the method. Wavelength of 240 nm was selected for the estimation of etoposide. Chromatograms of blank and three different concentrations of etoposide prepared in mobile phase are shown in Figure 4. Retention time of etoposide was 6.74 ± 0.31 min in selected mobile phase. Peak was having good resolution with asymmetric factor of 1.21 ± 0.10. Total run time for single injection was 10 min for this method.

b) Calibration Curve

Different concentrations (50, 200, 400, 600, 800 and 1000 ng/ml) and their peak areas were shown in the Table 9. At all concentration levels the standard deviation was low and the relative standard deviation (RSD) did not exceed 1.35 %. The predicted concentrations were matching with the nominal concentration. In selected mobile phase the linearity range was found to be 50-1000 ng/ml. The linear regression equation obtained was: Area (mV-sec) = 61.01 × Concentration (in ng/ml) + 401.19. These mean values were found to be within the 95% confidence limits. Goodness of fit of regression equation was supported by high regression coefficient value (0.9998), low calculated *F*-value (Calculated F-value - 4.49×10^{-4} and critical *F* (5, 24) - 2.62 at *P* = 0.05 level of significance) and low standard error of estimate (13.8). Lower values of parameters like standard error of slope, intercept and estimate indicated high precision of the proposed method.

c) Analytical Method Validation

Figure 5 shows chromatogram of etoposide present in marketed formulation. Retention time, asymmetric factor and area of the peak were not affected with excipients present in formulations of etoposide. Selected mobile phase does not have significant signal at retention time of etoposide. This indicates the proposed method is selective and sensitive to etoposide. Accuracy expressed as % relative error for three different concentrations ranged from -0.69 to 2.27 (Table 10). In standard addition studies, mean % recoveries (± SD) were found to be 99.01 (± 0.41), 102.59 (± 0.15) and 100.33 ± 0.05) for 100, 300 and 600 ng/ml concentrations respectively. High recoveries by standard addition method for respective pure drug concentration and low RSD (< 0.5 %) show that the method can estimate etoposide accurately.

In repeatability study RSD was ranged from 1.98 to 2.44. At all three concentration levels, precision showed satisfactory levels (Table 10). Intermediate precision expresses

variation in different days. Results of intermediate precision study, RSD values for each set (at three levels) were given in Table 11. In all the cases the RSD values were < 2.8 %, indicating that these methods have excellent repeatability and intermediate precision.

DL and QL were found to be 10.34 ng/ml and 33.62 ng/ml respectively. The mean % recovery (± SD) of the estimated QL was found to be 101.66 (± 2.79). When drug was estimated under varying pH and varying composition of mobile phase conditions the mean % recovery value was found to be 100.29 with low % RSD of 1.20, indicating the robustness of the method. The retention time and area of the bench-top stability and stock solution stability samples were not changed till 7 days and there were no extra peaks observed in the chromatograms during the run time of method.

d) Estimation of Etoposide in Commercial Formulations

The developed method was used for estimation of etoposide in pharmaceutical formulations and the results were shown in Table 12. For different formulations % assay ranged from 100.18 to 101.56 with standard deviation not more than 2.05. The estimated drug content with low values of standard deviation established the precision of the proposed method. Assay values of formulations were very close to the label claim thereby suggesting interference of formulation excipient matrix is insignificant in estimation of drug

3.6. Conclusions

In summary, all the developed methods were simple, rapid, accurate, and precise and can be used for routine analysis of etoposide in bulk, pharmaceutical formulations and for dissolution studies of formulations. They are simple and sensitive without the use of any complicated methods or sample preparation. Detection and quantitation limits of the proposed methods are much lower than reported methods for estimation of etoposide. The sample recoveries in all formulations were in good agreement with their respective label claims and thus suggested non-interference of formulation excipients in the estimation.

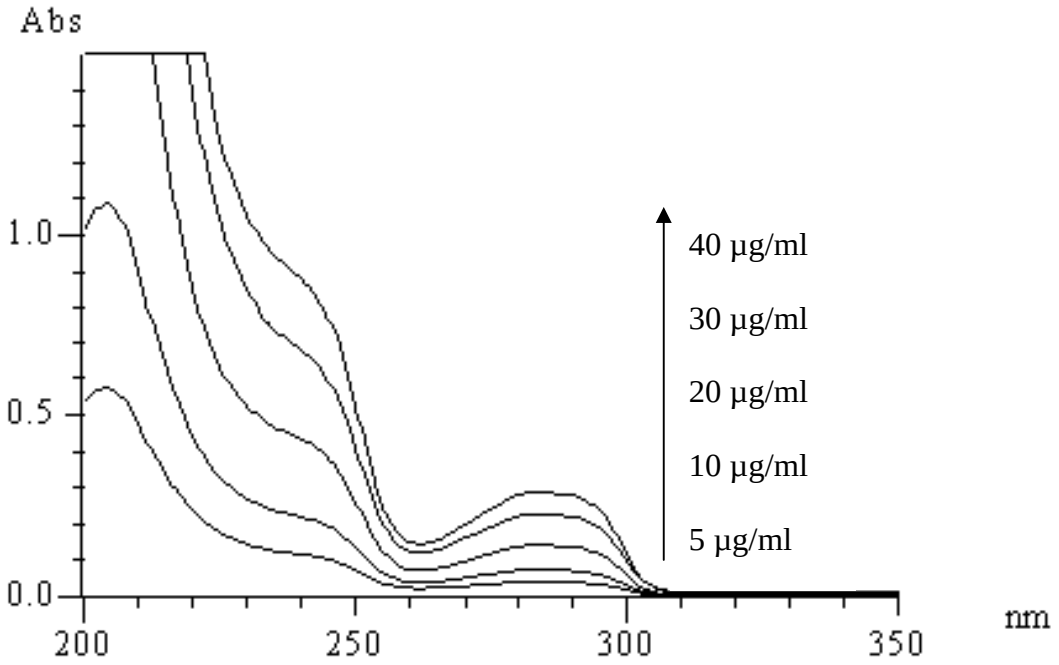

Figure 1: Overlay spectra of different concentrations of etoposide in ACN: TDW (50:50 v/v) medium by UV spectrophotometric method.

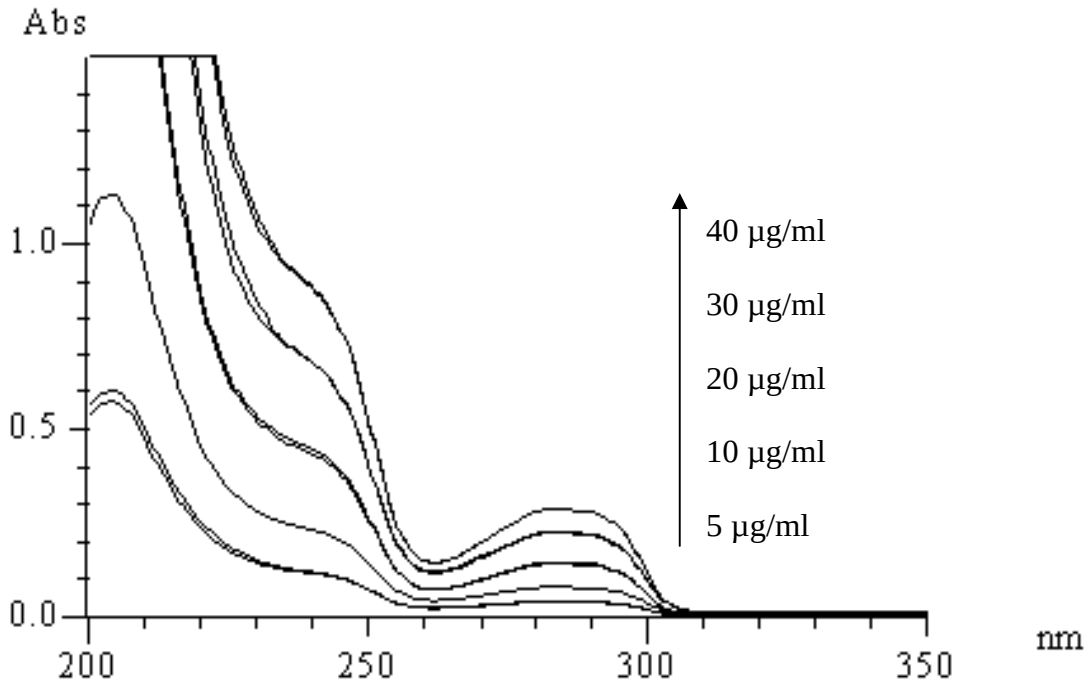

Figure 2: Overlay spectra of different concentrations of etoposide at zero time and 24 h in ACN: TDW (50:50 v/v) medium by UV spectrophotometric method.

Table 1: Calibration data for the estimation of etoposide by UV spectrophotometric method.

Etoposide (µg/ml)	Absorbance (± SD) [a]	RSD (%) [b]	Predicted Con. [c] (µg/ml)
5	0.120 ± 0.003	2.396	5.076
10	0.229 ± 0.003	1.151	10.008
20	0.447 ± 0.009	2.079	19.921
30	0.667 ± 0.010	1.445	29.911
40	0.892 ± 0.010	1.122	40.125

[a] - Each determination is an average of 6 separate determinations
[b] - RSD (%) of each point from the regressed line
[c] - predicted concentration calculated from the regression equation

Table 2: Accuracy and precision data for UV spectrophotometric method.

Level	Predicted con. (µg/ml) [a]			Mean % recovery (± SD)	Accuracy (%) [b]
	Range	Mean (± SD)	% RSD		
LQC	6.88 - 7.17	7.00 ± 0.09	1.24	99.98 ± 1.24	-0.02
MQC	14.86 - 15.08	14.97 ± 0.07	0.43	99.82 ± 0.43	-0.18
HQC	35.00 - 35.20	35.10 ± 0.05	0.14	100.28 ± 0.14	0.28

[a] - predicted concentration of etoposide was calculated by linear regression equation
[b] - accuracy is expressed in % relative error

Table 3: Intra-day and inter-day variability for UV spectrophotometric method.

Level	Intra-day repeatability % RSD (n=3)			Inter-day repeatability % RSD (n=18)
	Day 1	Day 2	Day 3	
LQC	0.552	0.303	0.491	1.274
	1.288	0.250	0.353	
MQC	0.229	0.151	0.242	0.413
	0.063	0.093	0.106	
HQC	0.160	0.065	0.213	0.064
	0.097	0.126	0.163	

Table 4: Determination of etoposide in pharmaceutical preparations by UV spectrophotometric method.

Preparation	Assay (± SD)	% Recovery (± SD)
Etosid soft gelatin capsules - 50 mg/capsule	49.87 ± 0.70	99.74 ± 1.40
Etosid injection - 20 mg/ml	19.67 ± 0.30	100.10 ± 2.28
Fytosid injection - 20 mg/ml	20.02 ± 0.46	98.33 ± 1.20

Each determination is an average of 5 separate determinations

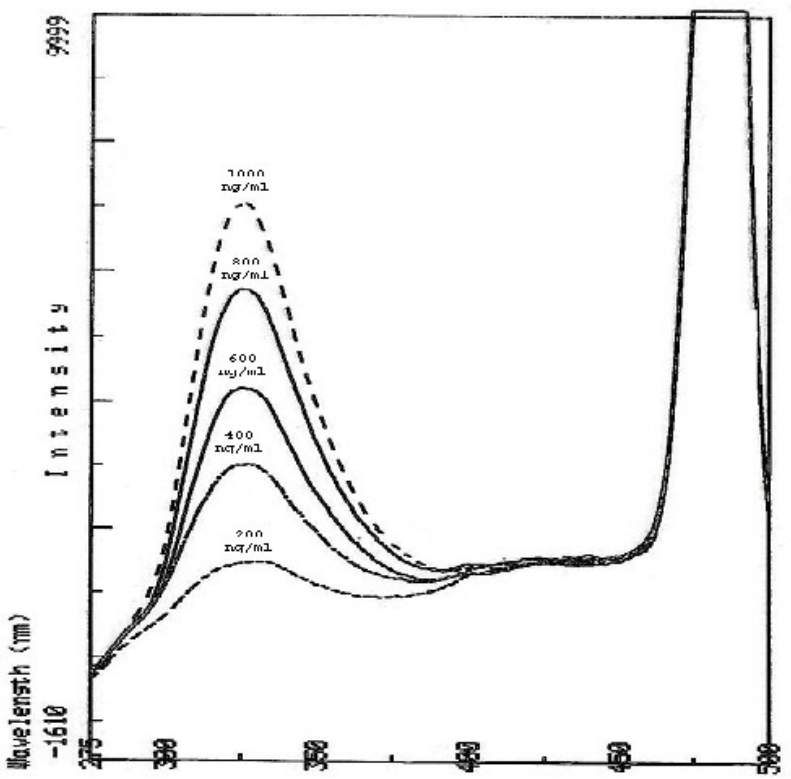

Figure 3: Emission spectra of different concentrations of etoposide in methanol: phosphate buffer pH 7.4 (70:30 v/v) medium by spectrofluorimetric method.

Table 5: Calibration data for the determination of etoposide by spectrofluorimetric method.

Etoposide (ng/ml)	Fluorescence intensity [a, b] (± SD)	RSD (%) [c]	Predicted Con. [d] (ng/ml)
200	1451.8 ± 18.21	1.25	199.34
400	2746.8 ± 0.67	0.02	392.50
600	4214.4 ± 55.22	1.31	611.42
800	5494.6 ± 57.30	1.04	802.37
1000	6782.0 ± 119.75	1.77	994.41

[a] - Each determination is an average of 9 separate determinations
[b] - Arbitrary units
[c] - RSD (%) of each point from the regressed line
[d] - predicted concentration calculated from the regression equation.

Table 6: Accuracy and precision data for the spectrofluorimetric method.

Level	Predicted con. (µg/ml) [a]			Mean % recovery (± SD)	Accuracy (%) [b]
	Range	Mean (± SD)	% RSD		
LQC	296.02 - 313.20	303.73 ± 3.86	1.27	101.24 ± 1.288	1.24
MQC	483.97 - 503.68	493.38 ± 5.22	1.06	98.68 ± 1.043	-1.32
HQC	872.03 - 919.67	890.72 ± 10.66	1.20	98.97 ± 1.184	-1.03

[a] - predicted concentration of etoposide was calculated by linear regression equation
[b] - accuracy is expressed in % relative error.

Table 7: Intra-day and inter-day variability for spectrofluorimetric method.

Level	Intra-day repeatability % RSD (n=3)			Inter-day repeatability % RSD (n=27)
	Day 1	Day 2	Day 3	
LQC	0.249	2.213	0.179	0.265
	2.123	0.582	0.176	
	0.930	0.462	1.430	
MQC	0.799	0.046	0.098	0.372
	1.435	0.097	0.426	
	0.621	0.744	0.446	
HQC	1.729	1.978	0.010	0.043
	0.747	0.072	0.587	
	1.477	1.529	1.548	

Table 8: Determination of etoposide in pharmaceutical preparations by spectrofluorimetric method.

Preparation	Assay (± SD)	% Recovery (± SD)
Etosid soft gelatin capsules - 50 mg/capsule	50.10 ± 0.88	100.21 ± 1.76
Etosid injection - 20 mg/ml	19.88 ± 0.15	99.40 ± 0.73
Fytosid injection - 20 mg/ml	19.92 ± 0.26	99.62 ± 1.27

Each determination is an average of 5 separate determinations

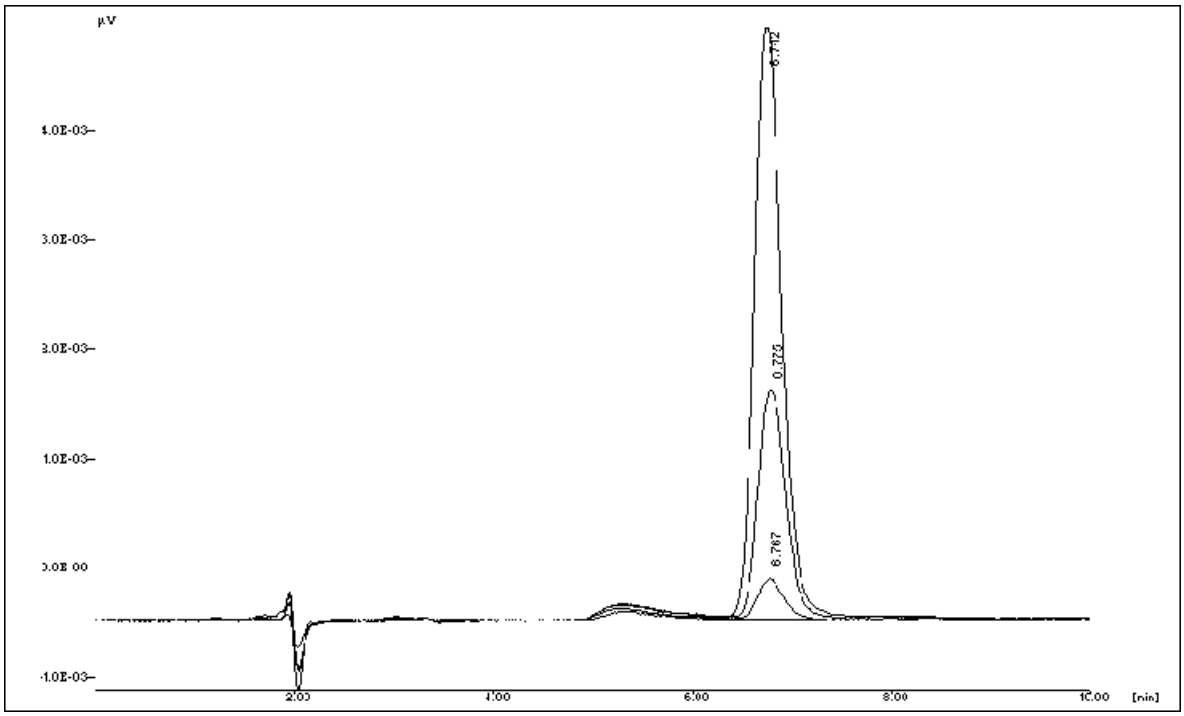

Figure 4: Chromatograms of mobile phase (methanol: ammonium acetate buffer 50:50 v/v), 50, 400 and 1000 ng/ml of etoposide obtained using HPLC.

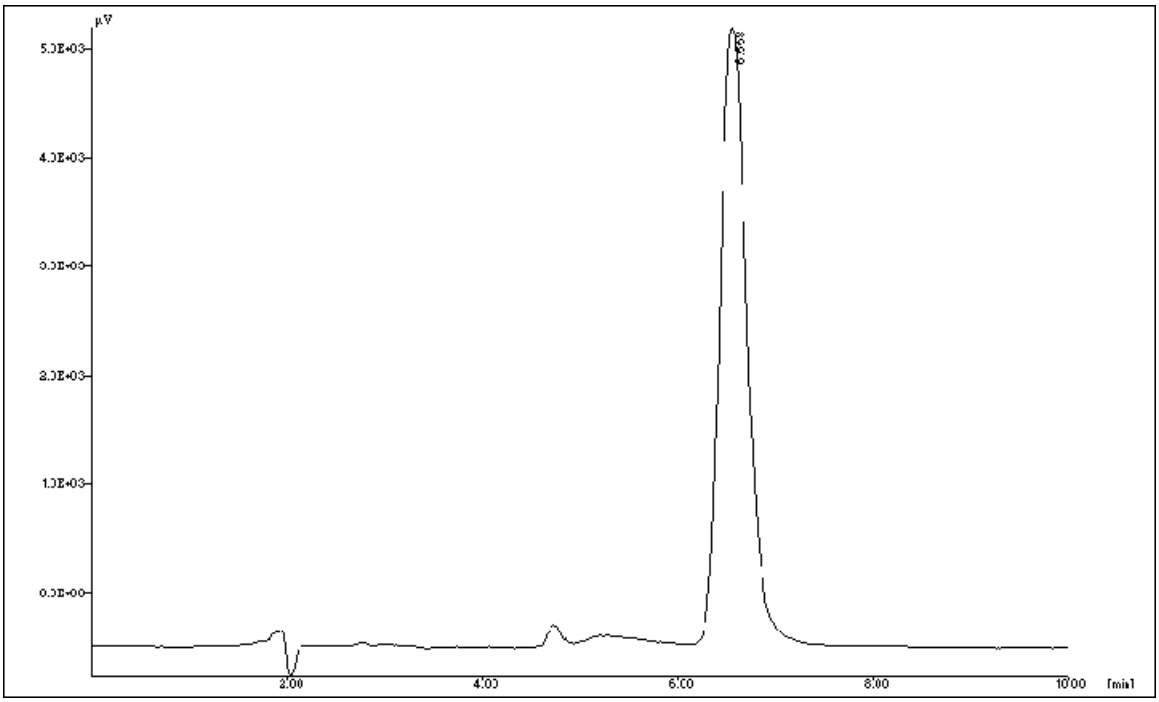

Figure 5: Chromatogram of etoposide present in marketed formulation (Etosid Injection) estimated using HPLC.

Table 9: Etoposide calibration curve data for HPLC method.

Etoposide (ng/ml)	**Area [a] (mV-sec) (± SD)**	**% RSD [b]**	**Predicted Con. [c] (ng/ml)**
50	3168.42 ± 32.62	1.03	49.53
200	11592.33 ± 149.27	1.29	201.91
400	22441.96 ± 302.96	1.35	398.17
600	33600.25 ± 149.08	0.44	600.01
800	45413.97 ± 134.97	0.30	813.70
1000	55145.41 ± 584.23	1.06	989.73

[a] - Each determination is result of 6 separate determinations
[b] - RSD (%) of each point from the regressed line
[c] - predicted concentration calculated from the regression equation.

Table 10: Accuracy and precision data for the developed HPLC method.

Level	Predicted con. (ng/ml) [a]			Mean % Recovery (± SD)	Accuracy (%) [b]
	Range	Mean (± SD)	% RSD		
LQC	96.69 - 106.61	102.27 ± 2.50	2.44	102.27 ± 2.50	2.27
MQC	484.61 - 518.19	496.57 ± 9.83	1.98	99.31 ± 1.97	-0.69
HQC	776.0 - 848.16	806.35 ± 18.34	2.27	100.79 ± 2.29	0.79

[a] - predicted concentration of etoposide was calculated by linear regression equation
[b] - accuracy is expressed in % relative error.

Table 11: Intra-day and inter-day precision of the developed HPLC method.

Level	Intra-day repeatability % RSD (n=3)			Inter-day repeatability % RSD (n=18)
	Day 1	Day 2	Day 3	
LQC	2.026	2.789	0.172	1.932
	2.393	0.489	0.347	
MQC	1.475	1.991	2.138	1.368
	1.929	1.589	0.147	
HQC	0.730	0.526	2.521	1.431
	0.361	1.484	2.170	

Table 12: Determination of etoposide in pharmaceutical preparations by HPLC method.

Preparation	Assay (± SD)	% Recovery (± SD)
Etosid soft gelatin capsules - 50 mg/capsule	50.78 ± 0.81	101.56 ± 1.39
Etosid injection - 20 mg/ml	20.24 ± 0.28	101.18 ± 2.05
Fytosid injection - 20 mg/ml	20.09 ± 0.59	100.46 ± 1.63

Each determination is an average of 5 separate determinations

References

Beijnen, J.H., Holthuis, J.J.M., Kerkdijk, H.G., van der Houwen, O.A.G.J., Paalman, A.C.A., Bult, A., Underberg, W.J.M., 1988. Degradation kinetics of etoposide in aqueous solution. Int. J. Pharm. 41, 169-183.

Bolton, S., 1997. In: Bolton, S., (Ed.), Pharmaceutical statistics: practical and clinical applications. Marcel Dekker, New York, pp. 216-514.

Eisenberg, E.J., Eickhoff, W.M., 1993. Determination etoposide in blood by liquid chromatography with electrochemical detection. J. Chromatogr. 621, 110-114.

Floor, B.J., Klein, A.E., Muhammad, N., Ross, D., 1985. Stability indicating liquid chromatographic determination of etoposide and benzyl alcohol in injectable formulations. J. Pharm. Sci. 74, 197-200.

Igwemezie, L.N., Kaul, S., Barbhaiya, R.H., 1995. Assessment of toxicokinetics and toxicodynamics following intravenous administration of etoposide phosphate in beagle dogs. Pharm. Res. 12, 117-123.

International Conference on Harmonisation (ICH), ICH Harmonised tripartite guideline. 1996. Topic Q2B, Note for Guidelines on Validation of Analytical Procedures: Methodology.

Liliemark, E., Petterson, B., Peterson, C., Liliemark, J., 1995. High performance liquid chromatography with fluorimetric detection for monitoring of etoposide and its *cis*-isomer in plasma and leukemic cells. J Chromatogr. B: Biomed. Sci. and Appl. 669, 311-317.

McLeod, H.L., Relling, M.V., 1992. Stability of etoposide solution for oral use. Am. J Hosp. Pharm. 49, 2784-2785.

Mross, K., Bewermeier, P., Kruger, W., Stockschlader, M., Zander, A. Hossfeld, D.K., 1994. Pharmacokinetics of undiluted or diluted high-dose etoposide with or without busulfan administered to patients with hematologic malignancies. J. Clin. Oncol. 12, 1468-1474.

Shah, J.C., Chen, J.R., Chow, D., 1989. Preformulation study of etoposide: identification of physicochemical characteristics responsible for the low and erratic bioavailability. Pharm. Res. 6, 408-412.

Sinkule, J.A., Evans, W.E., 1984. High performance liquid chromatographic analysis of the semisynthetic epipodophyllotoxins teneposide and etoposide using electrochemical detection. J. Pharm. Sci. 73, 164-168.

Strife, R.J., Jardine, L., Colvin, M., 1980. Analysis of the anticancer drugs VP 16-213 and VM 26 and their metabolites by high-performance liquid chromatography. J. Chromatogr. B. Biomed. Sci. and Appl. 182, 211-220.

Strife, R.J., Jardine, L., Colvin, M.; 1981. Analysis of the anticancer drugs etoposide (VP 16-213) and teneposide (VM 26) by high-performance liquid chromatography with fluorescence detection. J Chromatogr. B. Biomed. Sci. and Appl. 224, 168-174.

United States Pharmacopoeia (USP). 2003. Validation of compendial methods, Pharmacopoeial Convention, Inc., Rockville, MD. 2439-2440.

Van Opstal, M.A.J., van der Horst, F.A.L., Holthuis, J.J.M., Van Bennekom, W.P., Bult, A., 1989. Automated reversed phase chromatographic analysis of etoposide and teneposide in plasma using on-line surfactant-mediated sample clean-up and column-switching. J. Chromatogr. 495, 139-151.

Werkhoven-Goewie, C.E., Brinkman, U.A.T., Frei, R.W., Ruiter, C., de Vries, J., 1983. Automated liquid chromatographic analysis of the anti-tumorigenic drugs etoposide (VP 16-213) and Teneposide (VM 26). J. Chromatogr. 276, 349-357.

Chapter 4

Preformulation Studies

4.1. Introduction

For any formulation development, preformulation study is very critical and important. Preformulation studies help in the determination of critical physicochemical properties of a drug substance which are important to decide possible formulation. The goal of preformulation study is to choose the correct form of drug substance, evaluate its physical properties, and generate a thorough understanding of the material's stability under various conditions, leading to an optimal drug delivery system. An adequate understanding of the properties of the drug substance will minimize problems in formulation stages and reduce formulation costs. These studies generally include generation of pH - solubility data, pH - stability, partition coefficient, determination of dissociation constant of the drug, interaction with excipients and stability of drug in solution state and solid state. Scientific approach of preformulation study can make formulations easy, cheaper and effective.

For drugs with poor and erratic bioavailability, physicochemical study can also indicate reason of such problems (D'Incalci et al, 1982, Harvey et al, 1985). This knowledge can help to decide logical and effective approaches to design a suitable dosage form for better availability. pH-solubility and pH-stability profile of etoposide were established, with the pH range encountered in the gastro intestinal tract. Solid state stability of etoposide was done in presence of different polymers and excipients, which are being used in the design of etoposide formulations. In addition, n-octanol/water and chloroform/water partition coefficient of etoposide was also determined.

4.2. Materials, Equipment/Instruments and Reagents

4.2.1. Materials

Etoposide was received from Dabur research centre, Sahibabad as gift sample. Poly lactide co glycolide (PLGA 50/50, Molecular wt. 10000), Pluronic F 68 (F 68), Polyvinyl alcohol (PVA) and Poly e caprolactone (PCL, Mol wt. 40000) were purchased from Sigma Aldrich Chemicals. Other PLGA co polymers PLGA 75/25 (Purasorb® 75/25, Molecular wt. 10000) and PLGA 85/15 (Purasorb® 85/15, Molecular wt. 10000) were generously gifted by Purac chemicals, Netherlands. Eudragit L-100 (EuL-100) was gifted by Aurobindo Laboratories Ltd., Hyderabad, India. All other chemicals were purchased from Qualigens, Mumbai.

4.2.2. Equipment/Instruments

A constant temperature water bath (MAC instruments, India) was used for solubility studies. Stability studies were carried out in Frost-free-200 L Godrej refrigerator for the

studies at refrigerated condition, a humidity chamber (MAC Instruments, India) was used to maintain 40°C± 2°C/75 % RH. All pH measurements were performed using Elico pH meter equipped with combination glass electrode filled with potassium chloride gel and with auto temperature adjustments. Thermal analysis was performed using a Shimadzu (Japan) differential scanning calorimeter (model: DSC-60, integrator: TA-60WS thermal analyzer, integrating software: TA-60WS collection monitor version 1.51, analysis software: TA60, principle: heat flux type, temperature range: -150-600°C, heat flow range: ± 40 mW, temperature program rate: 0-99°C/min and atmosphere: inert nitrogen at 30 ml/min).

4.2.3. Reagents

Preparation of Buffered Solutions: Different buffer systems pH ranging from 1.2 to 10 with 0.1 M molar strength were prepared as given in USP (USP, 2003).

Preparation of Unbuffered Solutions: Unbuffered solutions of pH ranging 2 to 8 were prepared by using variable volumes of 0.1 N HCl and 0.1 N NaOH solutions.

4.3. Methods

4.3.1. Determination of Solubility

Different buffered and un-buffered systems (2.0-8.0) of varying pH from 2 to 8 were used to determine solubility of etoposide at 37 ± 2°C. Excess amount of etoposide was added to vials containing 10 ml of different buffers of pH 2.0, 3.0, 4.0, 5.0, 6.0, 6.8, 7.4 and 8.0. Unbuffered systems of above mentioned pH were also kept for shaking with excess of etoposide. The sample vials were agitated for 48 hr using water bath shaker at 37 ± 2°C. After 48 hr, two ml samples were taken and filtered through Whatman filter paper. Clear solutions obtained were diluted and analyzed using analytical method 1 described in chapter 3. For unbuffered pH, stirring was continued for 12 h only as pH found to be changed after that.

4.3.2. Determination of Partition Coefficient

Partition coefficient of etoposide was determined in n-octanol/water and chloroform/water systems. The n-octanol, triple distilled water (TDW) and chloroform TDW were pre-saturated with each other for 24 h. They were separated after 24 h by centrifugation at 2000 rpm for 5 min. Five ml of octanol and chloroform were taken separately in vials and then to each 5 ml of TDW containing 80 µg/ml of etoposide was added. These vials were kept for constant shaking on mechanical shaker at room

temperature. At the end of 24 h, one ml of aqueous phase was taken and centrifuged at 2000 rpm for 5 min. After equilibrating at room temperature for 15 min, aqueous phase was removed and analyzed by analytical method 2. Partition coefficient of etoposide was calculated by the following equation. Volume of both the media are same.

$$P_{o/w} = C_o/C_w -= (A_i-A_f)/A_f$$

Where, C_o = Concentration of drug in oily phase

C_w = Concentration of drug in aqueous phase

$P_{o/w}$ = Apparent partition coefficient;

A_i = Initial amount of drug in aqueous phase; and

A_f = Final amount of drug in aqueous phase

4.3.3. Determination of Stability

Both solution state stability and solid state stability of etoposide were determined. Solution state stability study was done with different buffer systems to establish pH - stability profile where as solid state stability was done in presence of different polymers and excipients at three different temperatures. Etoposide solution stability at different pH was also confirmed using thin layer chromatography (TLC).

a) Solution State Stability

A concentration of 20 µg/ml of etoposide was prepared in buffered solutions of different pH (1.2-10) and used in the study. These solutions were stored at room temperature in a closed container. Samples were taken at different time points, diluted suitably and analyzed by analytical method 2. TLC was done using methanol and chloroform (7:3 v/v ratio) as mobile phase, to check the degradation of etoposide in aqueous buffer systems. Etoposide dissolved in methanol was taken as control in all TLC plates. Etoposide in 0.01 N, 0.1 N HCl and 0.01 N, 0.1 N NaOH, acetate buffer (pH 4.0), TDW (pH 6.8) and phosphate buffer (pH 7.4) were used in the study to confirm the degradation of etoposide in aqueous media.

b) Solid State Stability Study

Etoposide (# 40 passed) and different excipients short listed for the preparation of nanoparticle formulations were physically mixed in a ratio of 1:10 (for polymers) and 1: 100 (for stabilizers). Excipients used for this study are PLGA 50/50, PCL, EuL-100, F 68 and PVA. Among all these excipients PLGA polymer was highly crystalline and was not forming uniform physical mixture. Thus etoposide and PLGA in 1:10 ratio were dissolved

in acetone and acetone was evaporated on hot plate and then vacuum dried. The remaining material was powdered and used for solid state stability study.

The drug and its corresponding physical mixtures with different excipients were prepared carefully, filled in vials and kept at different temperature conditions, room temperature (RT: 25 ± 2°C), refrigerated temperature (FT: 5 ± 2°C) and at accelerated condition (40°C ± 2°C/75 % RH). The samples were taken at predetermined time intervals in triplicate and analyzed for drug content after suitable dilution with analytical method 1.

c) Thermal Study of drug and excipient physical mixtures

Differential scanning calorimetry (DSC) was done for etoposide, individual excipients and physical mixture of etoposide with excipients (1:1). Around 2 to 2.5 mg of the material was taken and sealed in standard aluminum pans with lid. The temperature range of measurement was 30°C to 300°C with a heating rate of 10°C/min. After measurement, temperature was decreased back to starting temperature by cooling. Exothermic peaks recorded in the thermograms are directed upwards.

4.4. Results and Discussion

4.4.1. Solubility

The solubility of etoposide at 37 ± 2°C in various buffers and unbuffered solutions of different pH ranging from 2 to 8 is presented in Table 1. The pH - solubility profile of etoposide in both buffered and unbuffered pH solutions is shown in Figure 1. Solubility in buffered systems remained nearly same over the pH range of 2 to 5 (184.33 ± 2.15 at pH 2 and 185.88 ± 3.10 µg/ml) however solubility was decreased as pH increased from 6.0 to 8 (180.24 ± 1.63 µg/ml at pH 6.0 to 140.05 ± 2.56 µg/ml at pH 8.0). In case of unbuffered pH solutions, solubility decreased continuously as pH increased from 2 to 8. Between pH 2 to 6.8, solubility of etoposide was found to be slightly higher in buffer system. However, at 7.4 and 8 pH, solubility was same in both the systems.

Insufficient aqueous solubility of drug has been known to yield poor and erratic absorption with large inter and intra subject variations in blood levels (Martin et al, 2001). Potential bioavailability problems are often present when the aqueous solubility of a drug is less than 10 mg/ml. The low aqueous solubility of etoposide may be responsible for its poor and erratic oral absorption. Solubility of etoposide was very inadequate to result in complete dissolution of the usual oral dose of 50 mg in gastric fluids. Etoposide has a high melting point, which is indicative of strong crystal lattice energy. This high melting point is one of the factors responsible for lower solubility (Shah et al, 1989).

4.4.2. Partition Coefficient

The equilibrium partition of etoposide between n-octanol and water phase and chloroform and water phase was achieved in 24 hr. The partition coefficient for n-octanol/water and chloroform/water systems were 8.814 ± 0.158 and 6.147 ± 0.780 respectively (Table 2). Log P of etoposide in these systems was 0.945 ± 0.008 and 0.786 ± 0.055 respectively. Partition coefficient values of etoposide in both systems reflect the high lipophilicity of the drug. The inverse correlation between the partition coefficient and the rate and extent of absorption of a drug may also be reason for the poor and erratic absorption and has been reported by Shah et al, (1995).

4.4.3. Stability

a) Solution State Stability

Stability of etoposide was found to be poor at different pH with maximum stability at pH 5. The Log percent remaining to be degraded (Log % RTD) versus time profiles were presented in Figure 2. The linear profile for all plots at all pH's indicated first order degradation. Degradation rate constants obtained from the slopes of the curves were used to determine the half lives at various pH. The pH - stability profile of etoposide is shown in Figure 3. The degradation was rapid under highly acidic and alkaline conditions. The degradation half lives were 0.111 and 0.114 days at pH 1.2 and 10 respectively, while 5 to 6.0 was the pH range of maximum stability, with degradation half life of 57.673 and 45.973 days respectively. The degradation rate constants on the highly acidic and basic side were 6.241 $day^{-1}$and 6.096 day^{-1} respectively; therefore the degradation of etoposide is both acid and base catalyzed (Martin et al, 2001). Observed first order degradation rate constants (K_{deg}), $t_{1/2}$ and $t_{90\%}$, regression coefficient and MSSR, are listed in Table 3 for buffered solutions. These results were similar to that of the study conducted by Shah et al, (1989).

Orally administered drug needs to be stable during its transit through the gastrointestinal tract of various pH ranging from 1.2 to 8. Etoposide is most stable in the pH range of 5 to 7.4 and rapidly degraded at pH < 2.0 and pH > 8. The rapid degradation of etoposide in gastric fluid could also account for its low oral bioavailability. To effectively improve bioavailability of etoposide a formulation should be such that stability of etoposide is enhanced during its transit through gastric media.

TLC plate developed for 0.1 N HCl showed one extra spot other than etoposide under UV wavelength of 254 nm after 12 h of study. The same was observed for TLC plates developed for 0.01 N HCl, 0.1 N NaOH, and 0.01 N NaOH. This confirms the degradation

of etoposide at extreme lower and higher pH. When the TLC was done for etoposide in sodium acetate buffer (pH 4.0), TDW (pH 6.8) and phosphate buffer (pH 7.4), only one spot corresponding to etoposide was observed. This shows the stability of etoposide at these pH conditions. There was no difference in the retention factor (R_f) values of etoposide (R_f - 0.658) alone and etoposide in different buffers. These results correlate with the pH - stability study of etoposide.

b) Solid State Stability

Drug content in physical mixture of etoposide and formulation excipients, prepared in 1: 10 ratio (for polymers) and in 1:100 ratios for other excipients, was given in Table 4 to 9. Etoposide was stable at all temperatures in the study whereas etoposide with PLGA 50/50 was stable at refrigerated conditions for 12 months. After 24 months, the assay value of etoposide decreased to 89.29 % at RT, and to 94.29% at FT. Physical mixture of etoposide and PCL was stable for 12 months at both RT and 5°C ± 2°C. Assay values of etoposide after 24 months at these temperatures decreased to 90.79% and to 94.50% respectively. In presence of EuL-100, etoposide was stable for 24 months at RT and FT as there was no difference in the assay value of etoposide after 12 months and 24 months of storage at RT and FT.

Physical mixture of etoposide with F 68 was also stable at FT indicated by the assay value of 96.77% after 24 months. But the same physical mixture at room temperature was stable for only 12 months period of time showing degradation (% assay after 24 months 94.50%). Etoposide and PVA in 1:100 ratio was stable at both RT and at 5°C ± 2°C, represented by % assay (Table 9).

Etoposide alone was stable at 40°C± 2°C/75% RH for 6 months. At 40°C± 2°C/75% RH, in all physical mixtures degradation of etoposide was observed after some time indicating little incompatibility in combination with other excipients. This can be due to the low melting point of polymers and stabilizers used in the study (Lemoine et al, 1996). These results could also indicate the stability of etoposide when formulated using all these excipients. Storing at 40°C ± 2°C/75% RH may not maintain the stability of the preparation. They can be stored at RT and at FT conditions for longer period of time. This study gives valuable information regarding the stability of etoposide in presence of selected excipients at various storage conditions and for deciding formulation excipients.

c) Thermal Study of drug and excipient physical mixtures

DSC thermogram of etoposide shows that it exists in two polymorphic forms. There is sharp endothermic peak at 179.81°C, an exothermic transition at 218.49°C followed by another endotherm at 286.09°C. According to earlier reports etoposide exhibits polymorphism, the endotherm at 179.81°C corresponds to the melting of etoposide form Ia, the anhydrous form of etoposide, which soon begins to crystallize to a different polymorphic form, etoposide IIa (crystallization exotherm at 218.49°C). Another endotherm at 286.09°C is attributed to the melting point of the newly formed etoposide IIa. The polymorphic transition was concluded to be monotropic (Jasti et al, 1995). Thus present DSC of etoposide matches with the previous results.

Figures 4 to 9 represent thermograms of etoposide, excipient and physical mixtures of etoposide with different polymers and stabilizers selected for study. Melting endotherms of etoposide were well preserved in most of the cases. However, there were slight changes in the peak shape with little broadening or shifting towards the lower temperature, which could be attributed to the mixing process that lowers purity of each component in the mixture (Verma and Garg, 2004). In case of PLGA co polymers, there was no melting peak was observed for respective polymers (Figure 4 to 6). But glass transition was present and they were increased with increase in lactide content of the polymer (Table 10). Physical mixture of etoposide with these polymers showed the endothermic peaks and exothermic peak of etoposide. There was no change in enthalpy value of etoposide in these physical mixtures. Etoposide is compatible with PLGA co polymers.

Figure 7 shows the thermograms of pure etoposide, PCL and physical mixture of etoposide with PCL (1:1). PCL showed sharp endothermic peak at 64.44°C represents its melting. The endothermic and exothermic peaks of etoposide were retained in the physical mixture with a minute change in enthalpy value (Table 10). Based on the results, it was concluded that etoposide is compatible with PCL.

The DSC thermogram of F 68 showed an endothermic peak at 53.34°C (Figure 8). Endothermic peak of etoposide form Ia was very small or insignificant in the thermogram of the physical mixture of etoposide and F 68 (1:1). Exothermic peak, which is melting peak of form Ia was missing and the endothermic peak of the form IIa of etoposide, was shifted to lower temperature (231.34°C). There was no broadening or any change in shape of endothermic peak of etoposide. Degradation of F 68 was observed at and above 200°C. This might be causing the shift of etoposide form IIa endothermic peak. Enthalpy values of both the forms of drug were not changed significantly. This indicates there is no possible incompatibility between drug and Pluronic F 68.

Figure 9 shows thermograms of etoposide, PVA, physical mixture of etoposide and PVA in 1:1 ratio. PVA showed melting peak at 222.29°C and degradation endotherm at around 274°C. Thermogram of physical mixture showed endothermic peak of etoposide at 180.07°C with no difference in the enthalpy value between pure etoposide and physical mixture. This indicates there is no possible incompatibility between drug and PVA. Peak shape of exothermic peak of etoposide in the physical mixture was changed. This is because melting endotherm of PVA merged with the exotherm of etoposide. Endothermic peak of etoposide from IIa was shifted and was merged with degradation endotherm of PVA showing a split peak (Verma and Garg, 2004).

4.5. Conclusions

pH - solubility studies in different buffered and unbuffered systems showed low solubility of the etoposide. Degradation of etoposide in different aqueous buffer systems followed first order. Etoposide is compatible and stable for 12 months with all the polymers and stabilizers selected for the study at RT and FT. At 40°C± 2°C/75 % RH there was degradation of etoposide with all the excipients used. Extensive degradation was observed in presence of PLGA 50/50, PCL, and F 68 at 40°C± 2°C/75 % RH. There was no possible degradation of etoposide in presence of excipients used in the study at RT and FT. The low aqueous solubility, rapid degradation at pH 1.2 of etoposide may account for the low and erratic bioavailability of the drug. Therefore approaches to increase the aqueous solubility and prevent degradation in gastric fluid may effectively improve the oral bioavailability of etoposide.

Table 1: Solubility of etoposide at 37°C in buffered and unbuffered systems of various pH.

pH	Solubility (µg/ml) Mean ± SD	
	Unbuffered Systems*	**Buffered Systems**
2.0	172.45 ± 3.11	184.33 ± 2.15
3.0	170.55 ± 4.51	183.82 ± 2.26
4.0	163.94 ± 4.64	180.58 ± 3.42
5.0	158.58 ± 2.00	185.88 ± 3.10
6.0	151.09 ± 4.78	180.24 ± 1.63
6.8	149.24 ± 4.92	175.36 ± 1.42
7.4	148.94 ± 4.79	151.18 ± 4.42
8.0	143.03 ± 4.41	140.05 ± 2.56

Each value is mean of 3 independent determinations
* Study was done for 12 h

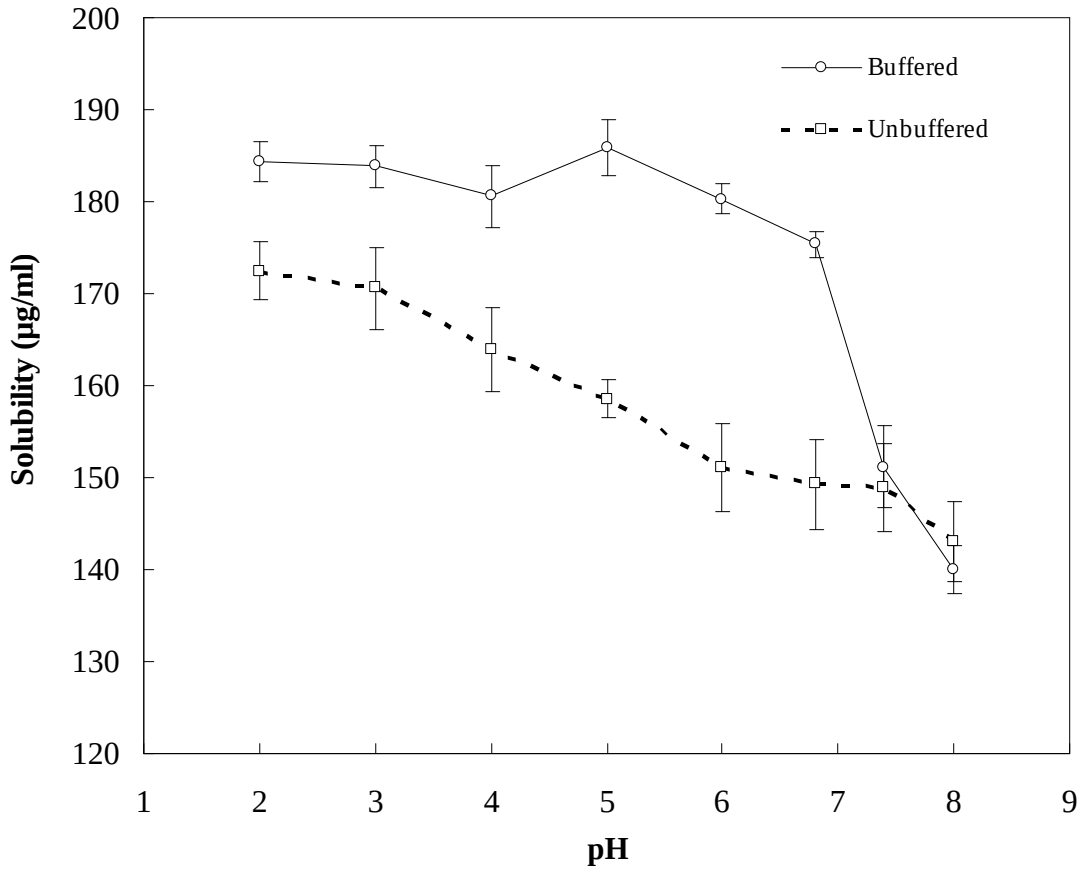

Figure 1: pH - solubility profile of etoposide. (Each point represents the mean of 3 determinations).

Table 2: Partition coefficient data of etoposide at different time points.

Time (h)	Octanol/Water system (Avg ± SD)		Chloroform/Water system (Avg ± SD)	
	$P_{o/w}$	Log $P_{o/w}$	$P_{Cl/w}$	Log $P_{Cl/w}$
12	3.559 ± 0.337	0.945 ± 0.008	4.659 ± 0.137	0.786 ± 0.055
24	8.814 ± 0.158		6.147 ± 0.780	

Each value is mean of 3 independent determinations

Table 3: pH - stability data for etoposide in buffered systems at room temperature.

pH	k_{deg} (day^{-1}) Mean ± SD	$t_{1/2}$ (days) Mean ± SD	$t_{90\%}$ (days) Mean ± SD	Regression	MSSR
1.2	6.241 ± 0.123	0.111 ± 0.002	0.017 ± 0.001	0.9980	0.004
2.0	0.697 ± 0.032	0.996 ±0.045	0.152 ± 0.007	0.9934	0.016
3.0	0.083 ± 0.004	8.359 ± 0.391	1.271 ± 0.059	0.9960	0.006
4.0	0.028 ± 0.001	24.853 ± 0.622	3.780 ± 0.095	0.9988	0.002
5.0	0.012 ± 0.001	57.673 ± 2.713	8.772 ± 0.413	0.9936	0.001
6.0	0.015 ± 0.000	45.973 ± 0.858	6.992 ± 3.132	0.9977	0.001
6.8	0.018 ± 0.001	38.383 ± 1.863	5.838 ± 0.283	0.9981	0.002
7.4	0.025 ± 0.000	27.450 ± 0.460	4.175 ± 0.070	0.9976	0.001
8.0	0.121 ± 0.001	5.747 ± 0.070	0.874 ± 0.011	0.9990	0.001
10.0	6.096 ± 0.009	0.114 ± 0.001	0.017 ± 0.000	0.9983	0.001

Each value is mean of 3 independent determinations

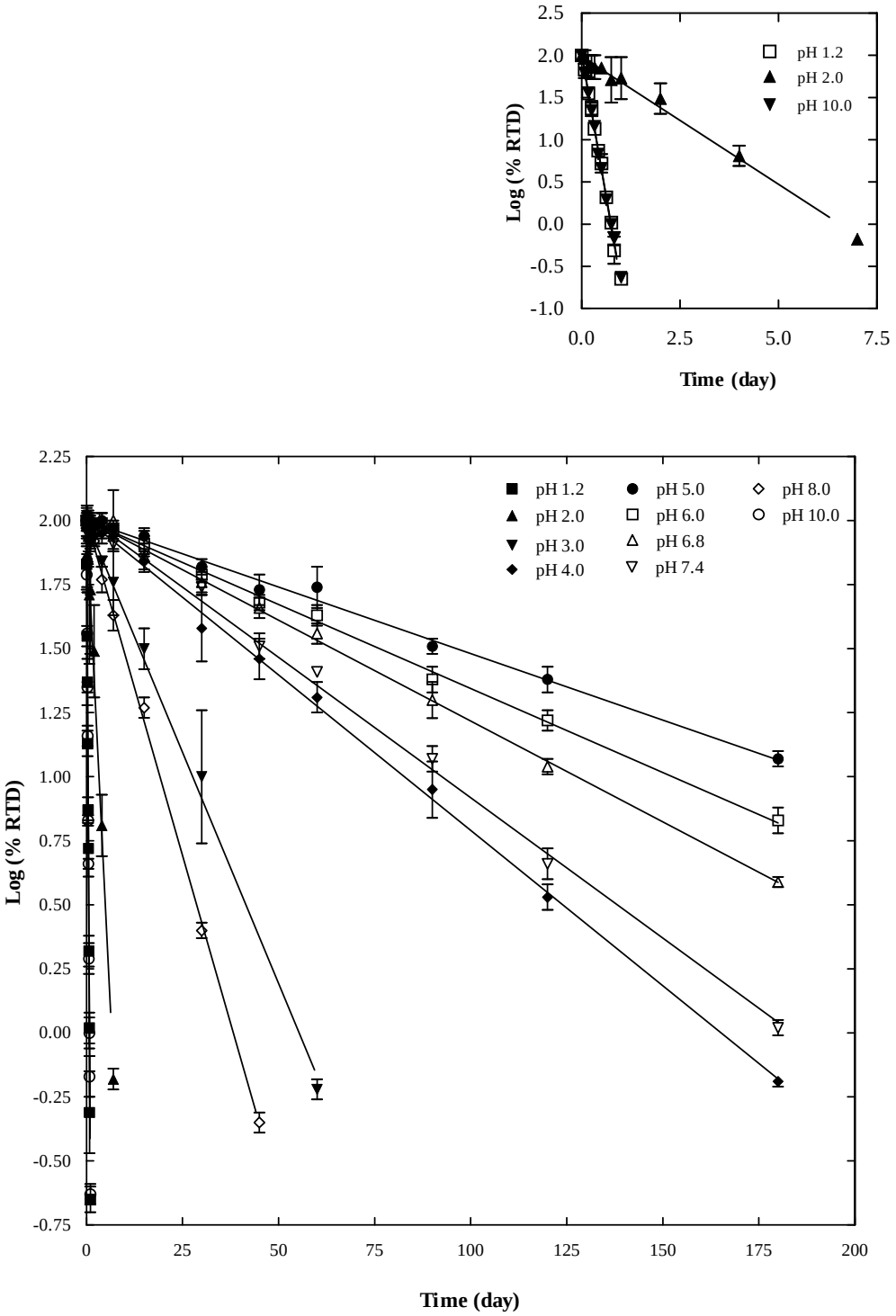

Figure 2: Log % RTD versus time plots for pH - stability of etoposide in buffered systems (Each value is the mean of 3 independent determinations).

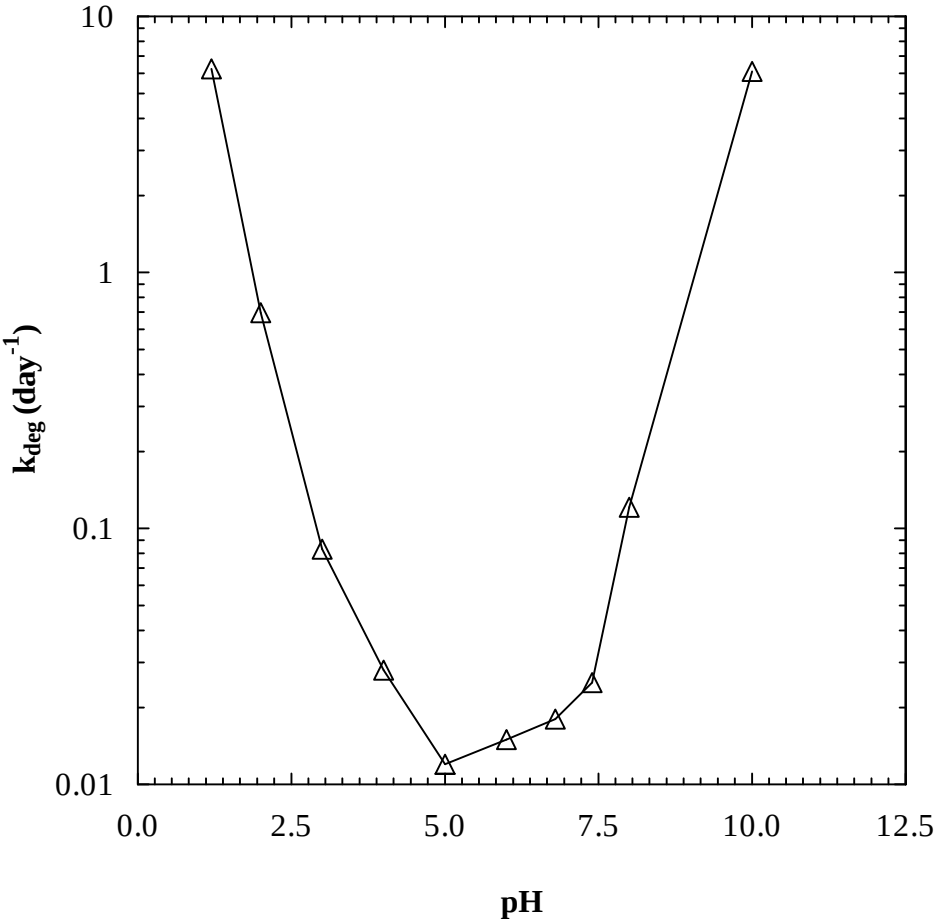

Figure 3: The pH - rate profile of etoposide at room temperature in buffered systems (each value represents the mean of 3 independent determinations).

Table 4: Stability of etoposide at different storage temperatures.

Time (months)	Assay (%) Mean ± SD		
	RT	5°C ± 2°C	40°C ± 2°C/75 % RH
0	100.12 ± 1.02		
0.5	99.21 ± 1.33	100.05 ± 0.13	100.02 ± 0.48
1.0	99.96 ± 0.22	99.44 ± 0.90	98.45 ± 0.97
3.0	99.58 ± 0.07	100.25 ± 0.61	97.58 ± 0.28
6.0	99.57 ± 0.92	99.66 ± 0.69	95.20 ± 0.57
9.0	97.65 ± 1.12	100.04 ± 0.50	-
12.0	97.62 ± 0.36	99.53 ± 0.40	-
24.0	95.96 ± 1.10	99.14 ± 0.89	-

Each value is mean of 3 independent determinations

Table 5: Stability of etoposide in presence of PLGA 50/50 (1:10) at different storage temperatures.

Time (months)	Assay (%) Mean ± SD		
	RT	**5°C ± 2°C**	**40°C ± 2°C/75 % RH**
0	100.06 ± 1.13		
0.5	99.20 ± 0.55	99.80 ± 0.48	100.17 ± 0.29
1.0	99.27 ± 1.86	100.20 ± 0.84	96.03± 0.78
3.0	99.10 ± 1.50	98.94 ±0.51	92.68 ± 0.71
6.0	99.44 ± 1.04	99.61 ±0.87	-
9.0	97.20 ± 0.91	100.04 ±0.35	-
12.0	96.96 ± 0.82	98.90 ±0.28	-
24.0	89.29 ± 0.56	94.29 ±0.14	-

Each value is mean of 3 independent determinations

Table 6: Stability of etoposide in presence of PCL (1:10) at different storage temperatures.

Time (months)	Assay (%) Mean ± SD		
	RT	**5°C ± 2°C**	**40°C ± 2°C/75 % RH**
0	99.94 ± 0.75		
0.5	100.10 ± 0.88	99.98 ± 0.26	99.92 ± 0.60
1.0	99.53 ± 0.60	100.14 ± 0.93	96.98 ± 1.58
3.0	99.55 ± 0.93	99.28 ± 1.35	91.59 ± 0.99
6.0	98.98 ± 1.23	99.57 ± 1.05	-
9.0	97.26 ± 0.52	99.98 ± 0.45	-
12.0	96.01 ± 0.82	97.69 ± 0.50	-
24.0	90.79 ± 0.51	94.50 ±1.00	-

Each value is mean of 3 independent determinations

Table 7: Stability of etoposide in presence of EuL-100 (1:10) at different storage temperatures.

Time (months)	Assay (%) Mean ± SD		
	RT	5°C ± 2°C	40°C ± 2°C/75 % RH
0	100.62 ± 1.04		
0.5	99.76 ± 0.51	100.25 ± 0.40	100.09 ± 0.24
1.0	100.07 ± 0.73	100.87 ± 0.37	100.19 ± 0.21
3.0	99.12 ± 1.38	99.49 ± 1.73	99.11 ± 0.45
6.0	99.86 ± 0.55	100.15 ± 0.60	94.01 ± 0.84
9.0	99.19 ± 0.94	99.83 ± 0.15	-
12.0	98.99 ± 0.77	99.75 ± 0.49	-
24.0	98.54 ± 0.72	98.66 ± 0.83	-

Each value is mean of 3 independent determinations

Table 8: Stability of etoposide in presence of F 68 (1:100) at different storage temperatures.

Time (months)	Assay (%) Mean ± SD		
	RT	5°C ± 2°C	40°C ± 2°C/75 % RH
0	100.04 ± 0.62		
0.5	99.79 ± 0.09	99.96 ± 0.41	97.37 ± 0.27
1.0	99.82 ± 0.39	100.15 ± 0.83	94.97 ± 1.44
3.0	100.02 ± 0.19	100.05 ± 0.10	79.72 ± 0.71
6.0	100.55 ± 0.18	99.90 ± 0.45	-
9.0	100.35 ± 0.55	100.24 ± 0.43	-
12.0	98.41 ± 0.03	99.25 ± 0.60	-
24.0	94.50 ± 0.67	96.77 ± 0.71	-

Each value is mean of 3 independent determinations

Table 9: Stability of etoposide in presence of PVA (1:100) at different storage temperatures.

Time (months)	Assay (%) Mean ± SD		
	RT	5°C ± 2°C	40°C ± 2°C/75 % RH
		99.98 ± 1.01	
0.5	100.17 ± 0.10	99.57 ± 0.69	100.85 ± 0.38
1.0	99.89 ± 0.42	99.54 ± 0.40	100.35 ± 0.70
3.0	101.18 ± 0.65	100.31 ± 0.32	99.90 ± 0.65
6.0	100.52 ± 0.37	100.61 ± 0.24	94.24 ± 0.69
9.0	98.63 ± 0.09	98.11 ± 0.17	-
12.0	97.61 ± 0.26	97.74 ± 0.22	-
24.0	96.76 ± 0.06	95.85 ± 0.10	-

Each value is mean of 3 independent determinations

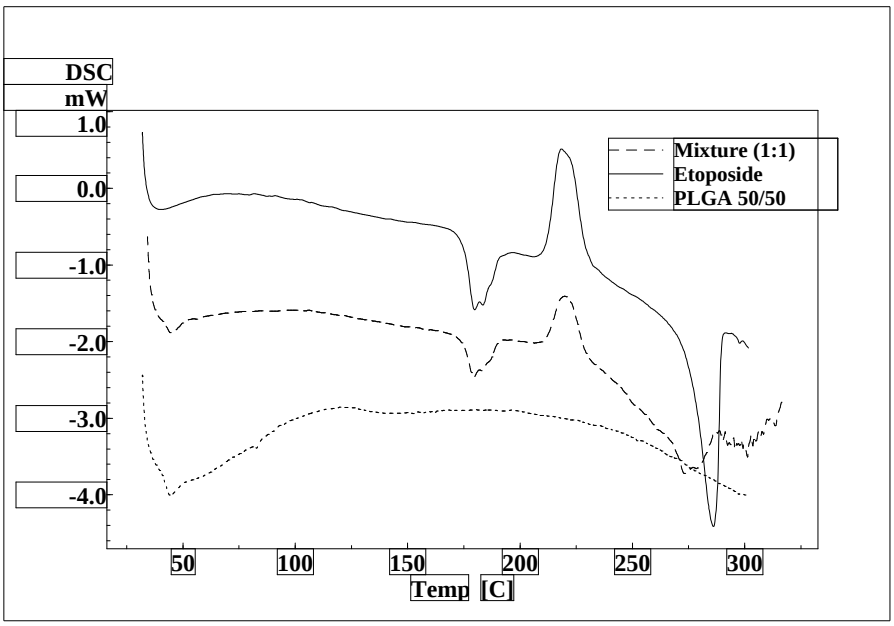

Figure 4: Thermograms of etoposide, PLGA 50/50 and mixture of both in 1:1 ratio.

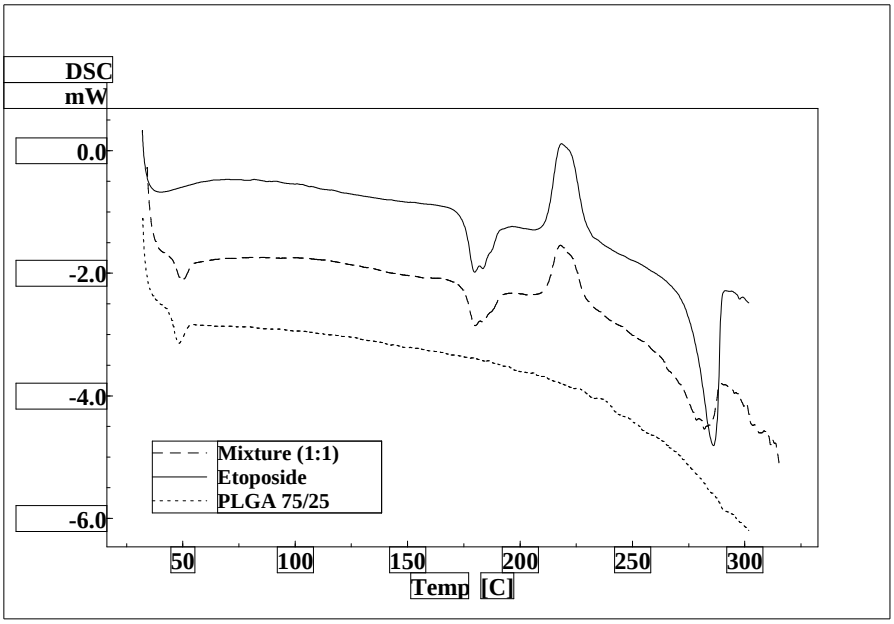

Figure 5: Thermograms of etoposide, PLGA 75/25 and mixture of both in 1:1 ratio.

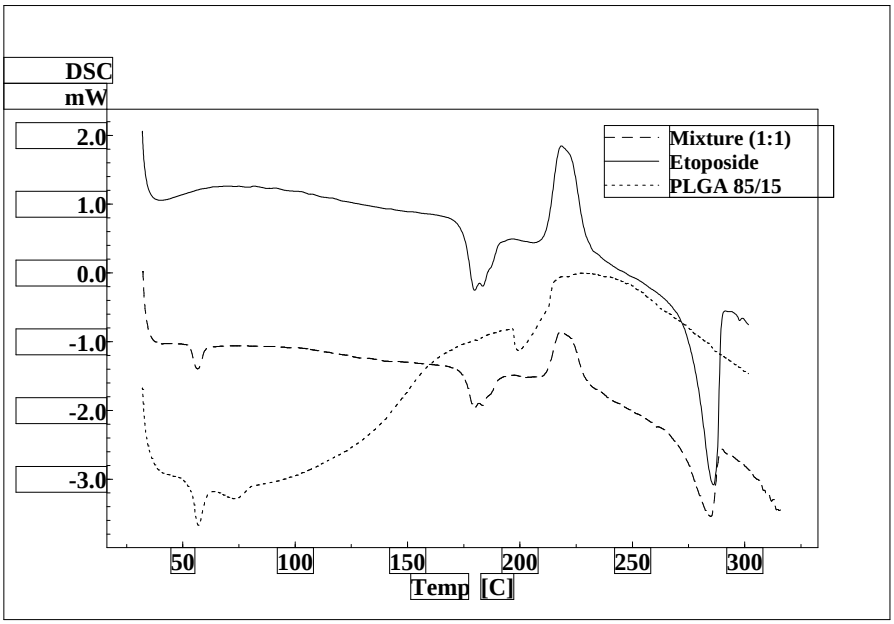

Figure 6: Thermograms of etoposide, PLGA 85/15 and mixture of both in 1:1 ratio.

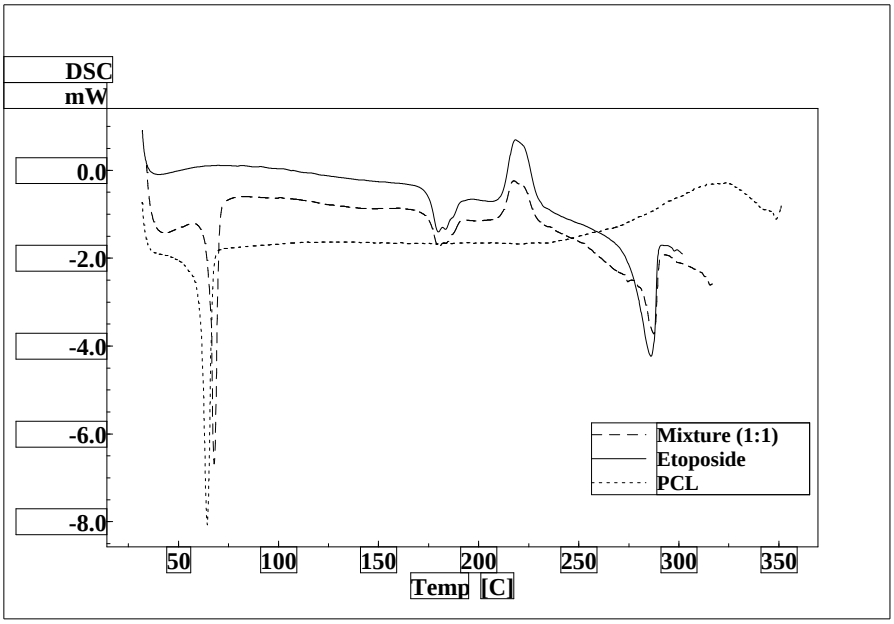

Figure 7: Thermograms of etoposide, PCL and mixture of both in 1:1 ratio.

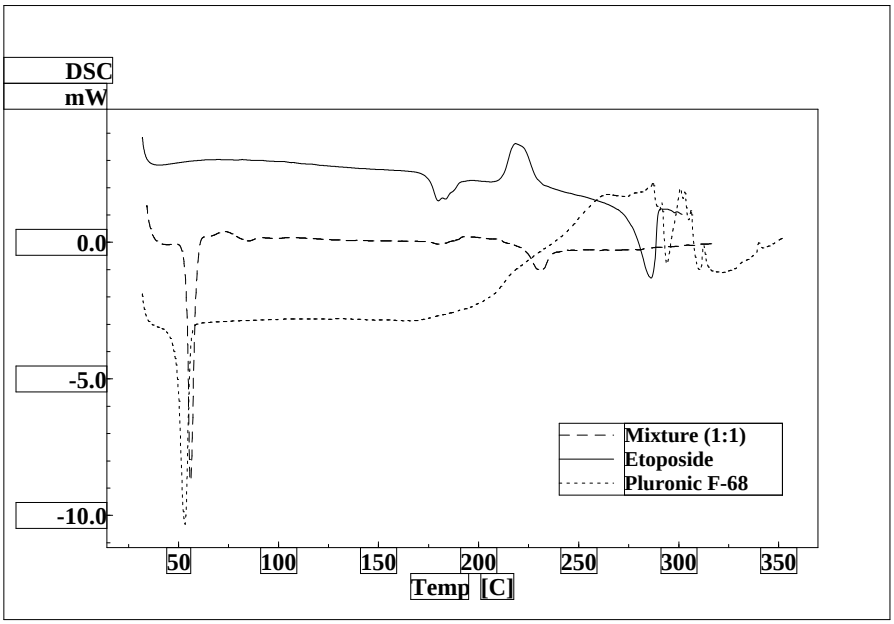

Figure 8: Thermograms of etoposide, F 68 and mixture of both in 1:1 ratio.

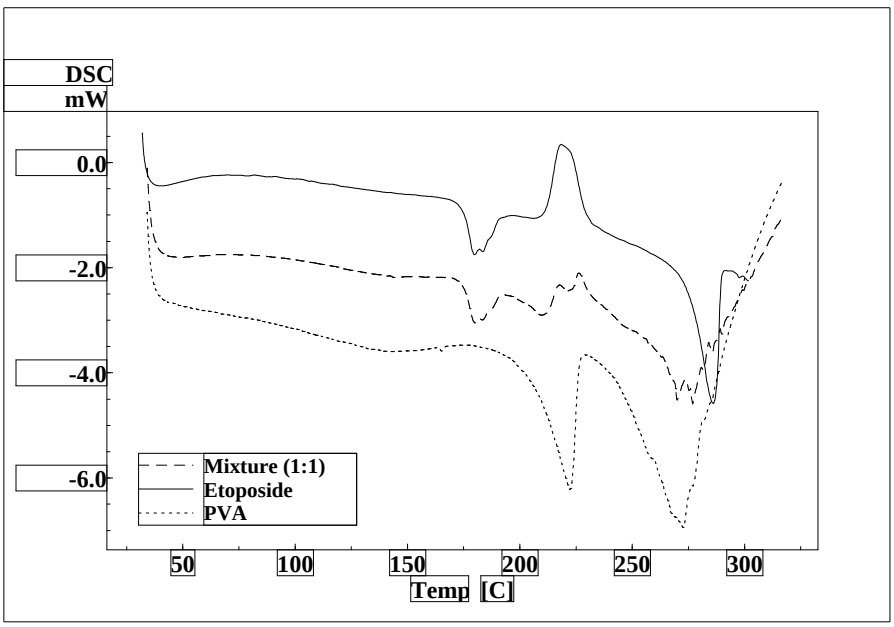

Figure 9: Thermograms of etoposide, PVA and mixture of both in 1:1 ratio.

Table 10: Thermal properties of drug, excipients alone and in combination.

Sample	Peak	Peak onset (°C)	Peak (°C)	Peak end set (°C)	Heat (J/g)
PLGA 50/50	Tg	-	42.77	-	-
PLGA 75/25	Tg	-	44.61	-	-
PLGA 85/15	Tg	-	51.64	-	-
PCL	Endo	60.69	64.44	67.20	-
F 68	Endo	49.2	53.34	55.81	-
PVA	Endo	207.94	222.29	226.24	-
Etoposide	Endo	175.08	179.81	189.76	-21.91
	Exo	211.93	218.49	229.25	43.40
	Endo	276.30	286.09	289.56	-58.12
Etoposide: PLGA 50/50	Tg	-	42.23	-	-
	Endo	174.82	179.48	190.05	-21.91
	Exo	212.32	219.85	228.37	43.67
	Endo	268.38	274.15	275.73	-60.78
Etoposide: PLGA 75/25	Tg	-	46.24	-	-
	Endo	175.13	180.14	191.05	-22.02
	Exo	211.56	217.90	228.30	43.33
	Endo	272.42	282.08	289.44	-58.28
Etoposide: PLGA 85/15	Tg	-	53.81	-	-
	Endo	175.18	179.75	190.18	-23.32
	Exo	211.78	218.24	228.30	41.85
	Endo	272.42	284.93	288.22	-58.48
Etoposide: PCL	Endo	65.97	67.82	70.11	-
	Endo	175.52	179.96	190.35	-23.55
	Exo	211.55	217.60	228.28	45.71
	Endo	282.58	287.59	289.84	-61.02
Etoposide: F 68	Endo	54.06	56.02	59.06	-
	Endo	178.05	179.81	184.56	-23.76
	Exo	-	-	-	-
	Endo	224.67	231.34	236.13	-52.51
Etoposide: PVA	Endo	-	-	-	-
	Endo	175.14	180.07	190.58	-20.82
	Exo	-	-	-	-
	Endo	-	-	-	-

Tg - Glass transition temperature; Endo - Endotherm; Exo - Exotherm

References

D'Incalci, M., Farina, P., Sessa, C., Mangioni, C., Conter, V., Masera, G., Rocchetti, M., Pisoni, M.B., Piazza, E., Beer, M., Cavalli, F., 1982. Pharmacokinetics of VP16-213 given by different administration methods. Cancer. Chemother. Pharmacol. 7, 141-145.

Harvey, V.J., Slevin, M.L., Joel, S.P., Smythe, M.M., Johnston, A., Wrigley, P.F.M., 1985. Variable bioavailability following repeated oral doses of etoposide. Eur J. Clin. Oncol. 21, 1315–1319.

Jasti, B.R., Du, J., Vasavada R.C., 1995. Characterization of thermal behavior of etoposide. Int. J. Pharm. 118, 161-167.

Lemoine, D., Francok, C., Kedzierewicz, F., Preat, V., Hoffman, M., Maincent, P., 1996. Stability study of nanoparticles of poly(e-caprolactone), poly(D,L-lactide) and poly(D,L-lactide-co-glycolide) Biomaterias. 17, 2191-2197.

Martin, A., Bustamante, P., Chun, A.H.C., 2001. In: Martin, A., (Ed.) Physical pharmacy: physical chemical properties in the pharmaceutical sciences, Lippincott Williams & Wilkins, Maryland, pp. 101-250.

Shah, J.C., Chen, J.R., Chow, D, 1995. Preformulation study of etoposide: II. Increased solubility and dissolution rate by solid dispersions. Int. J. Pharm. 113, 103-111.

Shah, J.C., Chen, J.R., Chow, D., 1989. Preformulation study of etoposide: identification of physicochemical characteristics responsible for the low and erratic bioavailability. Pharm. Res. 6, 408-412.

United States Pharmacopoeia. 2003. Validation of compendial methods, Pharmacopoeial Convention, Inc., Rockville, MD. 2439-2440.

Verma, R.K., Garg, S., 2004. Compatibility studies between isosorbide mononitrate and selected excipients used in the development of extended release formulations. J. Pharm. Biomed. Anal. 35, 449-458.

Chapter 5

Formulation Development and Characterization

5.1. Introduction

The controlled release of pharmacologically active agents to the specific site of action at the therapeutically optimal rate for intended period of time has been a major goal for formulation scientist. Several researchers discussed importance and utility of designing polymeric nanoparticle formulations with such characters (Jain, 2000; Soppimath et al, 2001).

These formulations have the ability to ensure specific drug targeting, as discussed in introduction, by both the oral route (Ponchel and Irache, 1998) and the parenteral route (Marty et al, 1978; Soppimath et al., 2001). Based on the size of the colloidal particles and the route of administration, certain drugs can be passively targeted to the areas of the body. This selective targeting of chemotherapeutic agents has two advantages. It allows for the maximum fraction of the delivered drug molecules to selectively reach and react with the cancer cells, and it minimizes side effects produced by many of the chemotherapeutic agents. The end result of targeted chemotherapy is an increase in effectiveness of the chemotherapeutic agent and decreased incidence of side effects (Schaefer and Singh, 2002). The advantages of the nanoparticles are the improvement of biodistribution, the increased therapeutic efficacy and the reduced toxicity. These drug carriers protect the drug being carried to everywhere and then target and control its release. It also provides drug protection against chemical and biological degradation related to the administration route. Therefore, the physico-chemical characteristics of the carriers themselves govern the types of application (Soppimath et al, 2001).

Erratic bioavailability of etoposide with high intra and inter subject variation is associated with its poor water solubility and stability (Shah et al, 1995). Several approaches have been tried to increase solubility and stability of etoposide: lipophilic capsules of etoposide suspension (Falkson et al, 1975); drinking ampoules (Nissen et al, 1976); hydrophilic, soft gelatin capsules containing etoposide solution (Lau et al, 1979) and solid dispersions (Shah et al, 1995). However, all these formulations yielded poor bioavailability (25-74%) with high intra and inter patient variability in the rate and extent of etoposide absorption (Phillips and Leuper 1983). Therefore, the development of a stable formulation with higher and more reproducible bioavailability than the present formulations is desirable.

Various polymers have been explored as sustained release and protective carriers of drugs to a target site and thus increase the therapeutic benefit, while minimizing side effects. Among these polymers, the thermoplastic aliphatic poly (esters) like poly (lactic acid) (PLA), poly (glycolic acid) (PGA) and especially poly (lactic co glycolic acid) (PLGA) (Leo et al, 2004), poly (e-caprolactone) (PCL) (Chawla and Amiji, 2002) has

generated tremendous interest due to their excellent biocompatibility and biodegradability and novel drug release behavior. Several of formulations using these polymers have received world wide marketing approval (Ogawa et al, 1988).

In this study, etoposide loaded nanoparticulate systems were prepared using different biodegradable and biocompatible polymers and their combination. Nanoparticles were prepared by two different techniques depending on the polymer used. Prepared nanoparticles were characterized and their in vitro release was established.

5.2. Materials, Equipment/Instruments and Reagents

5.2.1. Materials

Etoposide and other polymers were received as mentioned in the chapter 4. All other chemicals were purchased from Qualigens, Mumbai.

5.2.2. Equipment/ Instruments

Magnetic stirrer with temperature control (Remi, India), Cooling compufuge (Remi, India) was used during the preparation of nano dispersions. Lyophilizer (Heto Dry Lyo, Germany) was used for freeze drying of formulations. Zetasizer (Zeta sizer 3000HS, Malvern Instruments, UK available at Indian Institute of Chemical Technology, Hyderabad and Zeta sizer 1000HS, Malvern Instruments, UK available at Panacea Biotech, Lalru), Transmission Electron Microscopy (Morgagni, Philips, USA available at All India Institute of Medical Sciences, New Delhi), Atomic Force Microscopy (Nanoscope III, Digital Instruments, USA available at Central Electronics Research Institute, Pilani) were used for size distribution and morphological characterization.

5.2.3. Reagents

Pluronic F 68 Solution: Different concentrations, 0.5, 0.75, 1.0 and 2.0 % w/v of F 68 were prepared by dissolving 0.25, 0.375, 0.5, and 1.0 g of the same in triple distilled water and the volume was made up to 50 ml.

Polyvinyl alcohol Solution: Different concentrations of 0.5, 1.0 and 2.0 % w/v were prepared by dissolving 0.25, 0.375, 0.5 and 1.0 g of PVA in triple distilled water and subsequently volume was made up to 50 ml.

5.3. Experimental

Drug loaded and empty nanoparticles were prepared using PLGA 50/50, PLGA 75/25 and PLGA 85/15, PCL and EuL-100 polymers alone and in combination.

Nanoparticles were prepared by Nanoprecipitation technique (Fessi et al, 1989, Chen et al, 1994) and emulsion solvent evaporation method (Leroux et al, 1995) based on nature of the polymer used. However, the methods were modified according to present requirement.

At given conditions, acetone alone was not suitable to dissolve all the polymers used in this study. In order to dissolve these polymers, other solvents like ethanol and dichloromethane were tried. Finally acetone, dichloromethane, and ethanol were selected as solvents for PLGA co polymers, PCL and EuL-100 respectively.

Addition of stabilizer was necessary to maintain the stability of the system. F 68 and PVA were used as stabilizers in this study. Different process and formulation parameters were changed and final formulations were selected on the basis of size, zeta potential, drug loading and entrapment efficiency. Empty nanoparticles were prepared by the same methods of preparation for respective polymers with out adding etoposide.

5.3.1. Preparation of Nanoparticles with PLGA co Polymers

Etoposide loaded nanoparticles using different PLGA co polymers were prepared by the nanoprecipitation technique. To prepare the batches given in Table 1, typically, 25 to 200 mg of each PLGA co polymer was dissolved separately in acetone (10 ml) at room temperature (RT). Then a specified quantity of etoposide (2.5 to 20 mg) was added to the acetone solution. The resulting organic solution was added slowly with a syringe under moderate magnetic stirring into triple distilled water (TDW) containing stabilizer (25 ml). This aqueous phase immediately turns milky with formation of nanoparticle dispersion. The acetone, which rapidly diffused toward the aqueous phase, was then removed by evaporating under magnetic stirring or under reduced pressure at 35°C for approximately 1 h. After preparation, dispersion was centrifuged at 14000 rpm at 25°C for 10 min in three cycles. Supernatant containing free etoposide was analyzed for free drug content and the sediment containing nanoparticles loaded with etoposide was freeze dried.

5.3.2. Preparation of Nanoparticles with PCL

For preparing nanoparticles (Table 2) using PCL, 25 to 200 mg of PCL was dissolved in dichloromethane (10 ml) at RT. Then a specified quantity of etoposide (2.5 to 20 mg) was also dissolved in dichloromethane. Technique used for preparation of etoposide loaded PCL nanoparticles is emulsion solvent evaporation. In this, emulsion was formed when organic phase containing polymer and drug are added to the aqueous phase (TDW with stabilizer). The organic solvent was then removed by evaporating under magnetic

stirring or under reduced pressure at 35°C for approximately 1 h. Dichloromethane was selected as it is good solvent for PCL and drug and it produced nanodispersions without agglomeration and uniform size. Different parameters were changed one at a time and formulations were optimized.

5.3.3. Preparation of Nanoparticles with EuL-100

Nanoparticle dispersions containing etoposide were prepared by using ethanol as solvent for polymer. EuL-100 has not shown good solubility in acetone and dichloromethane, therefore ethanol was selected as solvent. Method used for the preparation of nanoparticles was nanoprecipitation method same as described above in section 5.3.1. Batches prepared using this polymer and composition of each batch prepared is given in Table 3.

5.3.4. Preparation of Nanoparticles with Polymer Combination

Nanoparticles were also prepared using combination of PLGA co polymers and PCL. The polymers were used in 1:1 ratio and dissolved in dichloromethane at RT. Then specified amount of etoposide was added to the dichloromethane solution. Nanoparticles were produced by emulsion solvent evaporation technique as mentioned in section 5.3.2. Composition and characters of the products are presented in Table 4.

5.3.5. Freeze Drying of Prepared Nanoparticles

After the preparation of nanoparticles, optimized formulations were freeze dried. Pre-freezing of samples was done at -20°C for 20 h, then the flasks were connected to freeze drier under vacuum (1 mbar, -110°C) and the process was continued till free flowing powder was obtained. Freeze drying was done to remove water from formulation so that system can be stable for longer time. After freeze drying, samples were stored at RT.

5.3.6. Effect of Various Formulation Parameters

a) Stabilizer Concentration

Different batches of nanoparticle dispersions were prepared using above mentioned polymers individually and in combination in the presence of two stabilizers, F 68 and PVA. Four different concentrations 0.5, 0.75, 1.0 and 2.0 %w/v of stabilizers were used to study the effect of stabilizer on various parameters. For each batch 50 mg polymer and 5 mg etoposide was taken. Batch codes and characters are mentioned in Tables 1 to 4 for different polymers.

b) Polymer Content

Formulations were prepared by varying the amount of polymer from 25 to 200 mg. Batches were prepared by taking specified quantity of polymer, 5 mg etoposide and constant 1.0 %w/v stabilizer. Batch codes and characters are mentioned in Tables 1 to 3.

c) Amount of Etoposide

Amount of etoposide taken for the preparation of nanodispersion was varied from 2.5 to 20 mg to study the effect on different formulation characters. Batches were prepared with 50 mg of each polymer or polymer combination, using 1.0 %w/v of stabilizer (Tables 1 to 3).

d) Effect of Freeze Drying

Effect of freeze drying on physical characteristics of nanoparticles like size, polydispersity index, zeta potential, drug loading and entrapment efficiency were studied. To measure size, polydispersity and zeta potential, freeze dried nanoparticles were dispersed in aqueous medium containing 1.0 % w/v of stabilizer.

5.3.7. Characterization of Prepared Nanoparticles

Characterization of the nanodispersions is a necessity for the control and achieving the quality product. The characterization methods should be sensitive to the key parameters of nanoparticles performance and should avoid artifacts. Size, zeta potential, polydispersity index, recovery, drug loading and entrapment efficiency for the prepared formulations were determined. In vitro release studies were done for optimized formulations. Freeze dried formulations were also checked for all the above parameters along with their redispersibility in TDW containing stabilizer (1 %w/v). Drug free nanoparticles were also prepared and characterized.

a) Morphology, Size and Polydispersity Index

Morphological examination of nanoparticles was performed using transmission electron microscopy (TEM) and atomic force microscopy (AFM). For TEM analysis, one or two drops of prepared nanoparticle dispersions were taken and mixed properly with 0.2%v/v of tungstic acid. Copper grids were placed on these drops for coating. The grids were removed, blotted with Whatman filter paper and viewed under microscope. In case of freeze dried samples, 2 mg of powder was weighed, dispersed in 0.5 ml of TDW containing 1 %w/v of stabilizer and analyzed.

For analysis of samples using AFM, a drop of nanodispersion was kept on mica and air dried. After drying, the sample was transferred to the sample holder for observation. Samples were analyzed under contact mode using AFM. Freeze dried samples were redispersed as described above and analyzed using AFM.

Average size and particle size distribution of the prepared nanoparticle dispersions was measured by Photon Correlation Spectroscopy using Zeta sizer. Instrument was calibrated with standard latex nanoparticle dispersion. An aliquot of drug loaded and empty nanoparticle dispersions were taken in the sample holder separately and measurements were performed at 90° angle to the incident light. Freeze dried samples were processed as described for TEM and analyzed.

b) Surface Potential

The zeta potential values of the samples were measured by Zetasizer which measures the distribution of electrophoretic mobility by using electrophoresis and laser doppler velocimetry. Nanodispersions were placed in a sample holder and electrodes were connected to it. A laser beam illuminates particles moving in an applied electric field, and the velocities of the particles are obtained from the Doppler frequency. Since zeta potential is directly related to the electrophoretic mobility of the particles, the analyzer calculates the individual potentials from the measured velocities.

d) Nanoparticle Recovery

The recovery of polymeric nanoparticles was defined as the weight ratio of prepared nanospheres to the initial loadings of polymer, drug and other excipients. Once the free drug is separated and the sediment was formed after centrifugation, dry weight was taken and the nanoparticle recovery (% w/w) was calculated using following equation.

$$\text{Nanoparticles recovery (\%)} = \frac{\text{Mass of nanoparticles recovered}}{\text{Mass of polymer, drug and any formulation excipient used in formulation}} \times 100$$

e) Drug Content and Entrapment Efficiency (EE %)

Drug content in nanoparticles was determined and measured as a ratio of drug present in nanoparticles to that of total mass of nanoparticles recovered after preparation. For drug content determination, after centrifugation, minimum 100 mg of the sediment was dissolved in acetonitrile and analyzed for etoposide using analytical method 1 for

formulations prepared with PLGA, PCL and combination of polymers and analytical method 2 for formulations prepared with EuL-100. Drug content (% w/w) was calculated using following equation.

$$\text{Drug content (\% w/w)} = \frac{\text{Mass of drug in nanoparticles}}{\text{Mass of nanoparticles recovered}} \times 100$$

For entrapment efficiency, 1 ml of nanodispersion was taken and centrifuged in 3 cycles at 14,000 rpm for 10 min per cycle. Free drug present in the dispersion will remain in the supernatant and nanoparticles settle to the bottom. Supernatant was collected and analyzed for etoposide using analytical method 1. Entrapped drug in nanoparticles was determined by dissolving the sediment formed after centrifugation in acetonitrile and analyzing for etoposide. Entrapment efficiency (%) was calculated by equation.

$$\text{Entrapment efficiency (\%)} = \frac{\text{Amount of etoposide in sediment}}{\text{Initial amount of etoposide taken}} \times 100$$

5.3.8. In vitro Drug Release

The etoposide release from prepared nanoparticles was evaluated by a dialysis bag diffusion technique (Levy and Benita, 1990). 2 ml of the nanodispersions were placed in the dialysis bag (Spectrapor, Cut off 12,500 Da), sealed and dropped into 200 ml of aqueous medium. Media used for in vitro release was phosphate buffer (pH 7.4). The entire system was kept at 37 ± 2°C with continuous stirring at 100 rpm. At specific time interval 5 ml of the medium was withdrawn and replaced by fresh buffer. Drug content in the samples was determined using analytical method 3. Since etoposide is insoluble in water, etoposide solution (2 mg/ml) in 1 % w/v of F68 in TDW was used to compare the diffusion of drug from the dialysis bag. In vitro data analysis was done using GraphPad Prism version 4.00 (Trial) for windows, GraphPad software, San Diego California USA. Different kinetic models (zero order, first order, Higuchi, Hixson-Crowell, Weibull models) were fitted for the release data and best fit was judged by Akaike's Information Criterion (AIC) and MSSR. AIC can be used to determine the 'best' model from a number of alternatives.

$$AIC = N * \ln(SSR) + 2 * M$$

where N is the number of data points, SSR is the sum of the squared residuals and M is the number of adjustable parameters. It is a measure of the goodness of fit between a

calculation line and the observed data. The lower the value of the AIC, the better the model describes the data (Yamaoka et al, 1978).

5.3.9. Stability Study of the Formulations

The physical stability of the nanosuspensions was evaluated after storage under different temperature conditions. Each optimized preparation, was stored in screw capped glass vials and placed at room temperature (RT: 25 ± 2°C), 5 ± 2°C and -20°C. Aliquots of 1 ml were withdrawn at specific time points to determine drug leakage. Dispersions were observed physically for the agglomeration and settling of particles. After 3 months, all the dispersions were checked for their size and entrapment efficiency.

Freeze dried samples were also kept under the same conditions and at every time point 2 mg was taken, redispersed in TDW containing 1.0 %w/v of stabilizer and evaluated for above mentioned parameters. As a part of stability, redispersibility of the nanoparticles was also determined. For freeze dried preparations, 2 mg of the preparation was taken and dispersed in 0.5 ml of TDW containing 1.0 %w/v of stabilizer. Redispersibility was also checked after centrifugation of prepared formulations. Supernatant was taken and checked for redispersibility by adding TDW containing 1.0 %w/v stabilizer.

5.3.10. Thermal Study of Nanoparticles

DSC study was done for freeze dried nanoparticles of batches ETNP/F68/03 and ETNP/PCL/03. Sample preparation was same as mentioned in section 4.3.3 of chapter 4. DSC experiments were carried out to define the physical state of the polymer and the drug in the formulation and to check for the possibility of any interactions between the drug and the polymer within the matrix (Espuelas et al, 1997). Exothermic peaks recorded in the thermograms are directed upwards.

5.4. Results and Discussion

The choice of the particular method of encapsulation is determined by solubility characteristics of the polymer and drug. In the present study nanoprecipitation method was used for PLGA co polymers and solvent evaporation technique was used for PCL and EuL-100 polymers, combination of PLGA and PCL since these were best suited for encapsulation of the selected drug etoposide.

Nanoparticle formation, in process used here, can be explained in terms of interfacial turbulence and the diffusion processes between two un-equilibrated liquid phases. When the organic phase containing polymer is poured into the aqueous phase and

converted to fine globules under stirring, due to the miscibility, the organic solvent diffuses into the water and carries with it some polymer which are still in solution. Then as solvent diffuses further into water, the associated polymer aggregate forming nanoparticles and the whole system is stabilized by a layer of stabilizer present in aqueous phase to provide a mechanical barrier to aggregation. Mechanism of nanoparticle formation can be described based on the solvent-polymer, water-solvent and water-polymer interactions (Chorny et al, 2002).

In solvent evaporation method, the first step is formation of an emulsion. The oil phase containing the drug and the polymer in the organic solvent is dispersed in the aqueous phase. This is followed by evaporation of the organic solvent. Since the particles formed by evaporation of solvent, are easy to aggregate in the aqueous medium, stabilizer is added. This method allows preparation of biodegradable nanoparticles with high drug loading capacity in an effective and reproducible manner. As acetone is miscible with water, it is suitable to form an emulsion. Therefore dichloromethane was preferred in solvent evaporation method (Mainardes and Evangelista, 2005).

Volume of solvent was an important factor, and control size of nanoparticles formed (Peltonen et al, 2002). After some preliminary study, volume of solvent was decided to 10 ml. An increase in the volume of the aqueous phase (5 to 25 ml) led to decrease in nanoparticle size to certain extent. Above 25 ml of aqueous phase volume there was no effect on nanoparticle formation. Aqueous phase volume, thus, was optimized and maintained as 25 ml for all the preparations. Nanoparticle codes, composition, particle size, drug content are presented in Tables 1 to 6.

5.4.1. Preparation of Nanoparticles with PLGA co Polymers

Nanoprecipitation method produced fine dispersions without any agglomeration for PLGA and its co polymers. Particle size found to vary depending on type of PLGA polymer and stabilizer used. Batch codes, composition, size of nanoparticles and their characters, drug content, entrapment efficiency and recovery of PLGA based nanoparticles are presented in Table 1. It was found that change in composition of lactide and glycolide content in PLGA polymers, polymer content, stabilizer and their percentage, amount of drug influenced size of the nanoparticles. Study of the particle size (Table 1) suggests that when quantity of drug and stabilizers percentage were kept constant, change of PLGA co polymers (vary in lactide and glycolide ratio) influence the particle size. For 5 mg quantity of drug and 0.5 %w/v of F 68, PLGA 50/50 produced nanoparticles of 160.7 ± 0.41 nm, where as PLGA 75/25 and PLGA 85/15 produced nanoparticles of 186.7 ± 0.28 nm and

181.4 ± 0.33 nm respectively. Same way, change of stabilizer concentration to 0.75 %w/v for PLGA 50/50 produced nanoparticles of 105.1 ± 1.36 nm, but PLGA 75/25 and PLGA 85/15 gave nanoparticles of 159.1 ± 0.24 nm and 162.1 ± 0.82 respectively. On increase in stabilizer percentage to 1.0 % and 2.0 % w/v, PLGA 50/50 produced nanoparticles of 91.8 ± 0.74 nm and 90.9 ± 0.42 nm respectively. Whereas for same stabilizer concentrations, PLGA 75/25 produced 103.7 ± 0.18 nm and 105.9 ± 0.29 nm respectively and PLGA 85/15 produced nanoparticles of 105.1 ± 0.38 nm and 106.3 ± 0.64 nm. Effect of stabilizer concentration, polymer content and etoposide amount are discussed later. On the basis of preliminary study, amount of drug was optimized to 5 mg, amount of polymer was optimized to 50 mg and concentration of stabilizer was optimized at 1.0 %w/v. Size distribution plots of etoposide loaded PLGA 50/50, PLGA 75/25 and PLGA 85/15 nanoparticles with optimized polymer content, drug amount and stabilizer concentration are shown in Figures 1A to 1F. TEM photographs of nanoparticles shows that all the nanoparticles are round, smooth with out showing any agglomeration (Figures 2A to 2F). AFM image (Figure 3) also confirms shape and surface properties of the formulation prepared with PLGA 85/15.

Polydispersity index is an indication of the size distribution with values ranging from 0 to 9 (Gurny and Alleman, 2002). Lesser the value of polydispersity indicate narrow size distribution of particles in the dispersion. Polydispersity was low for the batches prepared with F 68 as stabilizer (0.13, 0.14 and 0.11 for ETNP/F68/03, ETNP/F68/13 and ETNP/F68/17) than with PVA (0.16, 0.22 and 0.38 for ETNP/PVA/03, ETNP/PVA/13 and ETNP/PVA/17) showing homogenous and narrow size distribution. These polydispersity index values of these polymers were found to be was less than those reported by other scientists (Gurny and Alleman, 2002). Zeta potential of the prepared nanoparticles was found negative (around -33.38 to -1.29 mV) and the nanodispersions were found stable. There was no significant difference in the size, polydispersity and zeta potential values for empty nanoparticles prepared with the respective polymers and the values are given in Table 5. The prepared formulations were freeze dried and the effect of freeze drying on size, polydispersity and zeta potential was found and presented in Table 6.

5.4.2. Preparation of Nanoparticles with PCL

Solvent evaporation method adapted for the formation of nanoparticles using PCL produced fine dispersion. Use of acetone did not produced agglomeration of the particles and also required to be heated or used of large volume as solubility of PCL in acetone is less. Similar result was found by Jimenez et al, (2004). Thus, for PCL instead of acetone,

dichloromethane was used as solvent. The average diameter of the drug loaded PCL nanoparticles prepared by solvent evaporation method using F 68 and PVA stabilizers were 257.2 ± 0.96 nm, 391.4 ± 1.01 nm (Batch Code: ETNP/PCL/F68/03, ETNP/PCL/PVA/03) respectively. The polydispersity index values were very less indicating narrow size distribution. Low, negative zeta potential values of the dispersions indicated stability of the products. Size distribution profile and morphology of nanoparticles prepared with PCL, measured with Zetasizer, AFM, and TEM, are given in Figures 4A, 4B; 5, 6A and 6B respectively. Table 2 shows average size, zeta potential, drug content, entrapment efficiency and recovery for different batches prepared with PCL. Formulation characteristics of empty nanoparticles and freeze dried product are given in Table 5 and 6.

5.4.3. Preparation of Nanoparticles with EuL-100

Nanoprecipitation technique was used for the preparation of nanoparticles using EuL-100. Acetone was not suitable to dissolve EuL-100 therefore ethanol was selected as solvent for EuL-100. Fine dispersions were formed with EuL-100 but removal of ethanol form the dispersion took more time compared to dispersions prepared with acetone and also required higher temperature for evaporation. Size distribution profiles of nanoparticles prepared with EuL-100 are found to be broad and presented in Figures 7A and 7B. Nanoparticles prepared with EuL-100 as polymer has the size ranging from 70 nm to 1000 nm which is very wide. Polydispersity index was also very high compared with products prepared with other polymers. TEM and AFM images (Figures 8A, 8B and 9) also show the size variation and agglomeration of nanoparticles. Size, polydispersity, drug content, entrapment efficiency and recovery are presented in Table 3. Physical characters of empty nanoparticles and freeze dried are given in Tables 5 and 6 respectively. Drug entrapment was very low for these batches and a maximum of 15 % of entrapment was observed and is far less than that of batches with other polymers. Most of the drug added to the preparation was present in the supernatant after centrifugation. This suggests that EuL-100 is not a suitable polymer for etoposide nanoparticles. Another possible reason is long duration required for evaporation of ethanol, during which it was diffusing into the water but was not evaporated completely, polymer and drug are getting exposed to the aqueous environment and polymer is precipitating into bigger particles and drug is getting dissolved in the aqueous phase containing stabilizer. As the batches prepared with EuL-100 have failed to achieve narrow size distribution and entrapment efficiency, these batches were not taken up for in vitro release studies as well as in vivo studies.

5.4.4 Preparation of Nanoparticles with Polymer Combination

For the preparation of nanoparticles using combination of biodegradable polymers, solvent evaporation method was used. Polymers were completely dissolved in dichloromethane. Milky dispersion was formed at the end of preparation. Size distribution plots for these batches are given in Figures 10A to 10F respectively for ETNP1/F68, ETNP2/F68, ETNP3/F68, ETNP4/PVA, ETNP5/PVA and ETNP6/PVA. TEM and AFM images given in Figures 11A to 11F, 12A (ETNP1/F68) and 12B (ETNP1/PVA) confirm the spherical shape and size. Preliminary optimization was done for these batches and finally composition of polymer (50 mg) and stabilizer (1.0 %w/v) were selected similar to the batches prepared with individual polymers for comparison. Size of the particles was slightly bigger than the nanoparticles produced with individual PLGA co polymers. Drug content and entrapment efficiency were almost same as that of the batches prepared with same individual polymers alone. These values are given in Table 4.

5.4.5. Effect of Formulation Parameters

During the preparation of nanodispersions using different polymers, several parameters were assessed in order to achieve optimal preparation conditions, including amount of polymer, stabilizer content in the formulation and etoposide content. Only one parameter was changed in the each series of experiments.

a) Stabilizer Concentration

The effect of different concentrations (0.5, 0.75, 1.0 and 2.0 %w/v) of F 68 and PVA on size, zeta potential and polydispersity index of nanoparticle dispersions are shown in Tables 1 to 3. Increase in concentration of F 68 from 0.5 to 1.0 %w/v, made significant decrease in size from 160.7 to 91.8 nm for PLGA 50/50; 186.7 to 103.7 nm for PLGA 75/25, 181.4 to 105.1 nm for PLGA 85/15, 323.9 to 257.2 nm for PCL and 166.4 to 70.8 nm for EuL-100. Above 1.0 %w/v of F 68, there was no significant decrease in size of the particles. This was observed for all preparations in which F 68 was used as stabilizer. Polydispersity index of the formulations prepared with F 68 (in different concentrations) as stabilizer, (Table 1) was less indicating narrow and homogenous size distribution. There was decrease in polydispersity index with increase in stabilizer concentration from 0.5 to 1.0 %w/v. Therefore 1.0 %w/v of F 68 was considered as optimum for the preparation of nanoparticles and used for optimized products. Particles prepared with F 68 as stabilizer have negative surface charge (Table 1 to 3). It was observed that increase in stabilizer concentration changed the zeta potential towards positive value.

In case of formulations prepared with PVA as stabilizer, there was decrease in size of the particles as the PVA concentration was increased from 0.5 to 1.0 %w/v. Influence of PVA concentration on size, polydispersity and zeta potential of different batches was given in Tables 1 to 3. There was decrease in polydispersity index also with increase in PVA to 1.0 %w/v. But it was observed that polydispersity index was comparatively more for formulations with PVA as stabilizer than for F 68. Surface charge was negative and increased with increase in PVA concentration.

An optimum concentration of stabilizer leads to a reduced size of nanoparticles. Insufficient amount of stabilizer would fail in stabilizing and cause aggregation leading to larger nanoparticles (Feng and Huang, 2001). In the solvent evaporation and nanoprecipitation methods formation and stabilization of particles are crucial factors. The amount of surfactant plays an important role in the protection of particles, because it can avoid the agglomeration of particles. Lesser amount of stabilizer is unable to cover the dispersed nanoparticles completely by causing aggregation and larger particles (Feng and Huang, 2001). With increased stabilizer concentration, an improved protection of the particles from agglomeration was obtained, leading consequently to smaller particles. There was no much difference in size of the particles as the concentration of stabilizer was increased to 2 %w/v indicating excess stabilizer. Further increase in concentration of stabilizer increased particle size because of the viscosity of the aqueous phase, due to higher stabilizer concentration at specific stirring speed (Murakami et al, 1999).

Increase in stabilizer concentration upto 1.0 %w/v did not influence entrapment efficiency of etoposide. However, slight decrease in entrapment efficiency was obtained when the stabilizer concentration in increased to 2.0 %w/v. There was decrease in drug content with increase in stabilizer concentration. When the concentration of stabilizer is increased, it helps in solubilizing drug in the aqueous phase. Due to this, when organic solvent is added to the aqueous phase, more amount of etoposide was soluble in the aqueous phase and also helps in leaching of drug from nanoparticles.

b) Polymer Content

An increase in the polymer amount affected the morphology, particle size, polydispersity, zeta potential, drug content and encapsulation efficiency of the nanoparticles. Initially on increase from 25 to 50 mg there was no significant increase in mean size of the particles but polydispersity index was slightly increased. Nanoparticles prepared with 25 and 50 mg of polymer formed milky dispersions without any agglomerates. For formulations with PLGA co polymers, increase in amount to 100 mg

increased the size and there was formation of small agglomerates. But in formulations prepared with PCL, EuL-100 and combination of polymers, agglomeration started with 100 mg and when increased to 200 mg, agglomeration was very high leading to precipitation of polymer into large flakes. This is because aqueous phase containing stabilizer was not able to hold this amount of polymer making to precipitate into agglomerates. For these preparations (Tables 2 and 3) size measurement was not done. Effect of polymer content on size, polydispersity, drug content, entrapment efficiency and recovery for all polymers are given in Tables 1 to 3.

Increase in particle size was observed with an increase in biodegradable polymers by other authors also (Ogawa et al, 1988; Quintanar-Guerrero et al, 1996; Murakami et al, 1999; Kwon et al, 2001; Chorny et al, 2002). Increase in the polymer concentration led to increase in viscosity of the organic phase and this resulted in poor dispersibility of the organic phase into the aqueous phase. There is a resistance against the shear forces during the diffusion or emulsification. Coarse dispersions were obtained at higher polymer concentrations, which lead to formation of bigger particles during the diffusion process. This can also be due to the insufficient amount of stabilizer present in the aqueous phase for that particular polymer amount.

Entrapment efficiency was influenced by amount of polymer present in the formulation. When polymer amount was increased from 25 to 200 mg, there was increase in entrapment efficiency for batches prepared with PLGA co polymers (Tables 1 to 3). For batches prepared with PCL and EuL-100, entrapment efficiency was increased with polymer content from 25 to 50 mg. Increasing these polymer content above 50 mg lead to precipitation and aggregate formation. Therefore entrapment efficiency, drug content and recovery were not determined.

c) Etoposide Amount

Maintaining a constant initial mass of polymers (50 mg), the mass of etoposide was varied between 2.5 to 20 mg. Tables 1 to 3 shows the results of the influence of drug amount on nanoparticle mean diameter, polydispersity index and drug content and entrapment efficiency. It can be observed that the increase in the amount of etoposide increases the nanoparticle mean diameter and polydispersity index for all the batches prepared. The reason might be, when less amount of etoposidewas taken initially, smaller particles were produced after evaporation of organic solvent, whereas if the amount of etoposide added initially is increased, the mean particle size increases because of the high solid content after evaporation (Mainardes and Evangelista, 2005). The encapsulation

efficiency was increased for all batches when etoposide amount was increased from 2.5 to 10 mg, beyond which there was no effect. This could be due to inadequate amount of polymer present in the system and was not sufficient to entrap the drug inside the matrix.

d) Effect of Freeze Drying

Freeze dried nanoparticles which were optimized for stabilizer concentration, polymer content and etoposide amount were studied for size, zeta potential, polydispersity index, drug content and entrapment efficiency and are given in Table 6. It was found that there was no significant difference in the size of the formulations after freeze drying. TEM photographs confirmed the same. Figures 13, 14 and 15 shows the TEM photographs of freeze dried samples (F/ETNP/F68/17, F/ETNP/PCL/F68/03 and F/ETNP/PVA/17). Particles were spherical and there was no free drug crystals found in the picture.

5.4.6. Nanoparticle Recovery

For all the batches prepared with above mentioned polymers, drug recovery was good with a maximum of around 96 %. Percentage recovery of etoposide loaded nanoparticles for different batches is given in Tables 1 to 5. Batches prepared with higher amount of PCL and EuL-100 (100 and 200 mg), recovery was not determined as there was complete aggregation of particles and dispersion was not formed. Varying polymer content and etoposide content has not shown any affect on recovery. There was no change in the recovery of nanoparticles after freeze drying of the corresponding batches. These values are given in Table 6.

5.4.7. Redispersibility of Prepared Nanoparticles

Redispersibility of the freeze dried powder was very essential for administration of nanoparticles. Redispersibility was studied after freeze drying of the formulations and the sediment obtained after centrifugation of dispersions. Nanoparticles were redispersed in TDW and TDW containing 1 %w/v of F 68 or PVA. Qualitative evaluation was made in terms of excellent (if the dispersion is formed immediately after addition of medium), good (after 1 minute of shaking), fair (after 5 minutes of shaking), poor (after 5 minutes of sonication) and very poor (after 10 minutes of sonication) and by visual observation of agglomerates.

After freeze drying, all products have shown excellent redispersibility in TDW with and without stabilizers. But sediment formed after centrifugation of nanoparticles prepared using EuL-100 shown poor redispersibility. Formulations prepared with all other polymers

and combination of polymers has shown good redispersibility in both TDW and in presence of stabilizers. Excellent redispersibility was shown by formulations prepared with PLGA co polymers in both freeze dried and after centrifugation. Redispersibility of the different batches after freeze drying and centrifugation are given in Table 7.

5.4.8. In vitro Drug Release

In vitro diffusion profile of etoposide pure drug is given in Figure 16 and complete diffusion occured within 1.5 h. The cumulative in vitro release profiles of nanoparticle formulations prepared with PLGA co polymers with F 68 and PVA are given in Figures 16 and 17 respectively. There was initial burst release of around 41.08 % in the first hour for PLGA 50/50 (ETNP/F68/03). This rapid initial release may be attributed to the large fraction of drug that was adsorbed or exposed on the surface of the nanospheres. The small size of the nanoparticles is a major factor, which influences the release rate. The particles have a high surface area; therefore some amount of the drug will be at or near the particle surface and can be easily released. Further, the diffusion distances encountered in the particles are small which allows drug trapped in the core to rapidly diffuse out and also for the release medium to diffuse in. Release was decreased for batches prepared with PLGA 75/25 (20.65 %) and PLGA 85/15 (7.65 %) in the first hour of study. Release was extended for 24 h for PLGA 50/50 and it extended to 36 h and 48 h for PLGA 75/25 and PLGA 85/15 respectively. This decrease in release was due to increase in lactide content of the polymer and higher hydrophobic character. Similar effect was observed with formulations prepared with PLGA co polymers using PVA as stabilizer. Release of etoposide was relatively fast in case of formulations prepared using PVA as stabilizer than F 68.

Nanoparticles prepared with PCL extended etoposide release up to 48 h. Comparative release profile of ETNP/PCL/F68/03 and ETNP/PCL/PVA/03 is given in Figure 18. These batches released around 7.65 % and 27.44% in the first hour of study. This indicates less amount of etoposide was adsorbed or present on the surface of nanoparticles. Maximum amount of etoposide was present in the matrix along with PCL therefore release of etoposide was slow from these formulations. It was observed that ETNP/PCL/PVA/03 released etoposide completely in 40 h when compared with ETNP/PCL/F68/03. When the in vitro release profiles of formulations prepared with PCL were compared with those prepared with PLGA co polymers, maximum control in release was observed for PCL formulations (Figure 19).

In vitro release profiles of etoposide from formulations prepared with combination of PLGA co polymers and PCL with F 68 and PVA is shown in Table 20 and 21

respectively. From all the profiles, initial burst release was observed. But this was decreased with increase in lactide content of PLGA co polymer. This is due to the increase in hydrophobicity of the polymer with the increase in lactide content. Batch prepared with PLGA 50/50 and PCL combination (ETNP1/F68, ETNP1/PVA) retarded the release up to 40 h and for other batches ETNP2/F68, ETNP2/PVA, ETNP3/F68 and ETNP3/PVA release of etoposide was extended up to 48 h.

Comparative release profiles of formulations prepared with ETNP/F68/17, ETNP/PCL/F68/03 and ETNP3/F68 are given in Figure 22. Among these three formulations, formulation prepared with PCL released etoposide slowly from the nanoparticles. This retardation in release is due to more hydrophobic character of PCL than PLGA co polymers. The most crystalline and hydrophobic polymers exhibit the slowest degradation rate (Coffin and McGinity, 1992; Lemoine et al, 1996). As etoposide is also hydrophobic in nature, release from the PCL nanoparticle matrix was very less.

It was reported by other scientists that release can be extended from these polymers for about months because of slow degradation of polymers in the release medium (Lamprecht et al, 2000). In the present study release was extended up to 48 h. This might be due to the low molecular weight of the polymers used in the study.

All the in vitro release data was fitted into various mathematical models (zero order, first order, Higuchi, Hixson-Crowell, Weibull models) to know the release kinetics. Among all the models tried, data was best fitted into Peppas model. AIC and MSSR were calculated for all models and were found to be less for Peppas model indicating best fit. All the kinetic parameters for Peppas model (k, R^2, MSSR, n and AIC coefficient) are presented in Table 8. Value of ‘n’ in Peppas model indicates the mechanism of release of etoposide follows anomalous transport. All the polymers are biodegradable and their degradation depends on the molecular weight of the polymer and external medium. Release of drug from these polymers was mainly because of degradation/erosion of polymer.

5.4.9. Stability Studies of the Formulations

Stability of the dispersions and freeze dried preparations stored at different conditions were evaluated for agglomeration visually. All nanoparticle disperrsions prepared with PLGA and PCL stored at room temperature were stable for only 7 days. Visually agglomeration was observed in these within 7 days of storage. Nanodispersions prepared with EuL-100 were also not stable. After 2 days of storage sediment was formed at the bottom of the dispersion, which was not dispersible in TDW or TDW containing stabilizer. Drug was leached out from nanoparticles during the storage at room temperature.

After 7 days of storage of nanodispersions, there was no detectable amount of drug left in the nanoparticles.

Nanodispersions stored at 5°C ± 2°C were stable for 2 months but at the end of 3rd month there was significant change in the size and entrapment efficiency of etoposide loaded nanoparticles from the initial values (Table 9). Size of the nanoparticles was increased significantly and the entrapment efficiency was decreased from the initial values. Agglomeration of the nanodispersions stored at 5 ± 2°C can be seen in the TEM image in Figure 23. Nanodispersions stored at -20°C were quite stable for long period of time. There was not much variation observed in size and entrapment efficiency of the formulations after 3 months of storage. Size and entrapment efficiency values of nanodispersions stored at -20°C at zero time and after 3 months are given in Table 10. Redispersibility of nanoparticle preparations at 5 and -20°C are given in Table 11. Freeze dried formulations stored at all studied temperatures were stable and there was no difference in size and entrapment efficiency of the formulations after 1 year of storage (Tables 12, 13 and 14). This was confirmed by the TEM images showing PLGA and PCL freeze dried nanoparticles after 1 year of storage at RT (Figure 24 and 25). All freeze dried formulations have shown excellent redispersibility in TDW even after 1 year of storage.

5.4.10. Thermal Study of Nanoparticles

DSC thermograms of etoposide, PLGA 50/50, PCL, freeze dried etoposide ETNP/F68/03 and ETNP/PCL/F68/03 nanoparticles were shown in Figures 26 and 27. DSC thermogram of the drug loaded nanoparticles prepared with PLGA 50/50, showed glass transition temperature corresponding to PLGA 50/50 at 43.61°C (Figure 26) whereas thermogram of drug loaded nanoparticle formulation prepared by PCL, (Figure 27) showed endothermic melting peak of PCL at 58.84°C. The results show that when nanoparticles were prepared with PLGA 50/50 and PCL polymers, the encapsulated drug did not interact with the polymers and etoposide was encapsulated in the nanoparticle (Espuelas et al, 1997). Absence of drug peak can be attributed to complete encapsulation of etoposide or there might be very less adsorbed drug on the surface of nanoparticle and also low drug content in both formulations.

5.5. Conclusions

Etoposide loaded nanoparticles were prepared successfully using nanoprecipitation method (PLGA co polymers, EuL-100) and solvent evaporation method (PCL) in presence of F 68 and PVA as stabilizers. These methods found to be simple, reproducible and

produced nanoparticles with narrow size distribution and very good entrapment efficiency. Drug entrapment efficiency has been found to be as high as 85 % though drug content found to be very low as amount of polymer used was high. Use of different biodegradable polymers individually and in combination produced etoposide loaded nanoparticles with low polydispersity index and with high entrapment efficiency of etoposide. Change in the concentration of stabilizer, polymer and amount of etoposide found to vary size, polydispersity, drug content and entrapment efficiency of the prepared nanoparticles. Redispersibility of the formulations after freeze drying and centrifugation was good. Release from nanoparticles prepared with PLGA co polymers decreased with increase in lactide content in the polymer. In vitro release of etoposide from nanoparticles was extended to 48 h from formulations prepared with PLGA 85/15, PCL individually and combination of these two polymers in 1:1 ratio. By varying the proportion and nature of polymer, nanoparticles can be made for intended drug release. These formulations were stable for about 1 year after freeze drying without change in their size, entrapment efficiency and redispersibility. The derived correlations make it possible to optimize the formulation achieving higher efficacy and an improved safety profile of polymer based nanoparticulate formulation for intended administration. These results justify further investigation of the suitability of these nanoparticles for application in the controlled delivery and/or targeting of etoposide. These formulations can be an alternative to improve the stability of drug with probable enhancement in absorption and bioavailability of the etoposide. However, increasing the drug content per unit of nanoparticles can make total dose of formulation lower.

Table 1: Composition and effect of various parameters on the formulation characteristics of nanoparticles prepared with PLGA co polymers.

Code	Polymer (mg)			Stabilizer (% w/v)		Drug (mg)	Mean Size (nm) ± SD	PI[a] ± SD	Zeta potential (mV) ± SD	Drug Content (%)± SD	EE[b](%) ± SD	Recovery (%) ± SD
	PLGA 50/50	PLGA 75/25	PLGA 85/15	F68	PVA							
ETNP/F68/01	50	-	-	0.5	-	5.0	160.7 ± 0.41	0.16 ± 0.03	-28.71 ± 1.21	2.15 ± 0.07	66.88 ± 1.19	86.52 ± 1.25
ETNP/F68/02	50	-	-	0.75	-	5.0	105.1 ± 1.36	0.14 ± 0.02	-24.85 ± 0.56	1.51 ± 0.04	64.91 ± 1.07	88.35 ± 1.25
ETNP/F68/03	50	-	-	1.0	-	5.0	91.8 ± 0.74	0.13 ± 0.01	-21.23 ± 1.04	1.04 ± 0.06	57.64 ± 0.97	91.14 ± 0.28
ETNP/F68/04	50	-	-	2.0	-	5.0	90.9 ± 0.42	0.11 ± 0.02	-18.94 ± 0.37	0.49 ± 0.03	48.12 ± 0.82	88.22 ± 0.88
ETNP/F68/05	50	-	-	1.0	-	2.5	82.7 ± 1.11	0.11 ± 0.00	-19.28 ± 0.72	0.39 ± 0.01	42.81 ± 1.22	90.24 ± 0.64
ETNP/F68/06	50	-	-	1.0	-	10.0	92.4 ± 1.04	0.18 ± 0.01	-23.61 ± 1.08	2.21 ± 0.02	61.48 ± 0.54	89.66 ± 1.06
ETNP/F68/07	50	-	-	1.0	-	20.0	91.6 ± 0.68	0.22 ± 0.02	-24.28 ± 0.81	4.22 ± 0.01	61.97 ± 1.27	91.88 ± 1.01
ETNP/F68/08	25	-	-	1.0	-	5.0	85.8 ± 0.84	0.11 ± 0.01	-18.91 ± 1.38	0.99 ± 0.01	51.12 ± 1.19	92.25 ± 0.81
ETNP/F68/09	100	-	-	1.0	-	5.0	167.8 ± 0.81	0.24 ± 0.02	-26.90 ± 1.21	0.96 ± 0.03	62.90 ± 0.54	92.17 ± 1.07
ETNP/F68/10	200	-	-	1.0	-	5.0	235.4 ± 2.75	0.31 ± 0.02	-28.54 ± 0.27	0.82 ± 0.01	64.44 ± 0.18	86.28 ± 2.88
ETNP/F68/11	-	50	-	0.5	-	5.0	186.7 ± 0.28	0.34 ± 0.02	-31.71 ± 1.51	2.33± 0.11	73.08 ± 1.01	87.09 ± 0.97
ETNP/F68/12	-	50	-	0.75	-	5.0	159.1 ± 0.24	0.31 ± 0.01	-29.20 ± 1.09	1.56 ± 0.06	71.29 ± 0.12	94.44 ± 1.91
ETNP/F68/13	-	50	-	1.0	-	5.0	103.7 ± 0.18	0.14 ± 0.01	-28.06 ± 0.39	1.14 ± 0.02	66.11 ± 0.72	95.39 ± 0.91
ETNP/F68/14	-	50	-	2.0	-	5.0	105.9 ± 0.29	0.10 ± 0.02	-25.34 ± 0.87	0.53 ± 0.01	50.84 ± 1.38	85.99 ± 1.88
ETNP/F68/15	-	-	50	0.5	-	5.0	181.4 ± 0.33	0.32 ± 0.02	-33.38 ± 0.19	2.55 ± 0.41	83.27 ± 0.97	90.88 ± 4.17
ETNP/F68/16	-	-	50	0.75	-	5.0	162.1 ± 0.82	0.16 ± 0.02	-31.16 ± 1.05	1.82 ± 0.05	81.48 ± 1.07	92.36 ± 1.11
ETNP/F68/17	-	-	50	1.0	-	5.0	105.1 ± 0.38	0.11 ± 0.01	-29.41 ± 0.58	1.45 ± 0.11	78.99 ± 1.04	89.28 ± 0.58
ETNP/F68/18	-	-	50	2.0	-	5.0	106.3 ± 0.64	0.10 ± 0.01	-27.81 ± 0.34	0.61 ± 0.10	64.71 ± 2.71	94.81 ± 1.82

(Continued in the next page)

Table 1: (Contd.)

Code	Polymer (mg)			Stabilizer (% w/v)		Drug (mg)	Mean Size (nm) ± SD	PI[a] ± SD	Zeta potential (mV) ± SD	Drug Content (%)± SD	EE[b] (%) ± SD	Recovery (%) ± SD
	PLGA 50/50	PLGA 75/25	PLGA 85/15	F68	PVA							
ETNP/PVA/01	50	-	-	-	0.5	5.0	228.4 ± 3.59	0.21 ± 0.043	-13.48 ± 0.66	1.94 ± 0.02	61.87 ± 1.97	88.38 ± 0.39
ETNP/PVA/02	50	-	-	-	0.75	5.0	208.4 ± 5.34	0.19 ± 0.045	-12.36 ± 0.81	1.40 ± 0.01	58.28 ± 0.92	85.71 ± 0.46
ETNP/PVA/03	50	-	-	-	1.0	5.0	160.7 ± 0.45	0.16 ± 0.028	-9.74 ± 1.02	1.07 ± 0.05	56.99 ± 1.08	87.31 ± 0.99
ETNP/PVA/04	50	-	-	-	2.0	5.0	168.7 ± 1.05	0.13 ± 0.01	-1.29 ± 0.79	0.42 ± 0.01	42.01 ± 0.28	90.28 ± 1.15
ETNP/PVA/05	50	-	-	-	1.0	2.5	140.1 ± 1.01	0.13 ± 0.02	-6.24 ± 1.14	0.48 ± 0.03	51.08 ± 0.34	88.39 ± 0.33
ETNP/PVA/06	50	-	-	-	1.0	10.0	159.1 ± 2.10	0.31 ± 0.01	-8.91 ± 0.57	2.05 ± 0.02	57.18 ± 0.69	89.91 ± 0.73
ETNP/PVA/07	50	-	-	-	1.0	20.0	158.2 ± 0.58	0.32 ± 0.01	-10.81 ± 0.93	3.82 ± 0.01	56.58 ± 0.41	92.58 ± 1.44
ETNP/PVA/08	25	-	-	-	1.0	5.0	136.4 ± 1.26	0.14 ± 0.01	-6.8 ± 0.52	1.13 ± 0.01	53.82 ± 1.81	84.76 ± 0.96
ETNP/PVA/09	100	-	-	-	1.0	5.0	178.7 ± 1.08	0.21 ± 0.02	-11.13 ± 0.64	0.91.± 0.07	59.21 ± 0.92	91.81 ± 1.01
ETNP/PVA/10	200	-	-	-	1.0	5.0	232.5 ± 0.97	0.26 ± 0.01	-14.71 ± 1.88	0.75 ± 0.01	61.41 ± 0.37	89.39 ± 1.81
ETNP/PVA/11	-	50	-	-	0.5	5.0	337.2 ± 0.94	1.00 ± 0.51	-14.9 ± 1.11	2.13 ± 0.10	67.82 ± 0.18	88.64 ± 0.81
ETNP/PVA/12	-	50	-	-	0.75	5.0	323.9 ± 0.38	0.44 ± 0.09	-12.8 ± 1.08	1.59 ± 0.02	65.14 ± 1.03	84.28 ± 0.36
ETNP/PVA/13	-	50	-	-	1.0	5.0	255.0 ± 1.31	0.22 ± 0.01	-8.4 ± 1.16	1.11 ± 0.01	62.86 ± 1.11	92.84 ± 1.06
ETNP/PVA/14	-	50	-	-	2.0	5.0	260.0 ± 0.97	0.11 ± 0.02	-4.6 ± 0.38	0.57 ± 0.03	58.71 ± 0.85	93.44 ± 0.86
ETNP/PVA/15	-	-	50	-	0.5	5.0	348.3 ± 1.07	0.52 ± 0.14	-13.0 ± 0.46	2.45 ± 0.04	78.91 ± 1.81	89.54 ± 0.77
ETNP/PVA/16	-	-	50	-	0.75	5.0	322 ± 1.41	0.45 ± 0.07	-11.2 ± 1.07	1.66 ± 0.04	74.07 ± 0.96	91.87 ± 0.28
ETNP/PVA/17	-	-	50	-	1.0	5.0	280.1 ± 0.66	0.38 ± 0.03	-5.8 ± 1.38	1.32 ± 0.01	72.18 ± 1.44	89.86 ± 0.94
ETNP/PVA/18	-	-	50	-	2.0	5.0	283.1 ± 1.03	0.25 ± 0.01	-3.6 ± 0.33	0.63 ± 0.00	66.11 ± 0.94	95.28 ± 0.67

[a] - Polydispersity Index, [b] - Entrapment efficiency; Each value is mean of 3 independent determinations

Table 2: Composition and effect of various parameters on the formulation characteristics of nanoparticles prepared with PCL.

Code	Polymer (mg)	Stabilizer (% w/v)		Drug (mg)	Mean Size (nm) ± SD	PI[a] ± SD	Zeta potential (mV) ± SD	Drug Content (%)± SD	EE[b] (%) ± SD	Recovery (%) ± SD
		F68	PVA							
ETNP/PCL/F68/01	50	0.5	-	5.0	323.9 ± 0.97	0.44 ± 0.03	-31.33 ± 0.91	2.45 ± 0.07	82.19 ± 0.88	93.22 ± 0.44
ETNP/PCL/F68/02	50	0.75	-	5.0	293.3 ± 0.88	0.42 ± 0.01	-29.04 ± 1.70	1.74 ± 0.10	81.44 ± 0.89	96.71 ± 2.81
ETNP/PCL/F68/03	50	1.0	-	5.0	257.2 ± 0.96	0.10 ± 0.01	-27.70 ± 0.19	1.44 ± 0.09	80.15 ± 1.01	91.34 ± 0.87
ETNP/PCL/F68/04	50	2.0	-	5.0	234.9± 0.28	0.09 ± 0.01	-23.62 ± 1.14	0.69 ± 0.14	71.24 ± 1.21	92.71 ± 0.29
ETNP/PCL/F68/05	50	1.0	-	2.5	221.4 ± 1.13	0.91 ± 0.02	-26.70 ± 1.24	0.69 ± 0.02	74.84 ± 1.07	90.09 ± 1.41
ETNP/PCL/F68/06	50	1.0	-	10.0	255.7 ± 1.41	0.28 ± 0.04	-28.07 ± 0.99	2.88 ± 0.16	79.38 ± 0.57	89.02 ± 0.42
ETNP/PCL/F68/07	50	1.0	-	20.0	258.9 ± 1.05	0.13 ± 0.01	-29.89 ± 1.42	5.74 ± 0.88	81.21 ± 1.06	88.35 ± 1.80
ETNP/PCL/F68/08	25	1.0	-	5.0	214.1 ± 1.17	0.10 ± 0.03	-33.14 ± 0.85	1.38 ± 0.03	72.87 ± 1.46	94.55 ± 0.69
ETNP/PCL/F68/09	100	1.0	-	5.0	ND	ND	ND	ND	ND	ND
ETNP/PCL/F68/10	200	1.0	-	5.0	ND	ND	ND	ND	ND	ND
ETNP/PCL/PVA/01	50	-	0.5	5.0	437.2 ± 1.51	0.33 ± 0.01	-18.9-± 0.81	2.28 ± 0.10	78.94 ± 2.04	96.22 ± 1.61
ETNP/PCL/PVA/02	50	-	0.75	5.0	403.0 ± 0.77	0.14 ± 0.01	-16.5 ± 0.29	1.76 ± 0.11	76.91 ± 0.93	89.85 ± 1.00
ETNP/PCL/PVA/03	50	-	1.0	5.0	391.4 ± 1.01	0.10 ± 0.08	-13.8 ± 0.84	1.34 ± 0.03	74.18 ± 1.20	91.08 ± 1.09
ETNP/PCL/PVA/04	50	-	2.0	5.0	392.2 ± 1.08	0.21 ± 0.03	-8.1 ± 1.80	0.71 ± 0.07	70.01 ± 1.08	89.02 ± 0.68
ETNP/PCL/PVA/05	50	-	1.0	2.5	354.4 ± 2.51	0.09 ± 0.01	-12.81 ± 0.55	0.65 ± 0.04	69.46 ± 1.11	88.26 ± 1.21
ETNP/PCL/PVA/06	50	-	1.0	10.0	388.5 ± 1.14	0.15 ± 0.01	-14.28 ± 1.03	2.61 ± 0.05	75.01 ± 1.18	92.88 ± 1.07
ETNP/PCL/PVA/07	50	-	1.0	20.0	391.9 ± 2.06	0.18 ± 0.02	-16.24 ± 0.86	5.45 ± 0.09	74.91 ± 0.44	85.91 ± 2.08
ETNP/PCL/PVA/08	25	-	1.0	5.0	348.1 ± 0.25	0.08 ± 0.04	-17.95 ± 0.69	1.46 ± 0.01	71.08 ± 1.42	86.84 ± 1.81
ETNP/PCL/PVA/09	100	-	1.0	5.0	ND	ND	ND	ND	ND	ND
ETNP/PCL/PVA/10	200	-	1.0	5.0	ND	ND	ND	ND	ND	ND

ND - not determined, [a] - Polydispersity Index, [b] - Entrapment efficiency; Each value is mean of 3 independent determinations

Table 3: Composition and effect of various parameters on the formulation characteristics of nanoparticles prepared with EuL-100.

Code	Polymer (mg)	Stabilizer (% w/v)		Drug (mg)	Mean Size (nm) ± SD	PI [a] ± SD	Zeta potential (mV) ± SD	Drug Content (%) ± SD	EE[b] (%) ± SD	Recovery (%) ± SD
		F68	PVA							
ETNP/Eu/F68/01	50	0.5	-	5.0	166.4 ± 0.34	0.50 ± 0.04	-32.86 ± 0.72	0.46 ± 0.04	15.07 ± 1.01	90.84 ± 1.22
ETNP/Eu/F68/02	50	0.75	-	5.0	137.7 ± 0.17	0.42 ± 0.03	-26.22 ± 0.86	0.31 ± 0.01	13.17 ± 0.85	88.97 ± 0.83
ETNP/Eu/F68/03	50	1.0	-	5.0	70.8 ± 0.44	0.35 ± 0.01	-24.38 ± 1.21	0.24 ± 0.04	12.51 ± 0.76	84.82 ± 2.17
ETNP/Eu/F68/04	50	2.0	-	5.0	71.2 ± 0.11	0.33 ± 0.01	-18.49 ± 0.81	0.13 ± 0.04	12.38 ± 0.91	86.24 ± 1.13
ETNP/Eu/F68/05	50	1.0	-	2.5	70.4 ± 2.58	0.32 ± 0.10	-20.25 ± 1.32	0.10 ± 0.03	10.17 ± 0.54	87.22 ± 0.80
ETNP/Eu/F68/06	50	1.0	-	10.0	71.2 ± 1.51	0.35 ± 0.02	-23.49 ± 0.32	0.43 ± 0.06	11.08 ± 0.88	83.94 ± 0.73
ETNP/Eu/F68/07	50	1.0	-	20.0	70.2 ± 0.97	0.36 ± 0.02	-24.58 ± 1.47	0.93 ± 0.03	12.97 ± 0.31	87.29 ± 2.94
ETNP/Eu/F68/08	25	1.0	-	5.0	70.4 ± 0.82	0.32 ± 0.10	-26.08 ± 0.99	0.20 ± 0.02	9.88 ± 2.06	89.25 ± 1.08
ETNP/Eu/F68/09	100	1.0		5.0	ND	ND	ND	ND	ND	ND
ETNP/Eu/F68/10	200	1.0	-	5.0	ND	ND	ND	ND	ND	ND
ETNP/Eu/PVA/01	50	-	0.5	5.0	437 ± 1.18	1.00 ± 0.45	-2.32 ± 0.46	0.37 ± 0.04	11.92 ± 0.28	92.25 ± 2.94
ETNP/Eu/PVA/02	50	-	0.75	5.0	401 ± 0.93	0.59 ± 0.08	-1.25 ± 0.38	0.22 ± 0.01	10.04 ± 1.41	91.14 ± 2.41
ETNP/Eu/PVA/03	50	-	1.0	5.0	323.9 ± 0.71	0.44 ± 0.05	-0.84 ± 0.08	0.18 ± 0.02	8.99 ± 0.82	92.17 ± 3.01
ETNP/Eu/PVA/04	50	-	2.0	5.0	173.7 ± 1.91	0.35 ± 0.02	+0.32 ± 0.01	0.06 ± 0.01	5.14 ± 1.82	86.28 ± 1.94
ETNP/Eu/PVA/05	50	-	1.0	2.5	325.7 ± 1.07	0.39 ± 0.01	+1.06 ± 0.62	0.07 ± 0.02	7.24 ± 1.02	89.08 ± 1.11
ETNP/Eu/PVA/06	50	-	1.0	10.0	318.3 ± 1.24	0. 44 ± 0.01	-2.06 ± 0.37	0.36 ± 0.01	9.41 ± 0.68	85.05 ± 1.02
ETNP/Eu/PVA/07	50	-	1.0	20.0	322.0 ± 1.33	0.48 ± 0.02	-2.79 ± 0.94	0.79 ± 0.02	10.81 ± 1.29	86.01 ± 2.41
ETNP/Eu/PVA/08	25	-	1.0	5.0	318.3 ± 0.66	0.42 ± 0.05	-3.87 ± 0.19	0.15 ± 0.00	7.14 ± 0.89	83.91 ± 1.99
ETNP/Eu/PVA/09	100		1.0	5.0	ND	ND	ND	ND	ND	ND
ETNP/Eu/PVA/10	200	-	1.0	5.0	ND	ND	ND	ND	ND	ND

ND - not determined, [a] - Polydispersity Index, [b] - Entrapment efficiency; Each value is mean of 3 independent determinations

Table 4: Composition and effect of various parameters on the formulation characteristics of nanoparticles prepared with combination of PLGA co polymers and PCL.

Code	Polymer (mg)				Stabilizer (% w/v)		Drug (mg)	Mean Size (nm) ± SD	PI[a] ± SD	Zeta potential (mV) ± SD	Drug Content (%) ± SD	EE[b] (%) ± SD	Recovery (%) ± SD
	PLGA 50/50	PLGA 75/25	PLGA 85/15	PCL	F68	PVA							
ETNP1/F 68	25	-	-	25	1.0	-	5.0	202.3 ± 1.20	0.19 ± 0.01	-24.33 ± 0.57	1.26 ± 0.01	71.58 ± 0.99	92.81 ± 1.05
ETNP2/F 68	-	25	-	25	1.0	-	5.0	232.5 ± 0.95	0.18 ± 0.00	-27.82 ± 0.99	1.37 ± 0.06	76.82 ± 1.14	91.61 ± 0.63
ETNP3/F 68	-	-	25	25	1.0	-	5.0	234.9 ± 2.31	0.09 ± 0.06	-30.71 ± 1.08	1.49 ± 0.10	85.74 ± 1.08	94.13 ± 1.08
ETNP4/PVA	25	-	-	25	-	1.0	5.0	223.4 ± 1.52	0.04 ± 0.02	-18.85 ± 0.82	1.21 ± 0.04	69.27 ± 1.12	94.00 ± 2.01
ETNP5/PVA	-	25	-	25	-	1.0	5.0	283.1 ± 1.98	0.237 ± 0.01	-20.12 ± 0.33	1.30 ± 0.04	75.18 ± 2.01	95.14 ± 1.01
ETNP6/PVA	-	-	25	25	-	1.0	5.0	288.4 ± 1.87	0.411 ± 0.03	-22.91 ± 1.04	1.46 ± 0.01	81.01 ± 1.03	90.88 ± 0.94

[a] - Polydispersity Index, [b] - Entrapment efficiency; Each value is mean of 3 independent determinations

Table 5: Formulation characteristics for empty nanoparticles.

Code	Polymer (mg)				Stabilizer (% w/v)			Mean Size (nm) ± SD	PI[a] ± SD	Zeta potential (mV) ± SD	Recovery (%) ± SD
	PLGA 50/50	PLGA 75/25	PLGA 85/15	PCL	EuL -100	F68	PVA				
NP/F68/03	50	-	-	-	-	1.0	-	87.2 ± 0.25	0.14 ± 0.01	-18.3 ± 0.52	90.28 ± 0.88
NP/PVA/03	50	-	-	-	-	-	1.0	158.2 ± 1.51	0.15 ± 0.02	-16.8.± 1.00	88.07 ± 1.01
NP/F68/13	-	50	-	-	-	1.0	-	96.9 ± 1.06	0.12 ± 0.01	-17.2 ± 0.51	94.02 ± 1.33
NP/PVA/13	-	50	-	-	-	-	1.0	250.9 ± 3.41	0.12 ± 0.01	-16.9 ± 1.10	91.81 ± 0.72
NP/F68/17	-	-	50	-	-	1.0	-	106.1 ± 2.07	0.09 ± 0.03	-22.3 ± 1.18	91.28 ± 1.11
NP/PVA/17	-	-	50	-	-	-	1.0	283 ± 1.15	0.28 ± 0.04	-17.4 ± 0.66	88.29 ± 0.65
NP/PCL/F68/03	-	-	-	50	-	1.0	-	254.1 ± 1.00	0.13 ± 0.01	-28.1 ± 0.81	88.39 ± 1.42
NP/PCL/PVA/03	-	-	-	50	-	-	1.0	388.5 ± 2.81	0.15 ± 0.03	-14.5 ± 1.08	89.08 ± 1.58
NP/Eu/F68/03	-	-	-	-	50	1.0	-	70.9 ± 1.04	0.33 ± 0.02	-22.9 ± 0.44	82.99 ± 1.89
NP/Eu/PVA/03	-	-	-	-	50	-	1.0	318.3 ± 1.25	0.14 ± 0.01	-1.01 ± 0.21	85.15 ± 0.29
NP1/F 68	50	-	-	50	-	1.0	-	201.4 ± 0.92	0.15 ± 0.01	-22.8 ± 0.77	90.11 ± 1.03
NP2/F 68	-	50	-	50	-	1.0	-	225.9 ± 0.94	0.19 ± 0.07	-24.1 ± 0.41	91.06 ± 0.88
NP3/F 68	-	-	50	50	-	1.0	-	234.0 ± 1.03	0.17 ± 0.03	-31.5 ± 0.22	91.94 ± 0.61
NP4/PVA	50	-	-	50	-	-	1.0	221.4 ± 1.18	0.91 ± 0.01	-20.8 ± 1.01	95.48 ± 1.83
NP5/PVA	-	50	-	50	-	-	1.0	280.1 ± 0.88	0.38 ± 0.01	-22.9 ± 0.81	92.80 ± 1.30
NP6/PVA	-	-	50	50	--	-	1.0	287.8 ± 1.34	0.34 ± 0.08	-22.0 ± 1.06	93.84 ± 1.48

[a] - Polydispersity Index; Each value is mean of 3 independent determinations

Table 6: Effect of freeze drying on physical characteristics of nanoparticles.

Code	Mean Size in nm ± SD	PI[a] ± SD	Zeta Potential (mV) ± SD	Drug Content (%) ± SD	EE[b] (%) ± SD	Recovery ± SD
F/ETNP/F68/03	94.2 ± 1.10	0.14 ± 0.01	-22.17 ± 1.11	1.05 ± 0.04	57.28 ± 1.05	89.24 ± 1.21
F/ETNP/PVA/03	172.1 ± 0.50	0.18 ± 0.01	-10.01 ± 0.97	1.06 ± 0.10	54.23 ± 0.88	83.98 ± 0.51
F/ETNP/F68/13	106.8 ± 0.48	0.15 ± 0.03	-28.11 ± 0.41	1.15 ± 0.03	64.82 ± 2.11	92.38 ± 2.04
F/ETNP/PVA/13	260.2 ± 0.71	0.20 ± 0.02	-9.12 ± 1.27	1.16 ± 0.07	65.10 ± 1.98	92.07 ± 0.62
F/ETNP/F68/17	108.8 ± 052	0.16 ± 0.02	-28.08 ± 1.03	1.33 ± 0.01	74.04 ± 0.94	91.46 ± 1.18
F/ETNP/PVA/17	290.2 ± 1.39	0.24 ± 0.03	-6.09 ± 0.81	1.32 ± 0.01	71.58 ± 0.62	88.67 ± 0.60
F/ETNP/PCL/F68/03	264.3 ± 1.17	0.15 ± 0.01	-25.17 ± 1.24	1.35 ± 0.03	73.58 ± 0.44	89.08 ± 1.21
F/ETNP/PCL/PVA/03	382.6 ± 2.54	0.31 ± 0.04	-12.97 ± 1.07	1.27 ± 0.05	70.58 ± 1.51	90.85 ± 0.82
F/ETNP/Eu/F68/03	77.2 ± 1.63	0.39 ± 0.02	-25.21 ± 0.82	0.27 ± 0.02	14.18 ± 0.55	86.41 ± 1.04
F/ETNP/Eu/PVA/03	330.7 ± 0.94	0.41 ± 0.06	-1.04 ± 0.18	0.19 ± 0.03	10.04 ± 1.11	85.33 ± 0.72

[a] - Polydispersity Index, [b] - Entrapment efficiency; Each value is mean of 3 independent determinations

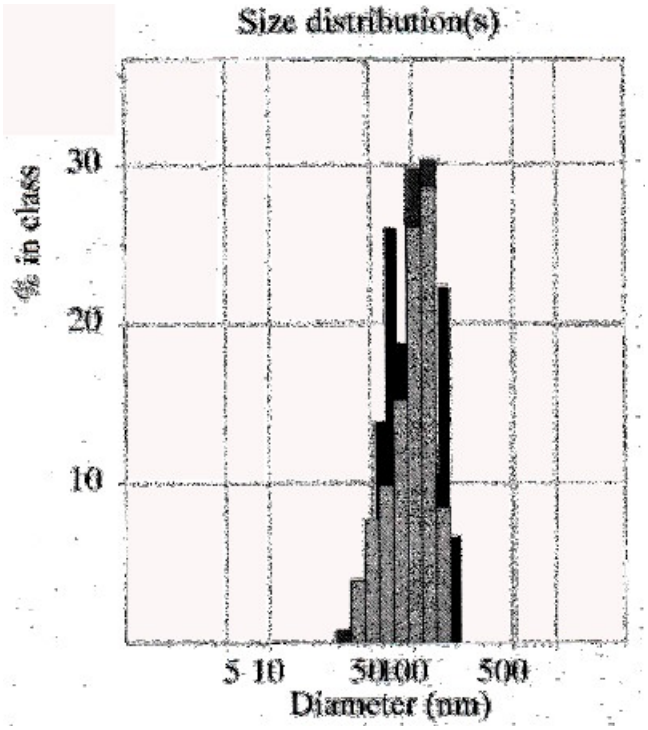

Figure 1A: Size distribution profile of nanoparticle formulation (ETNP/F68/03).

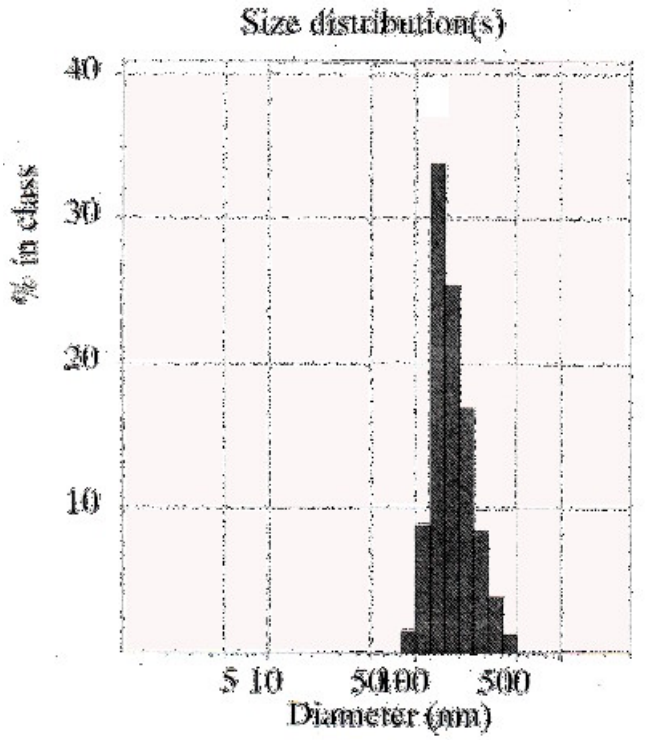

Figure 1B: Size distribution profile of nanoparticle formulation (ETNP/PVA/03).

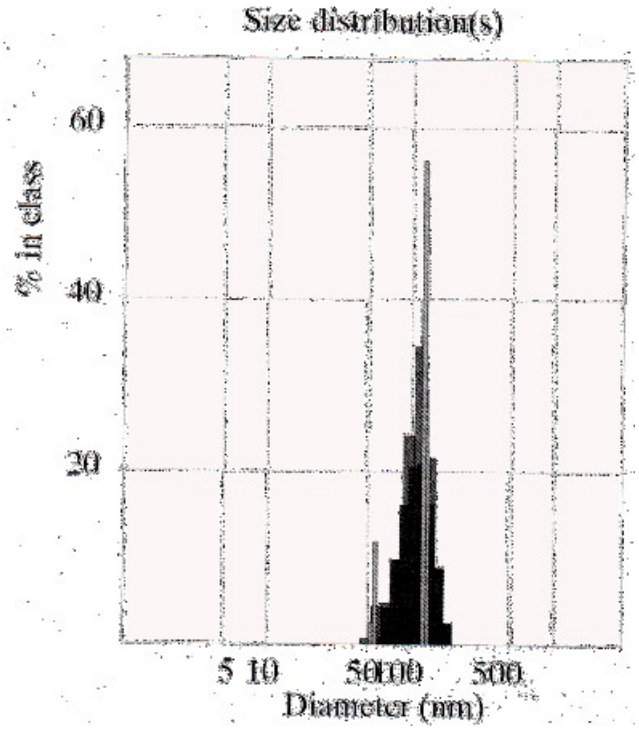

Figure 1C: Size distribution profile of nanoparticle formulation (ETNP/F68/13).

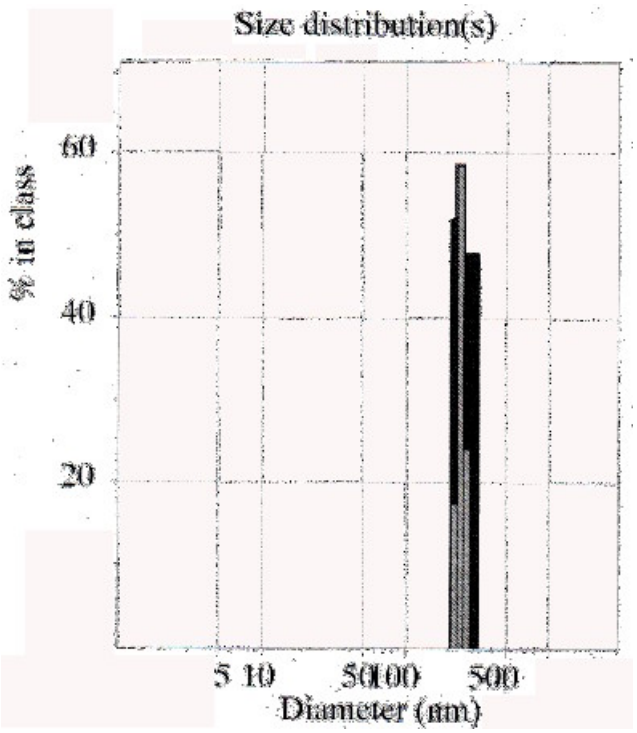

Figure 1D: Size distribution profile of nanoparticle formulation (ETNP/PVA/13).

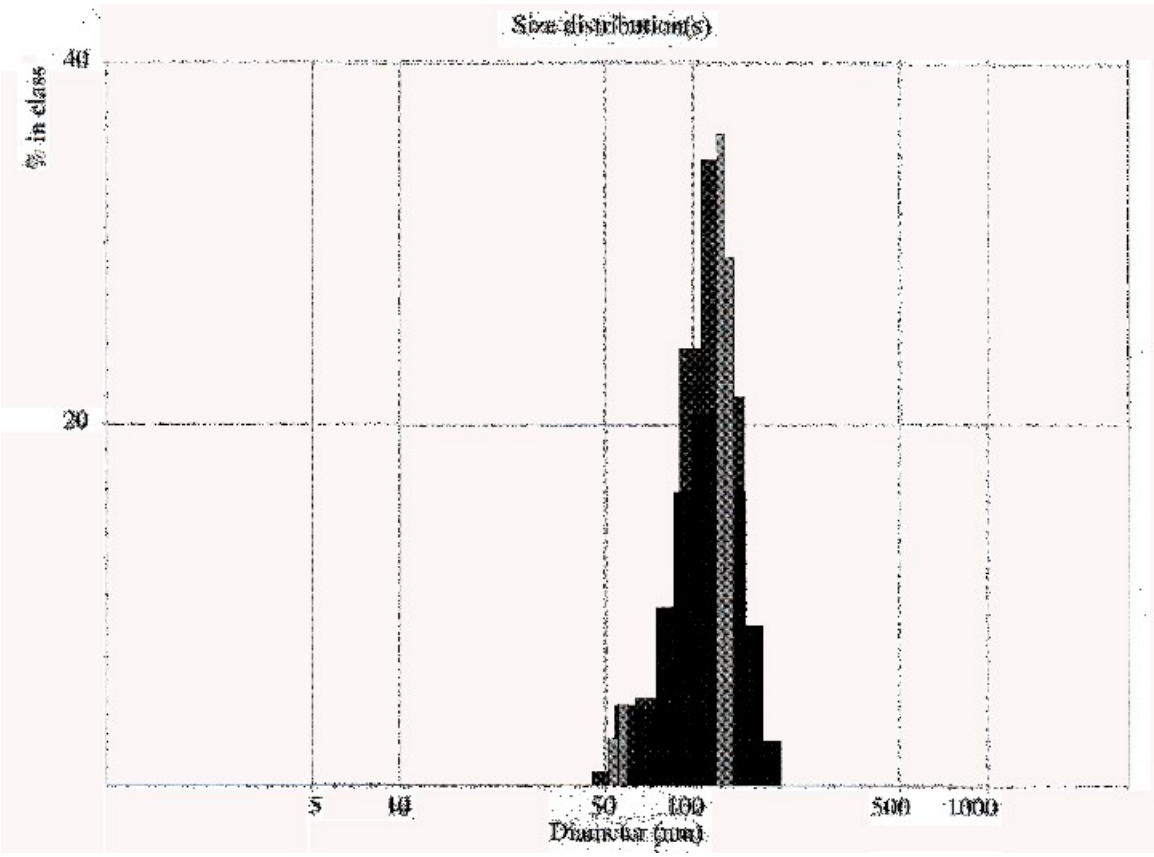

Figure 1E: Size distribution profile of nanoparticle formulation (ETNP/F68/17).

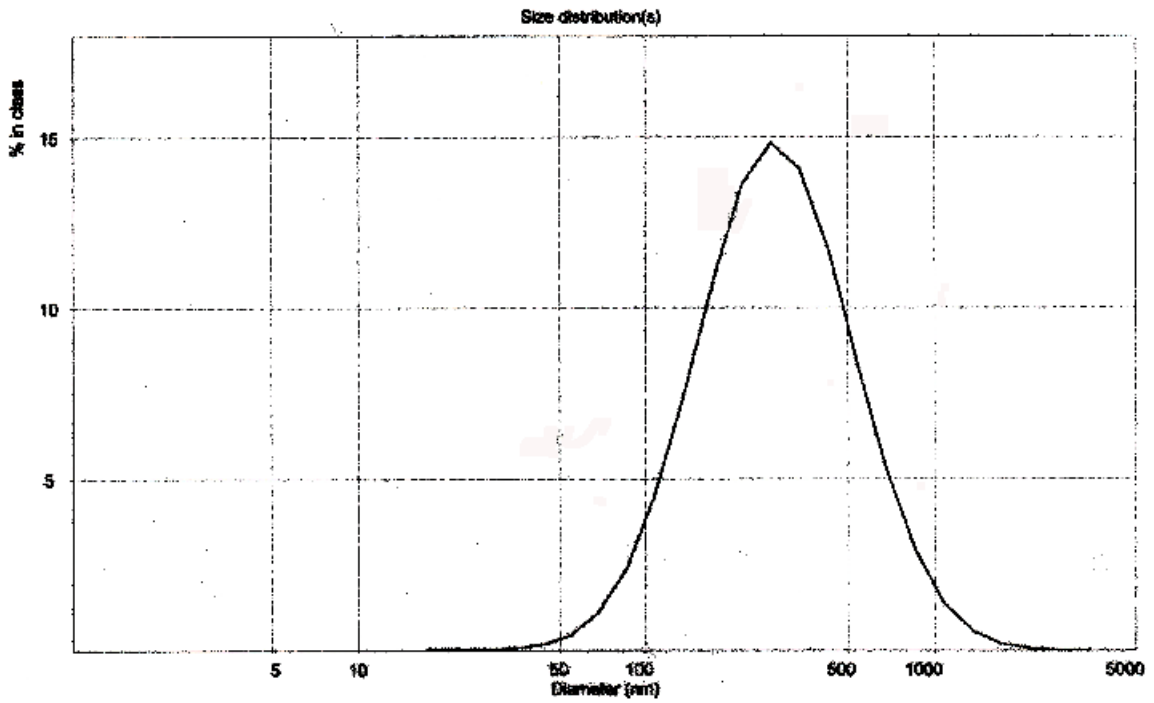

Figure 1F: Size distribution profile of nanoparticle formulation (ETNP/PVA/17).

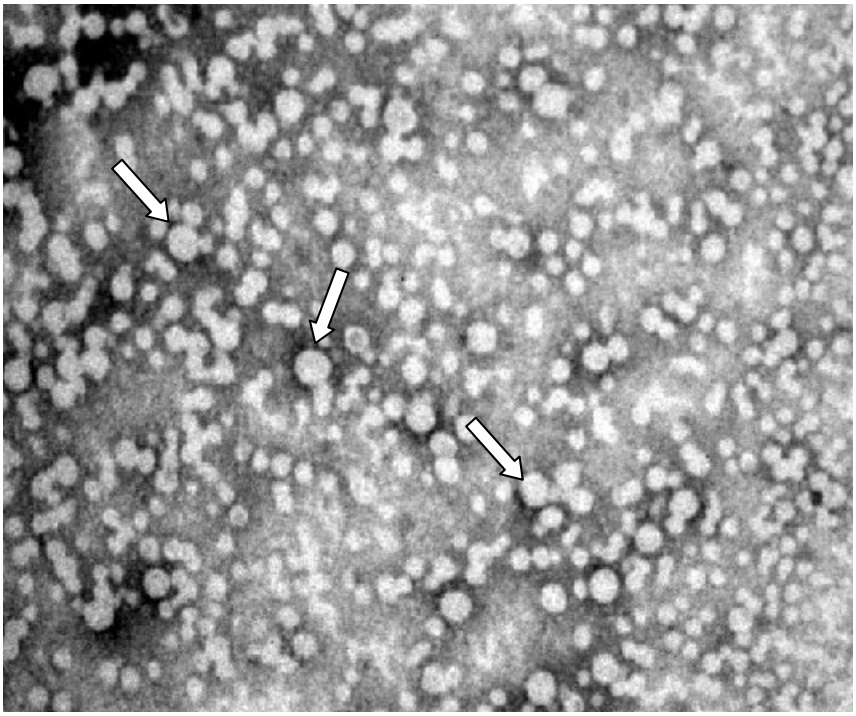

Figure 2A: TEM image of nanoparticle formulation (ETNP/F68/03) (× 24000 magnification). Arrows indicate nanoparticles.

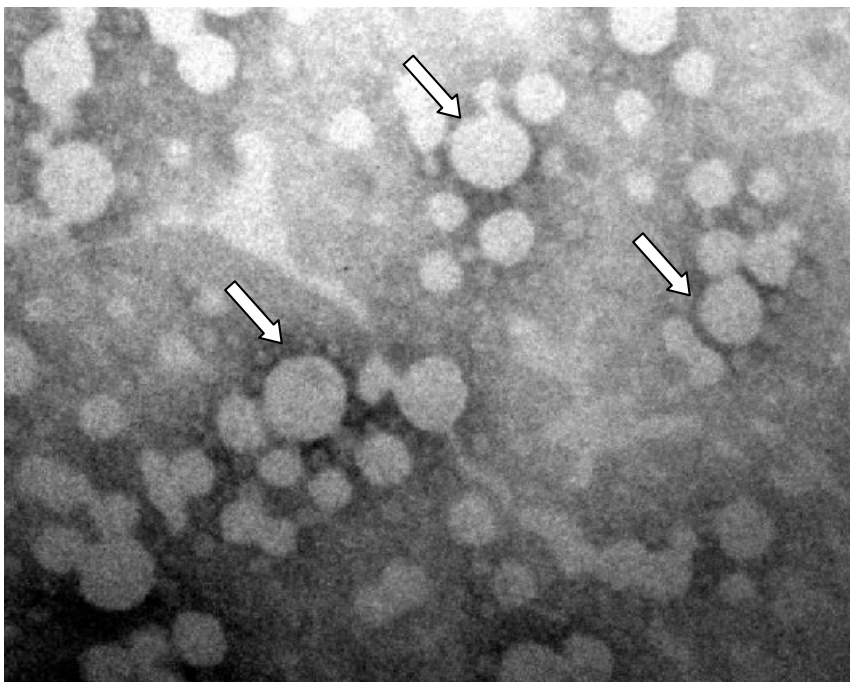

Figure 2B: TEM image of nanoparticle formulation (ETNP/PVA/03) (× 18000 magnification). Arrows indicate nanoparticles.

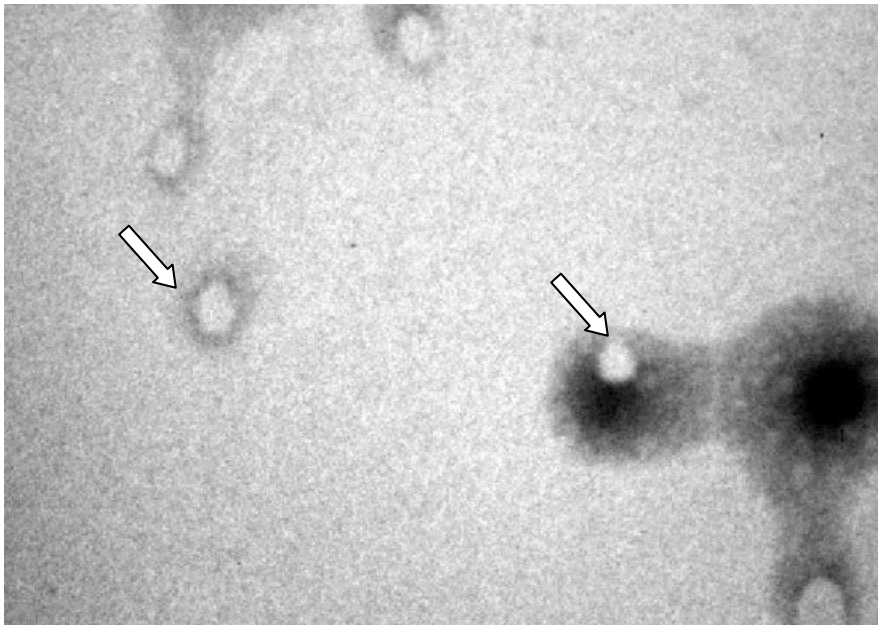

Figure 2C: TEM image of nanoparticle formulation (ETNP/F68/13) (× 20000 magnification). Arrows indicate nanoparticles.

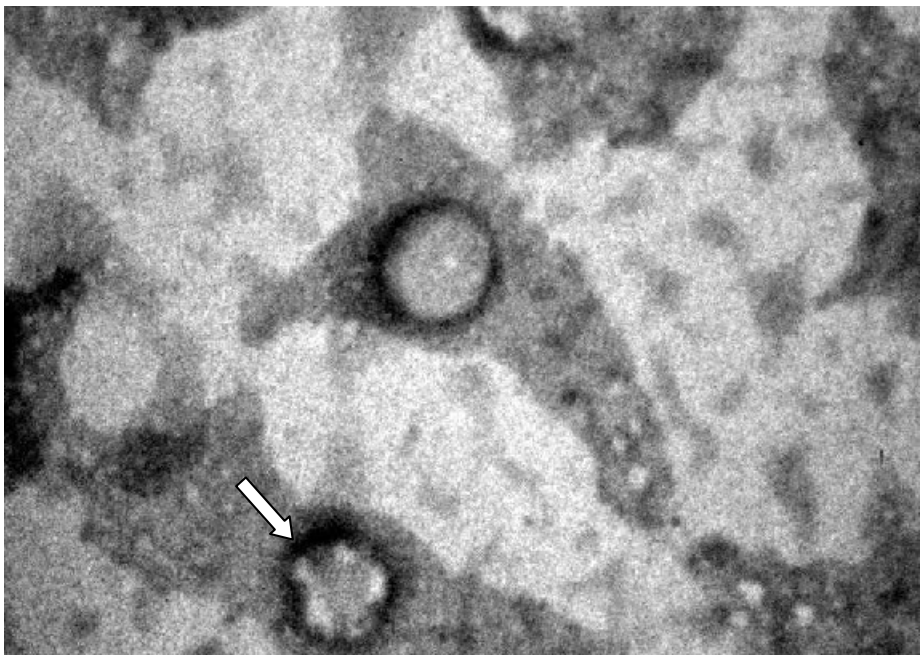

Figure 2D: TEM image of nanoparticle formulation (ETNP/PVA/13) (× 18000 magnification). Arrows indicate nanoparticles.

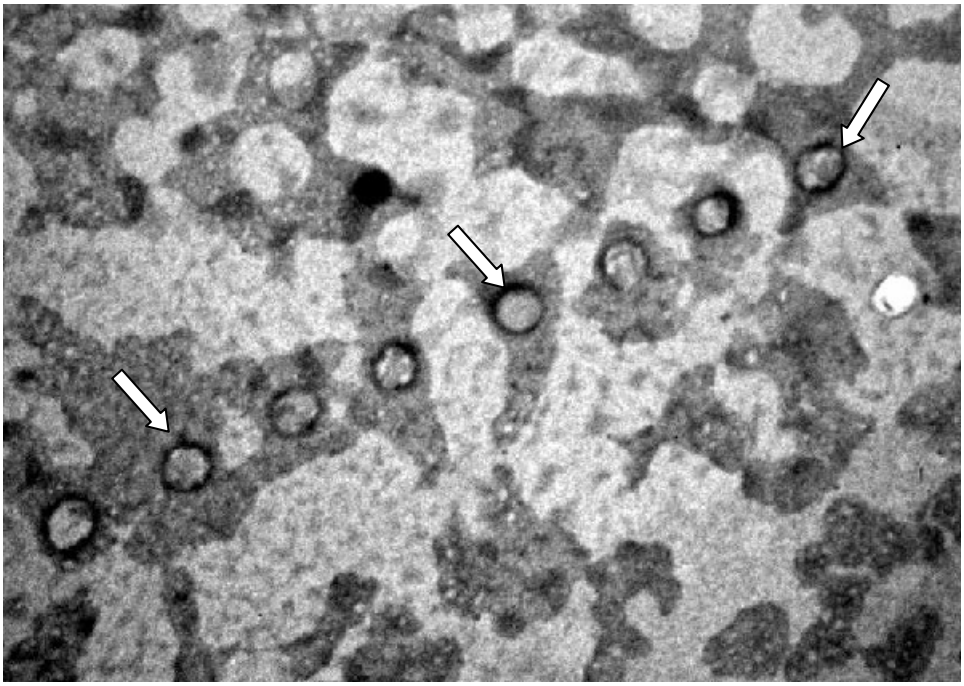

Figure 2E: TEM image of nanoparticle formulation (ETNP/F68/17) (× 21000 magnification). Arrows indicate nanoparticles.

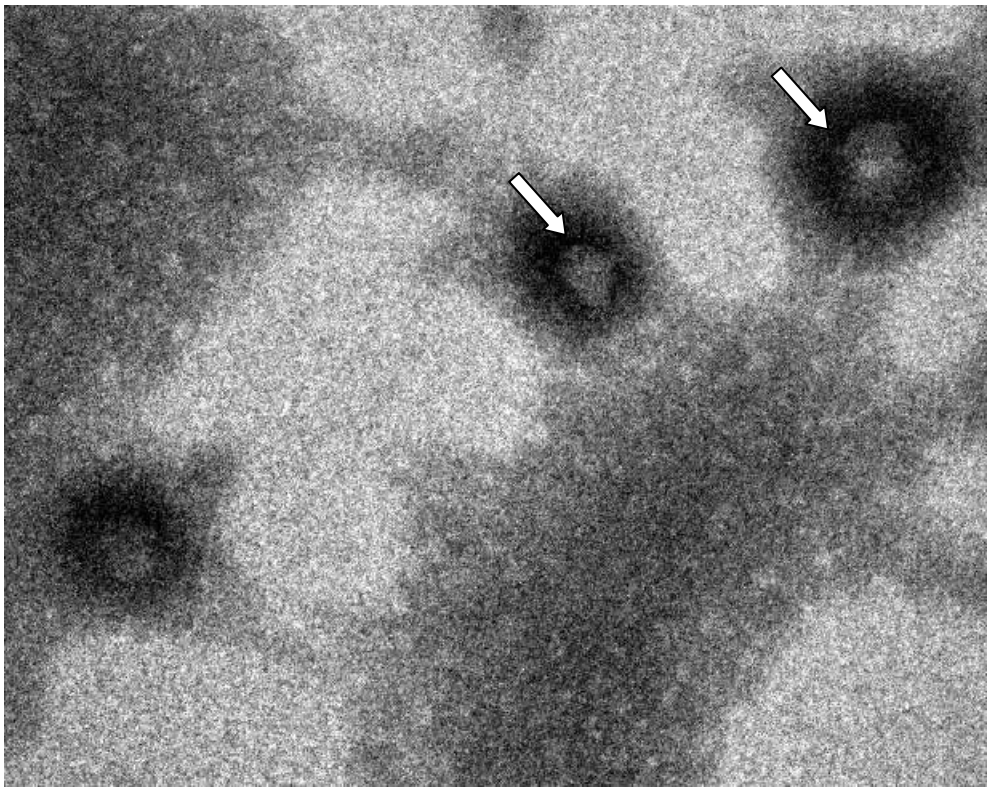

Figure 2F: TEM image of nanoparticle formulation (ETNP/PVA/17) (× 16000 magnification). Arrows indicate nanoparticles.

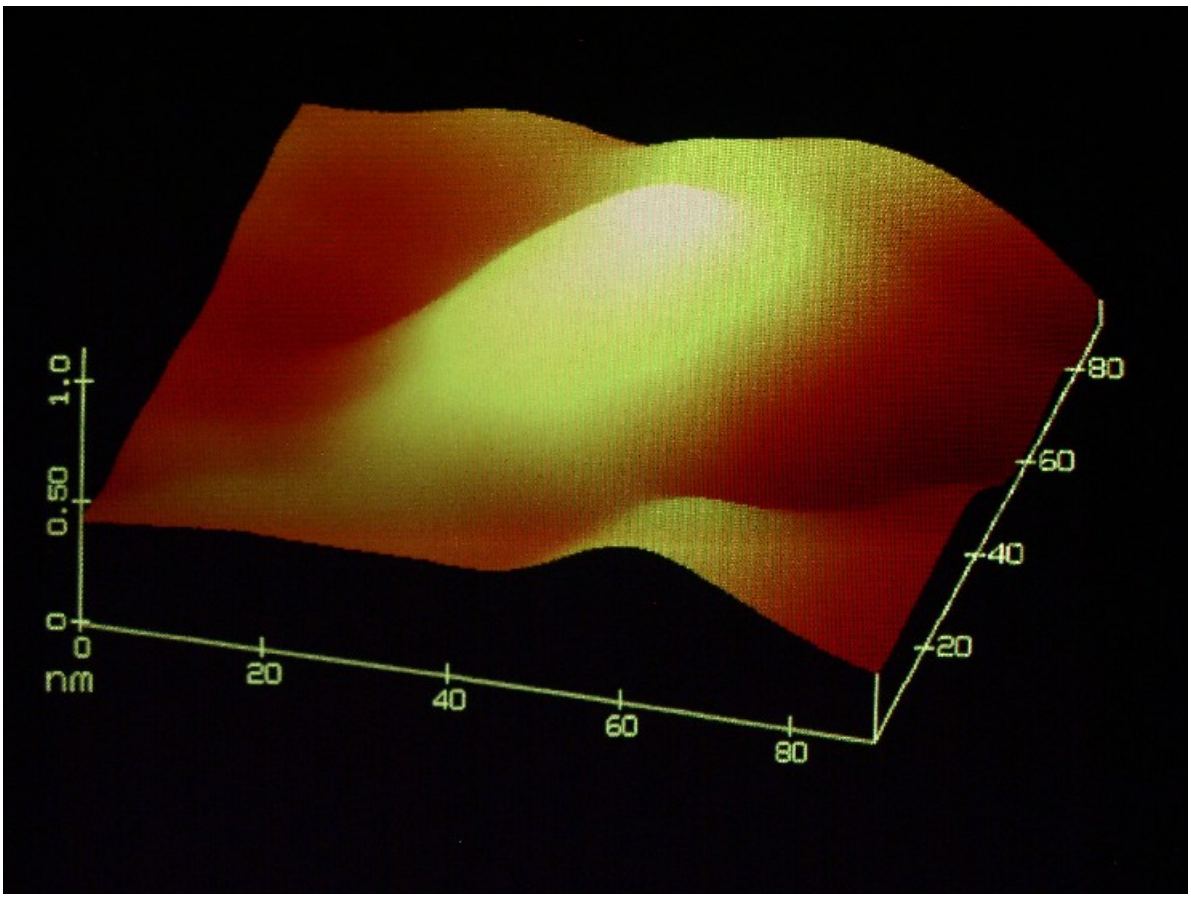

Figure 3: AFM image of nanoparticle formulation (ETNP/F68/17).

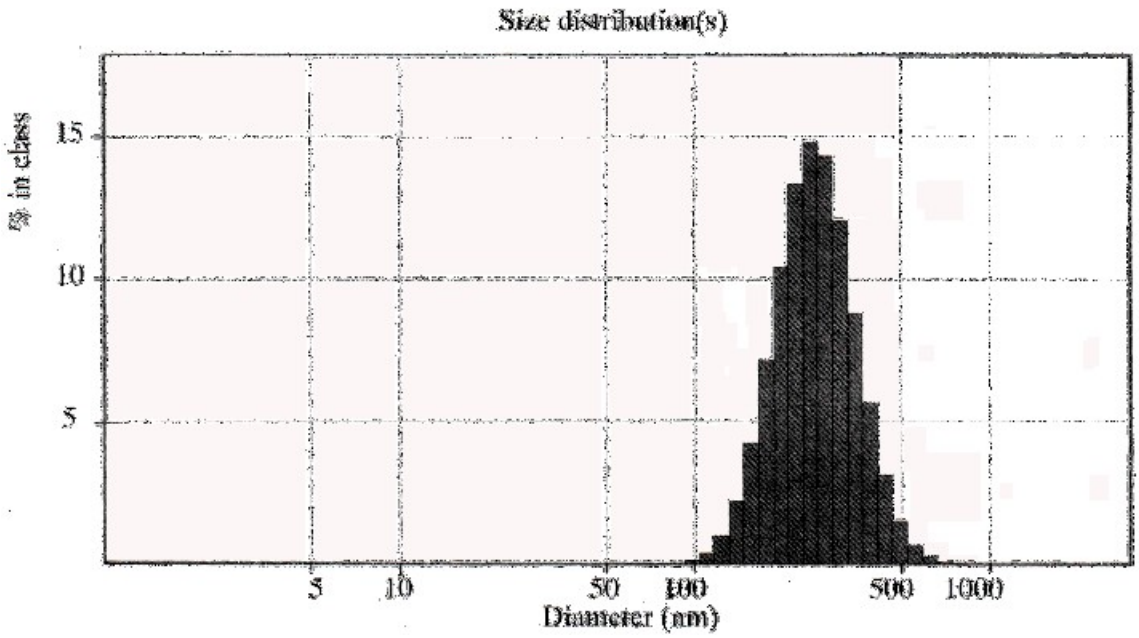

Figure 4A: Size distribution profile of nanoparticle formulation (ETNP/PCL/F68/03).

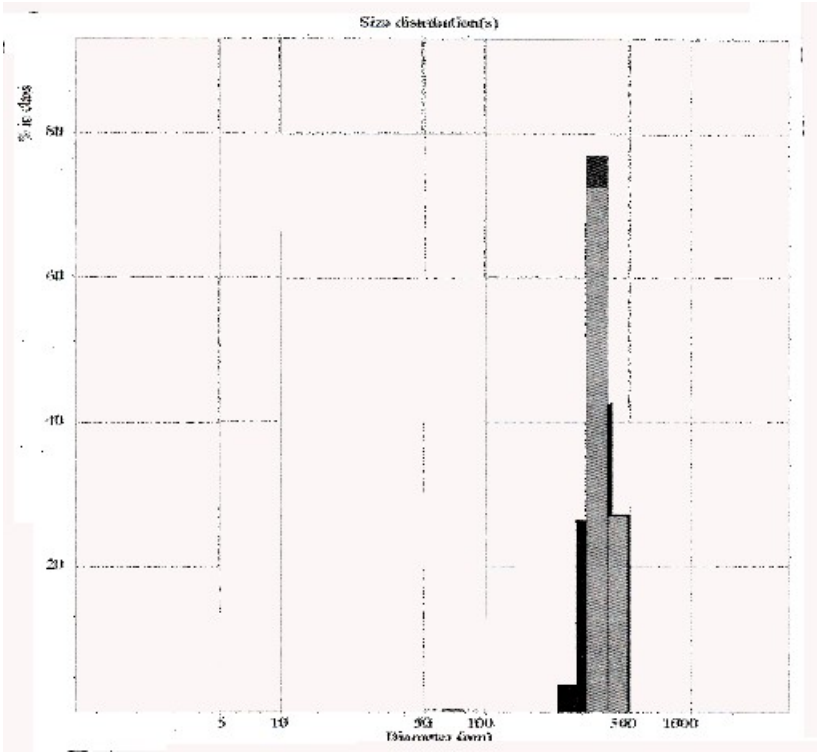

Figure 4B: Size distribution profile of nanoparticle formulation (ETNP/PCL/PVA/03).

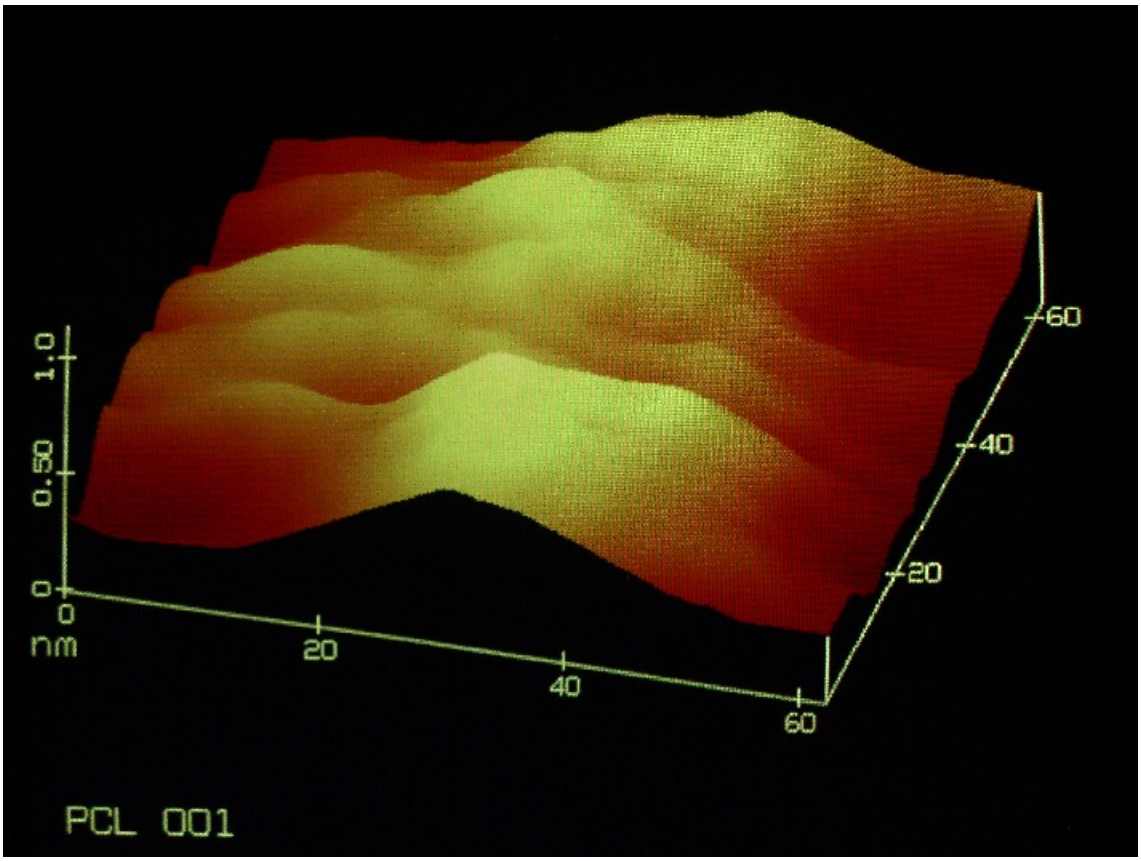

Figure 5: AFM image of nanoparticle formulation (ETNP/PCL/F68/03).

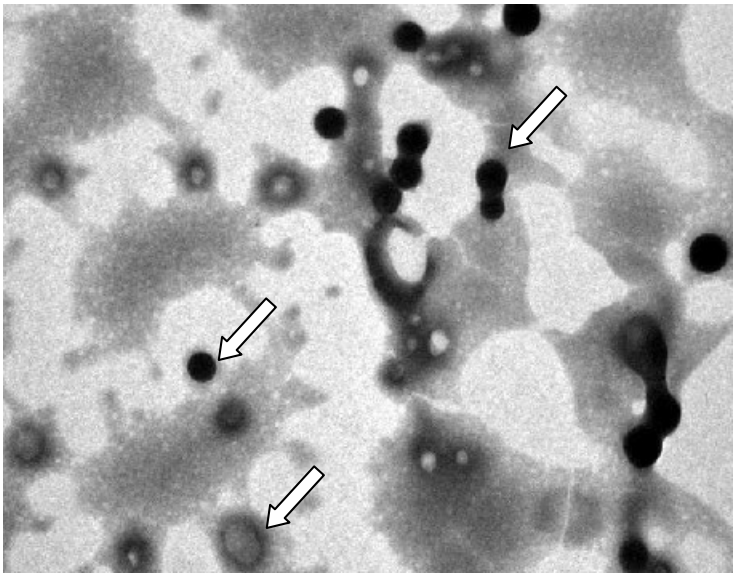

Figure 6A: TEM image of nanoparticle formulation (ETNP/PCL/F68/03) (× 24000 magnification). Arrows indicate nanoparticles.

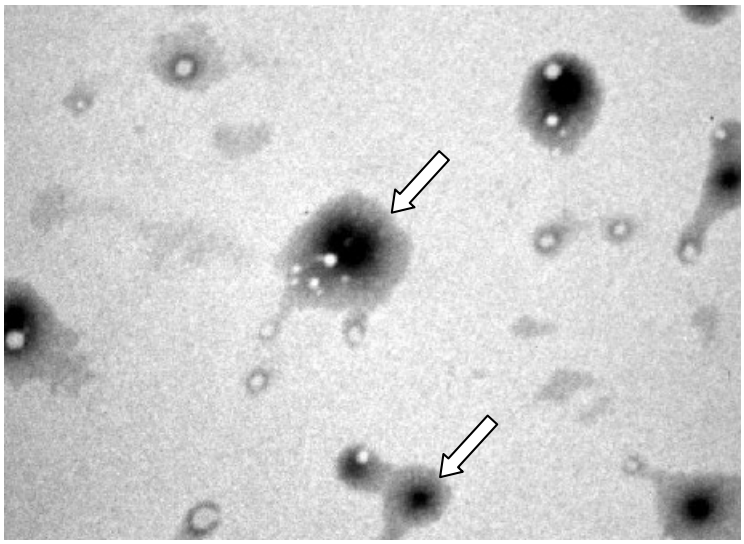

Figure 6B: TEM image of nanoparticle formulation (ETNP/PCL/PVA/03) (× 12000 magnification). Arrows indicate nanoparticles.

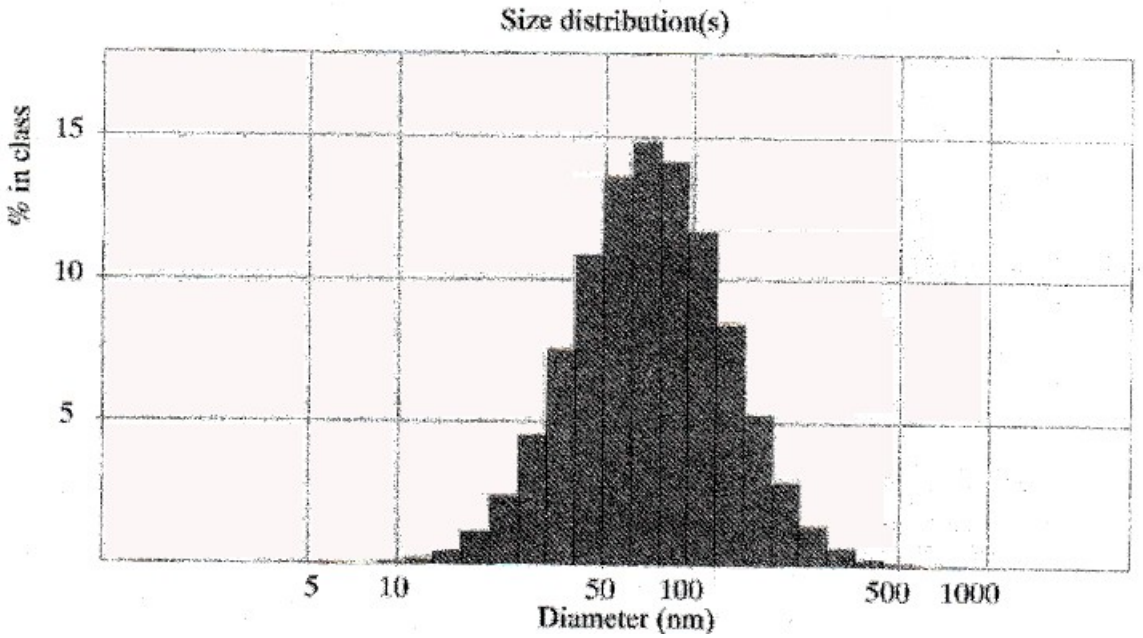

Figure 7A: Size distribution profile of nanoparticle formulation (ETNP/Eu/F68/03).

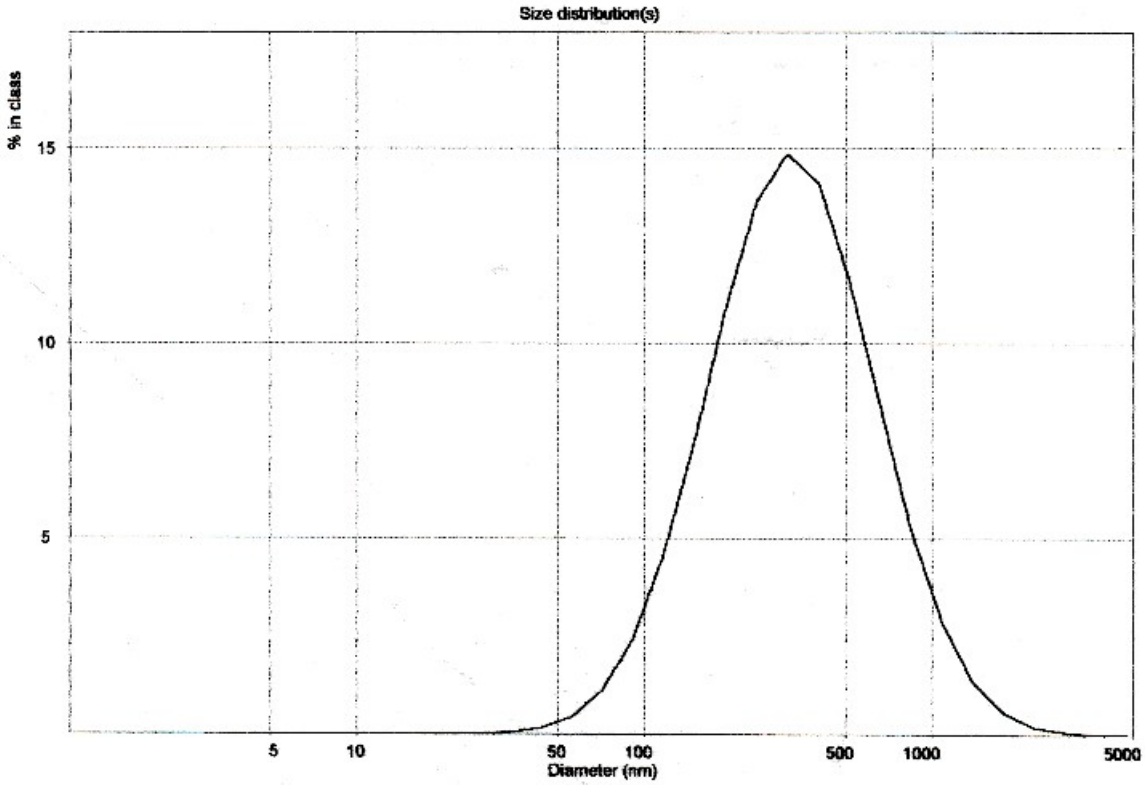

Figure 7B: Size distribution profile of nanoparticle formulation (ETNP/Eu/PVA/03).

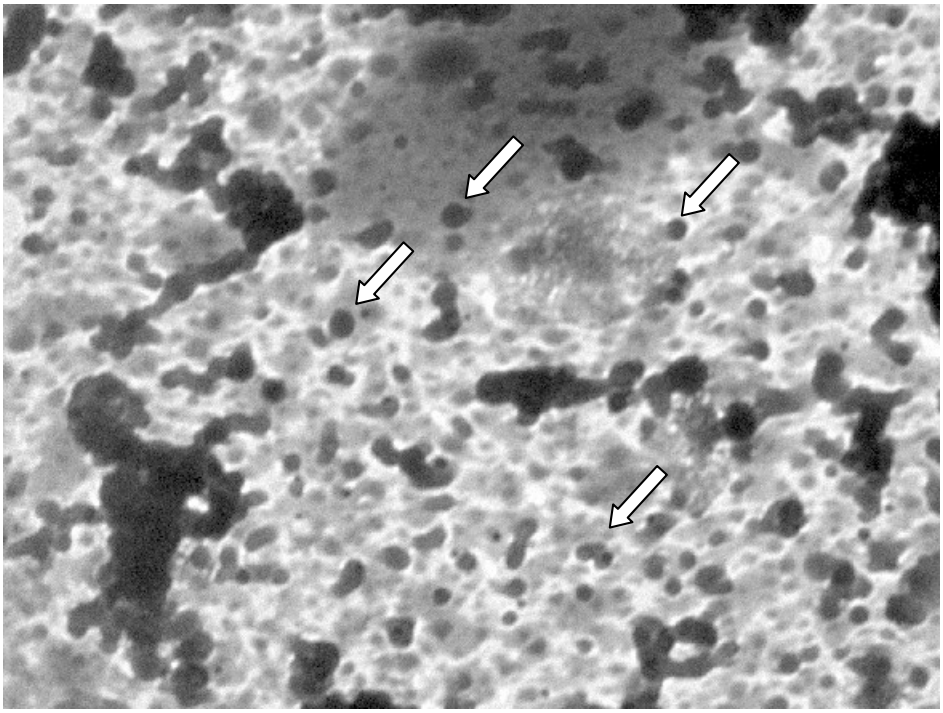

Figure 8A: TEM image of nanoparticle formulation (ETNP/Eu/F68/03) (× 24000 magnification). Arrows indicate nanoparticles.

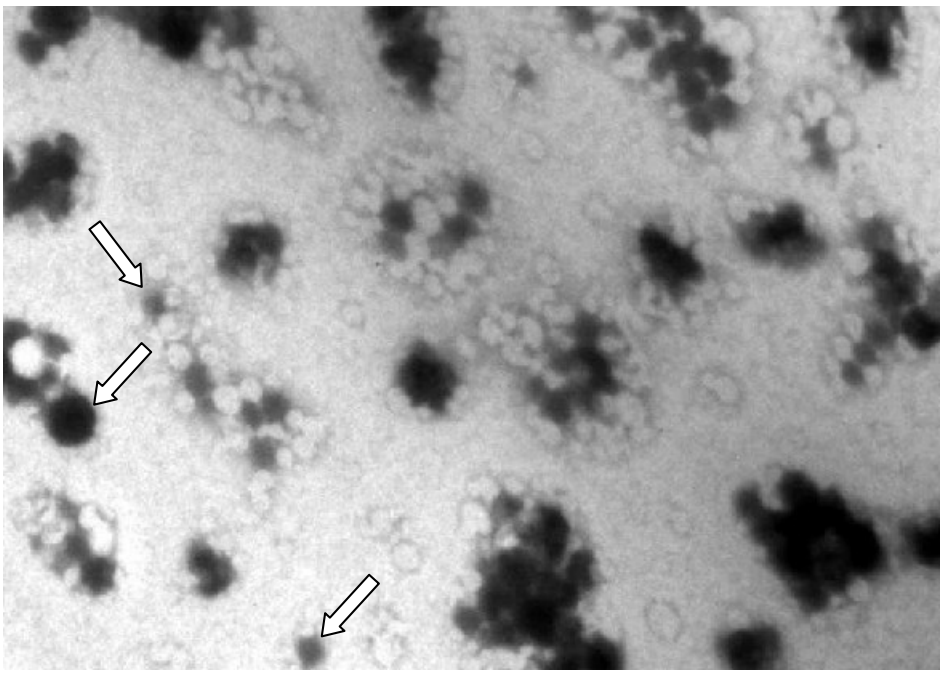

Figure 8B: TEM image of nanoparticle formulation (ETNP/Eu/PVA/03) (× 25000 magnification). Arrows indicate nanoparticles.

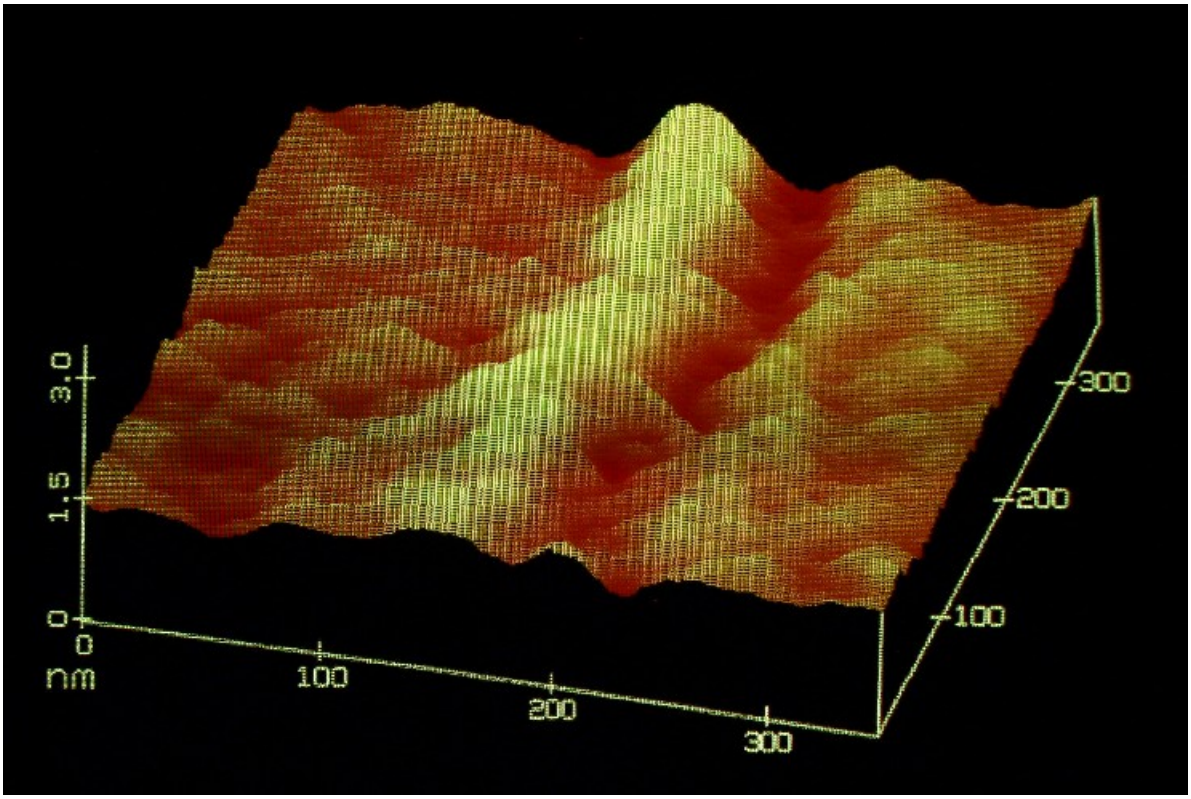

Figure 9: AFM image of nanoparticle formulation (ETNP/Eu/F68/03).

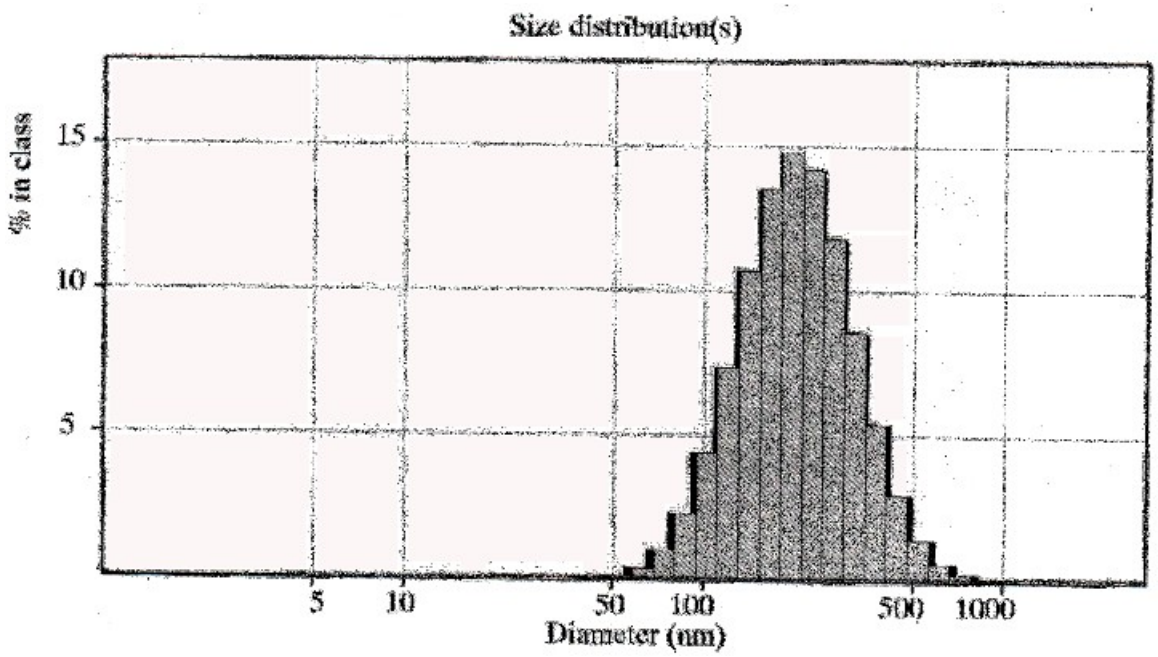

Figure 10A: Size distribution profile of nanoparticle formulation (ETNP1/F68).

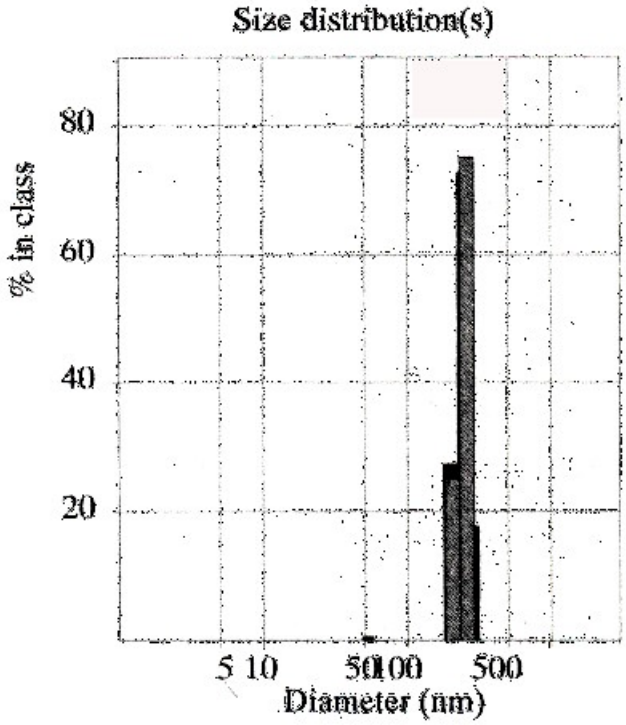

Figure 10B: Size distribution profile of nanoparticle formulation (ETNP2/F68).

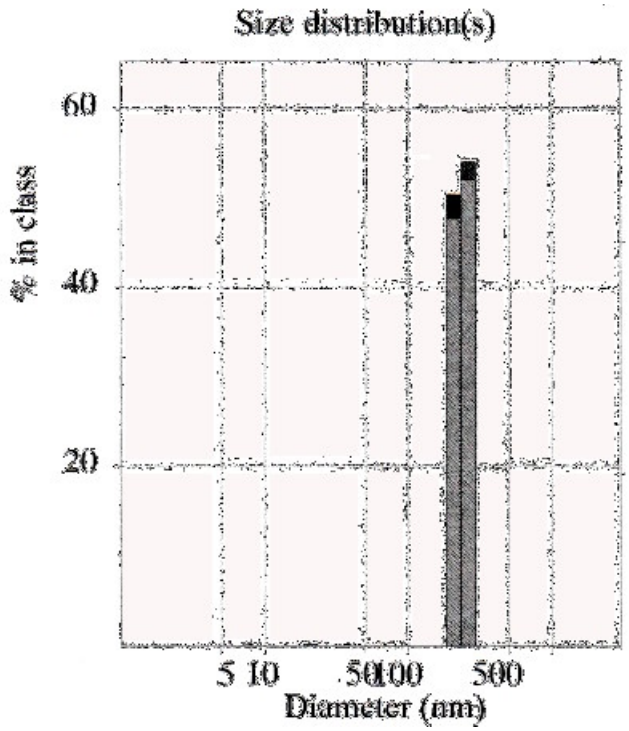

Figure 10C: Size distribution profile of nanoparticle formulation (ETNP3/F68).

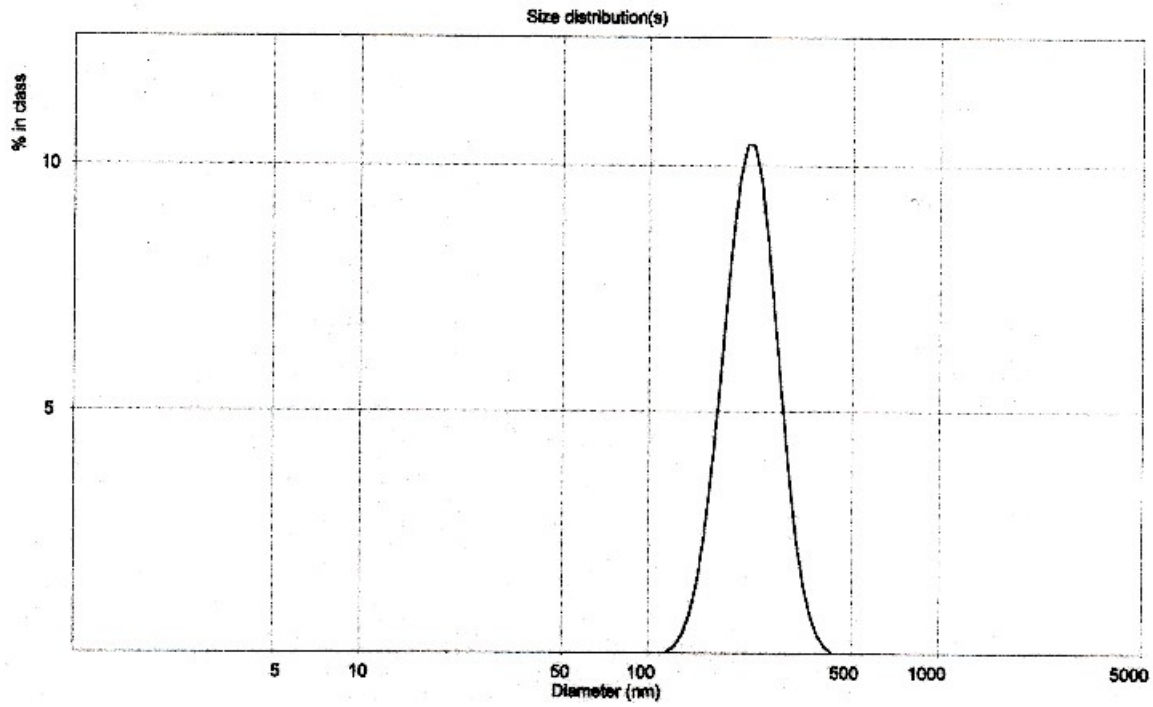

Figure 10D: Size distribution profile of nanoparticle formulation (ETNP4/PVA).

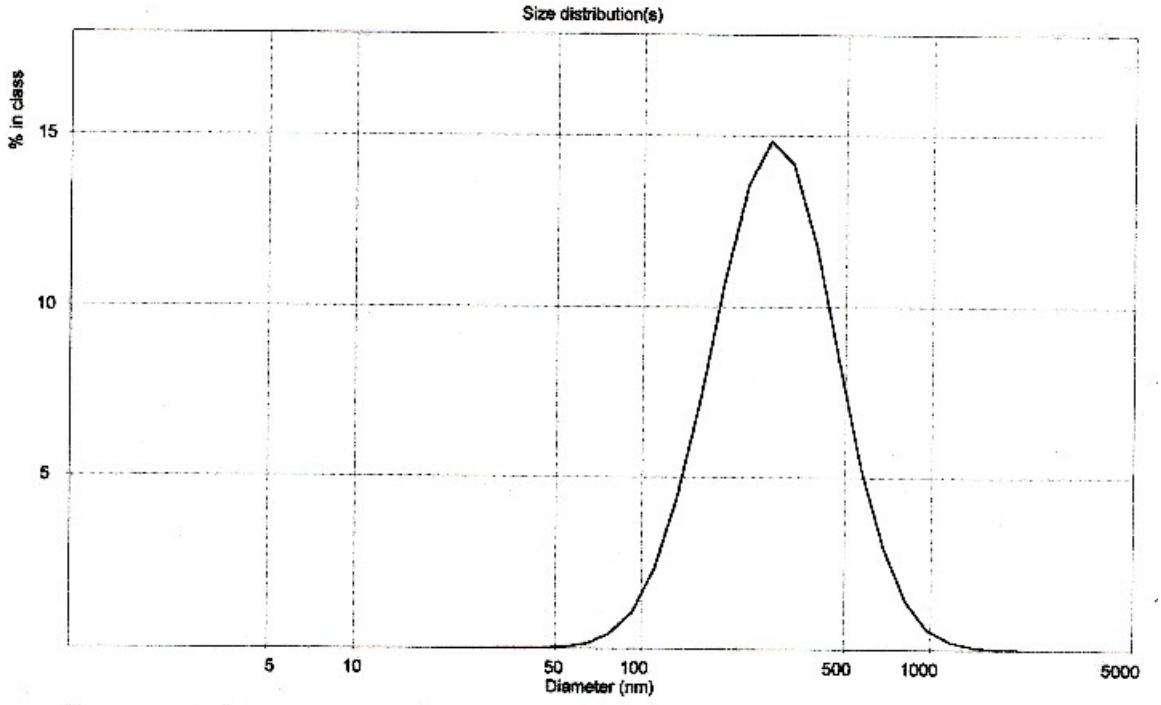

Figure 10E: Size distribution profile of nanoparticle formulation (ETNP5/PVA).

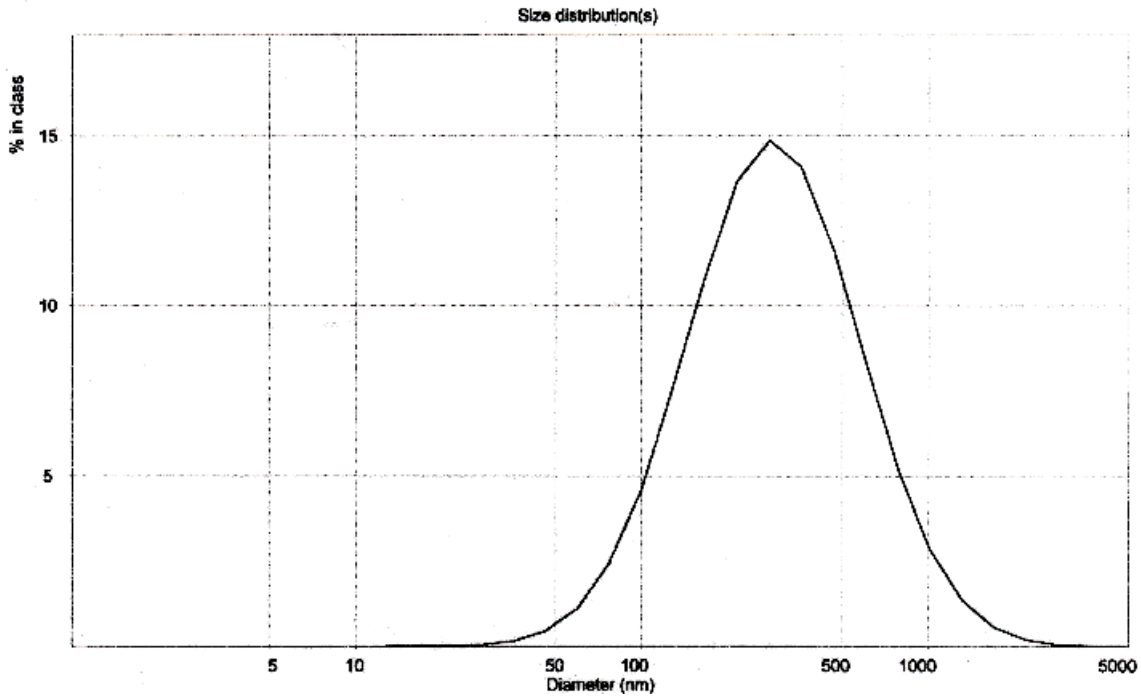

Figure 10F: Size distribution profile of nanoparticle formulation (ETNP6/PVA).

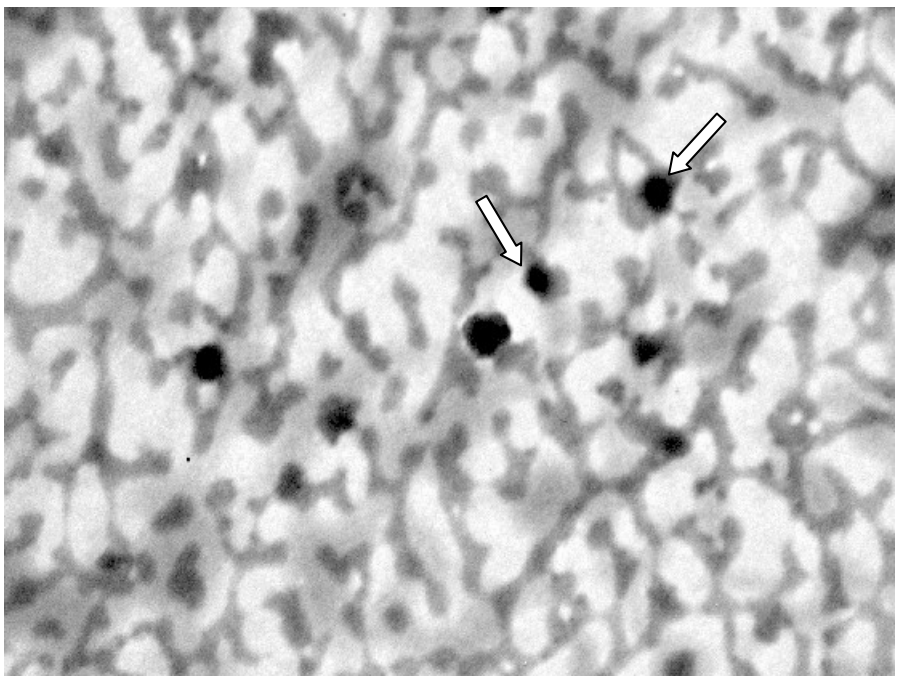

Figure 11A: TEM image of nanoparticle formulation (ETNP1/F68) (× 26000 magnification). Arrows indicate nanoparticles.

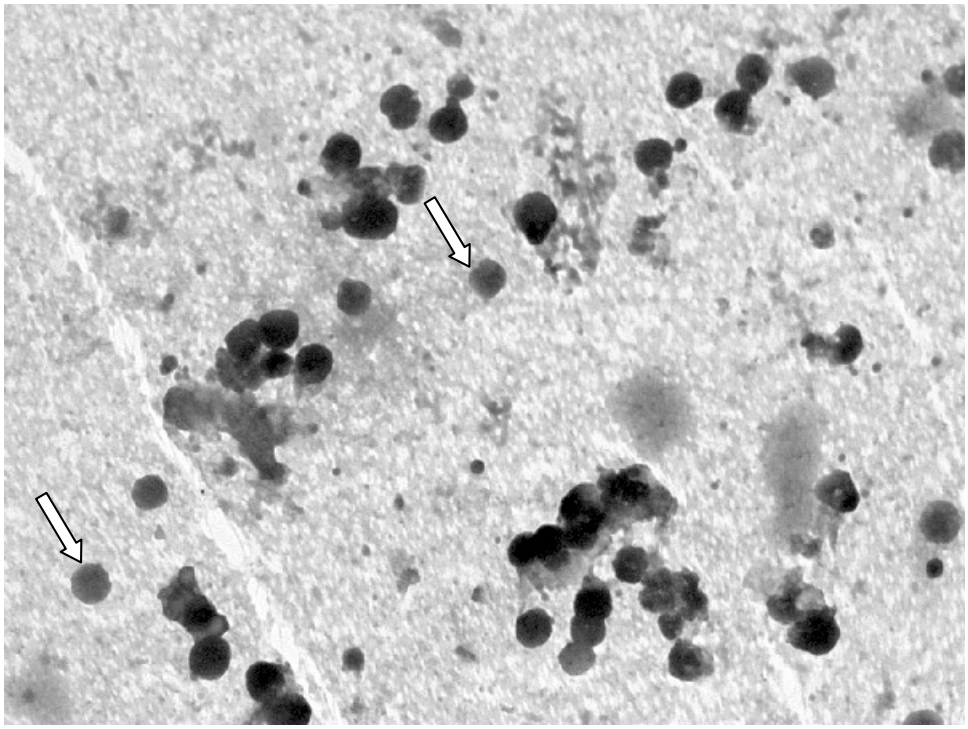

Figure 11B: TEM image of nanoparticle formulation (ETNP2/F68) (× 24000 magnification). Arrows indicate nanoparticles.

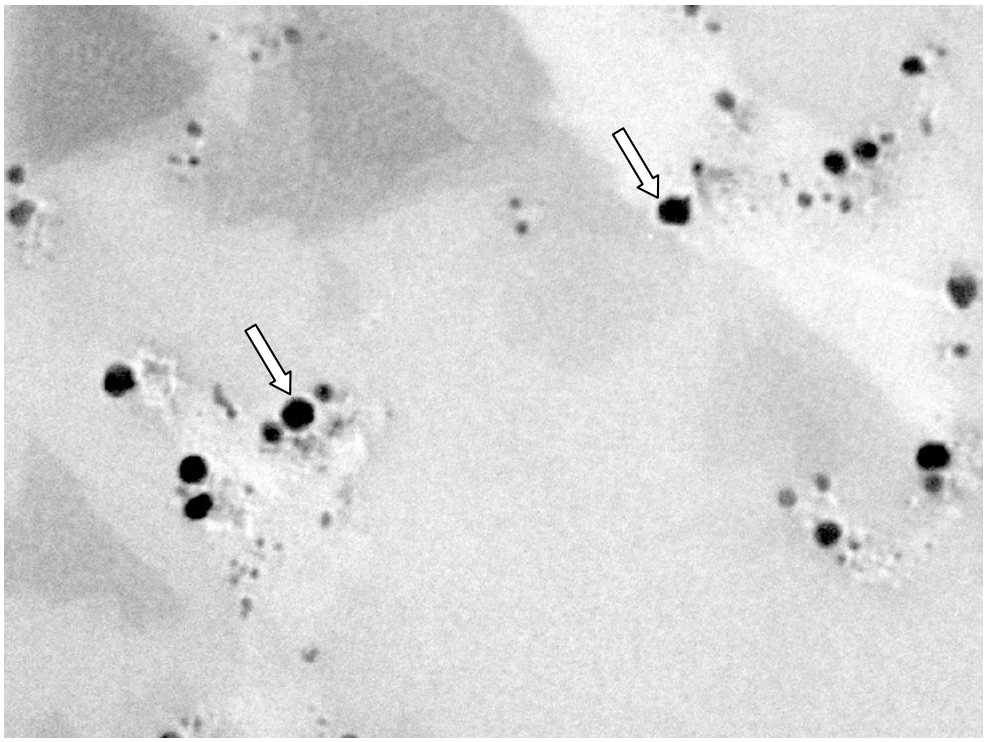

Figure 11C: TEM image of nanoparticle formulation (ETNP3/F68) (× 24000 magnification). Arrows indicate nanoparticles.

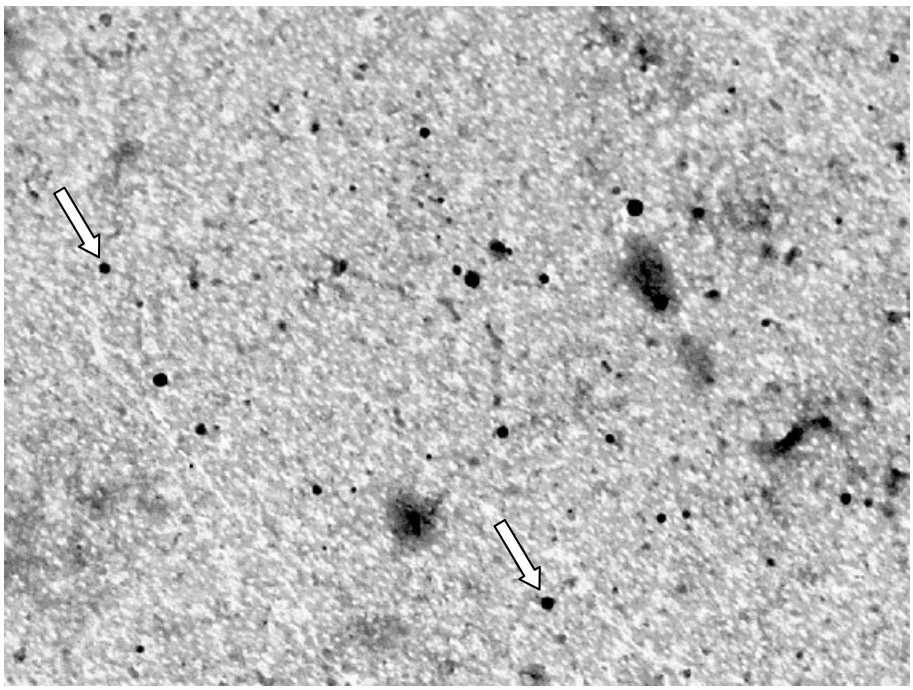

Figure 11D: TEM image of nanoparticle formulation (ETNP4/PVA) (× 20000 magnification). Arrows indicate nanoparticles.

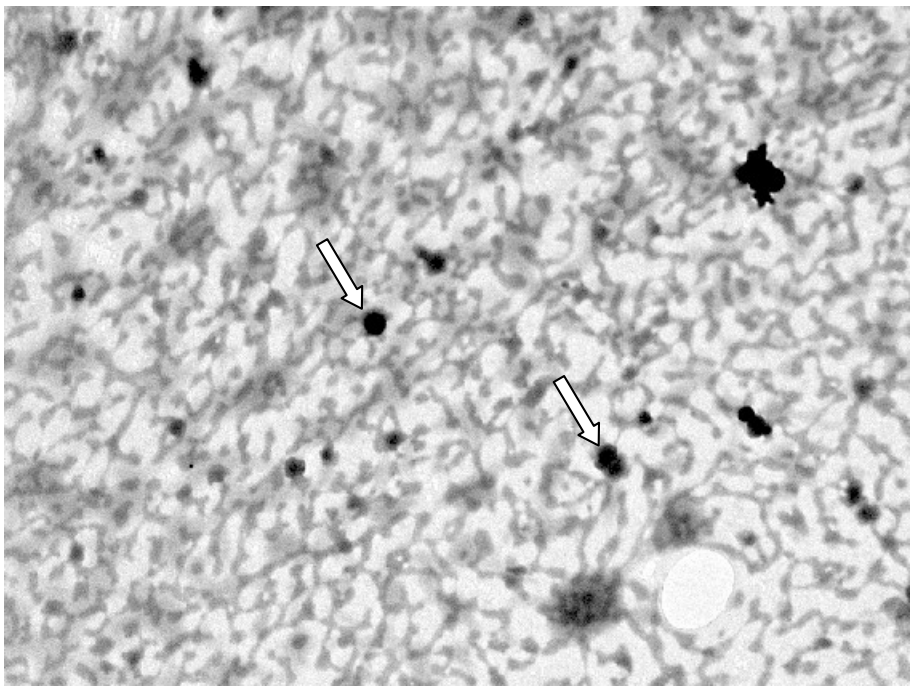

Figure 11E: TEM image of nanoparticle formulation (ETNP5/PVA) (× 25000 magnification). Arrows indicate nanoparticles.

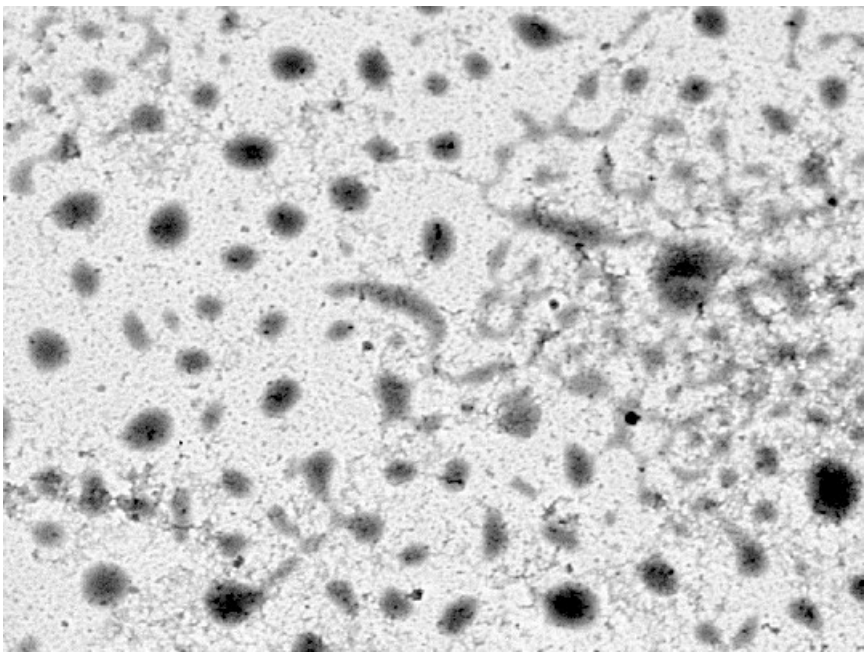

Figure 11F: TEM image of nanoparticle formulation (ETNP6/PVA) (× 24000 magnification). Arrows indicate nanoparticles.

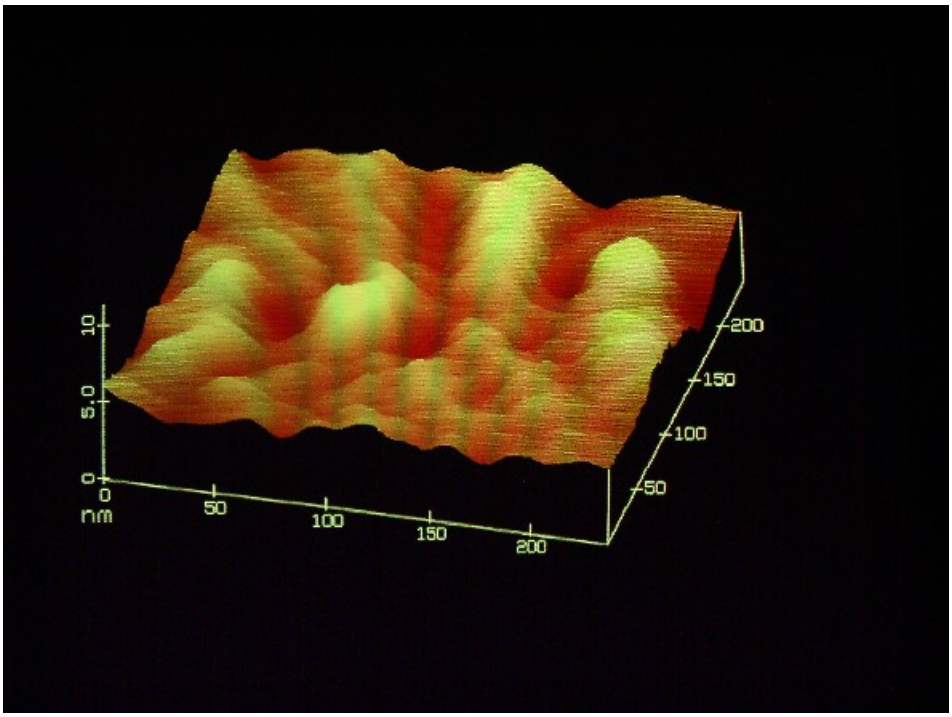

Figure 12A: AFM image of nanoparticle formulation (ETNP1/F68).

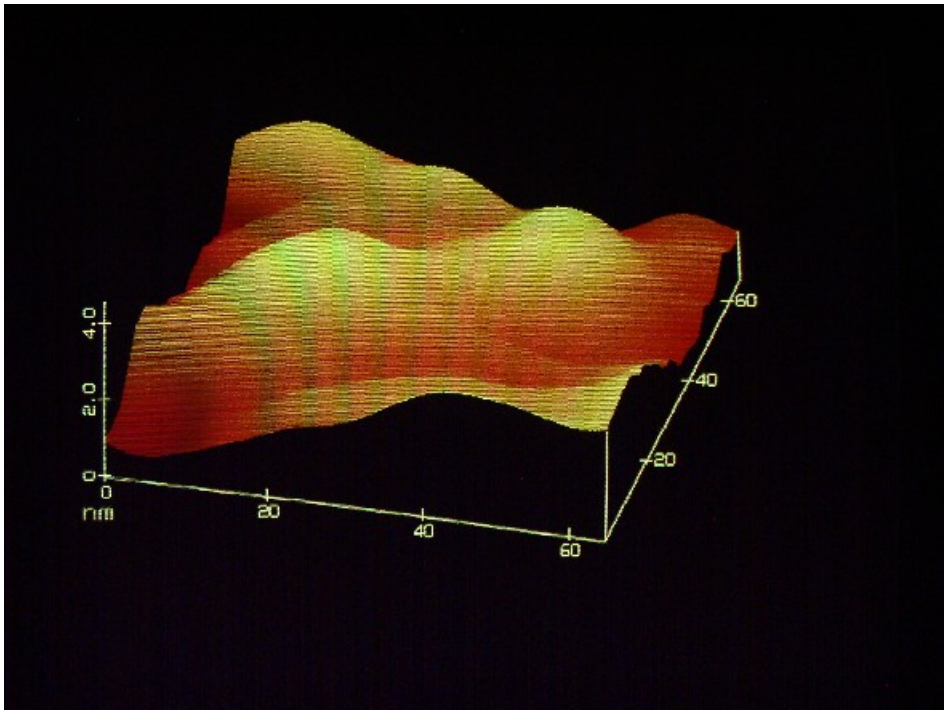

Figure 12B: AFM image of nanoparticle formulation (ETNP1/PVA).

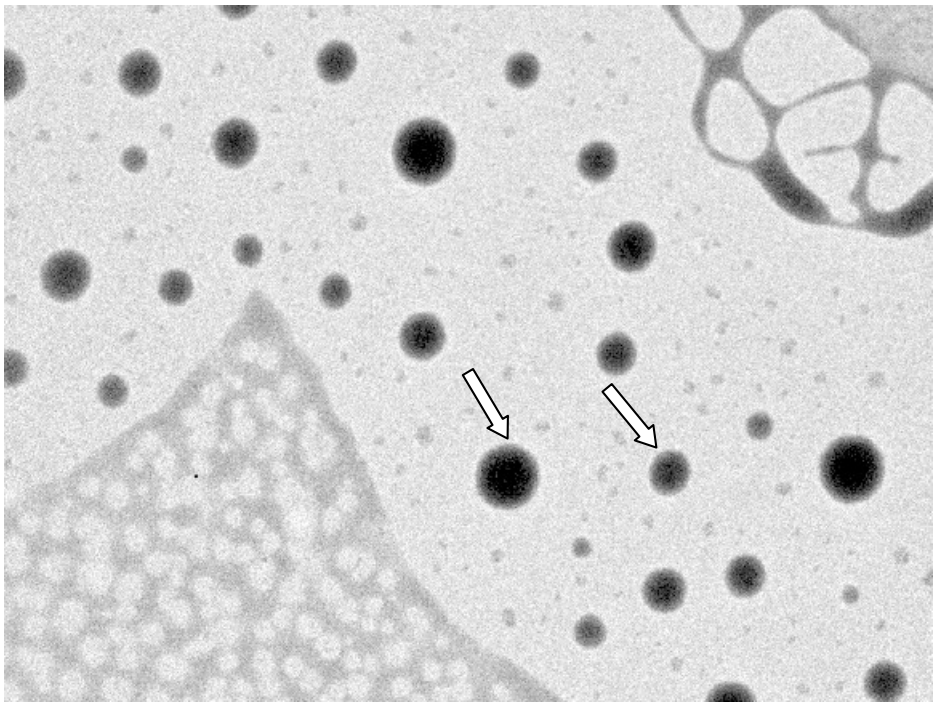

Figure 13: TEM image of nanoparticle formulation (F/ETNP/F68/17) after freeze drying (× 32000 magnification). Arrows indicate nanoparticles.

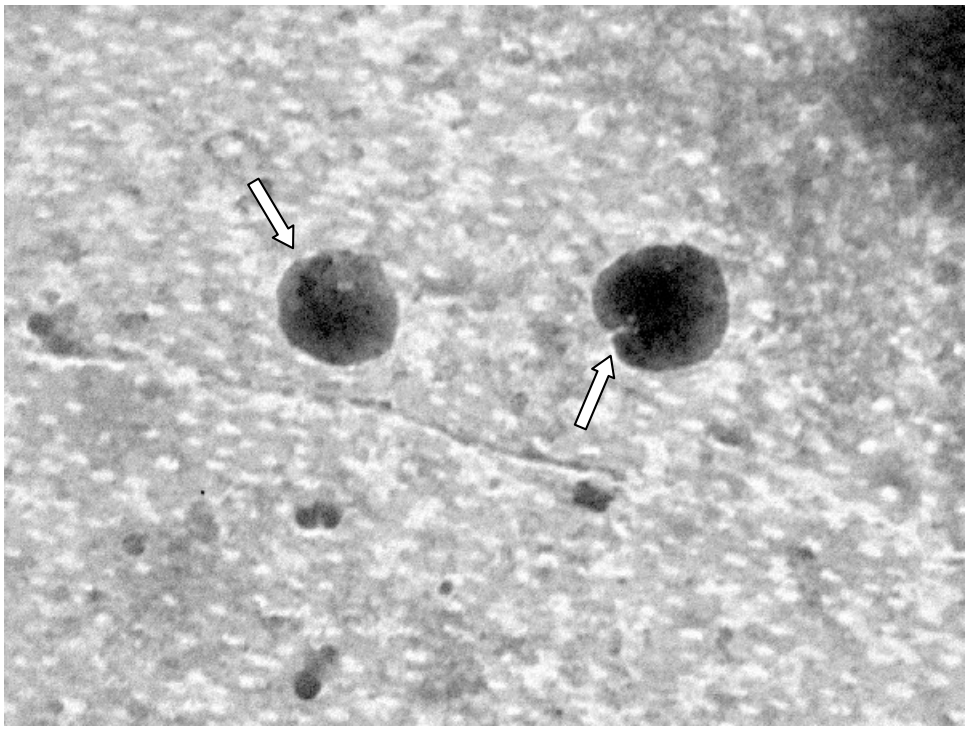

Figure 14: TEM image of nanoparticle formulation (F/ETNP/PCL/F68/03) after freeze drying (× 36000 magnification). Arrows indicate nanoparticles.

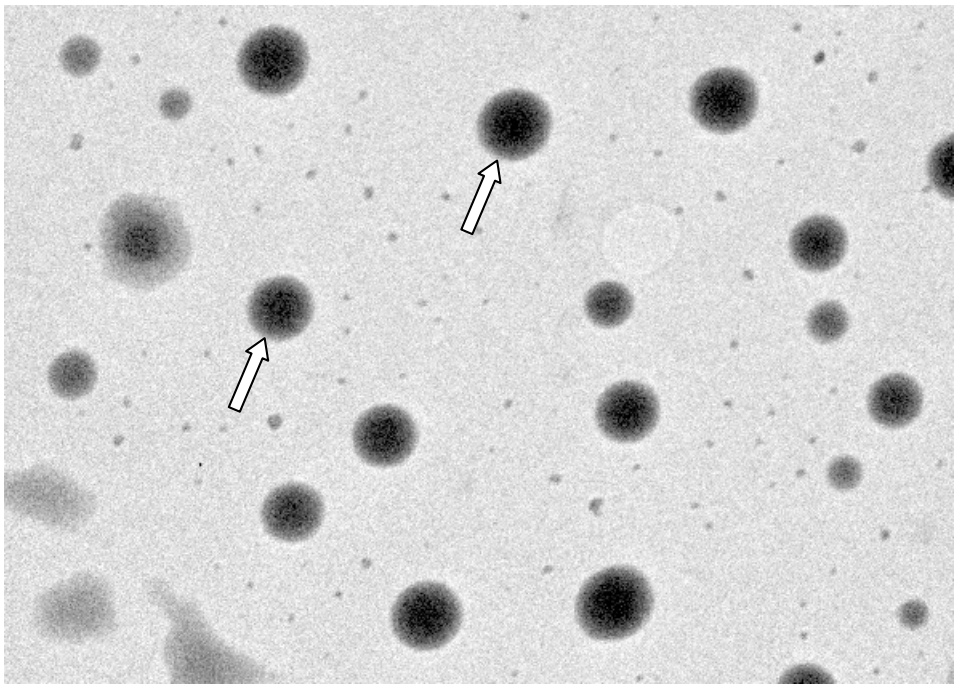

Figure 15: TEM image of nanoparticle formulation (F/ETNP/PVA/17) after freeze drying (× 32000 magnification). Arrows indicate nanoparticles.

Table 7: Redispersibility of the prepared formulations.

Code	Redispersibility in TDW		Redispersibility in Stabilizer solution	
	Freeze dried product	Sediment after centrifugation	Freeze dried product	Sediment after centrifugation
ETNP/F68/03	+ + +	+ +	+ + +	+ + +
ETNP/PVA/03	+ +	+	+ +	+ +
ETNP/F68/13	+ + +	+ +	+ + +	+ + +
ETNP/F68/17	+ + +	+ +	+ + +	+ + +
ETNP/PVA/13	+ +	-	+ +	+
ETNP/PVA/17	+ +	-	+ +	+
ETNP/PCL/F68/03	+ +	+	+ + +	+ + +
ETNP/PCL/PVA/03	+ +	- -	+ +	-
ETNP/Eu/F68/03	+ +	-	+ +	-
ETNP/Eu/PVA/03	-	- -	+	-

+ + + Excellent . + + Good, + Fair, - Poor, - - Very Poor

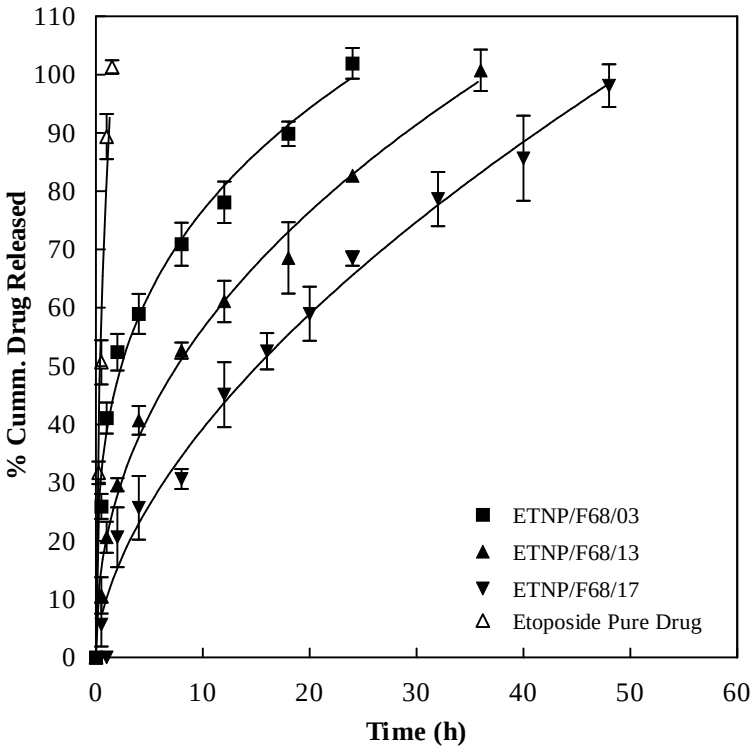

Figure 16: In vitro release profiles of etoposide and formulations prepared with PLGA co polymers with F 68 as stabilizer.

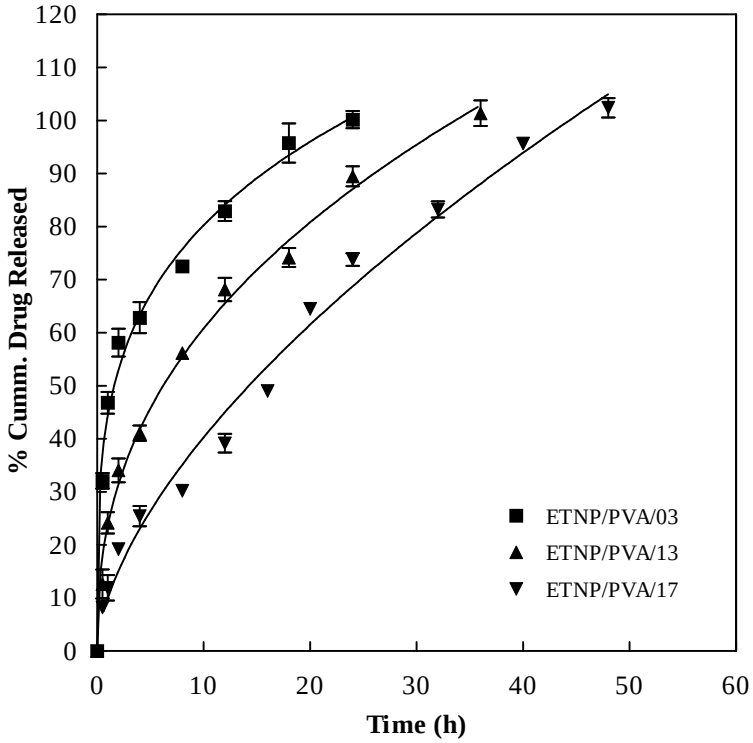

Figure 17: In vitro release profiles of nanoparticle formulations prepared with PLGA co polymers with PVA as stabilizer.

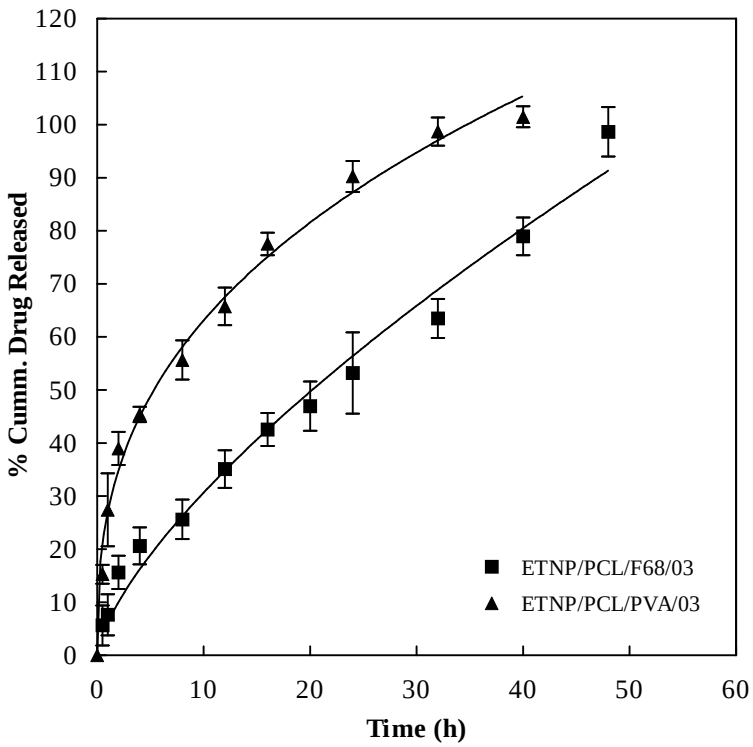

Figure 18: In vitro release profiles of nanoparticle formulations prepared with PCL.

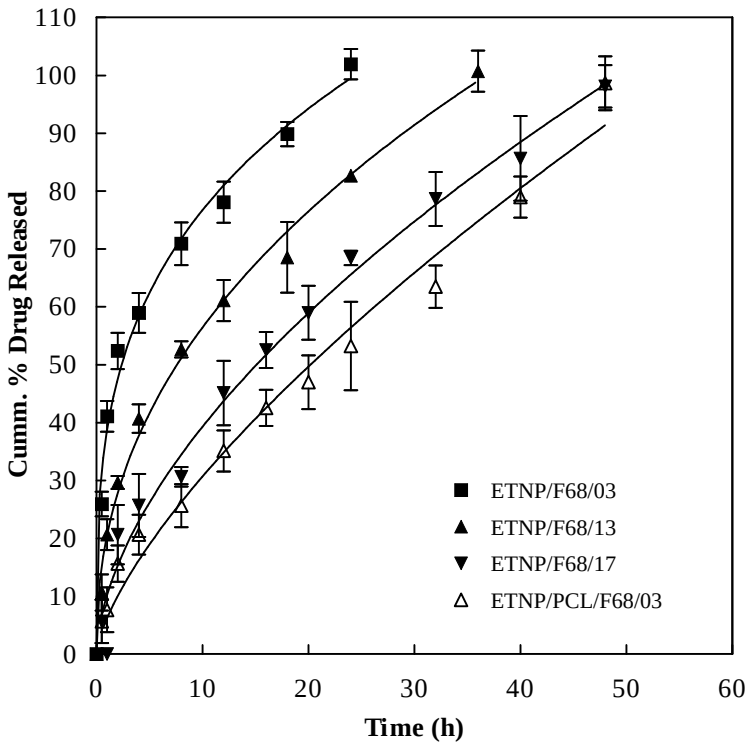

Figure 19: Comparative release profiles of nanoparticle formulations prepared with PLGA co polymers and PCL with F 68 as stabilizer.

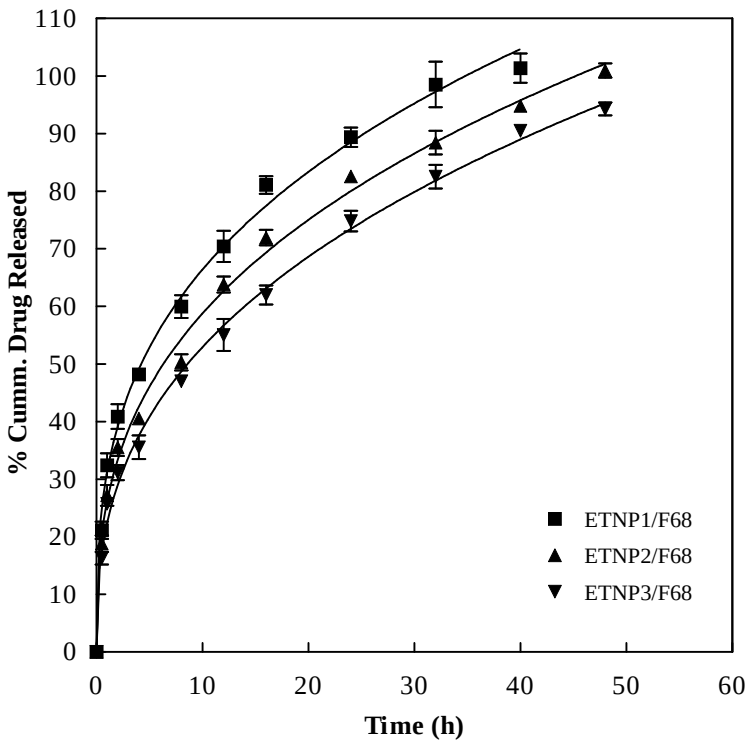

Figure 20: In vitro release profiles of nanoparticle formulations prepared with combination of PLGA co polymers and PCL with F 68 as stabilizer

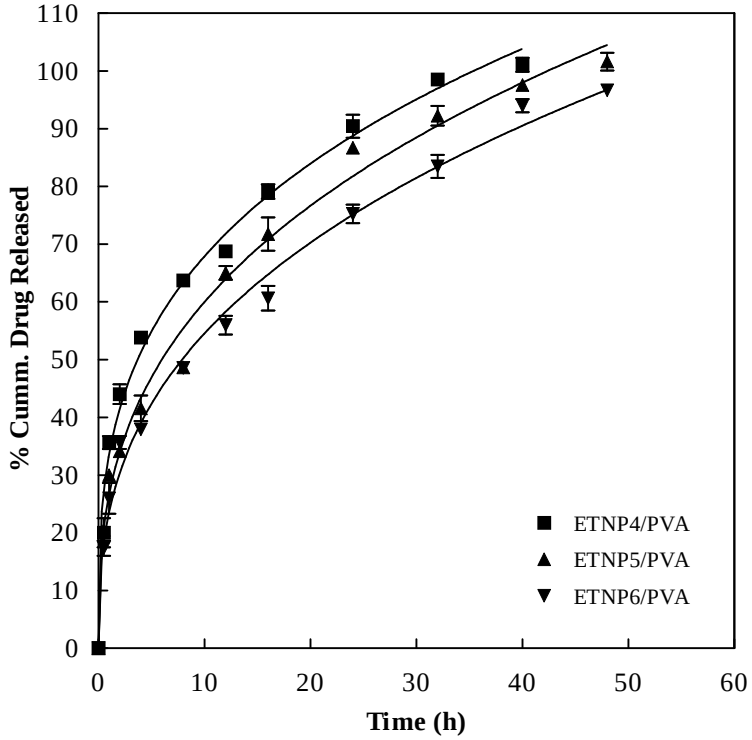

Figure 21: In vitro release profiles of nanoparticle formulations prepared with combination of PLGA co polymers and PCL with PVA as stabilizer.

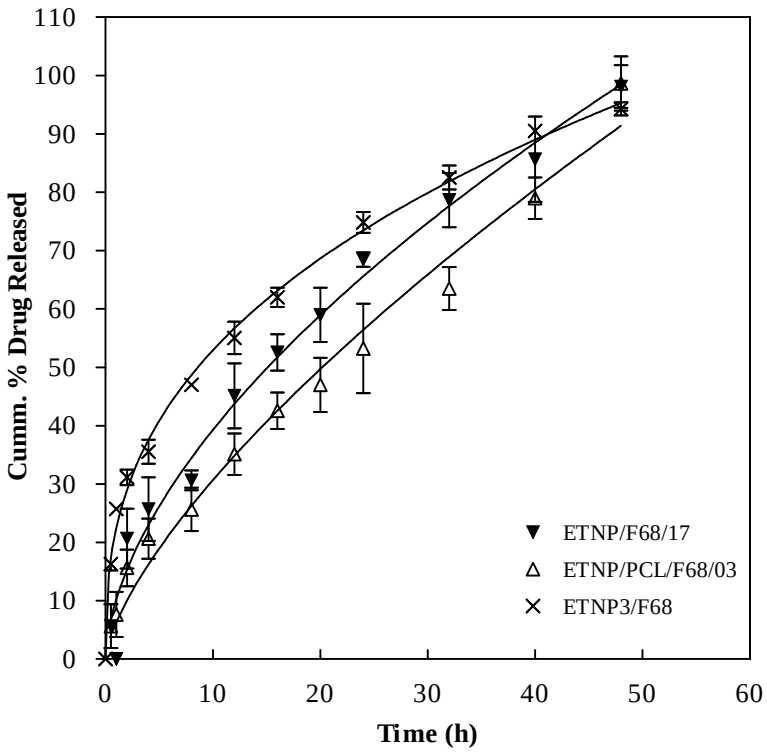

Figure 22: In vitro release profiles of nanoparticle formulations prepared with PLGA 85/15, PCL and a combination of these two polymers.

Table 8: Release kinetics of etoposide from nanoparticles using Peppas model.

Code	k (h^{-n})	n	R^2	MSSR [a]	AIC [b]
ETNP/F68/03	0.387	0.298	0.991	11.08	20.83
ETNP/F68/13	0.205	0.439	0.994	7.19	19.78
ETNP/F68/17	0.102	0.586	0.984	17.58	32.67
ETNP/PVA/03	0.443	0.258	0.991	10.77	20.64
ETNP/PVA/13	0.236	0.410	0.994	7.50	20.12
ETNP/PVA/17	0.099	0.611	0.987	15.67	31.52
ETNP/PCL/F68/03	0.062	0.696	0.984	15.95	31.69
ETNP/PCL/PVA/03	0.269	0.370	0.992	10.08	24.80
ETNP1/F68	0.312	0.329	0.996	5.37	19.12
ETNP2/F68	0.261	0.352	0.996	4.59	19.24
ETNP3/F68	0.223	0.375	0.997	3.36	16.11
ETNP4/PVA	0.335	0.307	0.992	9.99	24.72
ETNP5/PVA	0.265	0.354	0.992	9.85	26.87
ETNP6/PVA	0.235	0.366	0.993	7.44	24.06

[a] - Mean sum of the squared residuals; [b] - Akaike's information criteria

Table 9: Stability of nanodispersions stored at 5°C ± 2°C.

Code	Mean Size (nm) ± SD		EE[a] (%) ± SD	
	Initial	3 Months	Initial	3 Months
ETNP/F68/03	91.8 ± 0.74	518.2 ± 2.55	57.64 ± 0.97	46.08 ± 1.31
ETNP/F68/13	103.7 ± 0.18	681.1 ± 4.01	66.11 ± 0.72	58.29 ± 1.68
ETNP/F68/17	105.1 ± 0.38	576.7 ± 2.81	78.99 ± 1.04	72.34 ± 1.02
ETNP/PCL/F68/03	257.2 ± 0.96	869.3 ± 4.41	80.15 ± 1.01	69.41 ± 1.80
ETNP/Eu/F68/03	70.8 ± 0.44	1108.8 ± 3.34	12.51 ± 0.76	2.86 ± 1.81
ETNP/PVA/03	160.7 ± 0.45	910.0 ± 0.97	56.99 ± 1.08	39.97 ± 1.47
ETNP/PVA/13	255 ± 1.31	971.8 ± 2.81	62.86 ± 1.11	51.27 ± 0.94
ETNP/PVA/17	280.1 ± 0.66	1112.8 ± 3.84	72.18 ± 1.44	60.88 ± 1.15
ETNP/PCL/PVA/03	391.4 ± 1.01	1547.9 ± 7.81	74.18 ± 1.20	61.73 ± 1.81
ETNP/Eu/PVA/03	323.9 ± 0.71	1840.3 ± 6.82	8.99 ± 0.82	ND

ND - Not determined, [a] - Entrapment efficiency; Each value is mean of 3 independent determinations

Table 10: Stability of nanoparticle dispersions stored at -20°C.

Code	Mean Size (nm) ± SD		EE[a] (%) ± SD	
	Initial	3 Months	Initial	3 Months
ETNP/F68/03	91.8 ± 0.74	111.8 ± 2.01	57.64 ± 0.97	55.08 ± 1.08
ETNP/F68/13	103.7 ± 0.18	119.2 ± 2.50	66.11 ± 0.72	63.29 ± 1.88
ETNP/F68/17	105.1 ± 0.38	112.8 ± 3.82	78.99 ± 1.04	77.34 ± 1.74
ETNP/PCL/F68/03	257.2 ± 0.96	265.4 ± 2.58	80.15 ± 1.01	77.41 ± 1.24
ETNP/Eu/F68/03	70.8 ± 0.44	82.5 ± 3.22	12.51 ± 0.76	9.04 ± 0.47
ETNP/PVA/03	160.7 ± 0.45	172.8 ± 3.08	56.99 ± 1.08	54.07 ± 1.82
ETNP/PVA/13	255 ± 1.31	271.3 ± 2.97	62.86 ± 1.11	59.14 ± 2.81
ETNP/PVA/17	280.1 ± 0.66	291.8 ± 1.71	72.18 ± 1.44	69.81 ± 1.71
ETNP/PCL/PVA/03	391.4 ± 1.01	411.5 ± 1.81	74.18 ± 1.20	72.27 ± 3.01
ETNP/Eu/PVA/03	323.9 ± 0.71	338.5 ± 3.89	8.99 ± 0.82	4.12 ± 0.17

[a] - Entrapment efficiency; Each value is mean of 3 independent determinations

Table 11: Redispersibility of nanodispersions stored at 5°C ± 2°C and -20°C.

Code	Redispersibility	
	5°C ± 2°C	-20°C
ETNP/F68/03	+ +	+ + +
ETNP/PVA/03	+ +	+ +
ETNP/F68/13	+ +	+ + +
ETNP/F68/17	+ +	+ + +
ETNP/PVA/13	+	+
ETNP/PVA/17	-	-
ETNP/PCL/F68/03	+	+ +
ETNP/PCL/PVA/03	- -	-
ETNP/Eu/F68/03	- -	-
ETNP/Eu/PVA/03	- -	- -

+ + + Excellent . + + Good, + Fair, - Poor, - - Very Poor

Table 12: Stability of freeze dried nanoparticles stored at RT.

Code	Mean Size (nm) ± SD		EE[a] (%) ± SD	
	Initial	12 Months	Initial	12 Months
ETNP/F68/03	91.8 ± 0.74	108.2 ± 1.80	57.64 ± 0.97	57.81 ± 2.03
ETNP/F68/13	103.7 ± 0.18	110.1 ± 1.02	66.11 ± 0.72	65.14 ± 2.71
ETNP/F68/17	105.1 ± 0.38	108.7 ± 2.01	78.99 ± 1.04	77.58 ± 0.71
ETNP/PCL/F68/03	257.2 ± 0.96	261.3 ± 1.66	80.15 ± 1.01	81.07 ± 1.55
ETNP/Eu/F68/03	70.8 ± 0.44	71.8 ± 0.97	12.51 ± 0.76	11.94 ± 0.97
ETNP/PVA/03	160.7 ± 0.45	162.0 ± 1.67	56.99 ± 1.08	55.24 ± 1.44
ETNP/PVA/13	255 ± 1.31	257.8 ± 2.41	62.86 ± 1.11	62.04 ± 2.27
ETNP/PVA/17	280.1 ± 0.66	284.9 ± 2.64	72.18 ± 1.44	73.01 ± 5.14
ETNP/PCL/PVA/03	391.4 ± 1.01	405.1 ± 5.04	74.18 ± 1.20	73.41 ± 1.81
ETNP/Eu/PVA/03	323.9 ± 0.71	367.8 ± 4.10	8.99 ± 0.82	6.49 ± 0.64

[a] - Entrapment efficiency; Each value is mean of 3 independent determinations

Table 13: Stability of freeze dried nanoparticles stored at 5°C ± 2°C.

Code	Size in nm (mean ± SD)		% EE[a] (mean ± SD)	
	Initial	12 Months	Initial	12 Months
ETNP/F68/03	91.8 ± 0.74	104.9 ± 1.05	57.64 ± 0.97	55.38 ± 1.46
ETNP/F68/13	103.7 ± 0.18	162.0 ± 0.82	66.11 ± 0.72	66.91 ± 1.23
ETNP/F68/17	105.1 ± 0.38	107.6 ± 2.11	78.99 ± 1.04	79.04 ± 1.88
ETNP/PCL/F68/03	257.2 ± 0.96	255.8 ± 3.41	80.15 ± 1.01	80.28 ± 2.01
ETNP/Eu/F68/03	70.8 ± 0.44	74.5 ± 1.02	12.51 ± 0.76	13.18± 1.08
ETNP/PVA/03	160.7 ± 0.45	162.14 ± 1.06	56.99 ± 1.08	55.67 ± 1.67
ETNP/PVA/13	255 ± 1.31	259.1± 0.81	62.86 ± 1.11	62.55 ± 2.02
ETNP/PVA/17	280.1 ± 0.66	288.0 ± 1.25	72.18 ± 1.44	73.06 ± 1.57
ETNP/PCL/PVA/03	391.4 ± 1.01	394.8 ± 2.64	74.18 ± 1.20	73.69± 1.67
ETNP/Eu/PVA/03	323.9 ± 0.71	334.4 ± 3.92	8.99 ± 0.82	9.11 ± 1.02

[a] -Percent Entrapment efficiency; Each value is mean of 3 independent determinations

Table 14: Stability of freeze dried nanoparticles stored at -20°C.

Code	Mean Size (nm) ± SD		EE[a] (%) ± SD	
	Initial	12 Months	Initial	12 Months
ETNP/F68/03	91.8 ± 0.74	106.3 ± 0.68	57.64 ± 0.97	57.14 ± 1.81
ETNP/F68/13	103.7 ± 0.18	104.0 ± 2.33	66.11 ± 0.72	65.33 ± 2.17
ETNP/F68/17	105.1 ± 0.38	107.2 ± 1.41	78.99 ± 1.04	79.54 ± 1.07
ETNP/PCL/F68/03	257.2 ± 0.96	260.7 ± 0.66	80.15 ± 1.01	81.09 ± 1.71
ETNP/Eu/F68/03	70.8 ± 0.44	81.1 ± 3.14	12.51 ± 0.76	11.97± 1.56
ETNP/PVA/03	160.7 ± 0.45	164.8 ± 1.09	56.99 ± 1.08	57.44 ± 2.04
ETNP/PVA/13	255 ± 1.31	259.4 ± 1.58	62.86 ± 1.11	63.00 ± 1.48
ETNP/PVA/17	280.1 ± 0.66	285.3 ± 0.69	72.18 ± 1.44	72.98 ± 2.34
ETNP/PCL/PVA/03	391.4 ± 1.01	394.6 ± 1.02	74.18 ± 1.20	75.09 ± 2.41
ETNP/Eu/PVA/03	323.9 ± 0.71	326.1 ± 2.11	8.99 ± 0.82	8.12 ± 1.03

[a] - Entrapment efficiency; Each value is mean of 3 independent determinations

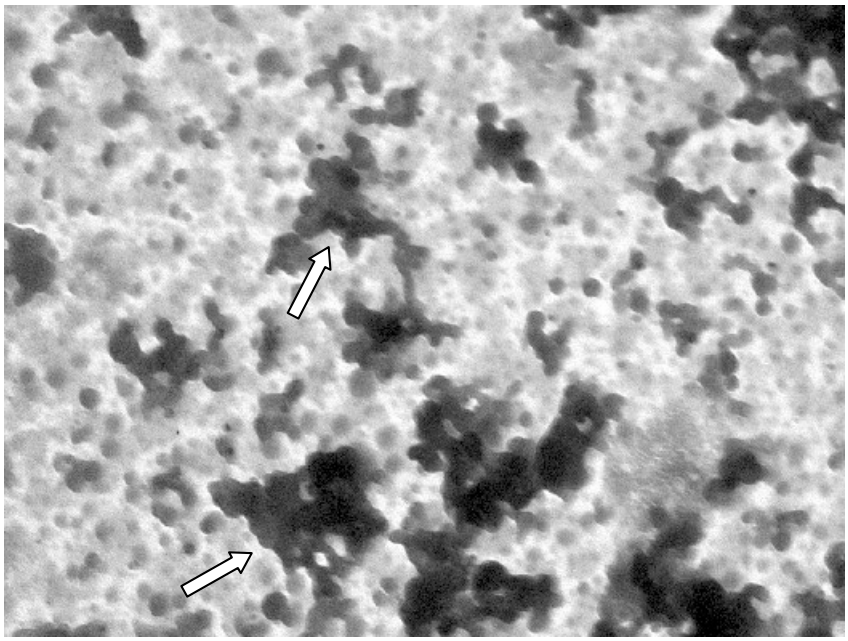

Figure 23: TEM image of nanoparticle formulation (ETNP/PCL/PVA/03) stored at 5°C ± 2°C after 3 months (× 28000 magnification). Arrows indicate agglomeration of nanoparticles.

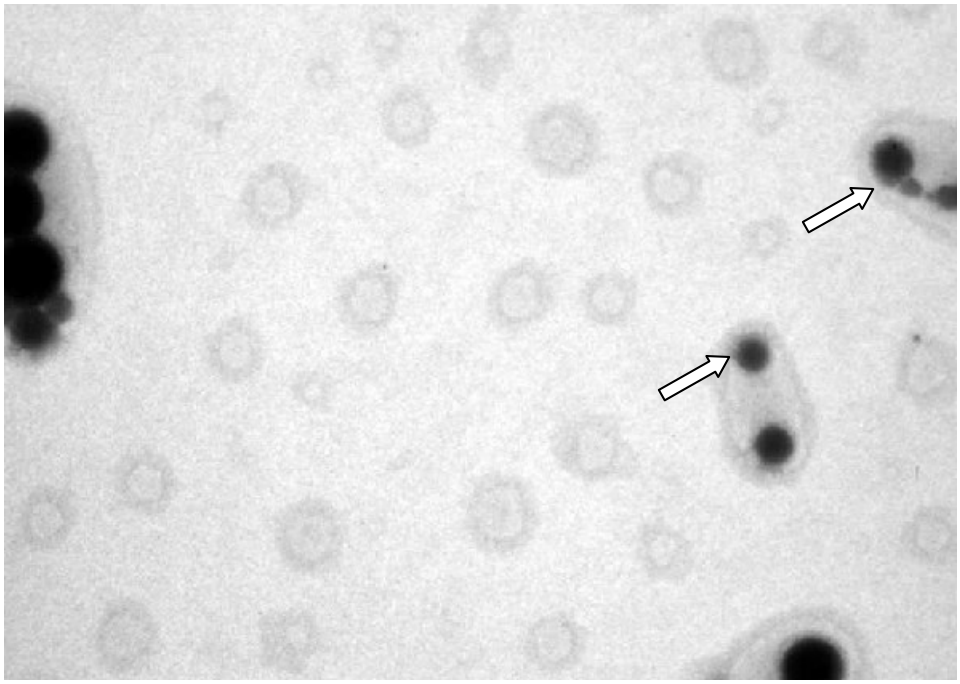

Figure 24: TEM image of freeze dried nanoparticle formulation (ETNP/F68/01) stored at RT after 1 year (× 36000 magnification). Arrows indicate nanoparticles.

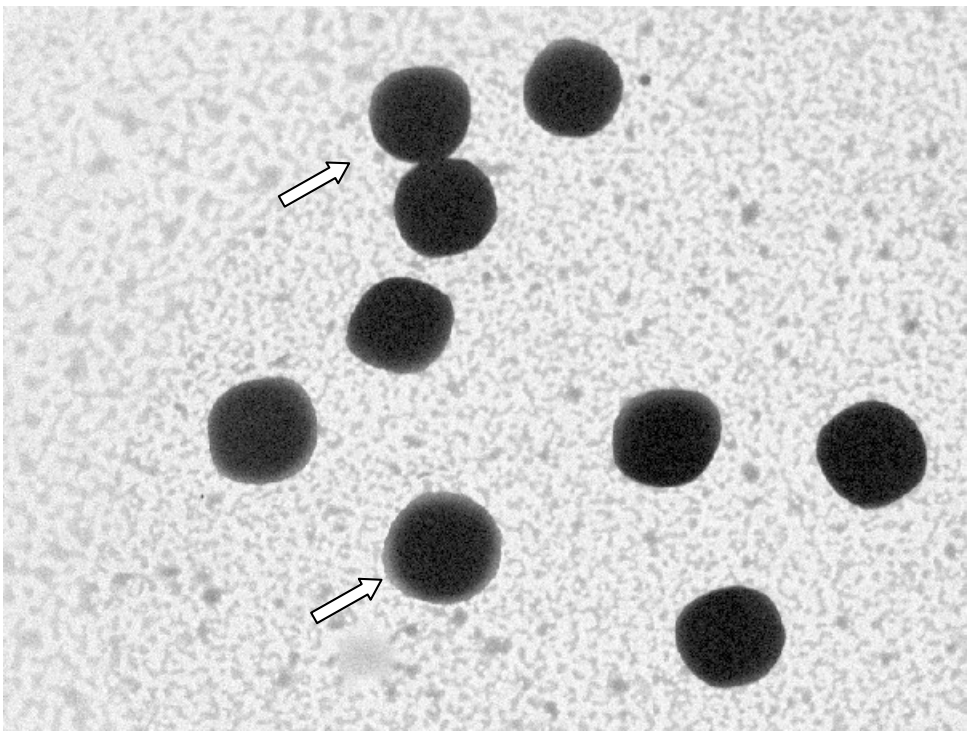

Figure 25: TEM image of freeze dried PCL nanoparticle formulation (ETNP/PCL/F68/03) stored at RT after 1 year (× 40000magnification). Arrows indicate nanoparticles.

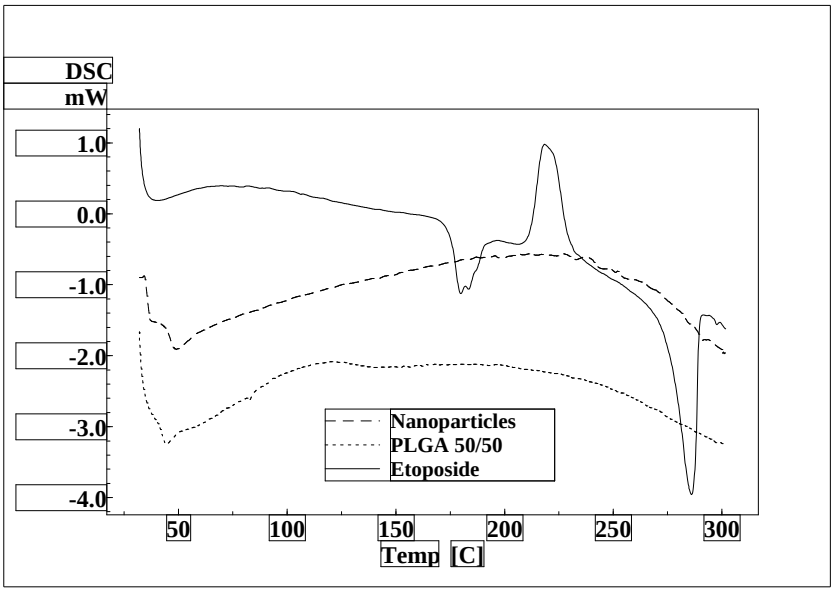

Figure 26: Comparative DSC thermograms of etoposide, PLGA 50/50 and nanoparticles (ETNP/F68/03).

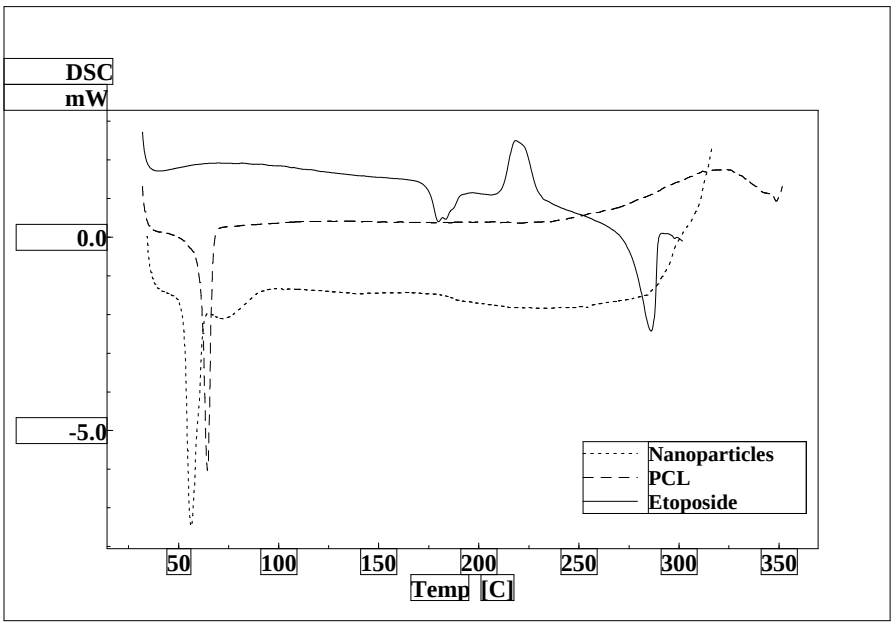

Figure 27: Comparative DSC thermograms of etoposide, PCL and nanoparticles (ETNP/PCL/F68/03).

References

Chawla, J.S., Amiji, M.M., 2002. Biodegradable poly (e-caprolactone) nanoparticles for tumor targeted delivery of tamoxifen. Int. J. Pharm. 249, 127-138.

Chen, G.Q., Lin, W., Combes, A.G.A., 1994. Preparation of human serum albumin microspheres by a novel acetone-heat denaturation method. J. Microencapsul. 11, 395-407.

Chorny, M., Fishbein, I., Danenberg, H.D., Golomb, G., 2002. Lipophilic drug loaded nanospheres prepared by nanoprecipitation: effect of formulating variables on size, drug recovery and release kinetics. J. Control. Release. 83, 389-400.

Coffin, M.D., McGinity, J.W., 1992. Biodegradable pseudolatexes: the chemical stability of poly (D,L-lactide) and poly(ocaprolactone) nanoparticles in aqueous media. Pharm. Res. 9, 200-205.

Espuelas, M.S., Legrand, P., Irache, J.M., Gamazo, C., Orecchioni, A.M., Devissaguet, J.P., Ygartua, P., 1997. Poly(o-caprolactone) nanospheres as an alternative way to reduce amphotericin-B toxicity. Int. J. Pharm. 158, 19-27.

Falkson, G., van Dyk, J.J., van Eden, E.B., van der Merwe, A.M., van den Bergh, J.A., Falkson, H.C., 1975. A clinical trial of the oral form of 4'-demethyl-epipodophyllotoxin-beta-D ethylidene glucoside (NSC 141540) VP 16-213. Cancer. 35, 1141-1144.

Feng, S., Huang, G., 2001. Effects of emulsifiers on the controlled release of paclitaxel (Taxol®) from nanospheres of biodegradable polymers. J. Control. Release. 71, 53–69.

Fessi, H., Puisieux, F., Devissaguet, J.P., Ammoury, J.P., Benita, S., 1989. Nanocapsule formation by interfacial polymer deposition following solvent displacement. Int. J. Pharm. 55, R1-R4.

Gurny, R., Alleman, E., 2002. Preparation and characterization of sterile and freeze-dried sub-200 nm nanoparticles. Int. J. Pharm. 233, 239-252.

Jain, R.A., 2000. The manufacturing techniques of various drug loaded biodegradable poly(lactide-co-glycolide) (PLGA) devices. Biomaterials. 21, 2475-2490.

Jimenez, M.M., Pelletier, J., Bobin, M.F., Martini, M., Fessi, H., 2004. Poly-epsilon-caprolactone nanocapsules containing octyl methoxy cinnamate: preparation and characterization. Pharm. Dev. Tech. 9, 329-339.

Kwon, H.-Y., Lee, J.-Y., Choi, S.-W., Jang, Y., Kim, J.-H., 2001. Preparation of PLGA nanoparticles containing estrogen by emulsification-diffusion method. Colloid Surf. A. 182, 123–130.

Lamprecht, A., Ubrich, N., Hombreiro-Perez, M., Lehr, C.M., Hoffman, M.P., 2000. Maincent a Influences of process parameters on nanoparticle preparation performed by a double emulsion pressure homogenization technique. Int. J. Pharm. 196, 177–182.

Lau, M.E., Hansen, H.H., Nissen, N.I., Pedersen, H., 1979. Phase I trial of a new form of an oral administration of VP-16-213. Cancer. Treat. Rep. 63, 485-487.

Lemoine, D., Francois, C., Kedzierewicz, F., Preat, V., Hoffman, M., Maincent, P., 1996. Stability study of nanoparticles of poly(ε-caprolactone), poly(D,L-lactide) and poly (D,L-lactide- co-glycolide). Biomaterials 17, 2191-2197.

Leo, E., Brina, B., Forni, F., Vandelli, M.A., 2004. In vitro evaluation of PLA nanoparticles containing a lipophilic drug in water-soluble or insoluble form. Int. J. Pharm. 278, 133-141.

Leroux, J.C., Allemann, E., Doelker, E., Gurny, R., 1995. New approach for the preparation of nanoparticles by an emulsification diffusion method. Eur. J. Pharm. Biopharm. 41, 14-18.

Levy, M.Y., Benita, S., 1990. Drug release from submicronized o/w emulsion: a new in vitro kinetic evaluation model, Int. J. Pharm. 66, 29–37.

Mainardes, R., Evangelista, R.C., 2005. PLGA nanoparticles containing praziquantel: effect of formulation variables on size distribution. Int. J. Pharm. 290, 137-144.

Marty, J.J., Oppenheim, R.C., Speiser, P., 1978. Nanoparticles-a new colloidal drug delivery system. Pharm. Acta. Helv. 53, 17-23.

Murakami, H., Kobayashi, M., Takeuchi, H., Kawashima, Y., 1999. Preparation of poly (dl-lactide-co-glycolide) nanoparticles by modified spontaneous emulsification solvent diffusion method. Int. J. Pharm. 187, 143–152.

Nissen, N.I., Dombernowsky, P., Hansen, H.H., Larsen, V., 1976. Phase I clinical trial of an oral solution of VP-16-213. Cancer. Treat. Rep. 60, 943-945.

Ogawa, Y., Yamamoto, M., Okada, H., Yashiki, T., Shimamoto, T., 1988. A new technique to efficiently entrap leuprolide acetate in microcapsules of co poly (lactic:glycolic acid). Chem. Pharm. Bull. 36, 1095–1103.

Peltonen, L., Koistinen, P., Karjalainen, M., Hakkinen, A., Hirvonen, J., 2002. The effect of cosolvents on the formulation of nanoparticles from low molecular weight poly (l) lactide. AAPS. Pharm. Sci. Tech. 3, 1-7.

Phillips, N.C., Lauper, R.D., 1983. Review of etoposide. Clin. Pharm. 2, 112-119.

Ponchel, G., Irache, J., 1998. Specific and non-specific bioadhesive particulate systems for oral delivery to the gastrointestinal tract. Adv. Drug. Deliv. Rev. 34, 191-219.

Quintanar-Guerrero, D., Fessi, H., Allemann, E., Doelker, E., 1996. Influence of stabilizing agents and preparative variables on the formation of poly (d,l-lactic acid) nanoparticles by an emulsification-diffusion technique. Int. J. Pharm. 143, 133–141.

Schaefer, M.J., Singh, J., 2002. Effect of tricaprin on the physical characteristics and in vitro release of etoposide from PLGA microspheres. Biomaterials. 23, 3465-3471.

Shah, J.C., Chen, J.R, Chow, D, 1995. Preformulation study of etoposide: II. Increased solubility and dissolution rate by solid dispersions. Int. J. Pharm. 113, 103-111.

Soppimath, K.S., Aminabhavi, T.M., Kulkarni, A.R., Rudzinski, W.E., 2001. Biodegradable polymeric nanoparticles as drug delivery devices. J Control. Release. 70, 1-20.

Yamaoka K., Nakagawa T., Uno T., 1978. Application of Akaike's information criterion (AIC) in the evaluation of linear pharmacokinetic equations. J. Pharmacokinet. Biopharm., 6, 165-175.

Chapter 6

Biodistribution and Pharmacokinetic Studies

6.1. Introduction

Any formulation or drug delivery systems are required to be studied in vivo for pharmacokinetic and therapeutic efficacy. The evaluation of drug delivery systems, including nanoparticulate systems, requires the study of the biodistribution and elimination in animal models and/or human volunteers. Biodistribution studies provide valuable information regarding passage and uptake of drug after administration of delivery systems by various routes to different organs, tissues of the body of the healthy animal. This is particularly important as it is expected that nanoparticulate form will change distribution and pharmacokinetic profile of drugs. This is more important for anticancer drug delivery systems to see distribution profile as it is necessary on toxicity point of view. It is expected that size and surface charge of nanoparticles will change the interaction of nanoparticles with the cell membrane, thus influencing the uptake by various organs of the body.

These studies can be done directly by radiolabeling of nanoparticles. Radiolabeling makes these studies easier and faster. A wide variety of radiopharmaceuticals are used nowadays for diagnostic purpose and also to know the fate of the formulation in the body. Rhodes et al, (1971) used Technetium (Tc^{99m}) microspheres for lung imaging. Larson et al, (1978) used Tc^{99m} RBC for blood pool imaging. Wistow et al, (1977) used various Tc^{99m} labeled complexes for imaging of hepatobiliary systems. Various radiopharmaceuticals were used for renal imaging (Chervu and Blaufox, 1982; Bhatnagar et al, 1997). The gamma imaging involves the application of gamma emitting radioactive materials, such as Tc^{99m}, Indium (In^{111}), Iodine (I^{131}), Gallium (Ga^{67}) and some other isotopes with variable decay times.

Gamma scintigraphy is a technique whereby the transit of a dosage form through its intended site of delivery can be non-invasively imaged in vivo via the judicious introduction of an appropriate short lived gamma emitting radioisotope (Turker et al, 2005). The observed transit of the dosage form can then be correlated with the rate and extent of drug absorption. Gamma scintigraphy study combined with knowledge of physiology and dosage form design can help define these variables. The resulting insight can be used to accelerate the formulation development process and help ensure success in early clinical trials. Combined with Pharmacokinetic analysis, this technique gives unique insight into performance of delivery systems. Gamma scintigraphy is a widely accepted, safe, non-invasive method of examining the deposition of a pharmaceutical in the body using standard radio labeling techniques (McDowell et al, 2005). Time sequenced images from the gamma camera are used to provide information on the deposition, residence and clearance of delivery systems. Computerized image of gamma emissions portrays overall product

deposition including color differentiation of test article concentration. Quantitative measurements of total deposited pharmaceutical, biopharmaceutical or other compounds by region can be assessed. Coupled with pharmacokinetic testing, the bioavailability and distribution characteristics of the test substance can be defined for all routes of administration (Newman, 1999). Nuclear medicine imaging techniques have an advantage over other imaging modalities as the whole body can be imaged in a single examination.

The current study was undertaken to document the biodistribution and pharmacokinetics of etoposide loaded nanoparticles labeled with Tc^{99m} in healthy and as well as tumor induced strain A mice. The radionuclide Tc^{99m} was chosen because of its short half life of 6.5 h and photon energy of 140 keV. Tc^{99m} is a Molybdenum (Mo^{99m}) generator product and available as Tc^{99m} pertechnetate ($^{99m}TcO_4^-$). It is used after elution from the Mo/Tc generator and may be used to label drugs, blood cells or other chemicals used to study their pharmacokinetics after various routes of administration. In the present study, comparison was made by studying radiolabeled empty nanoparticles and free etoposide also. Furthermore, free etoposide and all nanoparticle formulations were labeled using direct method in which $^{99m}TcO_4^-$ is reduced to lower valence state using stannous chloride as reducing agent (Blok et al, 1989). The majority of Tc^{99m} compounds employ the stannous reduction method, which makes use of the fact that stannous chloride is one of the most powerful reducing agents available to chemists.

6.2. Materials, Equipment/Instruments and Reagents

6.2.1. Materials

Etoposide, etoposide loaded nanoparticle dispersions, empty nanoparticles, Pluronic F 68, distilled water, freshly eluted Tc^{99m}, stannous chloride dihydrate ($SnCl_2$. 2 H_2O), 0.1N HCl, 0.01 N HCl, normal saline (0.9 %w/v sodium chloride, NaCl), 0.5 M sodium hydrogen carbonate (Na_2HCO_3), instant thin layer chromatography plates (Gelman Science Inc, Ann Arbor, MI), Dispovan syringes (1 and 2 ml) with 26G needles, Surgical spirit (70% IPA).

6.2.2. Equipment/Instruments

Gamma ray spectrometer (type GRS23C), Electronics Corporation India Ltd. Hyderabad, India, was used for measuring radio activity. Single Photon Emission Computed Tomography gamma camera (SPECT, LC 75-005, Diacam, Siemens, USA) was used for gamma imaging.

6.2.3. Reagents

Pluronic F 68 solution (0.1 % w/v): Pluronic F 68 (100 mg) was weighed and dissolved and final volume was made up to 100 ml using distilled water.

Hydrochloric Acid (0.1 N): Concentrated HCl, 8.56 ml was taken and diluted with distilled water to 1000 ml.

Hydrochloric Acid (0.01 N): Concentrated HCl, 0.856 ml was taken and diluted with distilled water to 1000 ml.

Stannous Chloride solution: Stannous chloride solution of 2 mg/ml was prepared by dissolving 2 mg in 1 ml of 0.1 N HCl.

Sodium Hydrogen Carbonate (0.5 M): To prepare 0.5 M sodium hydrogen carbonate solution, 4.2 g of this compound was taken and dissolved in distilled water and made up the volume to 100 ml.

6.3. Experimental

6.3.1. Radio Labeling

Radiolabeling of free etoposide and selected nanoparticle formulations, ETNP/F68/17, ETNP/PCL/F68/03, ETNP3/F68 and NP/F68/17 was done by direct method using stannous chloride as reducing agent (Babbar et al, 1991). Selection of formulations was made on the basis of evaluation and characterization of nanoparticles (Compositions and Characters of the formulations are given in Tables 1, 2, 4 and 5 of chapter 5). In the present method etoposide was weighed accurately and dissolved in 0.1 %w/v of F 68 solution, to get a concentration of 500 µg/ml. To this 50 µl of stannous chloride solution prepared in HCl (0.1 N) was added and mixed. To check the effect of pH on labeling it was varied from 3.0 to 7.5 using 0.5 M sodium hydrogen carbonate. To adjust the optimized pH of the preparation to 7.0, 10 µl of sodium hydrogen carbonate (0.5 M) solution was added. After mixing this preparation thoroughly, required quantity of $^{99m}TcO_4^-$ solution was added, mixed well and incubated for 15 min at room temperature. Final radioactivity present in the preparation was checked before starting the experiment using dosimeter. Volume and concentration of stannous chloride, final pH of the preparation; incubation time was optimized previously by changing one parameter at a time and performing quality control tests for the labeled complex. For optimizing amount of stannous chloride required for high labeling efficiency and low radio colloids, a range of 25 to 400 µg of stannous chloride was used.

6.3.2. Quality Control Tests for the Labeled Complexes

Quality control tests were performed as per the reported method (Babbar et al, 1991). The labeling efficiency of free etoposide and formulations was determined by ascending thin layer chromatography (TLC) using silica gel coated fiber sheets. The instant thin layer chromatography (ITLC) strips were used to determine free $^{99m}TcO_4^-$ and percentage of radio colloids in the preparation. Based on these two parameters, labeling efficiency of the preparation was calculated (Mishra et al, 1991). Figure 1 shows the developed TLC plates depicting free $^{99m}TcO_4^-$ and radio colloids in different solvent systems.

Figure 1: TLC plates depicting migration of labeled complex, free $^{99m}TcO_4^-$ and radio colloids in different solvent systems.

I = TLC plate developed with acetone showing migration of free $^{99m}TcO_4^-$

II = TLC plate developed with pyridine: acetic acid: water (PAW) showing migration of labeled complex along with free $^{99m}TcO_4^-$

A - Labeled complex and radio colloids B - Free $^{99m}TcO_4^-$

C - Radio colloids D - Free $^{99m}TcO_4^-$ and labeled complex

X = RB x 100/ (RA + RB)

Y = C x 100/ (RC + RD)

Where X is % free $^{99m}TcO_4^-$, Y is % radio colloids, RA is radioactivity shown by A, RB is radioactivity shown by B, RC is radioactivity shown by C and RD is radioactivity shown by D

% Labeling Efficiency (or) Labeled complex = 100 – X – Y

a) Percentage of Free $^{99m}TcO_4^-$

Labeling efficiency of the preparation was checked by using ITLC strips which were spotted with one or two drops of labeled complex at the bottom at least 1 cm above the solvent front. These strips were developed using acetone as the solvent system. The solvent front was allowed to reach up to a height of approximately 5 to 6 cm from the origin and the strip was cut into 2 pieces on the basis of location of samples. Radioactivity in each half was determined by well type gamma ray spectrometer. The free $^{99m}TcO_4^-$ present in the preparation migrates to the top portion (R_f value between 0.9 to 1.0) of the ITLC strip, leaving the labeled complex at the bottom.

b) Percentage of Radio Colloids

Incorporation of excess of stannous chloride for reduction of Tc^{99m} may lead to the formation of radio colloids, which is undesirable. Colloid formation was determined by using ITLC strips where the solvent system is a combination of pyridine: acetic acid: distilled water (PAW) in a ratio of 3:5:1.5. Radio colloids if present in the preparation will remain at the bottom of the strip, while both the free $^{99m}TcO_4^-$ as well as labeled complex migrated with the solvent front (Sundrehagen, 1982).

Percentage of free $^{99m}TcO_4^-$ and radio colloids in the preparations were calculated based on the radioactivity shown by samples in the developed ITLC strips. By subtracting these from hundred gives the percentage of Tc^{99m} labeled etoposide and formulations (labeling efficiency).

6.3.3. Assessment of In vitro Stability of the Labeled Complexes

Stability of the Tc^{99m} labeled etoposide, ETNP/F68/17, ETNP/PCL/F68/03, ETNP3/F68 and NP/F68/17 preparations was determined in vitro in rabbit serum, normal saline and 0.01 N HCl by ascending TLC technique. Rabbit blood was collected, centrifuged at 5000 rpm for 20 min and the supernatant serum was collected and used for this in vitro stability study. The labeled complex (0.1 ml) was incubated with freshly collected rabbit serum (0.9 ml) at room temperature. The samples were taken from this at regular intervals up to 24 h and ITLC strips were developed using above mentioned solvent systems. These strips were analyzed in gamma ray spectrometer and percentage labeling efficiency was calculated for etoposide and formulations. Similar stability study was carried out in presence of normal saline and HCl (0.01 N).

6.3.4. Animal Models Used for In vivo Studies

Strain A mice (25 to 30 g) were used for biodistribution, pharmacokinetic, tumor development and tumor uptake studies. Pharmacokinetic studies of radio labeled preparations were conducted in male New Zealand, white rabbits of 2 to 2.5 kg. Animals were kept in cages at constant temperature and humidity. Water and feed were given ad libitum.

Biodistribution, tumor development, tumor uptake and pharmacokinetic studies were carried out at Institute of Nuclear Medicine and Allied Sciences (INMAS), New Delhi after the prior approval (Sanction number: INM-302) and in accordance with the rules and regulations of the Animal Ethics Committee of INMAS, New Delhi. The Social Justice and Empowerment Committee further approved all the animal experiments for the purpose of control and supervision of experimental animals, New Delhi, India.

6.3.5. Biodistribution and Pharmacokinetic Study in Healthy Mice

a) Intravenous Administration (i.v.)

Tc^{99m} labeled etoposide and formulations: ETNP/F68/17, ETNP/PCL/F68/03, ETNP3/F68 and NP/F68/17 (100 µl) containing around 200 µCi of radioactivity were injected into the tail vein of healthy mice. For each preparation injected, three mice were used per time point. The mice were sacrificed at 0.5, 1, 2, 4 and 24 h post administration. Before sacrificing mice, at specific time points, mice were anaesthetized with excess amount chloroform and blood samples were collected by cardiac puncture and placed in pre weighed plastic tubes. Various organs like, the heart, liver, lungs, muscle, bone (femur), kidneys, spleen, gastrointestinal tract (GIT) and brain were then isolated. In the case of GIT, the whole tract was excised and separated into stomach, small intestine and large intestine. All the organs/tissues collected were thoroughly rinsed with saline, placed in pre-weighed plastic tubes and weighed. The radioactivity was determined in a well type gamma scintillation counter along with three aliquots of the diluted standard representing 100% of the injected radioactivity. Mean of this radioactivity was used to obtain the total injected radioactivity into the animal. The radioactivity present in organs/tissues was interpreted as percentage of the injected radioactivity per gram of organ/tissue (% A/g). Pharmacokinetic parameters were calculated for the blood samples collected in the study.

b) Oral Administration

Tc^{99m} labeled etoposide, ETNP/F68/17, ETNP/PCL/F68/03, ETNP3/F68 and NP/F68/17 (100 µl) containing around 200 µCi of radioactivity were administered orally.

All other conditions and procedures were kept same as mentioned in i.v. administration. The radioactivity present in all organs/tissues was determined using gamma scintillation counter along with the diluted standard representing 100% of the administered radioactivity. Mean of this radioactivity was used to obtain the total administered radioactivity into the animal. The radioactivity present in organs/tissues was interpreted as % A/g.

6.3.6. Biodistribution and Pharmacokinetic and Tumor Uptake Study in Dalton's Lymphoma Tumor Bearing Mice

a) Tumor Implantation and Development

The Dalton's Lymphoma solid tumor (DLS) cells were maintained in the peritoneum of Balb/C mice in the ascites form by serial weekly passages. Exponentially growing cells were harvested and tumor cells of 5×10^6 per mouse were injected subcutaneously in the thigh of right hind leg of the Strain A mice. After 8 to 10 days a palpable tumor in the volume range of 1.0 ± 0.1 cm^3 was observed and used for further studies.

b) Biodistribution, Pharmacokinetic and Tumor Uptake Study

Tc^{99m} labeled etoposide and ETNP/F68/17 (100 µl) containing around 200 µCi of radioactivity were injected into the tail vein of tumor bearing mice. For each injected preparation three mice were used per time point. The mice were sacrificed 1, 4, and 24 h post injection. Before sacrificing those mice, at specified time points, mice were anaesthetized with excess amount chloroform and blood samples were obtained by cardiac puncture and placed in pre-weighed plastic tubes. The heart, liver, lungs, muscle, bone (femur), kidneys, spleen, and brain were isolated.

Along with these organs, tumor was excised from the right hind leg. As a control; muscle from the right hind leg of a healthy animal, which was administered with the same preparation, was used. All the organs/tissues collected were thoroughly rinsed with saline, placed in pre-weighed plastic tubes and weighed. The radioactivity was determined as mentioned above.

6.3.7. Pharmacokinetic Study in Rabbits

a) Intravenous Administration

Tc^{99m} labeled etoposide, ETNP/F68/17, ETNP/PCL/F68/03 and NP/F68/17 (250 µl) containing around 6 mCi of radioactivity were injected into the marginal ear vein of rabbits. Study was conducted on grouping three rabbits per preparation. At specific time points, 5, 10, 15, 30 min, 1, 2, 3, 4, 6 and 24 h, blood samples were collected from the marginal vein

of the ear and placed in pre weighed plastic tubes and weighed. Radioactivity was checked using gamma counter. Along with the blood samples, standard solution, which was injected, also checked for radioactivity as it gives total injected radioactivity and it was taken as 100%. The radioactivity present in blood samples was interpreted as percentage of the injected radioactivity per gram of blood (% A/g).

b) Oral Administration

Tc^{99m} labeled etoposide, ETNP/F68/17 and NP/F68/17 (500 µl) containing around 6 mCi of radioactivity were administered orally for pharmacokinetic studies. Blood samples were collected after 0.5, 1, 2, 3, 4, 6 and 24 h post administration of preparations. All other conditions and procedures were kept same as mentioned in i.v. administration. The radioactivity present in blood was determined as above and represented as % A/g.

6.3.8. Gamma Scintigraphic Imaging

For gamma scintigraphic study of Tc^{99m} labeled etoposide and ETNP/F68/17, 100 µl of preparations containing 200 µCi of radioactivity was injected through the tail vein of the tumor bearing and healthy mice. Healthy mice were kept as control. At 4 and 24 h of post injection, mice were fixed on animal fixing tray board and imaging was performed with Single Photon Emission Computed Topography gamma camera. Gamma imaging was also done for rabbits after administering Tc^{99m} labeled etoposide and ETNP/F68/17 preparations containing 6 mCi of radioactivity through the marginal ear vein of rabbits.

6.3.9. Data Analysis

Results of the in vivo biodistribution studies were statistically evaluated by Student's t-test with $P<0.05$ as the minimal level of significance. Study was done in between free etoposide and etoposide loaded formulations.

Pharmacokinetic parameters were assessed using non-compartmental technique with the software program WinNonlin (version 2.1). The mean %A/g and time data was fitted to the model i.v. bolus for i.v. administration and extravascular for oral administration. Pharmacokinetic parameters like Area under the curve (AUC), Mean residence time (MRT), Clearance (Cl), $t_{1/2}$, T_{max}, C_{max} were calculated using this software.

6.4. Results and Discussion

6.4.1. Radiolabeling

Etoposide and its nanoparticle formulations ETNP/F68/17, ETNP/PCL/F68/03, ETNP3/F68 and NP/F68/17 were labeled with Tc^{99m} with high labeling efficiency by direct method. The direct labeling approach has the advantage that it can be carried out easily. Preliminary studies were done to optimize the pH, which is one of the most important parameters controlling labeling efficiency of the preparation. High labeling efficiency (from 98.26 to 99.34 %) for all preparations was observed at pH 7.0. Changing the pH below or above 7; there was increase in free $^{99m}TcO_4^-$ percentage. Therefore in all further studies pH 7 was maintained for labeling.

Chemically $^{99m}TcO_4^-$ is a rather non-reactive species and does not label any compound by direct addition. Being an oxidizing agent it can be reduced to lower oxidation state. When treated with certain reducing agents, the Tc^{+7} of the $^{99m}TcO_4^-$ can be reduced to lower oxidation states, usually Tc^{+3}or Tc^{+4}, where it becomes reactive species. The common agents, which have been normally used, are stannous chloride dihydrate ($SnCl_2.H_2O$), stannous tartarate, stannous citrate, sodium borohydride ($NaBH_4$), dithionite and ferrous sulphate. Among these, stannous chloride is the most commonly used reducing agent in acidic medium (Blok et al, 1989; Garron et al, 1991; Pauwels et al, 1993).

Amount of stannous chloride required to reduce $^{99m}TcO_4^-$ is very important in the labeling process. In the present study, the optimum amount of stannous chloride resulting high labeling efficiency and low amount of radio colloids was found to be 100 µg for all preparations. The influence of stannous chloride amount on labeling efficiency, percentage of free $^{99m}TcO_4^-$ and radio colloids present in Tc^{99m} labeled etoposide is shown in Table 1. This method was found to give good labeling efficiency (98.46 to 99.8%) with very less percentage of radio colloids (0.10 to 0.62 %) and free $^{99m}TcO_4^-$ (0.09 to 1.05 %) for etoposide and as well as for nanoparticle formulations. Incubation time in which maximum percentage of labeling occurred was also optimized as 15 min after the addition of $^{99m}TcO_4^-$ to the preparation. For optimizing above parameters at each time point, quality control tests were done by TLC using ITLC strips.

6.4.2. Assessment of In vitro Stability of the Labeled Complexes

Radiolabeled preparations were checked for their in vitro stability in rabbit serum, normal saline and 0.01 N HCl. These conditions were selected for stability study to mimic in vivo environment of the body like gastric pH, serum proteins and physiological pH. Stability data for all preparations was shown in Tables 2 to 4. All preparations are stable in

rabbit serum and normal saline for 24 h. At all time points % labeling was found to be more than 96 % in these media. Study in HCl was continued till 4 h but percentage labeled post 2.0 h was significantly reduced from that of initial. This stability in acidic pH was sufficient for preparations for oral administration, as within 2.0 h, material from stomach will reach intestine where the complex was found to be stable. The stability of the labeled complexes in different conditions indicates the usefulness of the label as a marker for the biodistribution studies.

6.4.3. Biodistribution and Pharmacokinetic Study in Healthy Mice

a) Intravenous Administration:

Free $^{99m}TcO_4^-$ and radio colloids were found to be very less (below 1.03 and 0.68 % respectively) after 24 h study of in vivo stability of the labeled complexes. These results are in accordance with the in vitro stability data. Blood and different organs/tissues were collected from mice at each time point. % A/g verses time curves were plotted for each set of experimental data (Figures 2 to 9).

Depending on the pure drug in solution or nanoparticle formulations, the distribution pattern appeared to be different. It was observed that the uptake and distribution of free etoposide and nanoparticles was different to different organs/tissues depending on the physical characters of the preparations. Comparative plots of radioactivity present in the blood of mice for all preparations (Figure 2) shows that free etoposide eliminated from the body at much faster rate than any of its nanoparticulate formulation. The administration of nanoparticle formulations led to an increase in the blood radioactivity than free etoposide solution. Residence time of free etoposide was less in the blood with quick elimination. In contrast all nanoparticle formulations showed a longer circulation time. At 24 h of post injection, % A/g of initial administration showed by all formulations; ETNP/F68/17 (1.01 %), ETNP/PCL/F68/03 (0.33 %), ETNP3/F68 (0.6%) and NP/F68/17 (1.13%) is 15.02, 4.96, 8.96 and 16.83 times more than free etoposide (0.07 %) respectively.

The pharmacokinetic parameters, calculated by non-compartmental modeling, for free etoposide and nanoparticle formulations are summarized in Table 5. There is significant difference in all parameters listed between free etoposide and formulations. Among nanoparticle formulations ETNP/F68/17 has significantly higher half-life ($t_{1/2}$), MRT and AUC and low clearance (Cl) value ($t_{1/2}$ - 20.09 h, MRT - 28.99 h, AUC_{0-8} - 100.22 %A.h/g, Cl - 0.99 g/h), as compared with other formulations (ETNP/PCL/F68/03: $t_{1/2}$ - 6.69 h, MRT - 9.66 h, AUC_{0-8} - 49.49 %A.h/g, Cl - 2.02 g/h, ETNP3/F68: ($t_{1/2}$ - 8.65 h, MRT - 12.48 h, AUC_{0-8} - 66.49 %A.h/g, Cl - 1.50 g/h) and free etoposide ($t_{1/2}$ - 1.28 h, MRT - 1.84 h,

AUC_{0-8} - 34.77 %A. h/g, Cl - 2.87 g/h). These results indicate that nanoparticles can circulate for a longer time in the blood than free etoposide. There was no significant difference in the pharmacokinetic parameters between empty nanoparticles (NP/F68/17) and etoposide loaded nanoparticles (ETNP/F68/17) indicating the results are based on the radioactivity shown by radiolabeled nanoparticles only and etoposide loading has not changed distribution pattern of nanoparticles in the body.

The distribution of nanoparticle formulations in tissues/organs, measured as radioactivity was significantly higher than those of free etoposide except in the heart. Radioactivity in case of nanoparticles in the heart was much lower than free etoposide at all time points. Etoposide levels in heart are related to the inherent cardiac toxicity. Therefore using nanoparticle formulations could reduce the cardiac toxicity of etoposide (Figure 3).

The formulations were found to reach the lung at relatively higher concentrations as indicated by radioactivity measured at particular time point. As etoposide is used in the treatment of lung cancer, nanoparticulate system can be a useful tool for better treatment of lung cancer with low dose and for longer period of time in a controlled manner. Free etoposide disappeared from lungs faster than nanoparticle formulations. There was significant difference in the radioactivity present in the lungs between free etoposide and formulations, whereas there was no significant difference between formulations (Figure 4).

Distribution of nanoparticle formulations loaded with etoposide in liver was significantly lower than that of free etoposide after 30 min of post injection. A comparison of the radioactivity detected in liver for free etoposide and nanoparticulate formulations can be seen in Figure 5. Highest radioactivity in liver was shown by ETNP/F68/17 among all formulations. It may be possible that the relatively small nanoparticles of ETNP/F68/17 can penetrate more efficiently than the bigger nanoparticles of ETNP/PCL/F68/03, ETNP3/F68 through fenestrae in the endothelial lining of the liver and associate with parenchymal cells. This would explain the increased liver accumulation of the ETNP/F68/17 nanoparticles compared with ETNP/PCL/F68/03 and ETNP3/F68, which are bigger in size. Stolnik et al, (2001) reported that their preliminary results suggest that small sterically stabilized particles can distribute mainly to the parenchymal cells of the liver after i.v. injection. These results show that free etoposide disappeared from the liver faster than formulations indicating nanoparticulate etoposide distribute more and stay for longer time than the free drug. Therefore these formulations could be used potentially in the treatment of liver cancer.

The overall uptake of formulations by spleen was significantly lower than free etoposide. The spleen uptake of ETNP/F68/17, ETNP/PCL/F68/03, ETNP3/F68 was initially low (2.25, 6.52, 4.35 and 2.41 % A/g at 30 min respectively) but increased with

time. ETNP/PCL/F68/03 has shown high radioactivity in spleen than ETNP/F68/17, ETNP3/F68 and NP/F68/17 (Figure 6). There was no significant uptake of formulations by kidney when compared to free etoposide. At initial time point, etoposide uptake was high indicating faster elimination of free etoposide (Figure 7). The lower kidney concentrations of all nanoparticle formulations indicated slow excretion and possibility of lower incidence of kidney toxicity.

Relatively higher radioactivity was found in bone for nanoparticles than free etoposide. This is one more useful indication for treatment of bone cancer. Higher concentration in bone owe to higher concentrations of nanoparticles in blood and their extended residence time in blood. All formulations reached at higher concentrations in bone at 1 h and then slowly eliminated from bone marrow. Significant radioactivity was present in bone after 24 h for formulations (ETNP/F68/17; 0.72, ETNP/PCL/F68/03; 0.75 and ETNP3/F68; 0.59 %A/g) than etoposide (0.09 %A/g). Higher accumulation of these particles in bone marrow may be the result of different physicochemical characters of nanoparticles. The major part of the radioactivity measured in bone is considered to result from the nanoparticle capture in phagocytic reticuloendothelial cells lining the vascular sinusoids of bone marrow. Radioactivity in case of NP/F68/17 was also same as ETNP/F68/17 formulation so blank nanoparticles can be used as diagnostic agents in the detection of tumor as they have specific uptake by bone (Figure 8).

Although overall brain uptake was relatively lower than other organs, formulations have reached brain and shown higher radioactivity than free etoposide (Figure 9). At all time points of study, radioactivity shown by free etoposide was significantly lower than ETNP/F68/17, ETNP/PCL/F68/03, ETNP3/F68 and NP/F68/17 formulations. At 24 h ETNP/F68/17 (0.07 %A/g), ETNP/PCL/F68/03 (0.08 %A/g), ETNP3/F68 (0.07 %A/g) have shown 4.23, 4.70, and 4.05 times higher radioactivity than that of free etoposide (0.02 % A/g). Formulations ETNP/F68/17, ETNP/PCL/F68/03, ETNP3/F68 and NP/F68/17 reached maximum in brain at 1 h and were present even after 24 h suggested that nanoparticles have greater brain transport. This helps in considering this system for the treatment of brain malignancies as etoposide is also used in the treatment of brain malignancies such as brain gliomas.

Radioactivity found in stomach, small intestine and large intestine for etoposide and formulations after i.v. administration is very low and is given in Tables 6 to 10. If the radioactivity in stomach is high after intravenous administration, then labeled complex is not stable indicating presence of higher percentage of free pertechnetate. A very low

radioactivity (< 1.0 %A/g for all preparations) recovered from stomach showed the in vivo stability of labeled complexes.

b) Oral Administration

In the biodistribution study after oral administration of radiolabeled free etoposide and nanoparticles, blood and different organs/tissues were collected from mice at different time points and percent administered activity (%A/g) verses time curves were plotted (Figures 10 to 20). In vivo stability of the labeled complexes was studied for 24 h by developing TLC of one or two drops of blood collected from mice at each time point. Free $^{99m}TcO_4^-$ and radio colloids were very less (below 1.15 and 0.59 % respectively).

High radioactivity levels were observed in the stomach up to 1 h after administration of nanoparticles, which then decreased with time (Figure 10). The free etoposide levels were high after 30 min of administration but then it decreased significantly proving its fast emptying from stomach than nanoparticles. Highest levels of radioactivity of about 42 % of administered dose were seen after 1 h in the small intestine for free etoposide. Radioactivity shown by nanoparticulate formulations was more after 2 h of administration when compared with free etoposide and even after 24 h there were high radioactivity levels in small intestine for nanoparticle formulations than free etoposide (Figure 11). This indicates the slow passage of nanoparticles through the GI tract along with the time and their uptake by the GI mucosa.

Maximum amount of radioactivity (50 %A/g) was appeared in large intestine after 2 h (Figure 12) of free etoposide administration. Formulations showed measurable radioactivity after 1 h but reached maximum radioactivity at 4 h. After 24 h also radioactivity was found in case of formulations in the intestine. This indicated fast movement of free etoposide from the GI tract where as formulations were still present in the intestine to release the drug. This could be due to the mucoadhesion of nanoparticles to the intestinal mucosa. Present study supported the observation of Sakuma et al, (1999). Their study showed that the bioadhesion of nanoparticles to GI mucosa occurs thereby increasing the salmon calcitonin absorption. Therefore the hypothesis of direct gastro intestinal uptake of nanoparticles (Florence, 1997) is supported by this present study also.

Three possibilities of uptake exist for nanoparticle formulations: an intracellular uptake, a paracellular uptake and an uptake via the M-cells and peyer's patches (Kreuter, 1991). Possibly a simultaneous uptake of by more than one pathway occurs. It seems that the quantitative contribution of each uptake pathway may be different at different sites of intestine. Nanoparticle uptake via intercellular spaces between the enterocytes in the

jejunum seems to be the prominent mechanism, 30 min after administration (Volkheimer, 1977; Alpar et al, 1989). In the opinion of these authors the paracellular pathway could explain the uptake and appearance in blood and other organs. In the large intestine, particles may seem to pass through M-cells and peyer's patches, both belonging to gut associated lymphatic tissue (GALT), in relatively large quantities (Jani et al, 1989; Jani et al, 1990; Jani et al, 1992a,b; Florence, 1997). To a lesser extent, normal intestinal tissue may be involved in particle uptake (Hillery et al, 1994). Besides particle size, surface properties of particles seem to influence their uptake. In addition, the surface properties also influence the bioadhesion and thus gastric transit time of small particles. Present study confirms the uptake of nanoparticles by the gastrointestinal tract.

The radioactivity data in blood after orally administration of nanoparticles and etoposide is presented in Figure 13. After 30 min of administration, radioactivity of free etoposide reached 0.1 %A/g of the administered dose where as in ETNP/F68/17, ETNP/PCL/F68/03, ETNP3/F68 and NP/F68/17 radioactivity reached 0.43, 0.51, 0.43 and 0.46 %A/g. Radioactivity concentration with the nanoparticle formulations increased with increase in time till 2 h reaching to a maximum of 1.38 % A/g administered dose for ETNP/PCL/F68/03 formulation. All formulations have higher residence time in blood than free etoposide. The pharmacokinetic parameters using non-compartmental modeling after oral administration of etoposide and formulations are summarized in Table 11. There is significant difference in all parameters listed between free etoposide and formulations. Among nanoparticle formulations ETNP/F68/17 has significantly higher half-life, MRT and area under the curve ($t_{1/2}$ - 37.56 h, MRT - 54.20 h, AUC_{0-8} - 53.46 %A.h/g, Cl/F - 1.87 g/h, C_{max} - 1.25 %A/g), as compared with other formulations (ETNP/PCL/F68/03: $t_{1/2}$ - 17.69 h, MRT - 25.53 h, AUC_{0-8} - 26.54 %A.h/g, Cl/F - 3.77 g/h, C_{max} - 1.38 %A/g), ETNP3/F68: ($t_{1/2}$ - 20.73 h, MRT - 29.92 h, AUC_{0-8} - 29.85 %A.h/g, Cl/F - 3.35 g/h, C_{max} - 1.19 %A/g) and free etoposide ($t_{1/2}$ - 5.59 h, MRT - 8.08 h, AUC_{0-8} - 8.97 %A.h/g, Cl/F - 11.14 g/h, C_{max} - 0.85 %A/g). These results indicated that nanoparticles circulated for a longer time in the blood circulation system than free etoposide.

Formulation ETNP/PCL/F68/03 showed a liver uptake of 3.48 %A/g at 1 h. After 24 h, radioactivity levels decreased to 0.53% of administered dose. Free etoposide showed highest levels of 5.8 %A/g at 1 h and drastically reduced to 0.15 %A/g (39 fold decrease) showing its faster elimination from the body. When compared with etoposide, all nanoparticle formulations showed significantly less uptake by liver as found from radioactivity data (Figure 14). In lungs, after oral administration of radiolabeled preparations, maximum radioactivity was shown by ETNP/PCL/F68/03 at 2 h. At all time

points radioactivity levels showed by formulations was more than etoposide. At 2 h, free etoposide showed 0.52 %A/g where as nanoparticle formulations, ETNP/F68/17, ETNP/PCL/F68/03, ETNP3/F68 and NP/F68/17 exhibited 1.06, 1.19, 0.98 and 1.12 %A/g respectively (Figure 15).

Another important organ for biodistribution study was spleen. From the Figure 16, it is evident that maximum amount of free etoposide was taken up by spleen. At 1 h of the study, 5.6 %A/g is present in spleen in case of free etoposide where as only 3.3, 3.8, 2.9 and 3.0 %A/g was present for formulations ETNP/F68/17, ETNP/PCL/F68/03, ETNP3/F68 and NP/F68/17 respectively. It indicated free etoposide was taken up by macrophages and thereby destroying it. Although radioactivity level in spleen for formulations was same after 2 h, significant radioactivity was present after 24 h also. Free etoposide has shown maximum radioactivity (0.9 %A/g) in heart at 1 h (Figure 17) when compared with formulations. But after 1 h, radioactivity of etoposide was reduced significantly with respect to formulations. Kidney concentrations in case of free etoposide was high and reached maximum (1.50 %A/g) at 1h and after that it decreased to minimum at 24 h (0.09 %A/g) indicating fast elimination of etoposide as free drug. For nanoparticle formulations, kidney radioactivity levels are less compared to etoposide till 4 h of the study. At 24 h formulations are still present in kidney indicating nanoparticle formulation was still present in the body of the animal and is available for elimination (Figure 18).

The Brain and Bone showed presence of relatively less radioactivity when compared to other organs of the animal. But significant differences were observed between free drug etoposide, and formulations regarding uptake by these two. In Figure 19, uptake of free etoposide and all formulations by bone are presented. It is clear that bone uptake for all formulations were more when compared to etoposide. Measurable radioactivity was present for free etoposide at 1 h (0.13 %A/g) where as in formulations ETNP/F68/17, ETNP/PCL/F68/03, ETNP3/F68 and NP/F68/17 levels are showing 0.82, 0.72, 0.84 and 0.89 %A/g respectively. Similar pattern was observed for brain also (Figure 20). Radioactivity levels reached maximum (0.06 %A/g) for etoposide at 1 hr. All formulations showed radioactivity significantly more than etoposide, which are 1.55, 1.38, 1.5 and 1.4 times more for formulations ETNP/F68/17, ETNP/PCL/F68/03, ETNP3/F68 and NP/F68/17 respectively than etoposide at 1 h.

Higher uptake and better distribution was shown by ETNP/F68/17 among all nanoparticle formulations in the study. This may be due to significantly low size of ETNP/F68/17 nanoparticles and also surface charge present on these particles. The present

study clearly demonstrates that nanoparticles can be taken up by the GIT after per oral administration although the uptake is rather low.

6.4.4. Biodistribution and Pharmacokinetic Study in Dalton's Lymphoma Tumor Bearing Mice

a) Tumor Implantation and Development

DLS tumor cells developed in the peritoneum of Balb/C mice were subcutaneously injected to Strain A mice. Measurable tumor was observed after 6^{th} day of implantation. It was allowed to grow further and measured on 10^{th} day of implantation. Tumor volume present in the right hind leg of strain A mice was measured with vernier calipers as 1.01 ± 0.2 cm^3.

b) Biodistribution and Pharmacokinetic Study

Biodistribution pattern of free etoposide and its nanoparticles (ETNP/F68/17) in tumor bearing mice is similar to that of in healthy mice with few exceptions. Radioactivity of ETNP/F68/17 measured from blood was more in tumor bearing mice (4.10 % A/g) than healthy mice (2.49 %A/g) 1 h post injection. Residence time of nanoparticles in blood is more compared with radiolabeled free etoposide as it is eliminated from the body at a faster rate (Figure 21). After 24 h of study, ETNP/F68/17 formulation is still present in blood circulation and radioactivity was 32 times more than that of free etoposide at the same time in blood. The pharmacokinetic parameters after non-compartmental modeling of Tc^{99m} labeled etoposide and ETNP/F68/17 nanoparticles are given in Table 12. There is significant difference in all pharmacokinetic parameters between etoposide and ETNP/F68/17 formulation, (etoposide: $t_{1/2}$ - 0.51 h, MRT - 0.74 h, AUC_{0-8} - 57.76 %A.h/g, Cl - 1.73 g/h), ETNP/F68/17: ($t_{1/2}$ - 9.74 h, MRT - 14..06 h, AUC_{0-8} - 136.97 %A.h/g, Cl - 0.73 g/h). After 1 h of injection, greater concentrations of free etoposide were found in heart, kidney, liver and spleen than formulation ETNP/F68/17. In the heart of tumor mice, uptake of formulation ETNP/F68/17 was less than etoposide at all time points of the study (Figure 22). Lungs have shown significant uptake of ETNP/F68/17 than etoposide but the uptake is less when compared with normal mice. Figure 23 shows the comparative biodistribution profile of free etoposide and formulation in lungs.

In tumor bearing mice also, liver is the major organ for uptake of free etoposide and formulation ETNP/F68/17. Highest radioactivity was found after 1 h of administration for free etoposide and ETNP/F68/17 (Figure 24). After 4 h, free etoposide concentrations (in terms of radioactivity) started decreasing indicating its elimination from the body but

nanoparticles were present in liver even after 24 h also which was indicated by the presence of radioactivity. Spleen uptake of etoposide was higher initially and decreased with time. Spleen capture of the formulation was less when compared to free etoposide. For formulation ETNP/F68/17, around 2.47 %A/g was found in spleen at 1 h post injection where as for etoposide %A/g found was around 9.20 (Figures 25). In kidney also, free etoposide got eliminated from the body earlier than ETNP/F68/17 (Figure 26). Interestingly uptake of ETNP/F68/17 formulation by bone near the tumor muscle in the right hind leg is significantly higher than the normal bone (Figure 27). Brain uptake was comparatively more for formulation than free etoposide. But radioactivity measured in brain was very less (Figure 28).

c) Tumor Uptake of Free Etoposide and Formulations

The tumor uptake of etoposide and ETNP/F68/17 nanoparticles was studied in DLS tumor induced mice at 1, 4 and 24 h post injection of the preparations. The uptake of free etoposide and ETNP/F68/17 nanoparticles increased with time till 4 h but found less at 24 h. ETNP/F68/17 nanoparticles showed significantly high tumor uptake compared to free etoposide at all time points studied. The tumor concentration of ETNP/F68/17 nanoparticles was 4.07 folds high at 1 h post injection, 7.11 fold high at 4 h post injection and 13.4 fold high at 24 h post injection (Figure 29). Radioactivity for both free etoposide and ETNP/F68/17 in tumor muscle was higher than normal muscle, which was used as control at all time points (Figure 30).

Etoposide amount was high in tumor muscle at all time points when compared with same muscle in healthy mice. This may be due to more blood perfusion to tumor than other muscles. Tumor vasculature is highly permeable than normal so free etoposide amount is high in the tumor. Amount of ETNP/F68/17 formulation present in tumor was high after 24 h also, where as free etoposide levels decreased significantly at 24 h. This is one advantage with nanoparticle formulation as they are available at tumor for more time to release drug. Residence time of ETNP/F68/17 nanoparticles in tumor can be due to more amount of formulation in blood of tumor bearing mice. Because of this, high amount is available at all time points and also tumor vasculature is made up of tight junctions which may not allow particles to leak out side the muscle tissue.

d) Gamma Scintigraphy

Scintigraphic images were taken after i.v. administration of etoposide and ETNP/F68/17 formulation to DLS tumor induced mice. Whole body of the mice was

viewed under gamma camera. As control, normal mice administered with free etoposide and ETNP/F68/17 formulations were used and radioactivity was measured under gamma camera. Figure 31 shows image taken after 4 h of administration of preparations and clearly indicate more radioactivity than 24 h image (Figure 32). Circled portions indicate radioactivity present in tumor or normal tissue/muscle. This indicated maximum radioactivity of ETNP/F68/17 formulation in tumor bearing mice than healthy mice at the tumor site. In all cases maximum radioactivity was present in liver. Radioactivity showed by free etoposide was less when compared to radioactivity shown by ETNP/F68/17nanoparticles in DLS tumor mice.

6.4.5. Pharmacokinetic Studies of Tc^{99m} Labeled Complexes

a) Intravenous Administration

Percentage injected activity verses time profiles obtained after intravenous administration of free etoposide, ETNP/F68/17, ETNP/PCL/F68/03 and NP/F68/17 in healthy rabbits are shown in Figure 33. The concentrations of free etoposide in blood declined biexponentially and ETNP/F68/17, ETNP/PCL/F68/03 and NP/F68/17 concentrations are significantly higher than that of free etoposide treated rabbit at all time points. The AUC_{0-8} obtained with ETNP/F68/17 formulation was greater than that of etoposide and ETNP/PCL/F68/03 (Table 13). Radioactivity shown by etoposide was 0.191 ± 0.11 %A/g after 6 h post administration of etoposide, 0.819 ± 0.12 %A/g and 0.50 ± 0.21% A/g for ETNP/F68/17, ETNP/PCL/F68/03 respectively. The clearance was low for ETNP/F68/17 and ETNP/PCL/F68/03 formulations when compared with free etoposide.

The overall pharmacokinetics of nanoparticle formulations were significantly different from free etoposide. Pharmacokinetic parameters after intravenous administration of etoposide, nanoparticle formulations ETNP/F68/17, ETNP/PCL/F68/03 and NP/F68/17 are listed in Table 13. Among the formulations, ETNP/F68/17 has more AUC, MRT and $t_{½}$ when compared to ETNP/PCL/F68/03 formulations. This is because of the bigger size of ETNP/PCL/F68/03 nanoparticles by which RES uptake is more and cleared from body at faster rate when compared to ETNP/F68/17. Empty nanoparticles were also studied for pharmacokinetic properties and found that drug loaded and blank formulations are behaving similar way in the rabbit body after intravenous administration. Nanoparticle formulations showed an improved pharmacokinetic profile than free etoposide. Better pharmacokinetic profile of nanoparticles can be attributed to slow clearance of formulations than that of free etoposide.

b) Gamma Scintigraphy

Rabbits were administered with etoposide and ETNP/F68/17 formulation and images were taken at 4 and 24 h post administration. Figures 34 and 35 shows the scintigraphic images of rabbits after i.v. administration of etoposide and ETNP/F68/17 at 4 and 24 h respectively. It was clearly shown that maximum radioactivity was in liver. Bone marrow uptake can be seen in case of rabbit administered with ETNP/F68/17 formulation (Figure 34). Whole body of the rabbit was captured and it indicated the presence of radioactivity in blood. In case of free etoposide administered rabbit, bone marrow uptake was less and there was very less radioactivity found in body after 24 h. With ETNP/F68/17 formulation there was radioactivity present in the rabbit body after 24 of administration indicating longer residence of nanoparticles.

c) Oral Administration

Pharmacokinetics of etoposide and nanoparticle formulations after oral administration was studied in rabbits. Percent administered dose present in blood at regular time intervals was plotted against time to know the pharmacokinetic parameters for preparations. Figure 36 shows pharmacokinetic profiles of orally administered free etoposide, ETNP/F68/17 and NP/F68/17. There was significant difference in the pharmacokinetic parameters between these preparations after fitting them into non-compartmental model of analysis. All pharmacokinetic parameters calculated for etoposide and nanoparticle formulations are tabulated in Table 13. From these parameters it was evident that free etoposide was eliminated from the body at faster rate than nanoparticle formulations. AUC, MRT of free etoposide were lower than all formulations in the study. Maximum concentration (C_{max}) reached for etoposide was 0.83 ± 0.04 % A/g at 2 hr. Time (T_{max}) to reach C_{max} was not changed for formulations but C_{max} was changed significantly from that of free etoposide. There was no significant difference between the pharmacokinetic parameters of drug loaded as well as empty nanoparticle formulations.

6.5. Conclusions

Etoposide and etoposide loaded nanoparticles were tagged with Tc^{99m} using rapid and simple direct labeling procedure. Labeling efficiency was high with 100 µg stannous chloride at pH 7. All labeled complexes are stable for 24 h in rabbit blood, normal saline and for about 2 h in 0.01 N HCl. In vivo stability of complexes has shown that all the complexes are stable for 24 h in blood. Nanoparticles observed to have more residence in blood after i.v. administration and thus advantageous for better therapy with lesser dose.

Higher brain concentrations after i.v. and oral administration of nanoparticles in healthy mice indicate their potential use in delivering etoposide to brain. The pharmacokinetic data after i.v. administration of etoposide and formulations to healthy mice shows their prolonged blood circulation and the order of preference is ETNP/F68/17 > ETNP/PCL/F68/03 > ETNP3/F68 > free etoposide.

Higher uptake of etoposide loaded nanoparticles by GI tract after oral administration proves the hypothesis of uptake of nanoparticles through GI mucosa. This also has potential use in treatment of GI tract malignancies. Pharmacokinetic parameters after oral administration of etoposide and formulations to healthy mice follows the order same as i.v. administration (ETNP/F68/17 > ETNP/PCL/F68/03 > ETNP3/F68 > free etoposide). Although recovered radioactivity in organs/tissues except GIT is comparatively less, etoposide loaded nanoparticles are taken up by all tissues after oral administration. Both routes of administration have their own advantages for the treatment of various malignancies signifying their use by both the routes of administration. Significant amount of radioactivity present in tissues/organs after 24 h indicates that these formulations were present in the body and can release etoposide till that time.

ETNP/F68/17 formulation is proved to be a better formulation after biodistribution and pharmacokinetic study than ETNP/PCL/F68/03 and ETNP3/F68 formulations. It has shown comparatively high residence time in blood after oral and i.v. administration and has shown increase in pharmacokinetic parameters than all other formulations and free etoposide. ETNP/F68/17 formulation is prepared by PLGA 85/15 polymer and has significantly lower size and negative charge present on the surface of particles. These properties also contribute to its better biodistribution pattern of the formulation. ETNP/PCL/F68/03 and ETNP3/F68 were prepared by PCL and a combination of PLGA 85/15 and PCL (1:1) and these formulations have significantly higher size the ETNP/F68/17. Because of difference in size between formulations, uptake and biodistribution patterns changed, lower the size of formulation, better distribution into organs/tissues. All the studied formulations here were prepared in presence Pluronic F 68 as stabilizer and the presence of stabilizer might have contributed to higher uptake and increased the residence time in blood for all nanoparticle formulations.

Difference in biodistribution of etoposide and nanoparticles between healthy and DLS tumor induced mice was evident. This indicates tumor affinity and targeting properties of etoposide loaded nanoparticles than free etoposide. The tumor concentrations of both free etoposide and nanoparticles increased with time and showed higher retention indicating their use in effective and prolonged tumor therapy. Tumor is supplied with numerous blood

vessels and due to this reason radioactivity corresponding to etoposide and etoposide loaded nanoparticles were found in higher concentration in blood of tumor induced mice than healthy mice after i.v. administration. Scintigraphic images confirm the presence of labeled complexes at the site of tumor for 24 h at maximum concentration than in the normal muscle. This study signifies that etoposide loaded nanoparticles is better delivery system to deliver etoposide to DLS tumor at greater concentrations for prolonged period of time and is expected to lead to greater antitumor effect and tumor regression. This might be a suitable drug delivery system for targeting of various types of tumors.

Pharmacokinetic studies done on i.v. and oral administration of etoposide and nanoparticle formulations have also shown that these formulations can increase the bioavailability of the loaded drug. Pharmacokinetic parameters like AUC, Clearance and MRT after fitting into non-compartmental model are better than those obtained with free etoposide administration. Scintigraphic images taken in rabbit after i.v. administration have shown that there is maximum uptake by liver. Whole body of the rabbit can be viewed in the image confirming the presence of radioactivity in blood. With all these results we can say that drug loaded nanoparticles could be a better delivery system than any conventional formulation. These systems can potentially avoid some problems associated with conventional formulations of etoposide.

Table 1: Influence of amount of stannous chloride on the labeling efficiency of etoposide.

$SnCl_2 . 2 H_2O$ (µg)	% Labeled ± SD	% Colloids ± SD	% Free ± SD
25	73.89 ± 1.58	0.89 ± 0.07	25.22 ± 1.72
50	85.79 ± 1.94	0.72 ± 0.39	13.48 ± 1.55
100	99.21 ± 1.01	0.62 ± 0.08	0.17 ± 0.09
200	97.92 ± 0.76	1.56 ± 0.91	0.52 ± 0.18
400	95.16 ± 1.21	3.93 ± 1.04	0.91 ± 0.29

Each value is the mean of 3 independent determinations

Table 2: In vitro labeling stability of Tc^{99m} labeled preparations in rabbit serum.

Time (h)	% Labeled ± SD				
	Etoposide	ETNP/F68/17	ETNP/PCL/ F68/03	ETNP3/F68	NP/F68/17
0.0	98.38 ± 1.82	96.54 ± 0.84	97.90 ±1.54	99.32 ± 1.81	98.48 ± 2.71
0.25	98.32 ± 2.14	98.48 ± 1.30	99.78 ± 1.38	99.85 ± 2.08	98.67 ± 1.97
0.5	97.86 ± 1.81	99.80 ± 1.45	98.49 ± 1.64	98.74 ± 2.42	98.81 ± 1.24
1.0	98.19 ± 1.02	98.90 ± 2.14	97.23 ± 1.70	96.99 ± 1.05	97.24 ± 1.55
2.0	97.99 ± 0.84	98.35 ± 2.70	98.75 ± 0.99	98.56 ± 1.08	98.26 ± 0.89
4.0	97.94 ± 1.05	97.89 ± 1.80	96.99 ± 1.03	98.93 ± 1.82	97.58 ± 1.98
6.0	97.74 ± 1.16	98.94 ± 1.12	99.45 ± 3.07	97.57 ± 1.46	98.21 ± 1.11
24.0	98.03 ± 3.04	98.19 ± 1.01	97.58 ± 3.91	97.40 ± 2.02	98.97 ± 1.23

Each value is the mean of 3 independent determinations

Table 3: In vitro labeling stability of Tc^{99m} labeled preparations in normal saline.

Time (h)	% Labeled (± SD)				
	Etoposide	**ETNP/F68/17**	**ETNP/PCL/ F68/03**	**ETNP3/F68**	**NP/F68/17**
0.0	96.85 ± 0.97	96.91 ± 1.83	97.81 ± 2.71	96.45 ± 1.58	97.87 ± 2.52
0.25	98.95 ± 0.99	98.06 ± 2.01	98.62 ± 2.08	98.61 ± 1.39	97.11 ± 1.82
0.5	97.19 ± 1.06	99.88 ± 2.12	97.51 ± 1.48	97.70 ± 2.81	98.71 ± 1.03
1.0	98.19 ± 1.16	96.16 ± 3.11	98.05 ± 1.83	97.29 ± 1.46	97.98 ± 1.64
2.0	96.31 ± 1.24	97.11 ± 1.84	96.09 ± 2.54	96.76 ± 1.85	97.44 ± 1.88
4.0	95.98 ± 1.28	97.32 ± 2.18	98.05 ± 2.66	96.40 ± 2.06	97.28 ± 2.07
6.0	96.10 ± 2.58	96.77 ± 1.26	97.57 ± 2.57	97.91 ± 1.88	97.22 ± 0.93
24.0	97.99 ± 1.83	97.42 ± 0.96	98.11 ± 2.08	97.47 ± 0.97	96.73 ± 1.45

Each value is the mean of 3 independent determinations

Table 4: In vitro labeling stability of Tc^{99m} labeled preparations in 0.01 N HCl.

Time (h)	% Labeled ± SD				
	Etoposide	**ETNP/F68/17**	**ETNP/PCL/ F68/03**	**ETNP3/F68**	**NP/F68/17**
0.0	98.97 ±1.81	97.10 ± 0.97	97.98 ± 2.06	98.07 ± 1.08	97.47 ± 2.82
0.25	98.02 ± 1.80	97.08 ± 2.11	98.85 ± 1.24	97.61 ± 2.64	97.11 ± 2.08
0.5	98.49 ± 0.89	96.18 ± 2.84	97.55 ± 1.85	97.18 ± 3.05	97.18 ± 1.86
1.0	94.47 ± 2.05	93.95 ± 1.06	94.89 ± 1.23	95.45 ± 2.48	93.17 ± 1.08
2.0	90.08 ± 1.55	91.89 ± 1.97	90.76 ± 1.90	91.21 ± 1.65	89.70 ± 1.51

Each value is the mean of 3 independent determinations

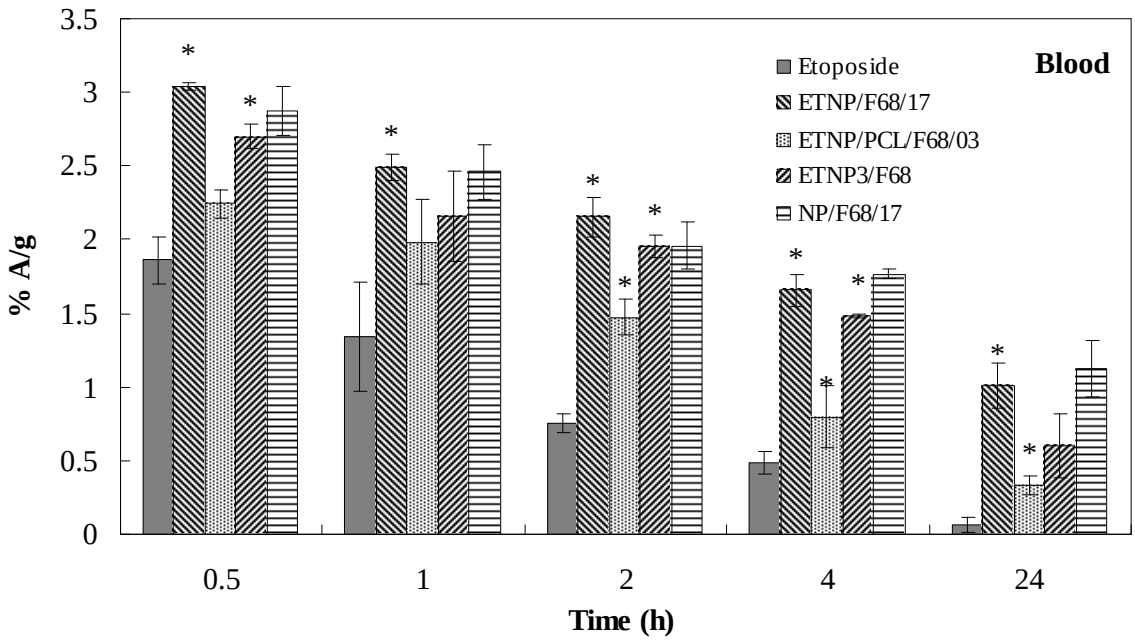

Figure 2: Comparative biodistribution profiles of drug and formulations in blood of healthy mice after i.v. administration (n=3). * - $P \leq 0.01$

Table 5: Pharmacokinetic Parameters for etoposide and nanoparticle formulations in healthy mice after intravenous administration.

Parameter	Etoposide	ETNP/F68/17	ETNP/PCL/ F68/03	ETNP3/F68	NP/F68/17
AUC_{0-8} (%A.h/g)	34.77	100.22	49.49	66.49	111.95
MRT (h)	1.84	28.99	9.66	12.48	33.72
$t_{1/2}$ (h)	1.28	20.09	6.69	8.65	23.37
Cl (g/h)	2.87	0.99	2.02	1.50	0.89

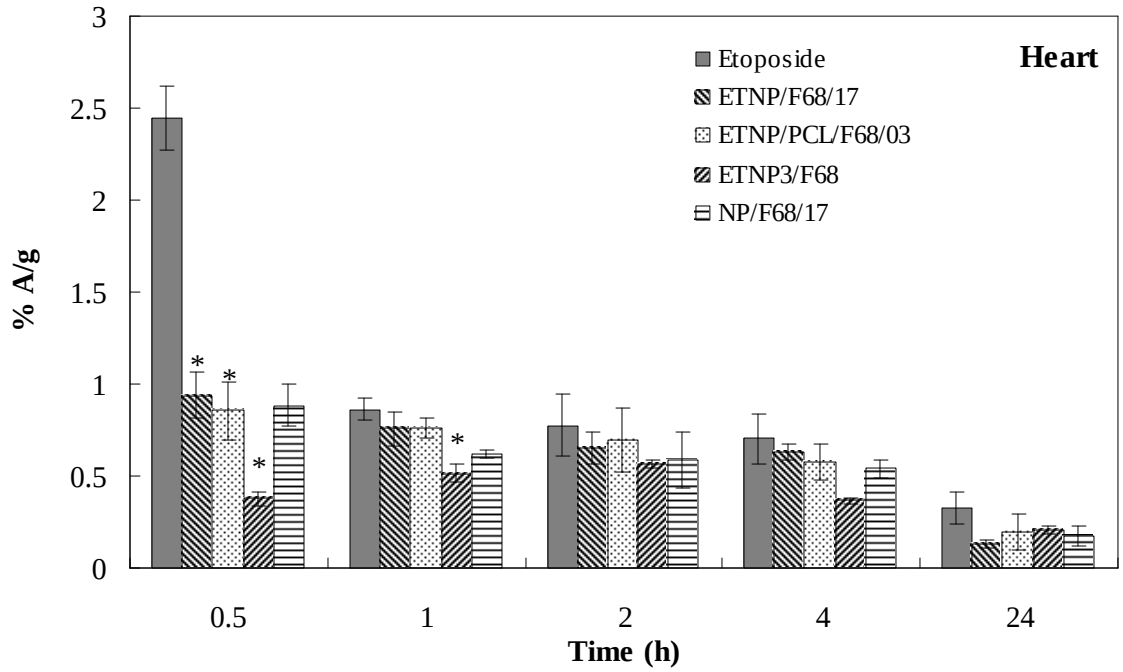

Figure 3: Comparative biodistribution profiles of drug and formulations in heart of healthy mice after i.v. administration (n=3). * - $P \leq 0.01$

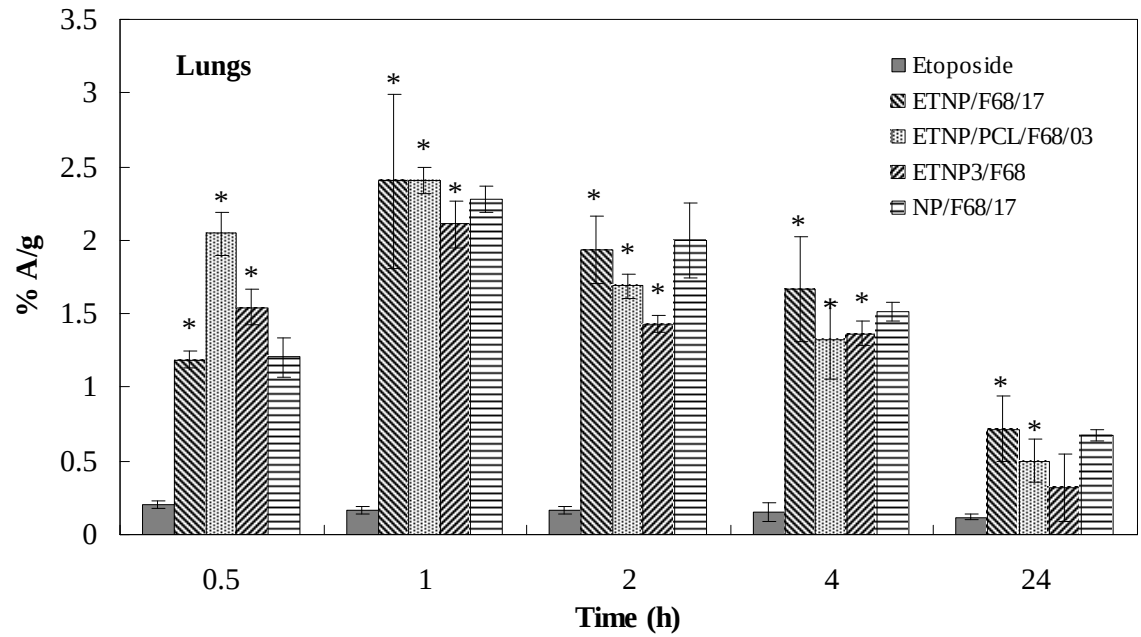

Figure 4: Comparative biodistribution profiles of drug and formulations in lungs of healthy mice after i.v. administration (n=3). * - $P \leq 0.01$

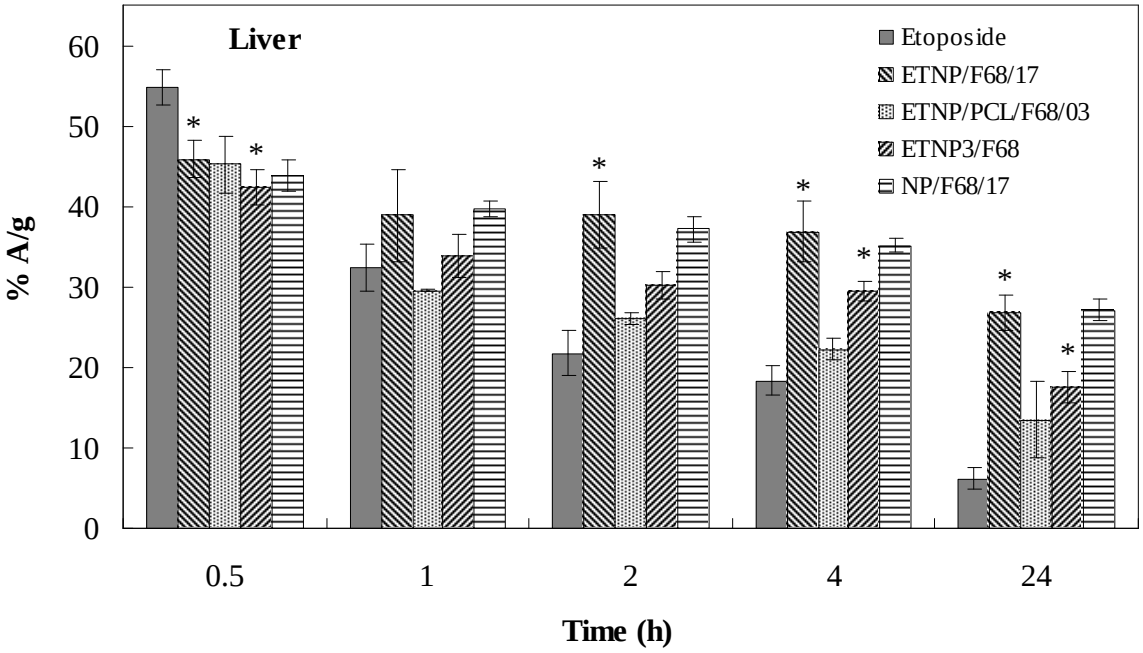

Figure 5: Comparative biodistribution profiles of drug and formulations in liver of healthy mice after i.v. administration (n=3). * - $P < 0.01$

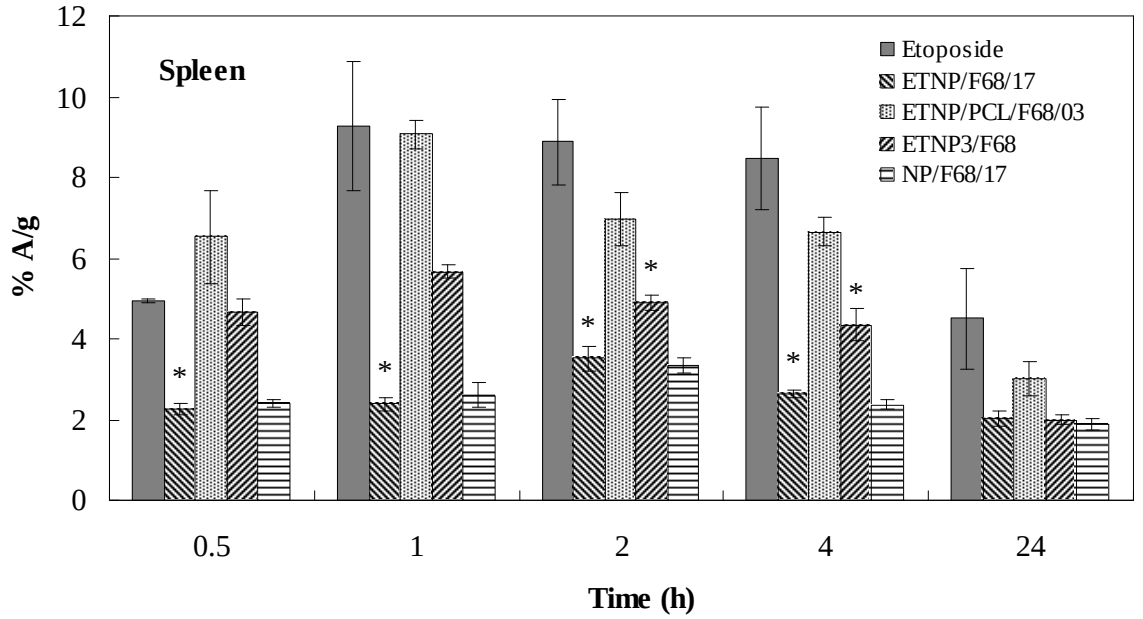

Figure 6: Comparative biodistribution profiles of drug and formulations in spleen of healthy mice after i.v. administration (n=3). * - $P \leq 0.01$

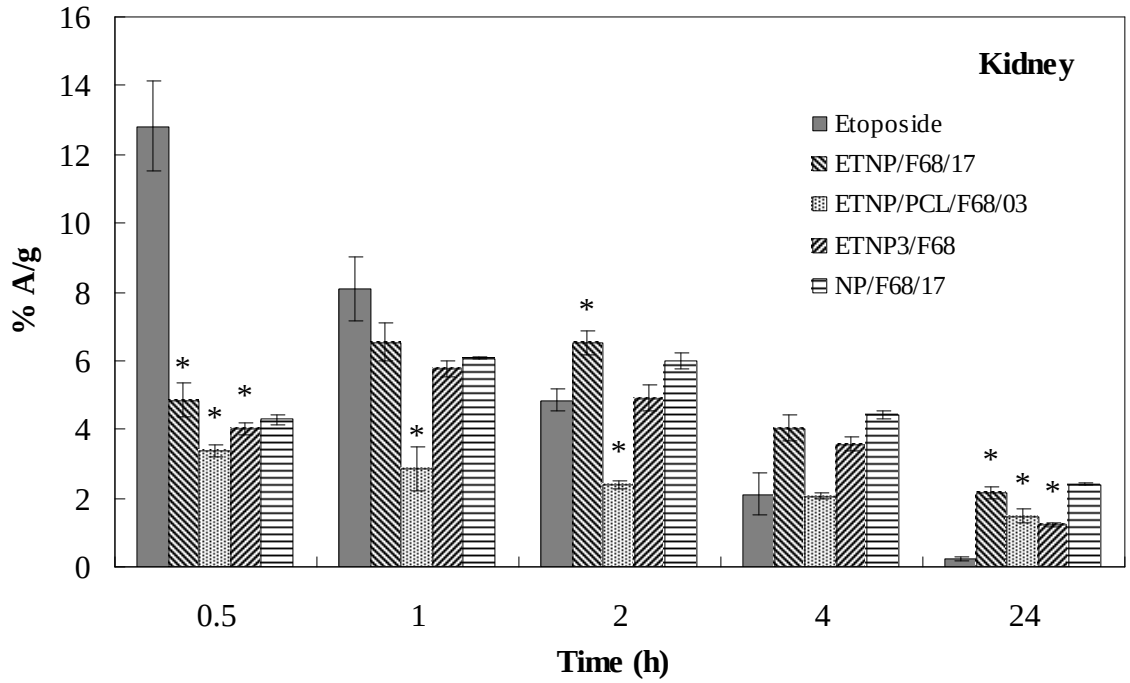

Figure 7: Comparative biodistribution profiles of drug and formulations in kidney of healthy mice after i.v. administration (n=3). * - $P \leq 0.01$

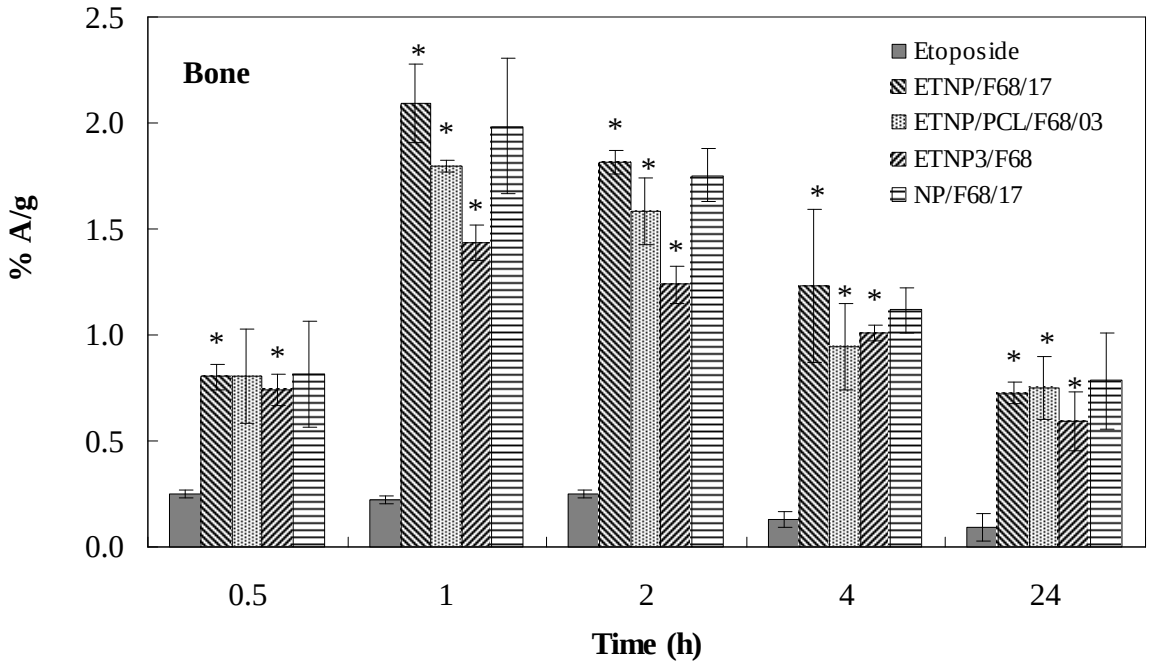

Figure 8: Comparative biodistribution profiles of drug and formulations in bone of healthy mice after i.v. administration (n=3). * - $P \leq 0.01$

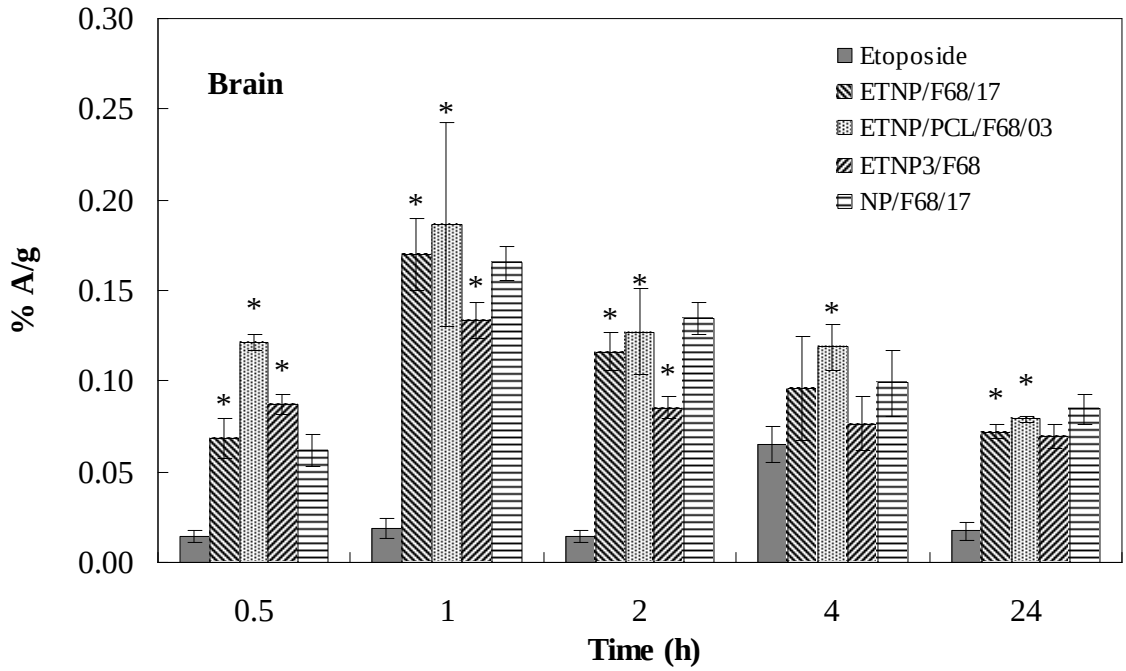

Figure 9: Comparative biodistribution profiles of drug and formulations in brain of healthy mice after i.v. administration (n=3). * - $P \leq 0.01$

Table 6: Tissue distribution kinetics of Tc^{99m} labeled etoposide in healthy mice - after i.v. administration.

Time (h) →	**% A/g ± SD**				
	0.5	**1.0**	**2.0**	**4.0**	**24.0**
Stomach	0.021 ± 0.003	0.057 ± 0.008	0.047 ± 0.015	0.078 ± 0.025	0.038 ± 0.016
Small Intestine	0.759 ± 0.094	1.169 ± 0.307	1.736 ± 0.091	2.143 ± 0.055	0.637 ± 0.131
Large Intestine	0.237 ± 0.052	0.607 ± 0.092	0.394 ± 0.005	0.246 ± 0.074	0.076 ± 0.012

Each value is the mean of 3 independent determinations

Table 7: Tissue distribution kinetics of Tc^{99m} labeled nanoparticle formulation (ETNP/F68/17) in healthy mice after i.v. administration.

Time (h) →	**% A/g ± SD**				
	0.5	**1.0**	**2.0**	**4.0**	**24.0**
Stomach	0.689 ± 0.063	0.870 ± 0.066	0.554 ± 0.104	0.403 ± 0.099	0.276 ± 0.101
Small Intestine	0.469 ± 0.021	0.540 ± 0.213	0.607 ± 0.254	0.962 ± 0.276	0.546 ± 0.327
Large Intestine	0.471 ± 0.074	0.860 ± 0.332	0.897 ± 0.143	0.587 ± 0.128	0.403 ± 0.07

Each value is the mean of 3 independent determinations

Table 8: Tissue distribution kinetics of Tc^{99m} labeled nanoparticle formulation (ETNP/PCL/F68/03) in healthy mice after i.v. administration.

Time (h) →	**% A/g ± SD**				
	0.5	**1.0**	**2.0**	**4.0**	**24.0**
Stomach	0.680 ± 0.049	0.991 ± 0.059	0.561 ± 0.098	0.421 ± 0.089	0.276 ± 0.101
Small Intestine	0.475 ± 0.009	0.603 ± 0.225	0.559 ± 0.286	1.081 ± 0.298	0.601 ± 0.365
Large Intestine	0.486 ± 0.084	0.984 ± 0.376	0.891 ± 0.151	0.661 ± 0.138	0.448 ± 0.062

Each value is the mean of 3 independent determinations

Table 9: Tissue distribution kinetics of Tc^{99m} labeled nanoparticle formulation (ETNP3/F68) in healthy mice - i.v. administration.

Time (h) →	**% A/g ± SD**				
	0.5	**1.0**	**2.0**	**4.0**	**24.0**
Stomach	0.589 ± 0.061	0.662 ± 0.039	0.631 ± 0.058	0.482 ± 0.044	0.492 ± 0.050
Small Intestine	0.743 ± 0.087	0.691 ± 0.048	0.522 ± 0.104	0.443 ± 0.081	0.585 ± 0.038
Large Intestine	0.927 ±0.217	0.882 ± 0.097	0.688 ± 0.185	0.439 ± 0.101	0.829 ± 0.111

Each value is the mean of 3 independent determinations

Table 10: Tissue distribution kinetics of Tc^{99m} labeled nanoparticle formulation (ETNP/F68/17) in healthy mice - i.v. administration.

Time (h) →	**% A/g ± SD**				
	0.5	**1.0**	**2.0**	**4.0**	**24.0**
Stomach	0.742 ± 0.082	0.807 ± 0.089	0.497 ± 0.069	0.362 ± 0.009	0.227 ± 0.035
Small Intestine	0.397 ± 0.038	0.620 ± 0.064	0.601 ± 0.088	0.943 ±0.051	0.483 ± 0.033
Large Intestine	0.508 ± 0.097	0.822 ± 0.091	0.721 ± 0.056	0.516 ± 0.055	0.496 ± 0.008

Each value is the mean of 3 independent determinations

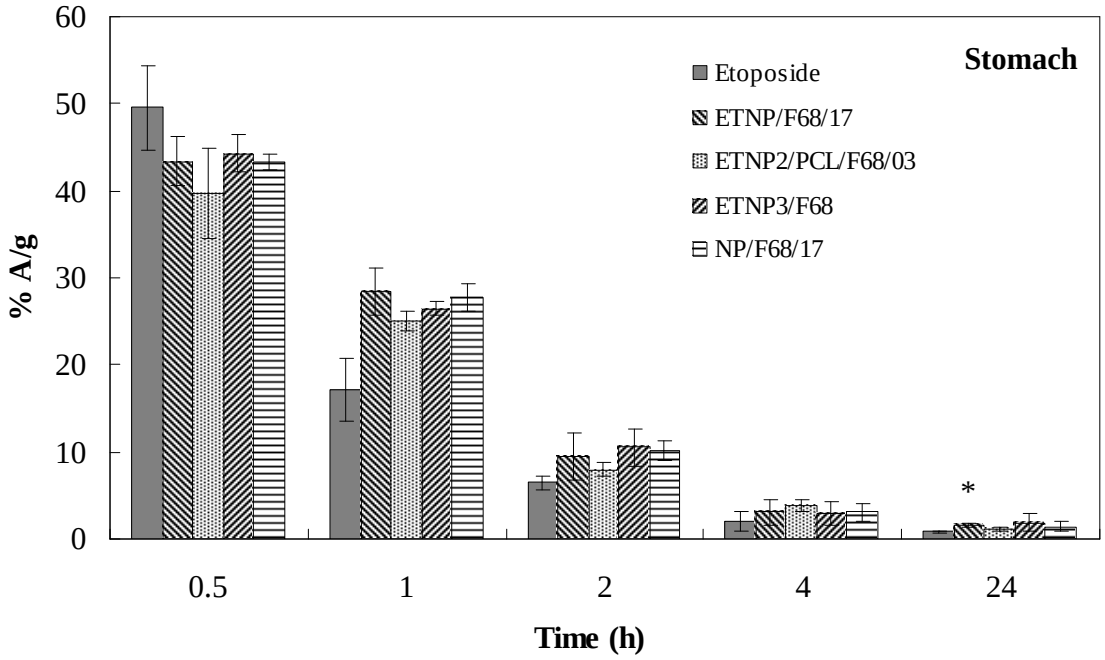

Figure 10: Comparative biodistribution profiles of drug and formulations in stomach of healthy mice after oral administration (n=3). * - $P \leq 0.01$

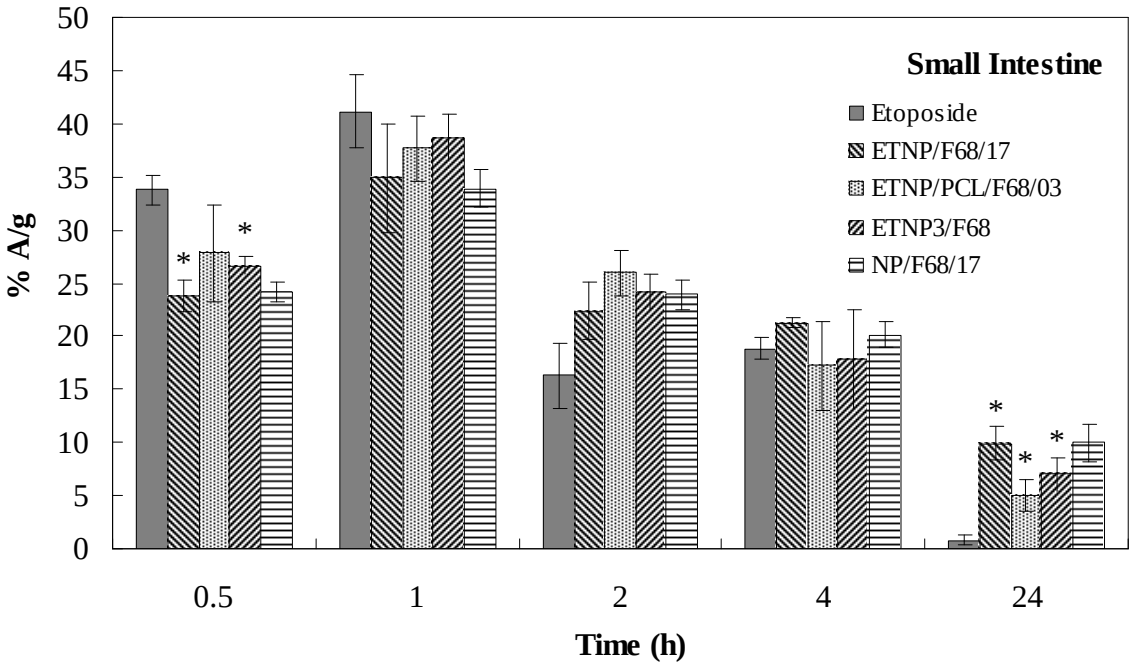

Figure 11: Comparative biodistribution profiles of drug and formulations in small intestine of healthy mice after oral administration (n=3). * - $P \leq 0.01$

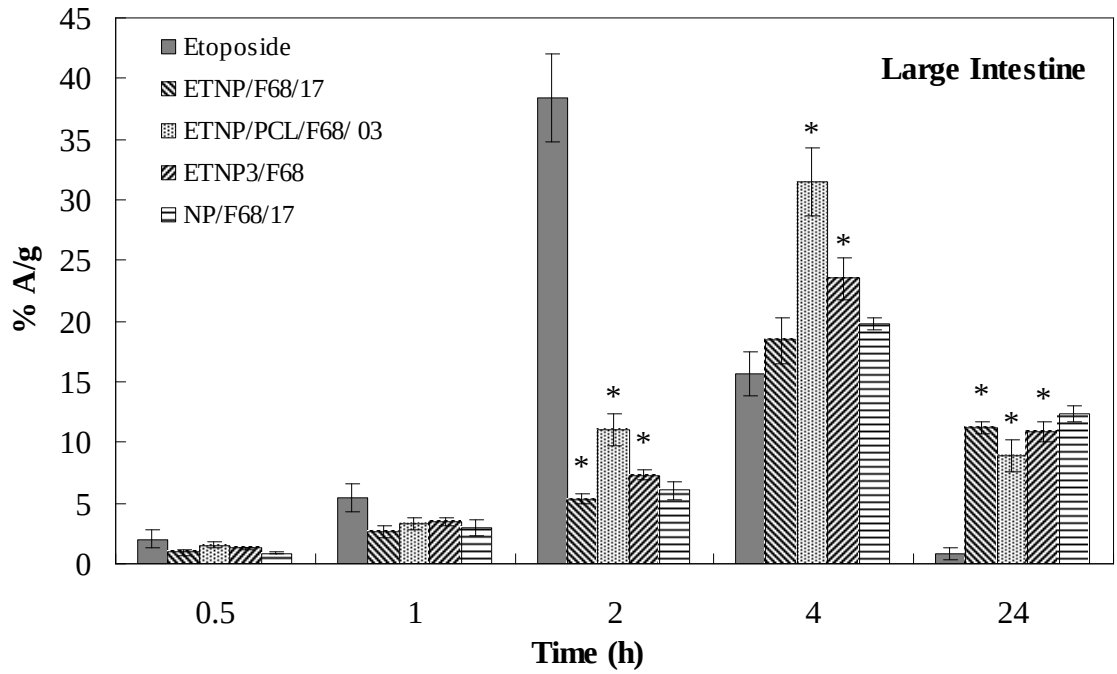

Figure 12: Comparative biodistribution profiles of drug and formulations in large Intestine of healthy mice after oral administration (n=3). * - $P \leq 0.01$

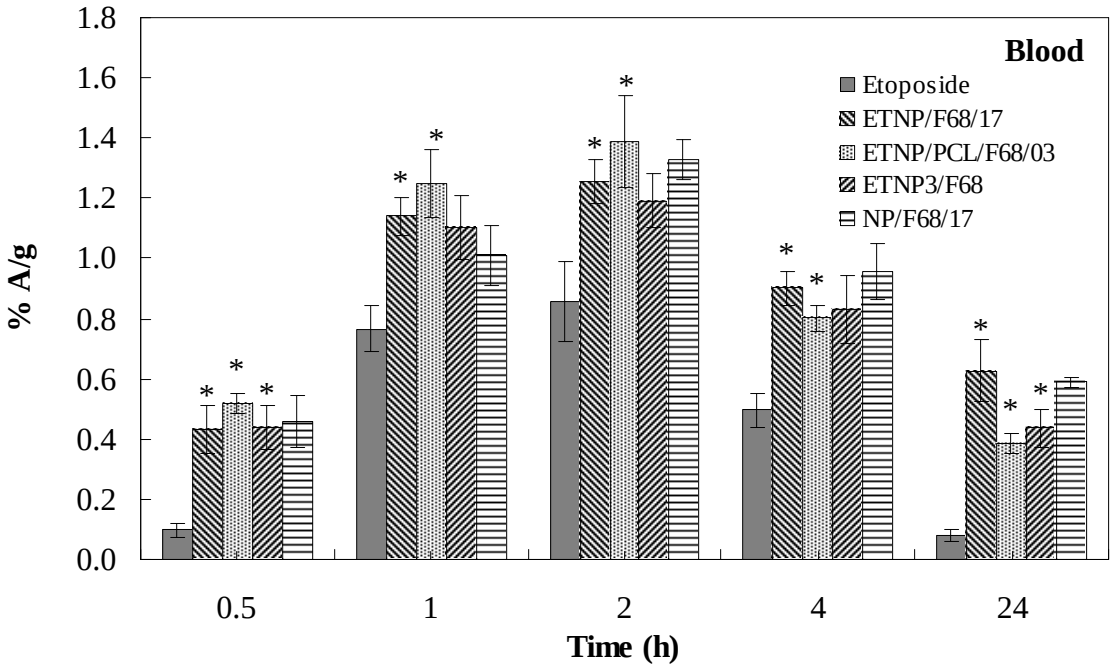

Figure 13: Comparative biodistribution profiles of drug and formulations in blood of healthy mice after oral administration (n=3). * - $P \leq 0.01$

Table 11: Pharmacokinetic parameters for etoposide and nanoparticle formulations in healthy mice after oral administration.

Parameter	Etoposide	ETNP/F68/17	ETNP/PCL/ F68/03	ETNP3/F68	NP/F68/17
AUC_{0-8} (%A.h/g)	8.97	53.46	26.54	29.85	43.52
MRT (h)	8.08	54.20	25.53	29.92	40.36
$t_{1/2}$ (h)	5.59	37.56	17.69	20.73	27.97
Cl (g/h)	11.14	1.87	3.77	3.35	2.29
C_{max} (%A/g)	0.85	1.25	1.38	1.19	1.32
T_{max} (h)	2.00	2.00	2.00	2.00	2.00

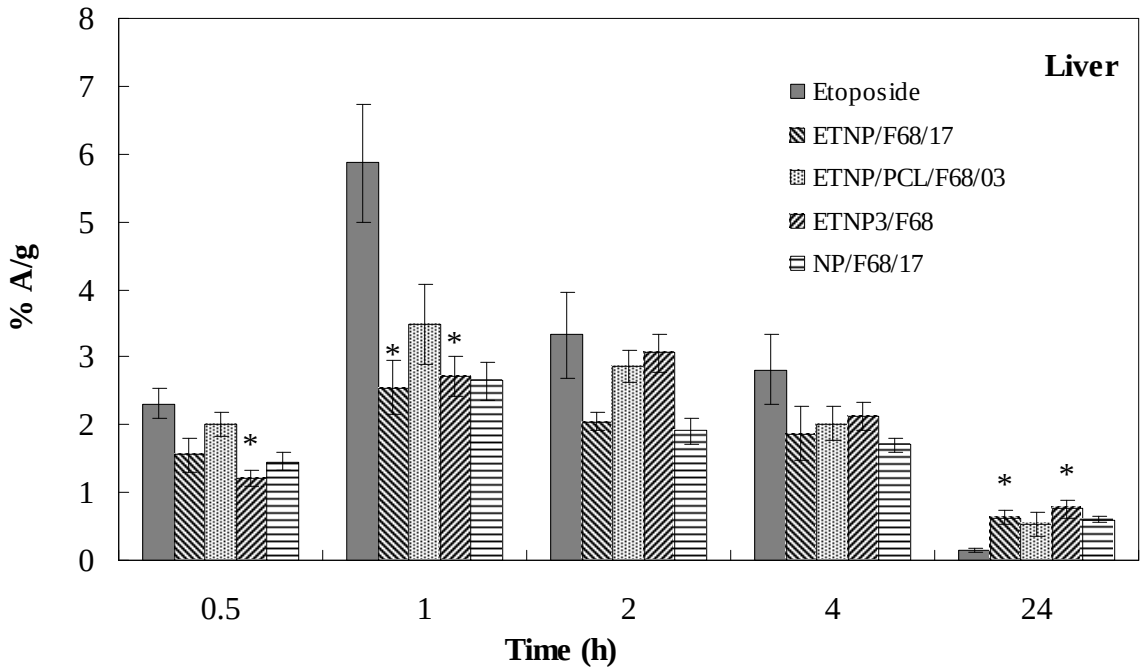

Figure 14: Comparative biodistribution profiles of drug and formulations in liver of healthy mice after oral administration (n=3). * - $P \leq 0.01$

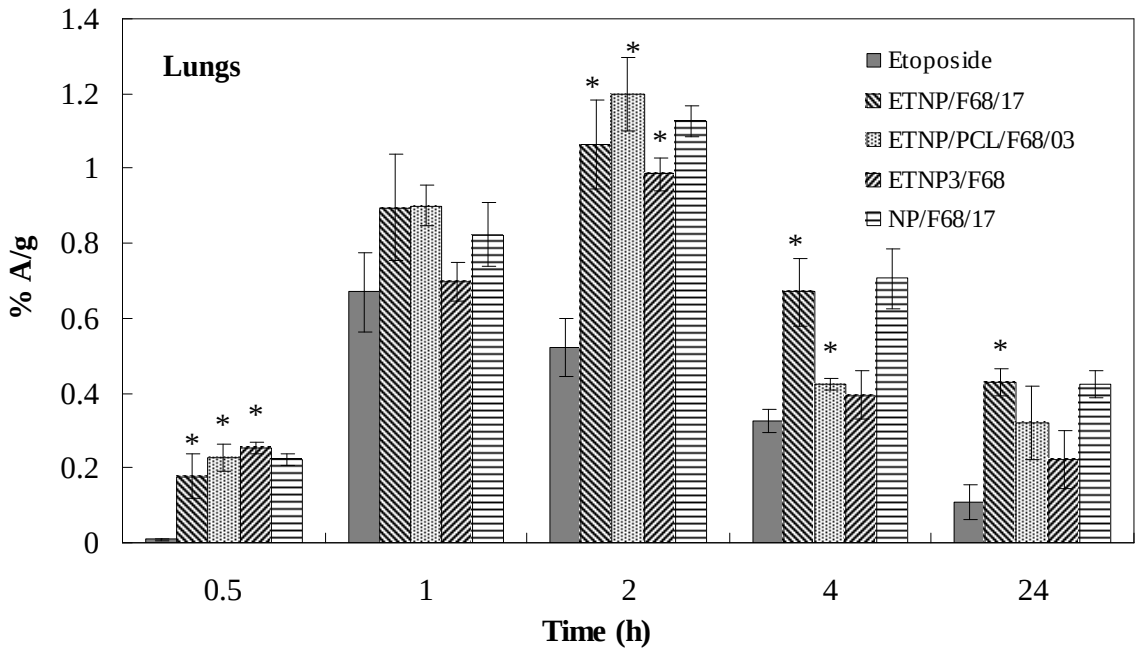

Figure 15: Comparative biodistribution profiles of drug and formulations in lungs of healthy mice after oral administration (n=3). * - $P \leq 0.01$

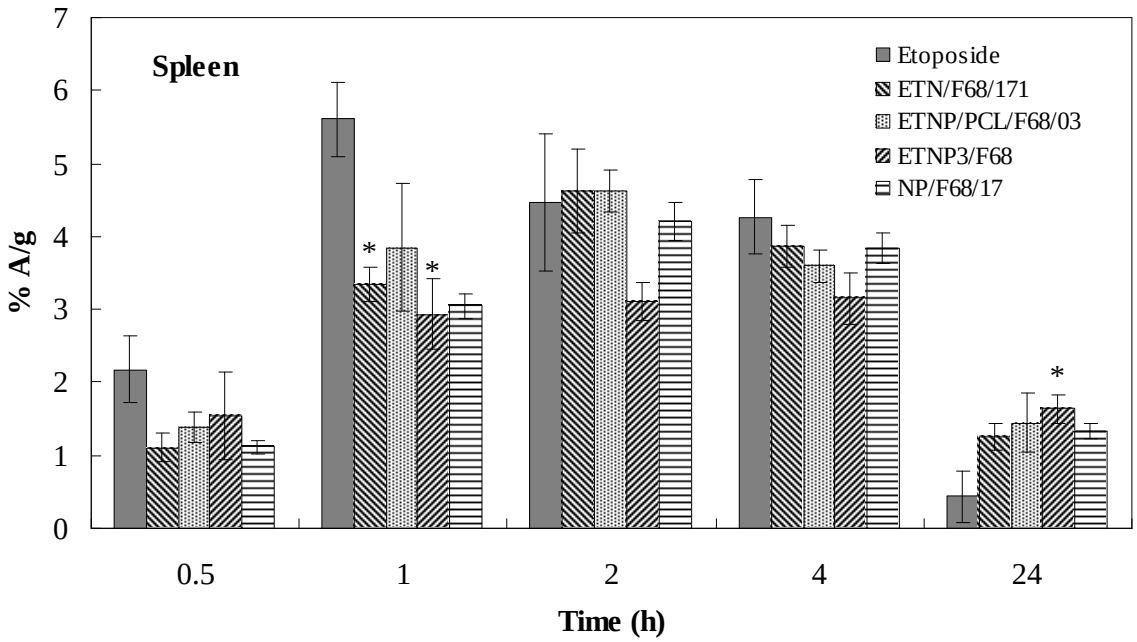

Figure 16: Comparative biodistribution profiles of drug and formulations in spleen of healthy mice after oral administration (n=3). * - $P \leq 0.01$

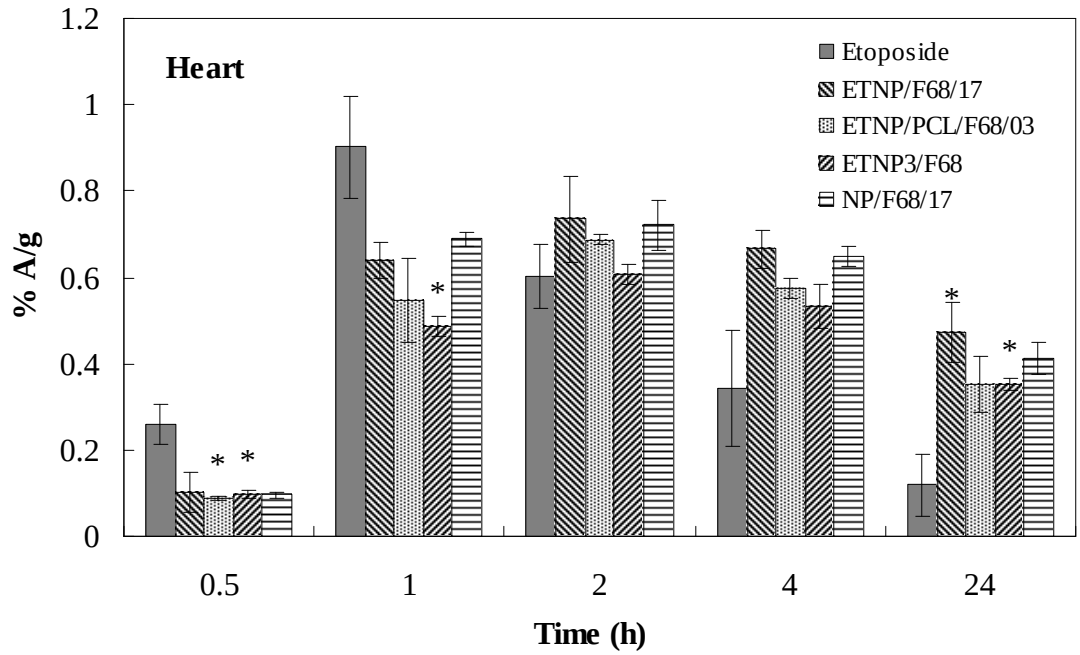

Figure 17: Comparative biodistribution profiles of drug and formulations in heart of healthy mice after oral administration (n=3). * - $P \leq 0.01$

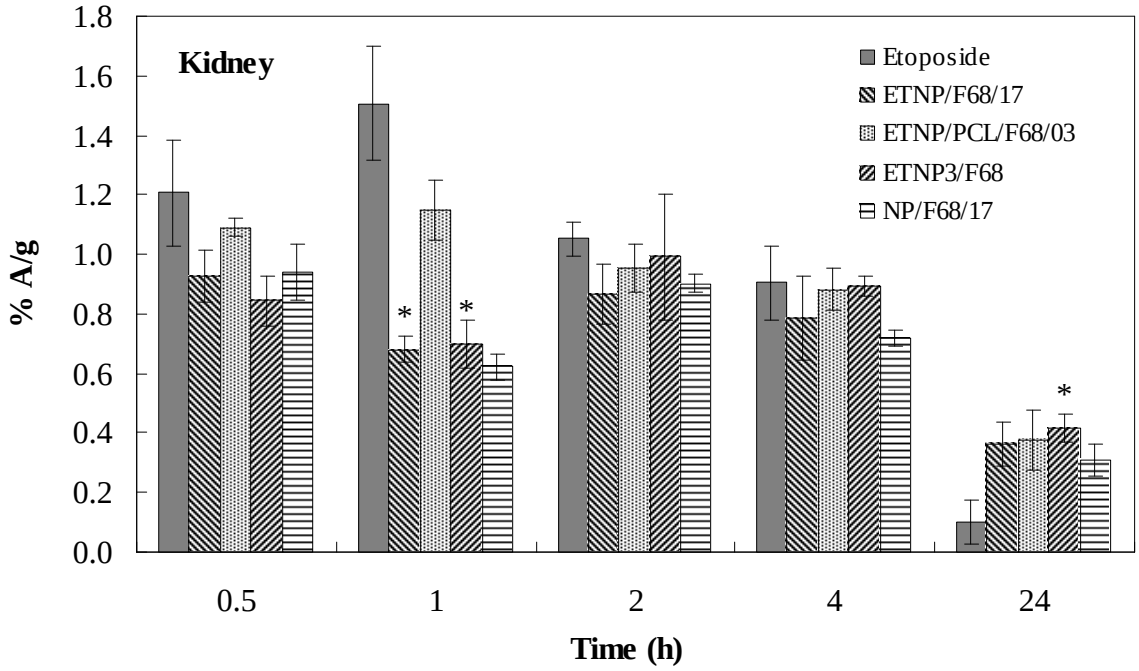

Figure 18: Comparative biodistribution profiles of drug and formulations in kidney of healthy mice after oral administration (n=3). * - $P \leq 0.01$

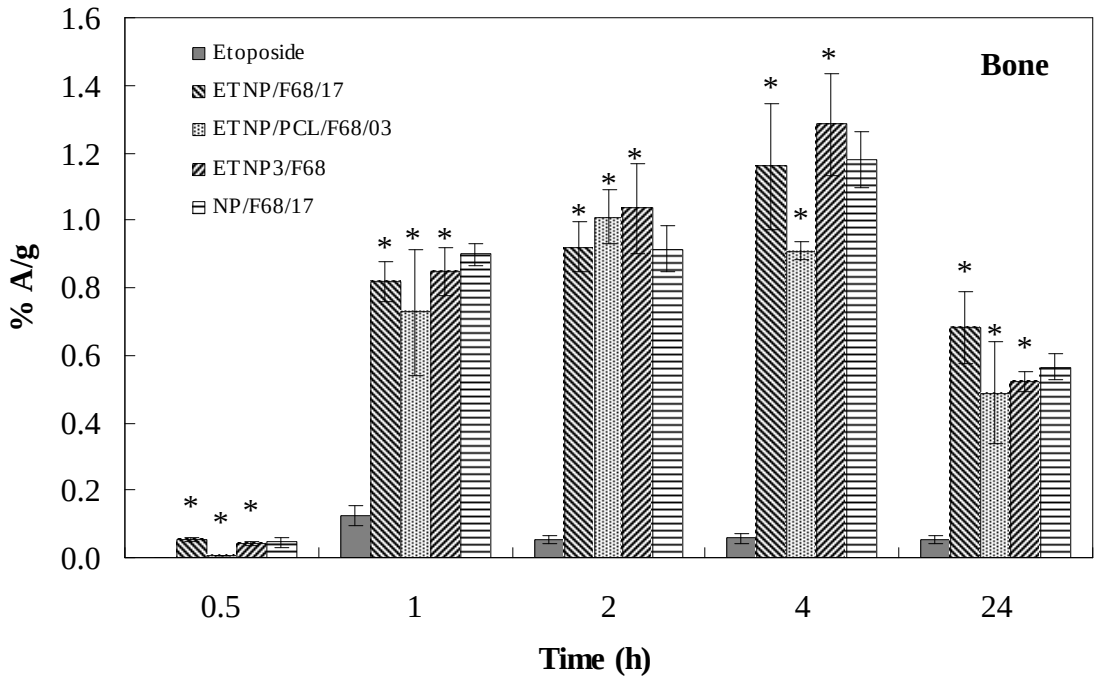

Figure 19: Comparative biodistribution profiles of drug and formulations in bone of healthy mice after oral administration (n=3). * - $P \leq 0.01$

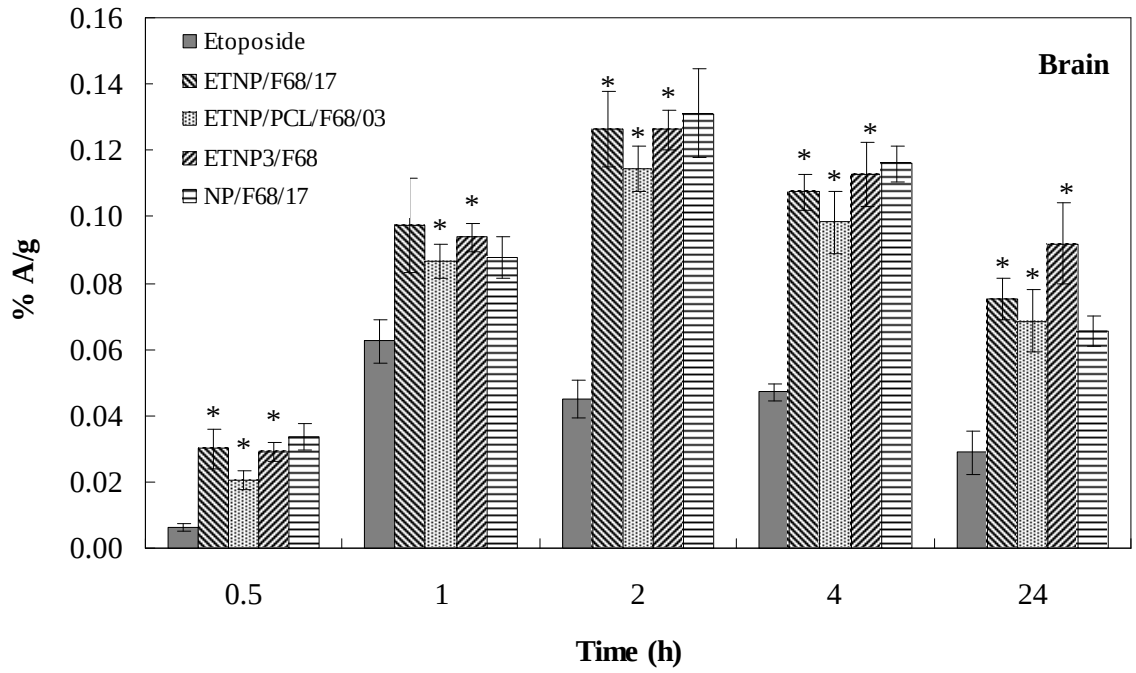

Figure 20: Comparative biodistribution profiles of drug and formulations in brain of healthy mice after oral administration (n=3). * - $P \leq 0.01$

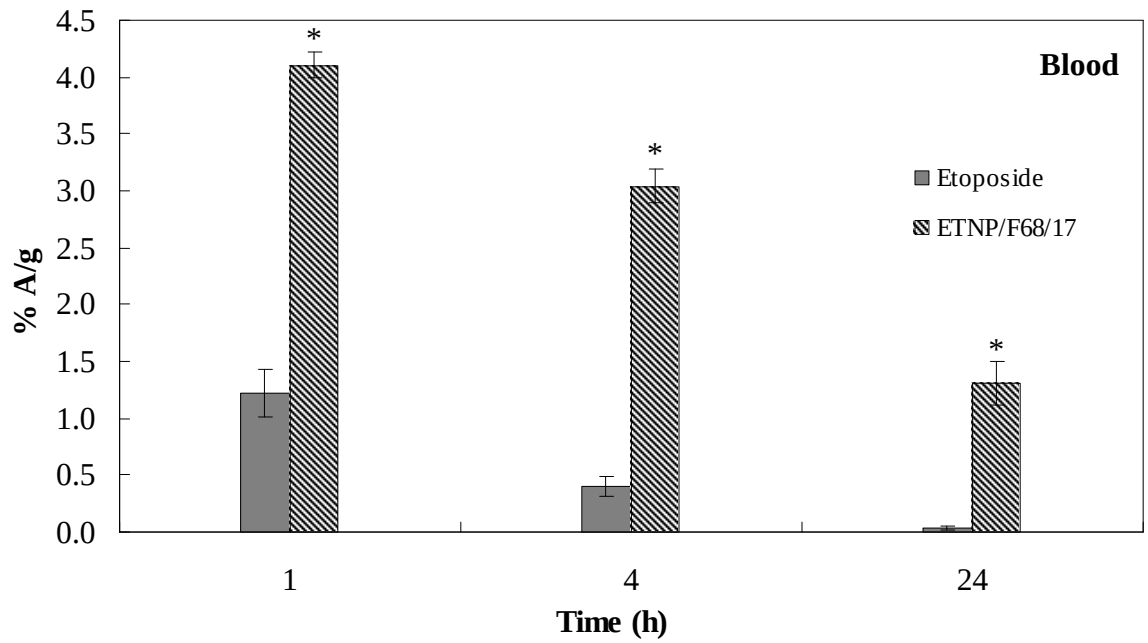

Figure 21: Comparative biodistribution profiles of drug and formulation in blood of DLS tumor induced mice after i.v. administration (n=3). * - $P \leq 0.01$

Table 12: Pharmacokinetic Parameters for etoposide and nanoparticle formulations in DLS tumor induced mice after intravenous administration.

Parameter	Etoposide	ETNP/F68/17
AUC_{0-8} (%A.h/g)	57.76	136.98
MRT (h)	0.74	14.06
$t_{1/2}$ (h)	0.51	9.74
Cl (g/h)	1.73	0.73

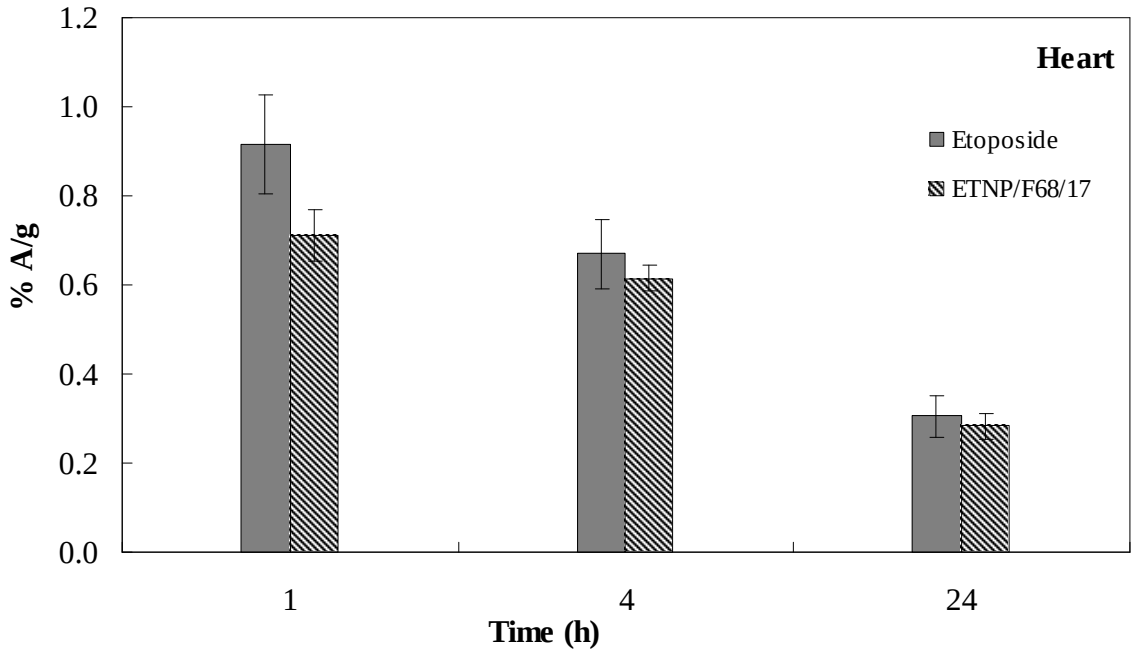

Figure 22: Comparative biodistribution profiles of drug and formulation in the heart of DLS tumor induced mice after i.v. administration (n=3).

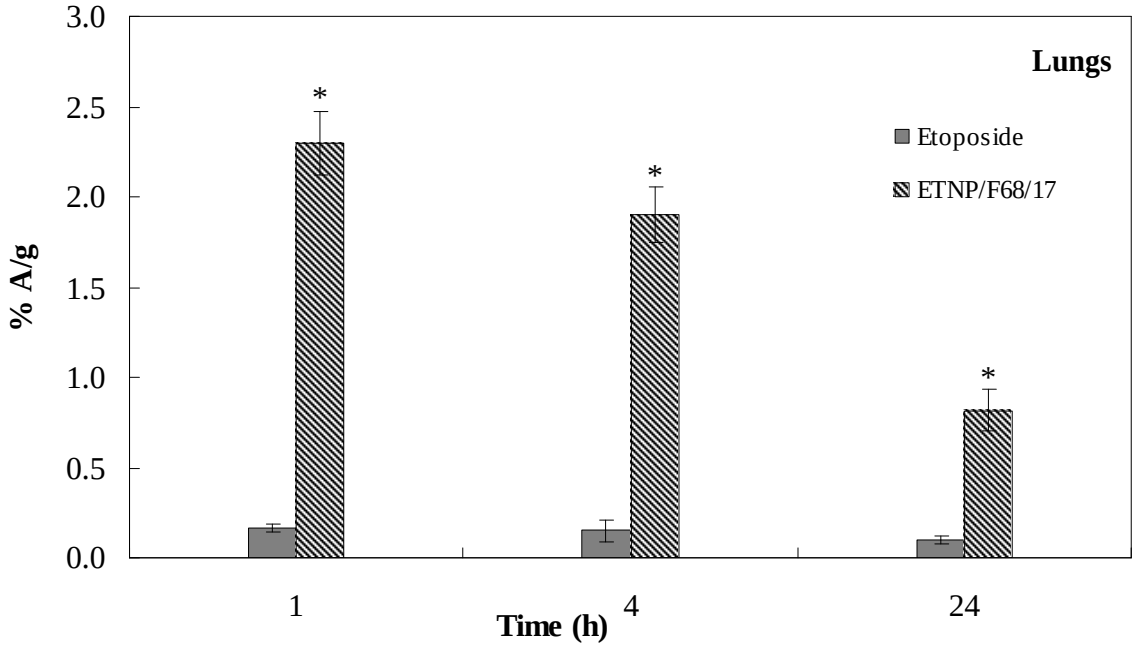

Figure 23: Comparative biodistribution profiles of drug and formulation in the lungs of DLS tumor induced mice after i.v. administration (n=3). * - $P \leq 0.01$

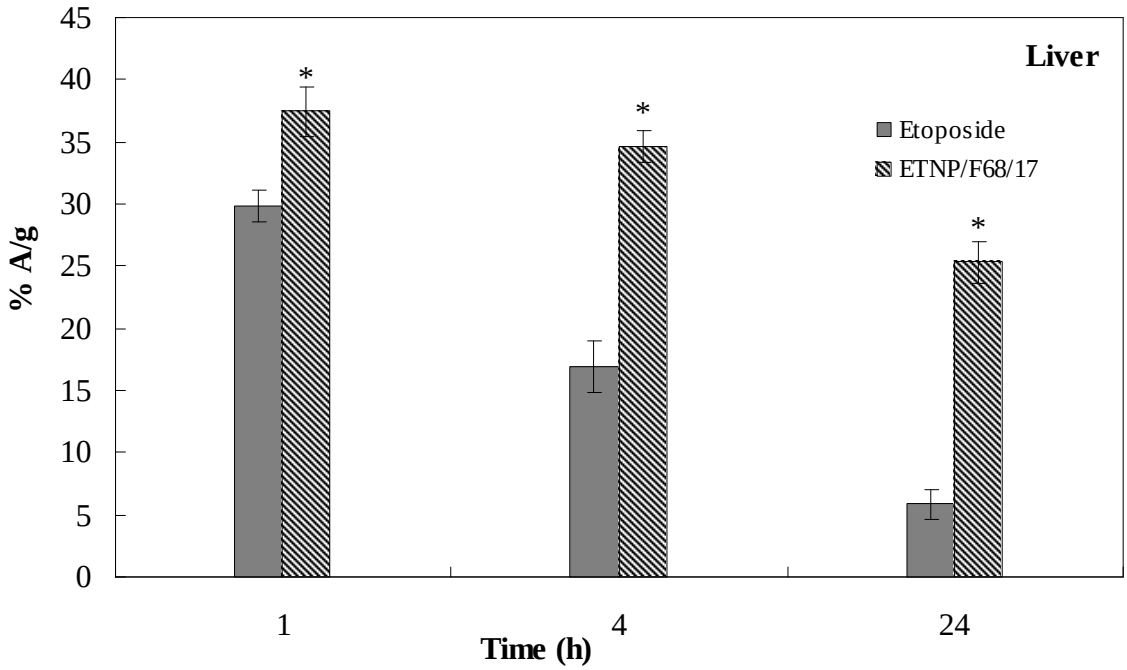

Figure 24: Comparative biodistribution profiles of drug and formulation in the liver of DLS tumor induced mice after i.v. administration (n=3). * - $P \leq 0.01$

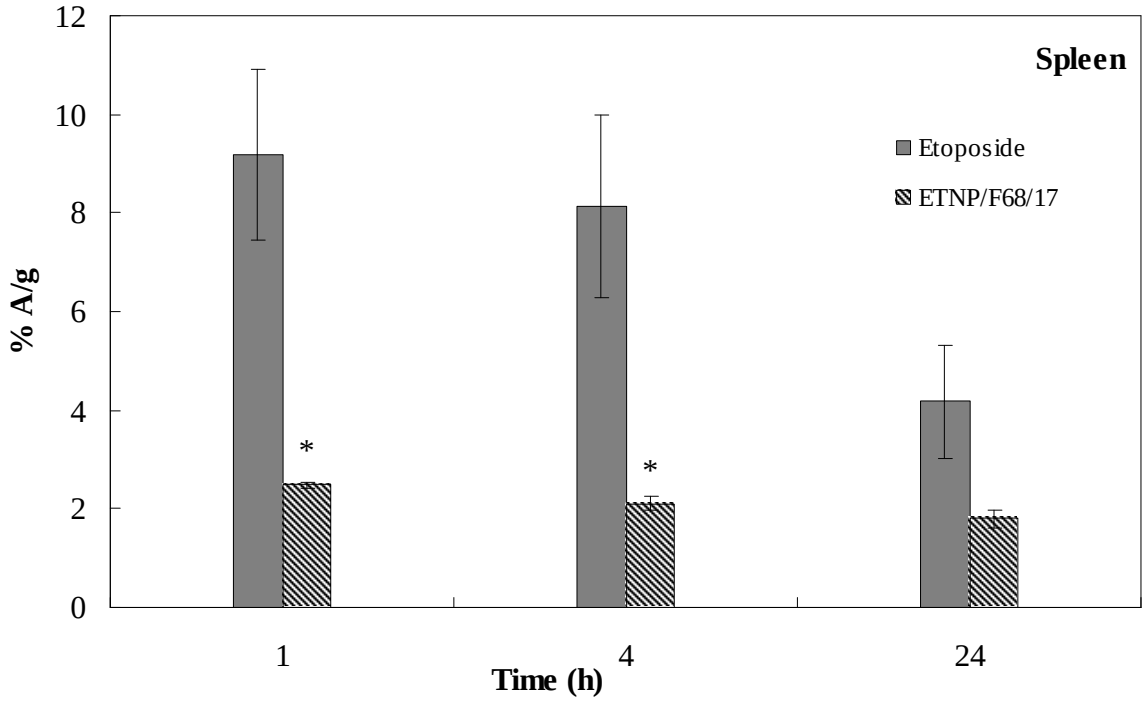

Figure 25: Comparative biodistribution profiles of drug and formulation in the spleen of DLS tumor induced mice after i.v. administration (n=3). * - $P \leq 0.01$

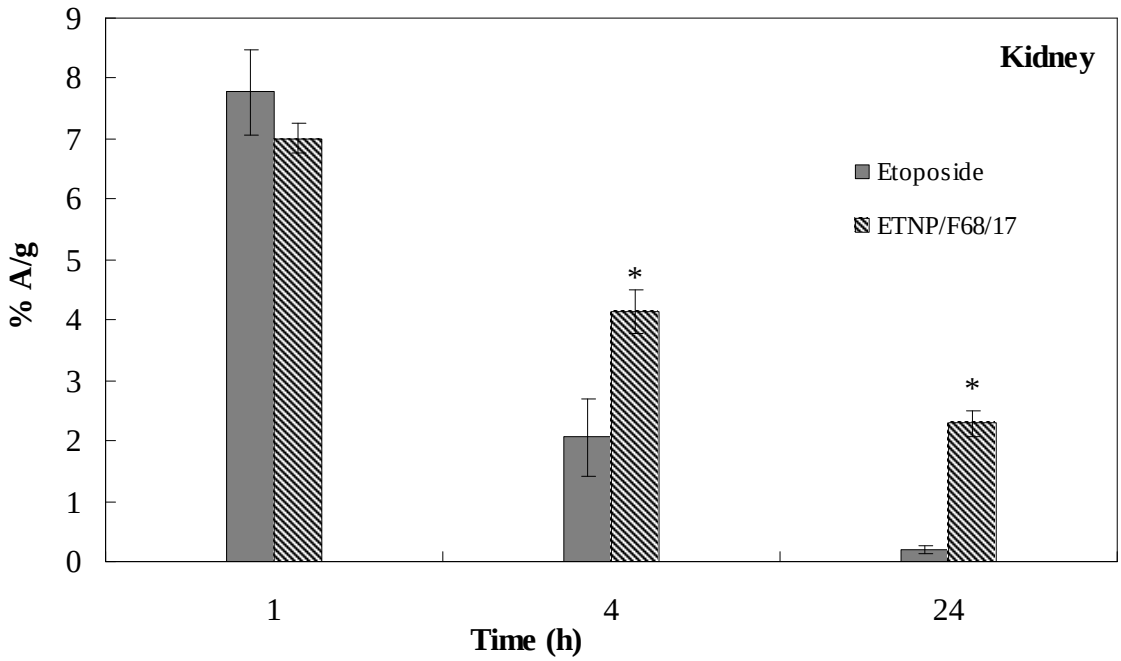

Figure 26: Comparative biodistribution profiles of drug and formulation in the kidneys of DLS tumor induced mice after i.v. administration (n=3). * - $P \leq 0.01$

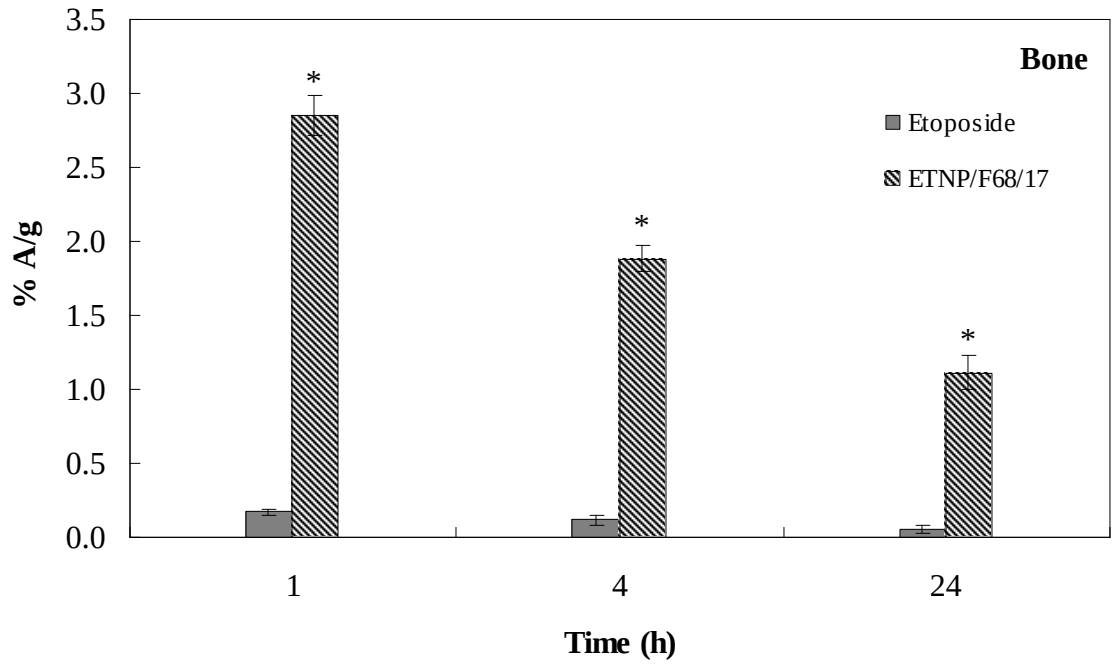

Figure 27: Comparative biodistribution profiles of drug and formulation in the bone of DLS tumor induced mice after i.v. administration (n=3). * - $P \leq 0.01$

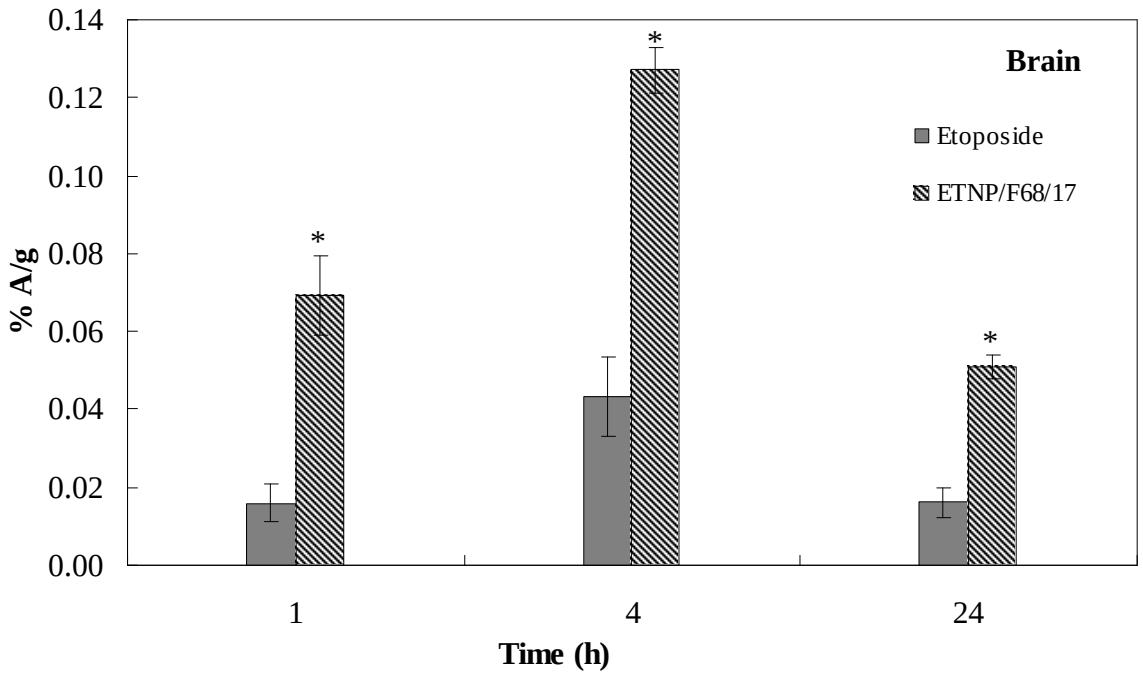

Figure 28: Comparative biodistribution profiles of drug and formulation in the brain of DLS tumor induced mice after i.v. administration (n=3). * - $P \leq 0.01$

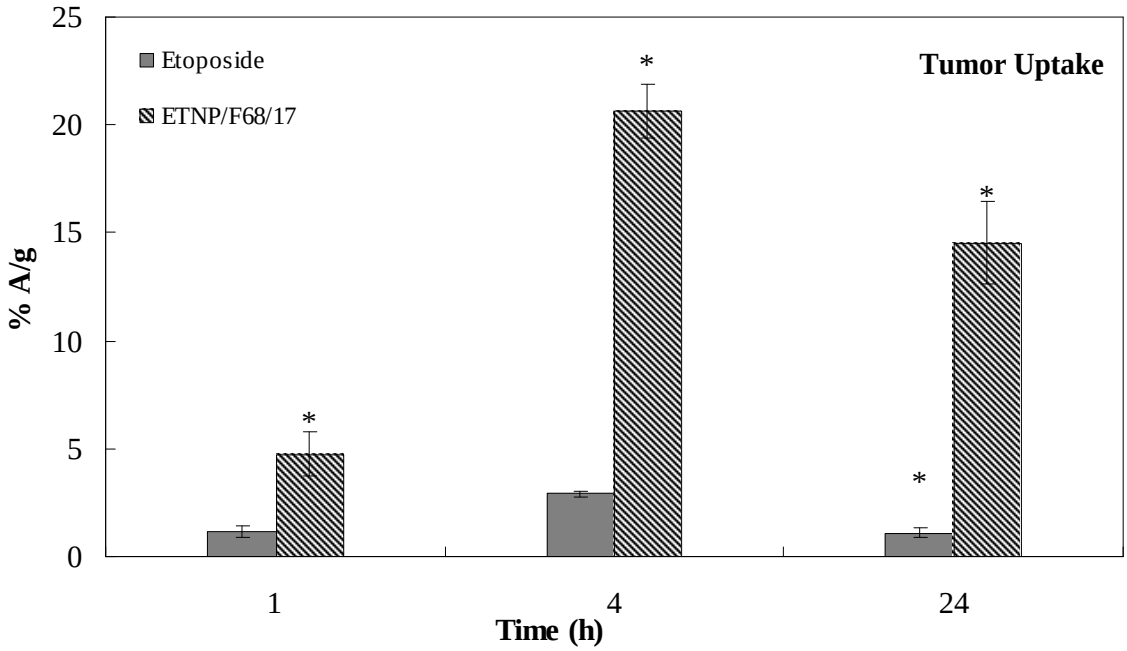

Figure 29: Comparative profile of drug and formulation in tumor muscle of DLS tumor bearing mice (n=3). * - $P \leq 0.01$

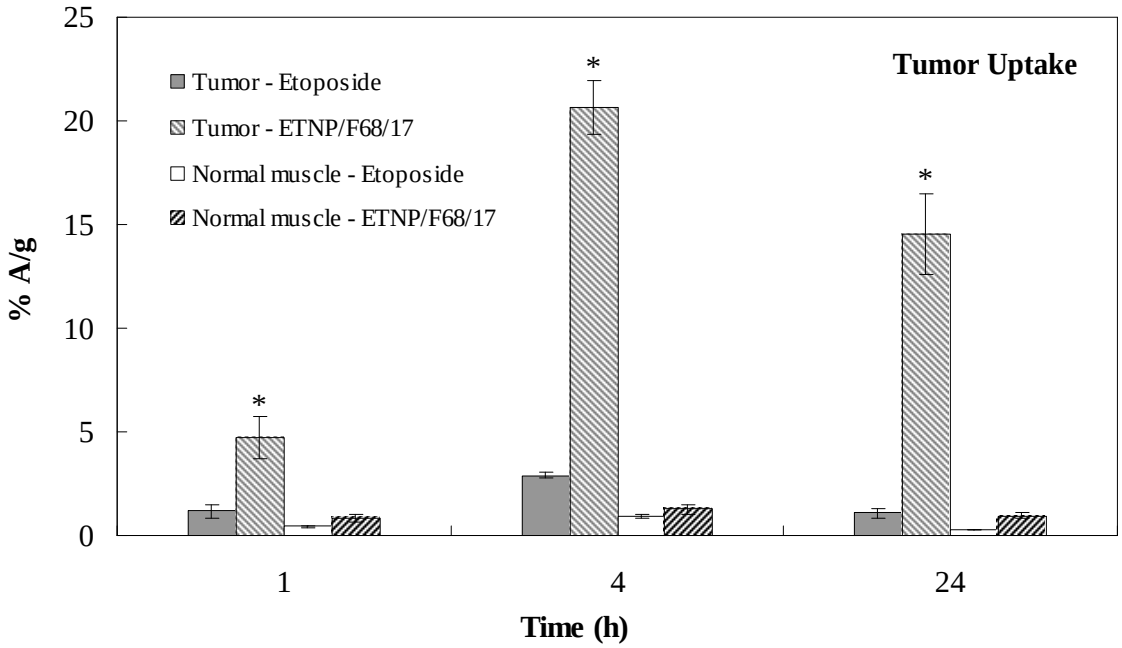

Figure 30: Comparative profiles of drug and formulations in tumor muscle and normal muscle (n=3). * - $P \leq 0.01$

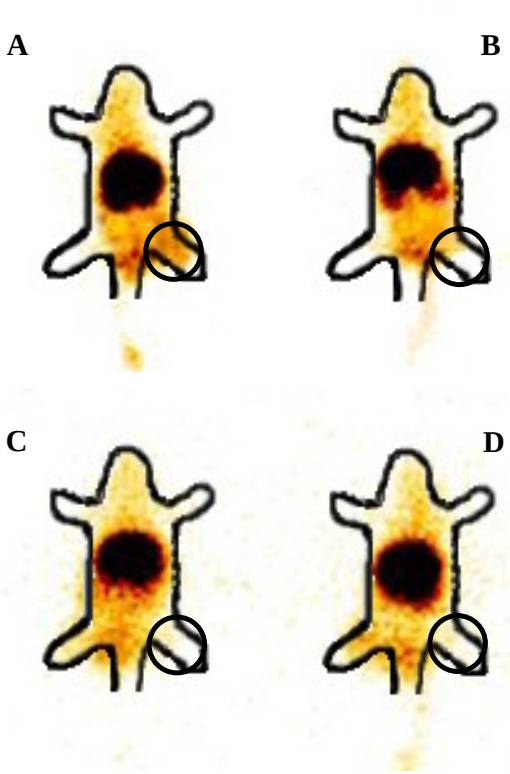

Figure 31: Gamma Scintigraphic images taken 4 h after i.v. administration of Tc^{99m} labeled complexes

A: Nanoparticle formulation (ETNP/F68/17) in DLS tumor induced mice
B: Free etoposide in DLS tumor induced mice
C: Nanoparticle formulation (ETNP/F68/17) in normal mice
D: Free etoposide in normal mice
Circled portions indicate radioactivity present in tumor and normal muscle/tissue. Darker the colour more the radio activity present at that part.

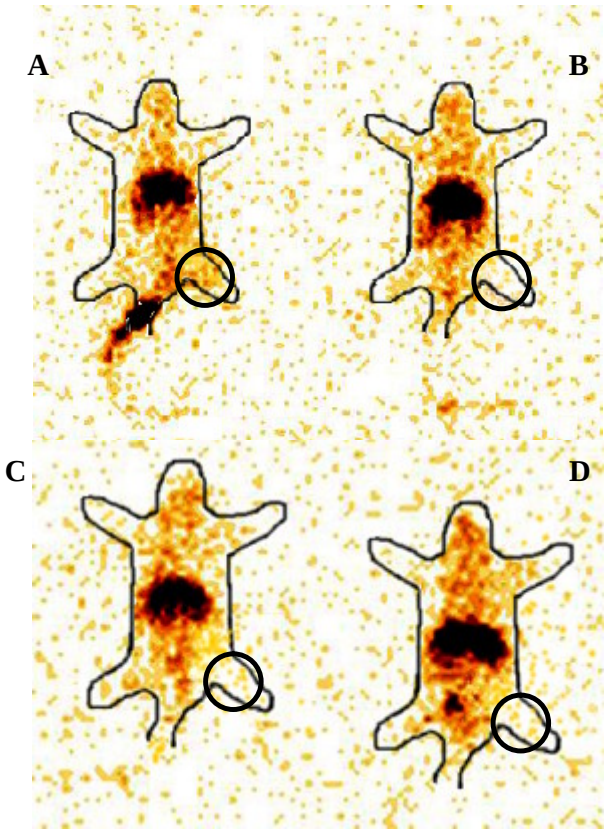

Figure 32: Gamma Scintigraphic image of DLS tumor induced and normal mice 24 h after i.v. administration

A: Nanoparticle formulation (ETNP/F68/17) in DLS tumor induced mice
B: Etoposide in DLS tumor induced mice
C: Nanoparticle formulation (ETNP/F68/17) in normal mice
D: Etoposide in normal mice
Circled portions indicate radioactivity present in tumor and normal muscle/tissue. Darker the colour more the radio activity present at that part.

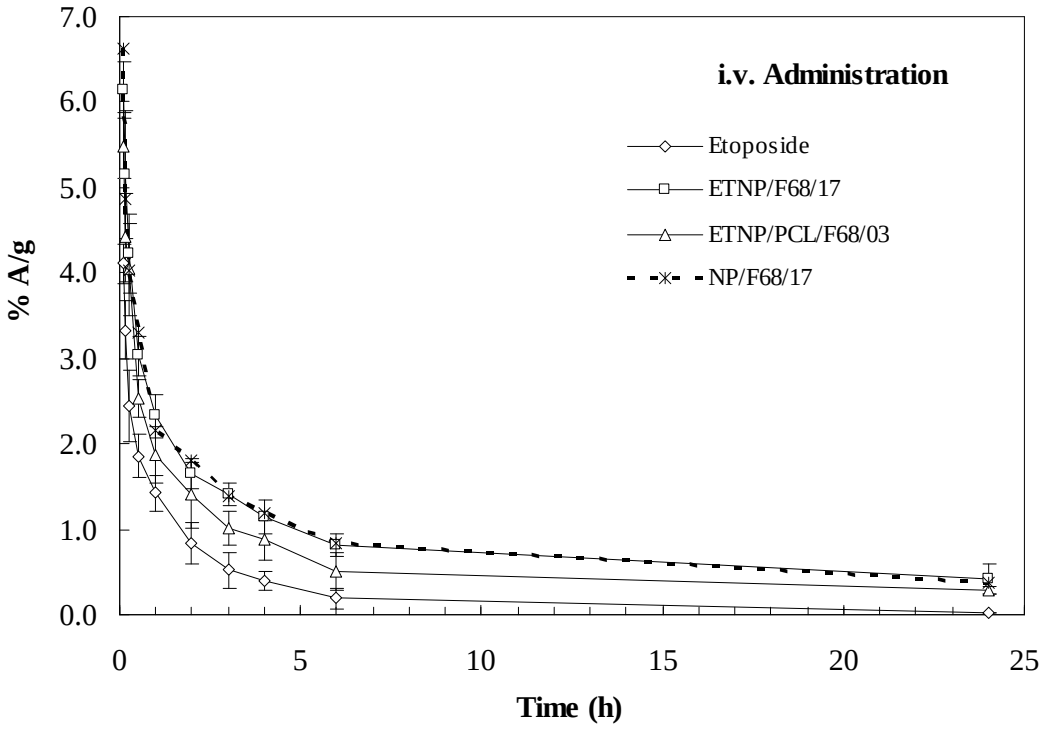

Figure 33: Pharmacokinetic profiles of Tc^{99m} labeled preparations in healthy rabbits after i.v. administration (n=3).

Table 13: Pharmacokinetic parameters for free etoposide and nanoparticle formulations in rabbits after intravenous and oral administration.

Parameter	i.v.				Oral		
	Etoposide	**ETNP/ F68/17**	**NP/ F68/17**	**ETNP/PCL /F68/03**	**Etoposide**	**ETNP/ F68/17**	**NP/F68/ 17**
AUC $_{0-8}$ (%A.h/g)	11.19	34.57	31.94	25.68	2.78	7.34	7.15
MRT (h)	2.55	16.67	13.56	15.36	4.18	8.31	6.95
$t_{1/2}$ (h)	1.77	11.55	9.39	10.64	2.89	5.76	4.82
Cl (g/h)	8.94	2.89	3.13	3.90	35.99	13.67	14.00
C_{max} (%)	-	-	-	-	0.83	1.22	1.16
T_{max} (min)	-	-	-	-	2.00	2.00	2.00

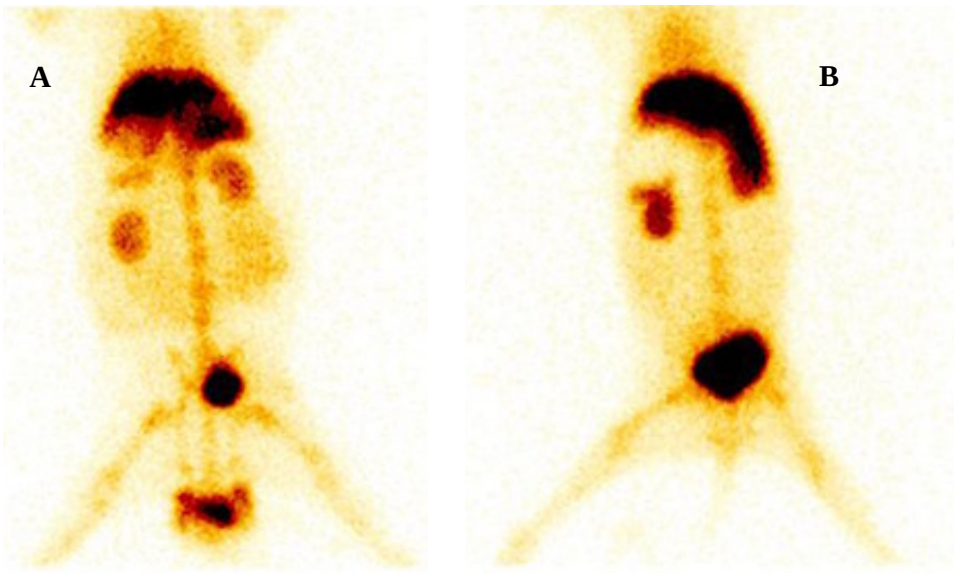

Figure 34: Gamma Scintigraphic image Rabbits after 4 h administration of A: Nanoparticle formulation (ETNP/F68/17) and B: Etoposide.
Darker the colour more the radio activity present in various organs/tissues.

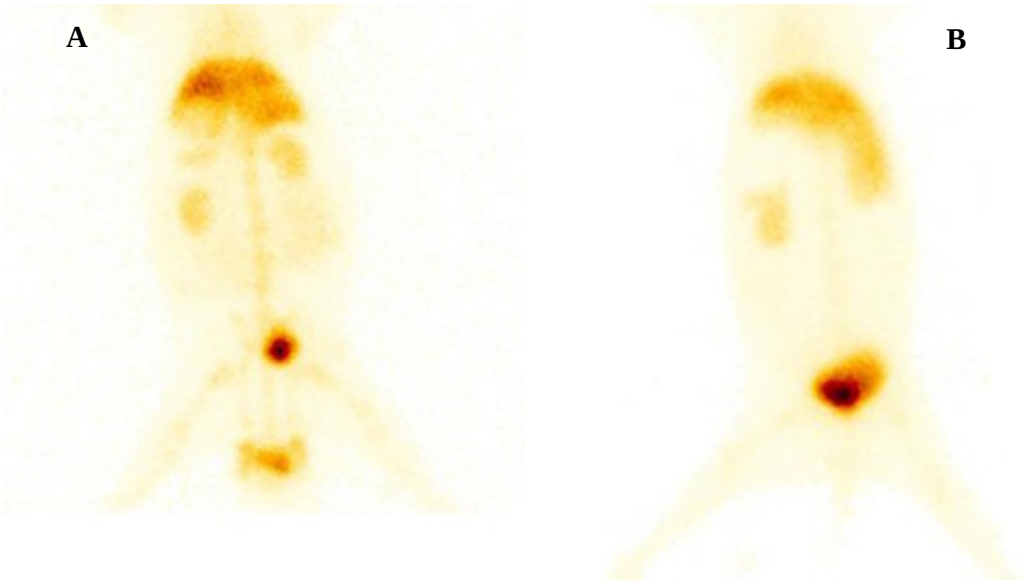

Figure 35: Gamma Scintigraphic image: Rabbits after 24 h administration A: Nanoparticle formulation (ETNP/F68/17) and B: Etoposide.
Darker the colour more the radio activity present in various organs/tissues.

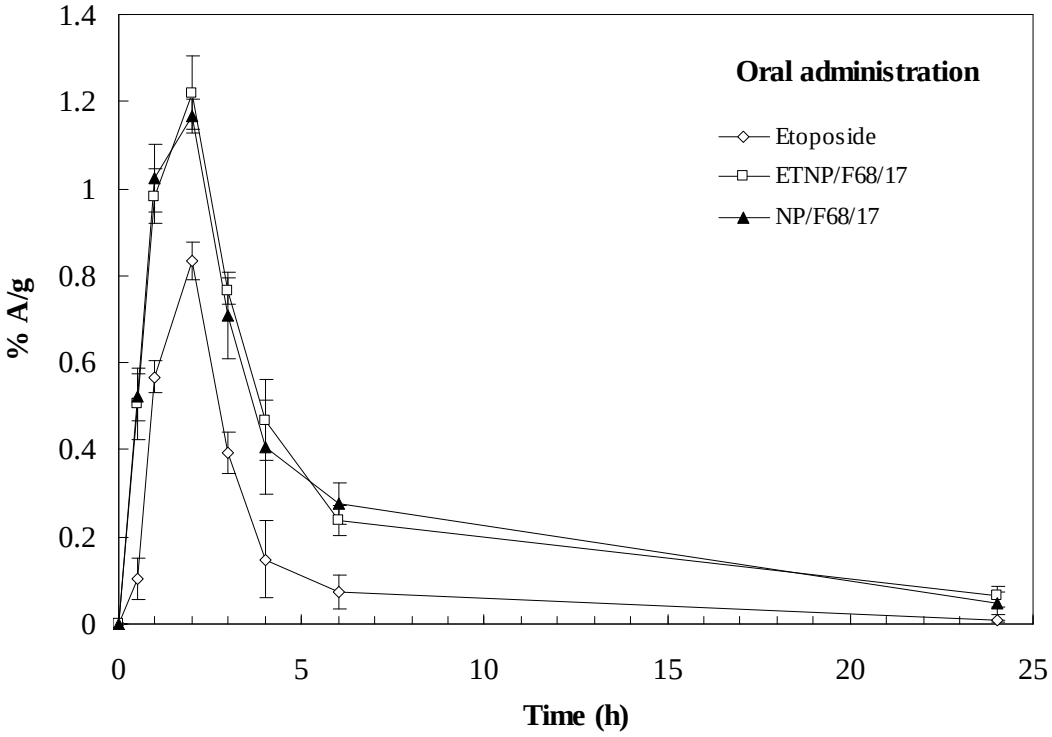

Figure 36: Pharmacokinetic profiles of Tc^{99m} labeled preparations in healthy rabbits after oral administration (n=3).

References

Alpar, H.O., Field, W.N., Hyde, R., Lewis, D.A., 1989. The transport of microspheres from the gastrointestinal tract to inflammatory air pouches in the rat. J. Pharma. Pharmacol. 41, 194-196.

Babbar, A., Kashyap, R., Chauhan, U.P., 1991. A convenient method for the preparation of 99mTc-labelled pentavalent DMSA and its evaluation as a tumour imaging agent. J. Nucl. Biol. Med. 35, 100-104.

Bhatnagar, A., Singh, A.K., Babbar, A., Soni, N.L., Singh, T., 1997. Renal imaging with 99Tc(m)-dextran. Nucl. Med. Commun. 18, 562-566.

Blok, D., Feitsma, R.I., Wasser, M.N., Nieuwenhuizen, W., Pauwels, E.K., 1989. A new method for protein labeling with 99mTc. Int. J. Rad. Appl. Instrum. B. 16, 11-16.

Chervu, L.R., Blaufox, M.D., 1982. Renal radiopharmaceuticals-an update. Semin. Nucl. Med. 12, 224-245.

Florence, A.T., 1997. The oral absorption of micro- and nanoparticulates: neither exceptional nor unusual. Pharm. Res. 14, 259-266.

Garron, J.Y., Moinereau, M., Pasqualini, R., Saccavini, J.C., 1991. Direct 99mTc labeling of monoclonal antibodies: radiolabeling and in vitro stability. Int. J. Rad. Appl. Instrum. B. 18, 695-703.

Hillery, A.M., Jani, P.U., Florence, A.T., 1994. Comparative quantitative study of lymphoid and non lymphoid uptake of 50 nm polystyrene particles. J. Drug. Target. 2, 151-154.

Jani, P., Halbert, G.W., Langridge, J., Florence, A.T., 1989. The uptake and translocation of the latex nanospheres and microspheres after oral administration to rats. J. Pharm. Pharmacol. 41, 809-812.

Jani, P., Halbert, G.W., Langridge, J., Florence, A.T., 1990. nanoparticle uptake by the rat gastrointestinal mucosa: Quantification and particle size dependency. J. Pharm. Pharmacol. 42, 821-826.

Jani, P.U., Florence, A.T., McCarthy, D.E., 1992a. Further histological evidence of the gastrointestinal absorption of polystyrene nanospheres in the rat. Int. J. Pharm. 84, 245-252.

Jani, P.U., McCarthy, D.E., Florence, A.T., 1992b. Nanosphere and microsphere uptake via Peyer's patches: observation of the rate of uptake in the rat after a single oral dose. Int. J. Pharm. 86, 239-246.

Kreuter, J., 1991. Peroral administration of nanoparticles. Adv. Drug. Del. Rev. 7, 71-86.

Larson, S.M., Hamilton, G.W., Richards, P., Ritchie, J.L., 1978. Kit - labeled technetium-99m red blood cells (Tc-99m-RBC's) for clinical cardiac chamber imaging. Eur. J Nucl. Med. 3, 227-231.

McDowell, A., Nicoll, J.J., McLeod, B.J., Tucker, I.G., Davies, N.M., 2005. Gastrointestinal transit in the common brushtail possum measured by gamma scintigraphy. Int. J. Pharm. 302, 125-132.

Mishra, P., Babbar, A., Chauhan, U.P., 1991. A rapid instant thin layer chromatographic procedure for determining radiochemical purity of 99Tcm-IDA agents. Nucl. Med. Commun. 12, 467-469.

Newman, S.P., 1999. Use of gamma scintigraphy to evaluate the performance of new inhalers. J. Aerosol. Med. 12, S25-31.

Pauwels, E.K., Welling, M.M., Feitsma, R.I., Atsma, D.E., Nieuwenhuizen, W., 1993. The labeling of proteins and LDL with 99mTc: a new direct method employing KBH_4 and stannous chloride. Nucl. Med. Biol. 20, 825-33.

Rhodes, B.A., Stern, H.S., Buchanan, J.A., Zolle, I., Wagner, H.N. Jr., 1971. Lung scanning with 99mTc-microspheres. Radiology. 99, 613-621.

Sakuma, S., Sudo, R., Suzuki, N., Kikuchi, H., Akashi, M., Hayashi, M., 1999. Mucoadhesion of polystyrene nanoparticles having surface hydrophilic polymeric chains in the gastrointestinal tract. Int. J. Pharm. 177, 161-172.

Stolnik, S., Heald, C.R., Neal, J., Garnett, M.C., Davis, S.S., Illum, L., Purkis, S.C., Barlow, R.J., Gellert, P.R., 2001. Polylactide-poly(ethylene glycol) micellar-like particles as potential drug carriers: production, colloidal properties and biological performance. J. Drug. Target. 9, 361-78.

Sundrehagen, E., 1982. Formation of 99mTc-immunoglobulin G complexes free from radiocolloids, quality controlled by radioimmunoelectrophoresis. Eur. J. Nucl. Med. 7, 549-52.

Turker, S., Erdogan, S., Ozer, A.Y., Ergun, E.L., Tuncel, M., Bilgili, H., Deveci, S., 2005. Scintigraphic imaging of radiolabelled drug delivery systems in rabbits with arthritis. Int. J. Pharm. 296, 34-43.

Volkheimer, G., 1977. Persorption of particles: physiology and pharmacology. Adv. Pharmacol. Chemother. 14, 163-187.

Wistow, B.W., Subramanian, G., Heertum, R.L., Henderson, R.W., Gagne, G.M., Hall, R.C., McAfee, J.G., 1977. An evaluation of 99mTc-labeled hepatobiliary agents. J Nucl. Med.18, 455-461.

Chapter 7

Conclusions

7. Conclusions

Nanoparticle drug delivery systems have caught attention of formulation pharmacist world over for better therapy with organ specific distribution and controlled release. It can provide an alternative solution for the more specific and selective delivery of drugs, particularly anticancer drugs, with less side effects or toxic effects. Thus, objective of this study was to design nanoparticle delivery systems for etoposide, an anticancer drug, and characterization, in vitro and in vivo evaluation of designed nanoparticles.

Analysis is a very important part for design and evaluation of drug delivery systems. Simple and accurate analytical methods are essential for success of design of formulations. Therefore, new UV spectrophotometric, spectrofluorimetric and HPLC methods were developed and validated for analysis of drug, formulations and study samples as required. The developed methods were found to be sensitive, accurate, and precise.

Preformulation studies showed that etoposide has poor aqueous solubility with rapid degradation at highly acidic and alkaline pH. Solid state stability indicated that there was no possible degradation of etoposide in presence of excipients used in the study for formulations.

Nanoprecipitation and emulsion solvent evaporation methods were found suitable to prepare nanoparticles with PLGA and PCL respectively. These methods produced nanoparticles in the range of 90 to 300 nm with PLGA co polymers, PCL and combination of these polymers with high entrapment efficiency. Nanoparticle morphology, size, recovery, entrapment efficiency, drug content was found to be effectively controlled by process parameters. However, to achieve high entrapment efficiency, high amount of polymer was used which produced low drug content. Effect of surfactant concentration, polymer and drug proportion was found to influence nanoparticle characteristics. Drug content, probably can be increased by modifying some process parameters or change of polymer.

Surfactants, F 68 and PVA, prevented aggregation, stabilized nanoparticles and hence produced lower size nanoparticles. PLGA produced finer particles compared with PCL with high drug entrapment efficiency. Further, size of the nanoparticles was finer with F 68 than PVA. Entrapment efficiency of etoposide was high with PCL because of its hydrophobic nature compared to PLGA co polymers. However, EuL-100 produced nanoparticles of wider and larger range. Formulations prepared with EuL-100 have very low level of drug entrapment.

Freeze drying was found to produce better nanoparticle products. There was no significant change in size, polydispersity index, entrapment, recovery after freeze drying of

nanoparticle dispersions. Nanodispersions were stable for 3 months when stored at -20°C without any significant change in their parameters. Freeze dried formulations were found to be stable for more than 1 year at room temperature and there was no change of characters. Redispersibility of nanoparticles after centrifugation and freeze drying was excellent for PLGA co polymers. In vitro release of etoposide from nanoparticles was extended upto 48 h. Increase in lactide content of the PLGA co polymers was found to slower the release of etoposide from nanoparticles. Use of PVA as stabilizer found to release etoposide from nanoparticles relatively faster when compared with those with F 68.

Biodistribution studies of radiolabeled etoposide and etoposide loaded nanoparticles in healthy mice after intravenous and oral administration produced different distribution profile compared with free drug. Higher concentrations of radio labeled etoposide loaded nanoparticles were observed in blood with increased residence time. There was preferential uptake by reticuloendothelial system with maximum amount of radioactivity observed in liver with lower clearance. Nanoparticles prepared with PLGA 85/15, PCL and their combination, were distributed more into liver, blood, lungs, bone and brain after i.v. and oral administration which might be useful in treatment of malignancies in the respective organs. Lower distribution of nanoparticles to heart, kidneys could reduce the side effects and toxicity. Higher uptake of nanoparticles by gut wall of GI tract after oral administration indicates potential use of nanoparticles in treatment of GI tract malignancies.

There was significant uptake of nanoparticles by tumor when administered to DLS tumor induced mice. Record of high amount of radioactivity in the tumor after 24 h of administration of radiolabeled nanoparticles indicated high uptake and localization of nanoparticles in tumor. This shows tumor affinity and targeting properties of etoposide loaded nanoparticles than free etoposide. Higher retention of nanoparticles in tumor could be useful for their effective use in cancer therapy.

Pharmacokinetic studies, in mice and rabbits, of free etoposide and nanoparticle formulations on oral administration, have shown an increased bioavailability and decreased elimination in case of nanoparticles. Non-compartmental analysis of data of both i.v. and oral administration indicated higher AUC, MRT and lower clearance for nanoparticulate formulations than those obtained with free etoposide administration.

Scintigraphic images confirm the presence of high level of labeled complexes at the site of tumor for 24 hr than in the normal muscle. Images taken in rabbit after i.v. administration have shown that there is maximum uptake by liver.

Findings of these study suggest that etoposide loaded nanoparticles could be a better delivery system than the conventional formulation to deliver etoposide to some specific

sites or organs with extended release of etoposide in the site. These systems can potentially avoid problems associated with conventional formulations of etoposide and demonstrated the promising potential of the etoposide loaded nanoparticles to improve the therapeutic efficacy of etoposide and reduce drug associated toxicity.

However, further work is required to be done to enhance the drug loading in nanoparticles by varying different parameters or change of polymer. Also in vivo therapeutic efficacy need to be done in cancer induced animals. On the basis of animal studies, clinical trial may be made in human volunteers to study the effectiveness and specificity.

List of Publications and Presentations

Papers Published/Communicated

1) **M. Snehalatha** and Ranendra N. Saha, "New, sensitive and validated spectrofluorimetric method for the estimation of etoposide in bulk and pharmaceutical formulations", Pharmazie, 61: 2006 (*In press*).
2) **M. Snehalatha** K. Venugopal, B. Girish and Ranendra N. Saha, "New, validated, reverse phase high performance liquid chromatography method for estimation of etoposide in bulk and formulations", Indian J. Pharm. Ed. Res, (*Communicated*).

Other papers from this study are under preparation.

Paper Presentations

1) **M. Snehalatha**, K. Venugopal, Ranendra N. Saha, "Preparation and characterization of Etoposide loaded nanoparticles", 32nd Annual Meeting and Exposition of the Controlled Release Society, 2005, Miami Beach, Florida, U.S.A.
2) **M. Snehalatha,** K. Venugopal and Ranendra N. Saha**,** "Formulation and characterization of Etoposide loaded nanoparticles using biodegradable polymers", AAPS Annual Meeting and Exposition, 2005, Nashville, TN, U.S.A.
3) **M. Snehalatha** and Ranendra N. Saha, "Preparation and characterization of Etoposide loaded PLGA and PCL nanoparticles", International Symposium on Recent Advances in Drug Design and Delivery Systems, 2005, Pilani, India.
4) Ranendra N. Saha., **M. Snehalatha.**, Archana R. and Charde, S. Y., "Novel delivery systems for orally administered drugs with biopharmaceutical limitations", International Symposium on Drug Design and Drug Delivery Systems, 2005, BITS, Pilani.
5) **M. Snehalatha** and Ranendra N. Saha., "Preparation and characterization of etoposide loaded PLGA nanoparticles", Sixth International Symposium on Advances in Technology and Business Potential of New Drug Delivery Systems, 2005, Mumbai, India.
6) **M. Snehalatha** and Ranendra N. Saha, "Nanoparticles for the delivery of anticancer drugs", International Symposium on Emerging Trends in Genomics and Proteomics Education and Research, 2003, BITS, Pilani.

Biography of Movva Snehalatha

Mrs. Movva Snehalatha has completed her bachelor degree in Pharmacy (B. Pharm) from K.V.S.R. Siddhartha College of Pharmaceutical Sciences, Vijayawada, A.P in the year 1999. She completed her post graduation (M. Pharm, Pharmaceutics) from Department of Pharmaceutics, Institute of Technology, Banaras Hindu University, Varanasi, U.P in 2001. She has been working as a senior research fellow at BITS, Pilani from 2001 to 2006. She has published/presented research articles in well renowned journals and several national and international conferences in India and abroad.

Biography of Prof. Ranendra N. Saha

Dr. Ranendra N. Saha is Professor of pharmacy and Dean, Faculty Division III and Educational Development Division, BITS, Pilani. He obtained his B. Pharm and M. Pharm (Pharmaceutics) degrees from Jadavpur University, Kolkata and Ph.D. from BITS, Pilani. He has more than 25 years of teaching and research experience and guided several doctoral, M. Pharm and B. Pharm students. He has many publications in reputed international and national journals and presented papers in international and national conferences in India and abroad. He has successfully completed several government and industry sponsored projects and continuing so. Dr. Saha has developed commercial products for industries and transferred technologies of production to industries and filed patents. He is expert member to various committees of UGC and other agencies and selection committee members of CSIR laboratories and several universities and colleges. He is also member of Board of studies of several universities and colleges and visiting Professor to few universities.